Benefits of Multi-energy System Integration for Decarbonizing Energy Sectors

Zhang, Xi

Department of Electrical and Electronic Engineering

Imperial College London

This thesis is submitted for the degree of

Doctor of Philosophy

Nov-2018

Declaration

I hereby declare that the contents of this thesis are original and have not been submitted in whole or in part for consideration for any other degree or qualification in this, or any other University. This thesis is the result of my own work, except where specific reference is made to the work of others. Any use of the first-person plural is for reasons of clarity.

Zhang, Xi

Nov-2018

Acknowledgements

I would like to express my deep gratitude to my supervisor, Prof. Goran Strbac, for his patient guidance and consistent dedication in my doctoral work. I feel very grateful for all his supervisions and supports which are crucial for me to overcome the challenges on the way towards a fulfilling PhD. His professional expertise and innovative ideas of system operation and planning inspired me to make efforts in these areas with certain contributions.

I would also like to show many thanks to my colleagues in the Control and Power Group at Imperial College London, especially Dr. Robert Sansom, Dr. Fei Teng, Dr. Danny Pudjianto, Dr. Marko Aunedi, and Dr. Mingyang Sun for all their valuable helps and suggestions in the field of multi-energy system modelling, electricity system operation, and representative data selecting.

I am also very grateful to my church, where I met many lovely people who gave me a lot of help when I first came to a new country.

My deep appreciation goes out to those important people in my life who gave me sweet memories and my friends in Imperial College who always accompany with me and support me when I had difficulties in the process of study and life. Especially Chi Luo, Min Yu, Jochen Cremer, Xin Xiang, Luis Badesa Bernardo, Zihang Dong, Cheng Hu, Yu Sang, Peng Fu, Hossein Ameli, Yijun Li, Boli Chen, Temitayo Oderinwale, Kaiwen Chen, Simon Phung, Jun Zhong and Dawei Qiu. Special thanks to Huayuan Jin, for her considerate care and supports.

Lastly, I would also like to express my heartfelt thanks to my parents for their sustained supports and selfless love. It is impossible for me to complete this thesis without their encouragement and care.

List of Publications

Journal Papers

X. Zhang, G. Strbac, F. Teng, and P. Djapic, "Economic assessment of alternative heat decarbonisation strategies through coordinated operation with electricity system – UK case study," *Applied Energy,* vol. 222, pp. 79-91, 2018/07/15/ 2018.

X. Zhang, G. Strbac, N. Shah, F. Teng and D. Pudjianto, "Whole-System Assessment of the Benefits of Integrated Electricity and Heat System," in *IEEE Transactions on Smart Grid*, vol. 10, no. 1, pp. 1132-1145, Jan. 2019.

M. Sun, F. Teng, **X. Zhang**, G. Strbac and D. Pudjianto, "Data-Driven Representative Day Selection for Investment Decisions: A Cost-Oriented Approach," in *IEEE Transactions on Power Systems*. DOI: 10.1109/TPWRS.2019.2892619.

P. Fu, D. Pudjianto, **X. Zhang**, G. Strbac. "Integration of Hydrogen into Multi-Energy System Optimization", *CSEE Journal of Power and Energy Systems*, submitted for review.

Conference Papers

X. Zhang, G. Strbac, P. Djapic, and F. Teng, "Optimization of Heat Sector Decarbonization Strategy through Coordinated Operation with Electricity System," *Energy Procedia,* vol. 142, pp. 2858-2863, 2017/12/01/ 2017.

P. Fu, D. Pudjianto, **X. Zhang**, G. Strbac. "Evaluating Strategies for Decarbonising the Transport Sector in Great Britain“, *13th IEEE PES PowerTech Conference*, 2019, submitted for review.

Abstract

Heat accounts for approximately half of the total energy consumption and is responsible for over 25% of carbon emissions in the U.K. Therefore, decarbonization of the heat sector is one of the key challenges in achieving the 80% carbon reduction target by 2050. The utilisation of various low-carbon heating technologies to replace gas boilers, which currently dominate the UK heating sector, is crucial in facilitating the transition to a low-carbon future energy system. Additionally, the building thermal characteristics can also provide us an alternative perspective to realise the carbon target while alleviating the burden of new investment at the end-side.

This thesis first proposes a District Heating Network (DHN) investment model by using a fractal-image-based algorithm. Through this model, the investment cost of DHNs driven by different user penetrations in different representative areas can be quantified and the DHN investment cost functions can be incorporated into the whole system investment model to optimize the penetration of DHNs. This thesis also investigates the value of pre-heating through inherent building thermal storage. By comparing the operational costs between the case where pre-heating is enabled and the case where additional TES is installed, the economic value of pre-heating can be evaluated while the capability of the inherent storage of buildings under given thermal parameters of buildings can be quantified. We then propose a novel whole-system integrated electricity and heat system model in which, for the first time, operation and investment timescales are considered while covering both the local district and national level infrastructures. The modelling of DHN investment and pre-heating are also integrated into this whole-system model.

A series of case studies are then carried out to investigate the benefits of different heating technologies. Electric HPs, hybrid heating technology and DHN are the main low-carbon heating technologies that can deliver the ambitious carbon reduction target in the UK. The optimal design of the heating system on a national scale to maximize the economic benefits regarding both investment cost and operation cost while satisfying the carbon target remains an open question. This thesis compares the economic advantages as well as the associated impacts on the electricity system under the full deployments of ASHP, hybrid HP-Bs (ASHP and gas boilers), DHNs and hydrogen boilers by using the whole-system integrated electricity and heat system model. The optimized strategy for heat sector decarbonisation is also

demonstrated, providing an outline of the optimal deployment for different heating technologies in terms of their penetrations and deployed areas. The UK case study suggests the significant economic advantage of the hybrid HP-B over the other three heating technologies, while DHN may play an important role in urban areas under the optimized heat decarbonisation strategy. The results also clearly demonstrate the changes in the electricity side driven by the different decarbonisation strategies in the heating system.

Additionally, the benefits through considering the interaction between electricity and heat systems at the planning stage are investigated, as the system integration will play an important role in facilitating the cost effective transition to a low carbon energy system with high penetration of renewable generation. The whole-system integrated electricity and heat system model is applied to optimize decarbonization strategies of the UK integrated electricity and heat system, while quantifying the benefits of the interactions across the whole multi-energy system, and revealing the trade-offs between portfolios of (a) low carbon generation technologies (renewable energy, nuclear, CCS) and (b) district heating systems based on heat networks and distributed heating based on end-use heating technologies. Overall, the proposed modeling demonstrates that the integration of the heat and electricity system (when compared with the decoupled approach) can bring significant benefits by increasing the investment in the heating infrastructure in order to enhance the system flexibility that in turn can deliver larger cost savings in the electricity system, thus meeting the carbon target at a lower whole-system cost.

Last but not least, a cost-oriented representative-day-selection approach that can significantly reduce the computational burden of the whole-system integrated electricity and heat system model is proposed. Through a series of case studies, we demonstrated the superior performance of the proposed cost-oriented representative-day-selection approach against the widely used input-based approach.

Contents

List of Figures

List of Tables

Nomenclature

Acronyms for all chapters

ASHP	Air Source Heat Pump
CAPEX	Capital Cost
CCGT	Combined Cycle Gas Turbine
CCS	Carbon Capture and Storage
CHP	Combined Heat and Power
COP	Coefficient of Performance
DHN	District Heating Network
DN	Distribution Network (electricity)
EGB	End-use Gas Boiler
ETES	End-use TES
HP	Heat Pump
IHP	Industrial Heat Pump
IGB	Industrial Gas Boiler
ITES	Industrial TES
LG	Low Carbon Generation
OPEX	Operation Cost
OCGT	Open Cycle Gas Turbine
NG	Natural Gas
RES	Renewable Energy Source
TES	Thermal Energy Storage
SMR	Steam methane reforming

Chapter 2

Constants

A	The size of area of representative districts [m^2]
A^{tot}	The total size of area of the Great Britain [m^2]
C^{unit}	Unit cost of heat network [£/km]
D^h	Annual heat demand of representative areas [GWh]
$D^{h,tot}$	Annual heat demand of the Great Britain [GWh]
N^c	The number of consumers in representative districts
N^{ra}	The number of each representative areas
P	The population of representative areas
P^{tot}	The total population of the Great Britain
l	The length of heat networks [km]
$\overline{p}^{CHP}/\underline{p}^{CHP}$	The maximum/ minimum electricity output of CHP [kW]
$\overline{s}$	Maximum discharging/charging rate of TES [kW]
z	Conversion rate from electricity to heat for CHP [p.u.]
η^s	The static efficiency of storage [%]
η^{in}/η^{out}	The efficiency of energy charging/discharging [%]
λ	Ratio of heat to electricity for CHP [p.u.]
τ	Fractal dimension of representative districts [p.u.]
τ^s	The duration that storage can be fully charged from being empty [h]
$\overline{p}^{HP}$	Electric power rating of HPs [kW]
COP^{HP}	Coefficient of performance of HPs [p.u.]

Variables

α^{hn}	DHN penetration in different representative areas [%]
ec	Energy content in TES [kWh]
p^{CHP}/h^{CHP}	Electricity/heat output of CHP [kW_{th}]
s^{in}/s^{out}	Charging/Discharging rate of TES [kW]
p^{HP}	Electricity consumption of HPs [kW];
p_t^{exd}/h_t^{exd}	Extended electricity/heat output through coordination in DHNs [kW]

Sets

R	The set of representative districts
T	The set of time horizon

Chapter 3

Constants

C^{im}	Price of importing electricity from the grid [£/kWh]
C^{ex}	Price of exporting electricity to the grid [£/kWh]
C^{PR}	Price of providing primary response to the grid [£/kWh]
C^{SR}	Price of providing secondary response to the grid [£/kWh]
C^{h}	Price of providing high frequency response to the grid [£/kWh]
C^{f}	Price of providing flexible frequency response to the grid [£/kWh]
w_x	Predefined temporal windows during which flexible response can be called [h]
P^{el}	Electricity demand excluding HVAC-driven electricity consumption [kW]
η^{HVAC}	Conversion rate from electricity to heat of HVAC appliances [p.u.]
a, b	Linear coefficient/constant term of COP for ASHP [$°C^{-1}$], [p.u.]
P_{max}^{HVAC}	Maximum power rating of HVAC appliances [kW]
Δt	Time interval [hour]
U^{wall}	Heat transfer coefficient of the walls [$W/(m^2 \cdot K)$]
U^{win}	Heat transfer coefficient of the windows [$W/(m^2 \cdot K)$]
A^{wall}	The area of wall surface [m2]
A^{win}	The area of window surface [m2]
α^{w}	Absorbance coefficient of the external surface of the wall [p.u.]
R^{se}	The external surface heat resistance for convection and radiation [$m^2 \cdot K/W$]
I^{T}	The total solar radiation on the walls/windows surface [kW/m^2]
τ^{win}	The glass transmission coefficient of the windows [p.u.]
SC	The shading coefficient of the windows [p.u.]
Q^{in}	Internal heat gains from people, appliances and lighting [kW]
ρ	The density of the air in buildings [kg/m^3]
C	The specific heat capacity of the air in buildings [$J/(kg \cdot °C)$]
V	The volume of the air in buildings [m^3]
T^{set}	Set point of the comfortable temperature inside buildings [°C]
$\overline{T}, \underline{T}$	The upper and lower limits of the temperature inside buildings [°C]
ε^{s}	Ratio of the energy capacity to power rating of TES [h]
η^{s}	Static efficiency of TES [p.u.]

η^{in}	Charging efficiency of TES [p.u.]
η^{out}	Discharging efficiency of TES [p.u.]

Variables

P^{im}/P^{ex}	Imported/exported electricity [kW]
P^{PR}	Primary response provision [kW]
P^{SR}	Secondary response provision [kW]
P^{h}	High frequency response provision [kW]
P^{f}	Flexible frequency response provision [kW]
P^{PV}	PV output [kW]
P^{HVAC}	HVAC-driven electricity consumption [kW]
Q^{HVAC}	Thermal power of HVAC [kW_{th}]
T^{am}	Ambient temperature [°C]
s^{in}/s^{out}	TES charging/ discharging rate [kW]
s^{ec}	Energy content in TES [kW]

Sets

J	The set of wall/window surface orientation
T	The set of time horizon

Chapter 4

Constants

α^{dsr}	Proportion of flexible electricity load that can provide DSR [%]
$\alpha^{hp,res}$	Proportion of HPs output that can be interrupted to provide operating reserve service [%]
α^{p}	Percentage of electricity demand supplied by representative distribution networks [%]
α^{PH}	Proportion of heat load that can provide pre-heating [%]
ε^{s}	Ratio of the energy capacity to power rating of TES [h]
η^{PH}	Heat storage efficiency of pre-heating [%]
η^{s}	Storage efficiency of TES [%]
λ	Maximum ratio of heat to electricity for CHP [p.u.]
ς^{W}	Forecasting error of wind output [%]

ς^{PV} Forecasting error of PV output [%]

ς^{D} Forecasting error of electricity demand [%]

τ Total time horizon [h]

a^{HP}/b^{HP} Linear coefficient [1/°C]/constant [p.u.] term of COP for ASHP

a^{L}/b^{L} Linear coefficient [p.u.]/constant [p.u.] term of LOLP function

$\overline{cap}^{DN}$ Peak electricity load that can be accommodated without distribution network reinforcement [GW]

h Heat demand [GW_{th}]

p Electricity demand [GW]

$\underline{p}^{chp}/\overline{p}^{chp}$ Minimum/maximum electricity output of CHP units [GW]

$\underline{p}^{g}/\overline{p}^{g}$ Minimum/ maximum electricity output of generation units [GW]

r^{up}/r^{dn} Ramp-up/ramp-down limit for generators [GW/h]

vre^{af} Renewable energy availability factor [p.u.]

$\overline{rsp}^{g}$ Maximum response generation units can provide [p.u.]

z Conversion rate from electricity to heat for CHP [p.u.]

AF Annuity factor of different assets [p.u.]

C^{d} Capital cost of various district heating assets [£/GW]

C^{e} Capital cost of various end-use heating appliances [£/GW]

C^{f} Capital cost of transmission networks [£/GW/km]

C^{g} Capital cost of generators [£/GW]

C^{fix} Fixed O&M cost of various assets [£/GW/year]

$C^{ins,e}$ Installation cost of end-use appliances [£]

C^{DN} Reinforcement cost of representative distribution networks [£/kVA/year]

C^{DN} Capital cost of heat networks per length [£/km]

Cap^{L} Capacity of the largest generator [GW]

$\overline{CO2}$ Overall carbon target [g/kWh]

COP^{a} Coefficient of performance of air source HPs [p.u.]

COP^{w} Coefficient of performance of water source HPs [p.u.]

$\overline{AAF}$ Annual availability factor of generators [p.u.]

$\overline{LOLE}$ Reliability criterion that sum of LOLP across the year should meet [p.u.]

OC^{gb} Operation cost of various types of gas boilers [£/GWh]

OC^{nl} No-load cost of various generation [£/h]

OC^{st}	Start-up cost of various types of generation [£]
OC^{var}	Variable operation cost of various types of generation [£/GWh]
N^{h}	Number of households
N^{DN}	Number of representative distribution networks
N^{HN}	Number of representative heat networks
$\underline{OR}$	System operating reserve requirement [GW]
$\underline{FR}$	System frequency response requirement [GW]
T^{a}	Ambient temperature [°C]

Variables

μ	Number of synchronized generation units
ω^{d}/ω^{e}	Penetration of district /end-use heating technologies [%]
ω^{HN}	Penetration of HNs in each representative district [%]
cap^{x}	Capacity of plant/appliance x [GW]
cap^{DN}	Expanded capacity of distribution networks due to reinforcement [GW]
h^{chp}	Heat output of CHP [GW_{th}]
h^{d}/h^{e}	Heat demand of district heating/end-use heating [GW_{th}]
h^{d+}/h^{d-}	Increased/reduced heat demand due to pre-heating in district heating [GW_{th}]
h^{e+}/h^{e-}	Increased/reduced heat demand due to pre-heating in end-use heating [GW_{th}]
h^{gb}	Heat output of different types of gas boilers [GW_{th}]
h^{hp}	Heat output of different types of HPs [GW_{th}]
h^{PH}	Accumulated heat through pre-heating [GWh_{th}]
p^{chp}	Electricity output of CHP [GW]
p^{ele}	Electricity load not related to heat [GW]
p^{ele+}/p^{ele-}	Increased/decreased non-heat electricity demand through DSR [GW]
p^{heat}	Heat-driven electricity load [GW]
p^{g}	Electricity output of generators [GW]
vre	Output of variable RES [GW]
vre^{ava}	RES available for generation [GW]
vre^{W}/vre^{PV}	Wind power/PV output [GW]
$res^{hp,e}$	Operating reserve provided by end-use HPs [GW]
res^{x}	Operating reserve provision from source x [GW]
$rsp^{hp,e}$	Frequency response provided by end-use HPs [GW]

rsp^x	Frequency response provision from source x [GW]
s^+/s^-	Discharging/charging rate of different types of TES [GW_{th}]
s^{cap}	Maximum discharging/charging rate of TES [GW_{th}]
s^{ec}	Energy content of TES [GWh_{th}]
$CO2$	Carbon emission from various sources [t]
CM	Capacity margin of generation [p.u.]
IC^{HN}	Investment cost of representative HNs [£]
$LOLP$	Estimated Loss of Load Probability [p.u.]

Superscripts

chp	CHP related
d	District heating assets related
e	End-use heating appliances related
f	Transmission network related
g	Generator related
gb	Gas boiler related

Functions

$F(\cdot)$	DC Power flow function
$F_L^{HN}(\cdot)$	Heat network length function
F^{LOLP}	LOLP function

Sets

H_d/H_e	Set of district/end-use heating technologies
D_x	Set of time steps in the xth day (starting at midnight)
DN/HN	Set of representative distribution/heat networks
DN_i	Set of components included in distribution network i
F	Set of transmission corridors
G	Set of generation types
L	Set of locations
T	Set of operating time steps

Chapter 1 Introduction

1.1 Background

The Climate Change Act that was passed by the UK government in 2008 claims that 'It is the duty of the Secretary of State to ensure that the net UK carbon account for the year 2050 is at least 80% lower than the 1990 baseline'[1]. To achieve this goal, it is essential to decarbonize the current energy system through large-scale deployment of various low-carbon energy sources while improving the energy efficiency of different energy sectors.

At present, heat occupies the largest proportion of the energy consumption in the UK [2], and is responsible for around one third of the total carbon emission. Heat can be classified into low grade and high grade usage. The former includes domestic heating and commercial heating. The latter mainly refers to the heat for industry process. Most of the heat is consumed for domestic heating, which includes space heating and water heating. In order to achieve the 2050 carbon target, substantial reductions of carbon emission in heat sectors have to be delivered.

In the first half of the 20th century, primary energy source was dominated by coal in the UK. With the exploitation of the North Sea natural gas since 1960s, gas rapidly substituted coal to serve as the most important primary energy source, supplying the major energy demand of electricity production as well as for heating sectors. In the early 1970s, the UK government suggested that the combined heat and power (CHP) plants might be an effective option to deal with the oil price crisis. However, as the availability of natural gas significantly brought down the market price of heat, the competitiveness of CHP in the short and medium term was seriously damaged. At present, only around 1% of commercial and domestic heat is supplied by CHP while nearly 80% of heat is covered by natural gas. In contrast, CHP is deployed on s large scale in many other countries, such as Denmark, in which CHP is responsible for over half of the total power demand. With the absence of natural gas, CHP is more attractive for

heat production in Denmark. Given that most of the CHP deployed in Denmark is heavily dependent on fossil fuels, the Danish government has proposed to build a fossil-fuel-free heating system by 2050, the core of which is to deploy biomass and waste-to-heat CHP in heat networks while generalizing the application of renewable electricity based HPs [3].

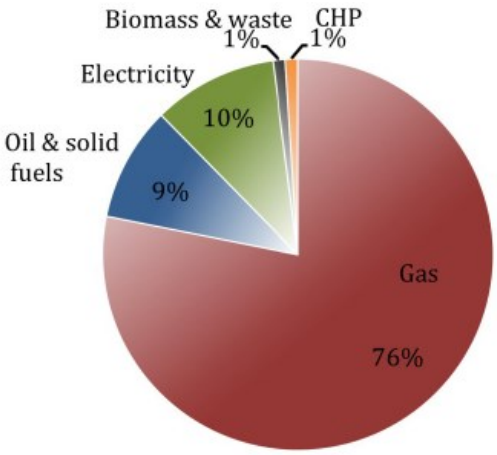

Figure 1.1– The structure of energy source for domestic heating in the UK

The structure of energy source for domestic heating in the UK is demonstrated in Figure 1.1 [2]. It can be observed that more than 90% of the heat for space and water heating comes from fossil fuel energy, leaving an intense carbon level in the heat sector. The application of low-carbon heating technologies such as district heating, HPs, and hydrogen, is still quite limited in UK.

District heating, end-use HPs as well as hydrogen are prospective low-carbon heating technologies to decarbonize the heat sector while having the potential to directly shape the future electricity system [4-7]. At present, around 80% of the households in the UK are using natural gas boilers for residential heating including both space and water heating. As most of the residential natural gas boilers are still in operation, it is challenging for customers to decommission their natural gas boilers and reinvest in new heating equipment, especially when the natural gas boiler still remains to be the most economic heating technology in the UK. As potential alternatives for end-use natural gas boilers in low-carbon scenarios, HPs, heat networks and hydrogen have different advantages and disadvantages.

1. District Heating

District heating networks (DHN) can provide thermal energy for space and hot water heating to a wide range of sectors. In DHNs, heat is produced from a central heat source and distributed through primary heat networks (as shown in Figure 1.2) to substations located in buildings. After heat exchange in the substations, heat is transferred into secondary heat networks inside the buildings and distributed to different rooms. Typically, heat is delivered via the medium of hot water (or steam which is not commonly used at present). Both the mass flow rate and temperature of the medium can potentially be adjusted to change the heat output of DHN. Different countries apply different control mode. In Europe, the control mode of variable mass flow rate and constant temperature is widely applied. The authors in [8] have performed case studies showing the advantages and disadvantages of different DHN control mode.

Figure 1.2– Primary distribution heat network

Although DHNs have been widely deployed in many countries, there are many concerns regarding large scale deployment of DHN within the UK. On the one hand, significant energy savings can be delivered through the application of DHN as it can feed on renewable energy sources, geothermal energy, or waste heat from industrial processes [9, 10]. Meanwhile, increased energy efficiency can also be achieved by using high efficiency forms of heating technologies (e.g. CHPs, industrial-sized HPs). Moreover, DHN can provide significant flexibility to the electricity system through coordinated operation of different heating technologies. For instance, CHP, by adjusting its power-to-heat ratio, and industrial-sized HPs, through temporary interruption or reduced operation, can provide balancing and ancillary services to the electricity system. TES (particularly referring to hot water tank) can facilitate

the accommodation of renewable energies, while reducing the requirement of back-up generation [11]. On the other hand, considerable heat losses can occur in the distribution networks of large centralised DH systems, impairing its competitiveness. Overall, the construction of DHNs is highly capital-intensive, which is the key limitation for its large scale deployment. However, the competitiveness of DHNs will be enhanced with the increase of heat density for the deployed area. More specifically, it is more economic to apply DHNs in urban areas rather than in rural areas, as more consumers can be supplied by per unit length of DHN pipelines, even though the capital cost of DHNs is higher in more populous areas due to congestion of existing underground utility and more serious impacts of disruption.

Basically, DHN is widely deployed in cold regions with high population density as it can offer attractive prices for thermal energy provision in these regions. Due to the adaptiveness of DHN to a wide variety of heat sources which brings energy diversification opportunities, it can reduce the dependence of heat sectors on fossil fuels, potentially contributing to the decarbonization of the future energy system.

2. Electrical HP

Electric HPs can transfer heat energy, mainly from air water or ground source to buildings, for space and hot water heating by consuming electricity. One unit of electricity can drive the transfer of multiple units of heat energy from the heat source to the heat sink (buildings). Figure 1.3 illustrates the operation of a HP. It should be stressed that HPs cannot generate, they actually upgrade heat which cannot be used directly.

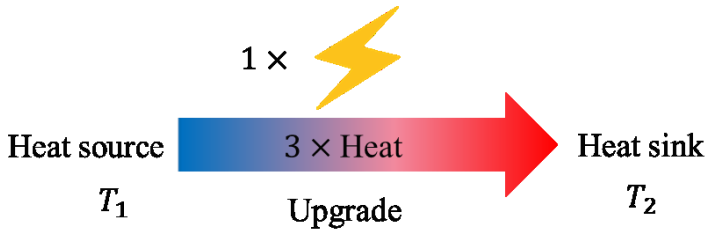

Figure 1.3– Operation of HP with COP of 3

The efficiency of HPs can be quantified by the coefficient of performance (COP) which is defined as the ratio of the useful heat supplied by the HP to the work required to drive the operation of the HP, as formulated in (1.1),

$$COP_t = \frac{h_t}{p_t} \tag{1.1}$$

where h_t is the heat output of HPs at time *t* while p_t is the electricity consumption at time *t*. COP is not a constant, it is relative to the difference between the flow temperature and heat source temperature. For air source HPs, COP can vary significantly in a day because it is very sensitive to the ambient temperature. However, for water source or ground source HPs, their COP is much more stable. Basically, the COP of ground-source HP is higher than that of air-source HP, but it is also more expensive.

Large-scale deployment of end-use HPs to substitute natural gas boilers remains to be regarded as one of the most effective options to fulfil the decarbonisation target of the heat sector. In this analysis, we only focus on the application of air-source HPs which is more suitable for large-scale deployment than ground-source HPs due to its improved affordability. However, growing concerns over high capital cost restricts the shift of heating technology from gas boilers to end-use HPs. Moreover, large-scale deployment of end-use HPs requires corresponding reinforcement of the distribution network, increasing the capital cost of HPs.

Similar to industrial-sized HPs applied in DHNs which have been mentioned above, end-use HPs can also provide considerable amount of flexibility to the electricity system [12, 13], particularly through short term interruption of operation and coordinated operation with end-use heat storage.

3. Hybrid Heating

Hybrid heating technologies allow consumers to combine different heating devices, e.g. electric HPs, natural gas boilers and resistance heaters. Through smart control, operation can be switched between these devices in accordance with their real-time operational efficiencies. Therefore, hybrid heating technologies, through combining new-invested HPs and existing natural gas boiler, can help alleviate the pressure of large investment in new heating equipment by allowing consumers to continue using gas boilers while spending less money on low-carbon heating technologies to meet the carbon target. A series of combinations of different heating technologies have been analysed in [13], manifesting the advantages of hybrid HP-Bs over the

other hybrid heating technologies. Considering the high penetration of natural gas boilers in the UK, it is tempting to apply hybrid HP-B on a large scale, as a solution to the concerns about the cost issues of ASHPs. Hybrid HP-Bs inherit all advantages from ASHP, while improving the cost-effectiveness of ASHPs by 1) delivering substantial savings in capital cost due to significant switch of investment from capital-intensive ASHPs to gas boilers while barely increasing the carbon emission; 2) reducing the costs of distribution networks reinforcement driven by large-scale deployment of ASHPs; 3) enhancing the load factor of ASHPs, considering that ASHPs only need to supply the base load while the peak load is covered by gas boilers.

4. Hydrogen

Hydrogen can potentially serve as a zero-carbon alternative to natural gas. Many countries are performing pilot schemes to investigate the economy of large-scale deployment of hydrogen plants as a promising measure for decarbonisation. As a gaseous fuel, hydrogen has the potential to adapt to most technologies that are based on natural gas while still providing a similar level of service. This means the transition from natural gas based technologies to hydrogen based technologies would barely incur hassle for customers given that very few appliances need to be replaced, thus driving significant savings from investment cost. Furthermore, hydrogen can potentially be injected into the existing gas networks and be delivered to consumers. At present, pure hydrogen cannot be directly transported through the existing gas networks due to the limitation of the material of pipelines, so only a small portion of hydrogen is mixed up with natural gas and injected into the gas networks, bringing limited benefits in terms of CO2 emission reduction. However, there are some research indicating that the existing distribution gas networks are suitable for the delivery of pure hydrogen [14], although further investigations need to be performed for a better understanding of the necessary conversion of networks related to the adaptation of hydrogen [15].

The most suitable method for industrial production of hydrogen is steam methane reforming (SMR), which accounts for about 95% of the world production. At high temperatures, water vapour reacts with methane to produce hydrogen and carbon monoxide, as presented in (1.2):

$$CH_4 + H_2O \rightarrow CO + 3H_2 \quad (1.2)$$

Extra hydrogen can be recovered through the reaction between carbon monoxide and water steam, with the presence of the catalyst of iron oxide, as shown in (1.3):

$$CO + H_2O \rightarrow CO_2 + H_2 \quad (1.3)$$

Since SMR produces CO2 as a by-product, its application in a low-carbon scenario would be highly dependent on the availability of CCS. After being captured (as a procedure of CCS), CO2 has to be transported to suitable sites for storage which are usually far away from the load centre, so the issues related to the delivery of CO2 have to be handled properly. CO2 network is a potential solution to transport large volume of CO2, but it requires considerable investment of infrastructure. If SMR plants are built close to the storage sites, hydrogen transmission infrastructures have to be considered, because existing high pressure gas transmission networks are likely unsuitable for hydrogen transmission due to material issues [16]. However, coastal SMR plant is convenient to transport the carbon emissions and seal them under the sea. On the contrary, if SMR plants build closing to the load centre, existing local gas distribution systems are potentially compatible with hydrogen use [17], but carbon transportation needs to be considered in this plan.

Another potential method for industrial bulk production of hydrogen is the electrolysis of water, which is more energy-intensive. Electrolysis uses surplus electricity from wind to produce only small fraction of hydrogen for its high capital investment costs, so they could be located near wind farms to provide more flexibility for electricity grid. The chemical equation is given as (1.4):

$$2H_2O \rightarrow 2H_2 + O_2 \quad (1.4)$$

The industrial production and transmission of hydrogen are investigated in [18] and [19]. Reference [20] presents a future hydrogen supply chain for UK transportation demand, which considers the hydrogen production, distribution and storage. A wind-electricity-hydrogen model, which integrated with electricity network to determine the optimal design and operation of hydrogen and electricity systems is developed in [21].

1.2 Research Questions

This thesis focuses on developing and proposing a multi-energy-system investment model to investigate the various decarbonisation strategies and the potential technology portfolio that can deliver a low-carbon future energy system in different scenarios. The Research Questions of this PhD thesis can be summarised as:

RQ1: How to model DHNs on the national level while considering the local distinctions of networks across different types of areas characterised with different geographical features and population density?

DHN is a potential heating method that can pave the pathway to a low-carbon future heat system. In order to identify the economically optimal heating technology portfolio to achieve the carbon reduction target, we cannot circumvent the potential contribution of DHNs. Therefore, it is necessary to comprehensively model the investment cost of DHNs infrastructure on the national level.

A lot of previous researches have been carried out to investigate the benefits that DHNs can bring to the energy system, especially considering how the coordinated operation of various heat sources in DHNs, such as CHP, TES, gas boilers, etc., improves the operational performance of the electricity system. However, most of the previous work has been focused on the operation of DHNs, how to quantify the investment cost of DHNs driven by different user penetrations and incorporate the DHN investment cost model into the national level multi-energy system investment optimisation problem remains to be an open question.

RQ2: How to evaluate the values of pre-heating through the inherent thermal storage of buildings? How to quantify the capability of pre-heating while considering the comfort requirement of customers?

While the advanced low-carbon technologies are crucial for decarbonising the future energy system, the improvement of energy management at the end-side is also an important means to achieve this goal. Pre-heating through the inherent thermal storage of buildings provides us the possibility to improve the building energy management, bringing significant economic benefits

to both the energy system and consumers. Therefore, it is important to model the process of pre-heating.

The dynamic thermal energy balancing process of pre-heating can be simplified as a storage model, however, it is not clear how much storage should be used to depict the capability of pre-heating given the thermal parameters of a building. Another concern is that the comfort requirement of consumers cannot be fully considered in a storage model. If we can find out the equivalent size of thermal storage to depict the capability of pre-heating while taken into account of the comfort requirement, then we can use the storage model to represent the functionality of pre-heating in more complex models.

RQ3: How to address the investment planning of the integrated electricity and heat system, while considering both operation and investment timescales with spatial granularity including local and national level infrastructure?

In order to identify the optimal decarbonisation strategy to achieve the carbon reduction target, it is imperative to assess the advantages and disadvantages of different heating technologies and identify the optimal design of the heating system on a national scale to maximize the economic benefits regarding both investment cost and operation cost. Additionally, as there is growing evidence that the interaction between electricity and heat systems will be important in facilitating cost effective transition to a lower carbon system by efficiently accommodating RES, it is necessary to quantify the benefits of the interactions across the multi-energy system. To achieve such, a comprehensive multi-energy system investment model would be essential.

Previous research on the investment and operation optimization of the multi-energy systems mostly focused on either the national or the local level infrastructure, with few investigating both. However, the decarbonisation through the adoption of different low-carbon technologies may potentially have significant impacts on the investments across different sectors, including local-level distribution networks and heat networks and national-level transmission network and generation. In order to research the whole-energy-system implications of various heating pathways towards the 2050 low-carbon energy system, it will be necessary to propose a modeling framework for the whole-system optimization of the combined electricity and heat

system while considering both operation and investment timescales with spatial granularity including local and national level infrastructure.

RQ4: How to reduce the computational burden of the integrated-electricity-and-heat-system investment-model, while ensuring that the results are near-optimal?

The complexity of investment planning models while taking into account a large number of operational conditions directly leads to dramatic computational burdens. Running the proposed integrated-electricity-and-heat-system investment-model over a whole year with hourly resolution is very time-consuming, so it is crucial to simplify the calculation so that this model can be solved within a reasonable time. One research direction to find the solution to this challenge is to reduce the size of input data by selecting a set of representative periods from the total number of operating snapshots. The selected periods have to retain most of the characteristics of the original data while guaranteeing that the investment decisions made are near-optimal.

Different algorithms have been investigated for the selection of representative periods. Most of the selection methods are performed according to the operational information in the input domain, which is convenient and straightforward for the implementation of the selection. However, since the investment decisions can be significantly non-linear to the input variables for the long-term investment planning problems, the input domain may not be the most appropriate domain to do the clustering. Additionally, few studies have considered the inter-temporal information in the operation constraints by performing representative-period selection to simplify the calculation of energy system planning problems. In this context, it is highly meaningful to investigate a more advanced method for the selection of representative days to further enhance the efficiency of calculation without compromising the accuracy.

1.3 Original Contributions

To address the research questions presented above, this PhD thesis makes the following original contributions to knowledge:

- Proposing a novel DHN investment model, through which the investment cost of DHNs driven by different user penetrations in different representative areas can be quantified and incorporated into the national-level multi-energy system investment model.
- Evaluating the economic value of pre-heating and quantifying the capability of the inherent storage of buildings under given thermal parameters of buildings.
- Presenting a novel combined electricity and heat system modeling framework considering both operation and investment timescales with spatial granularity including local and national level infrastructure. The proposed model simultaneously optimizes, for the first time, the investment in electricity generation (including conventional and low carbon generation), heating plants/appliances, DHNs, reinforcement of electricity transmission and distribution networks while considering system operation cost and taking into account frequency regulation and operating reserve requirements.
- Assessing the annual system cost coving multiple energy-sectors under the heating strategies of HP-only (electric HP is the only option of heat provision), hybrid HP-Bs and DHNs; analysing the impact of different heating strategies on the electricity system; and presenting the optimized portfolio of heating technologies to achieve the decarbonisation.
- Quantifying the benefits of the integrated planning of electricity and heat systems and demonstrating the impact on the technology mixes in both electricity and heat sectors; investigating the enhanced benefits TES and pre-heating bring to the multi-energy system; and demonstrating the major impact of the level of balancing service requirements on the value of the system integration.
- Proposing a novel cost-oriented method to select representative operating days for the multi-energy system investment planning problem with inter-temporal operating conditions considered. Performing a set of comprehensive analysis to demonstrate the superior performance of the proposed cost-oriented approach.

1.4 Thesis Structure

This thesis is constructed into seven chapters to address the proposed research questions, the summaries of which are presented as the following.

In Chapter 2, a novel linear District Heating Network (DHN) investment model is proposed by using the fractal-image-based algorithm. Through this model, the investment cost of DHNs driven by different user penetrations in different representative areas can be quantified and the DHN investment cost functions can be incorporated into the whole-system investment model proposed in Chapter 4 to optimize the penetration of DHNs. The operational principles of various heat sources in DHNs, including CHP plants, HPs and TESs are investigated, following which, the coordinated operation of these heat sources to increase the flexibility of the energy system is explored.

In Chapter 3, the value of pre-heating through the inherent building thermal storage is evaluated by using linear programming. The utilisation of the inherent thermal storage of buildings as an alternative way to reduce the operational costs while taking into account the comfort conditions in buildings is researched in a building energy management optimisation problem. In this problem, pre-heating through building thermal storage is enabled by allowing temperature variations within a pre-defined comfort zone. Through pre-heating, energy consumption can be managed in an economic-benefit-oriented way. By comparing the operational costs between the case where pre-heating is enabled and the case where additional TES is installed, the economic value of pre-heating can be evaluated while the capability of the inherent storage of buildings under given thermal parameters of buildings can be quantified.

In Chapter 4, a novel MILP modelling framework for the whole-system optimisation of the integrated heat and electricity systems, considering operation and investment timescales and covering both local and national level infrastructure. The proposed optimization model can simultaneously optimize, for the first time, the investment in electricity generation (including conventional and low carbon generation as well as CHP), heating devices, heat networks, reinforcement of electricity transmission and distribution networks while minimizing the system operation cost, taking into account frequency response and operating reserve requirements. The impact of integrated systems reducing system inertia on the frequency response requirement is explicitly modelled in the constraints. Carbon emission and security constraints are also included.

In Chapter 5, a set of comprehensive case studies are carried out to compare the economic advantages as well as the associated impacts on the electricity system under the full

deployments of ASHP, hybrid HP-Bs (ASHP and gas boilers) DHNs and hydrogen boilers by using the whole-system integrated electricity and heat system model. A series of sensitivity studies are also performed to illustrate the robustness of the heating strategies to the cost uncertainty of heating technologies. The optimized strategy for heat sector decarbonisation is demonstrated, providing an outline of the optimal deployment for different heating technologies in terms of their penetrations and deployed areas. The UK case study suggests the significant economic advantage of the hybrid HP-B over the other three heating technologies, while DHN may play an important role in urban areas under the optimized heat decarbonisation strategy. The results also clearly demonstrate the changes in the electricity side driven by the different decarbonisation strategies in the heating system.

In Chapter 6, the benefits through considering the interaction between electricity and heat systems at the planning stage are investigated, as the system integration will play an important role in facilitating the cost effective transition to a low carbon energy system with high penetration of renewable generation. The whole-system integrated electricity and heat system model is applied to optimize decarbonization strategies of the UK integrated electricity and heat system, while quantifying the benefits of the interactions across the whole multi-energy system, and revealing the trade-offs between portfolios of (a) low carbon generation technologies (renewable energy, nuclear, CCS) and (b) district heating systems based on heat networks and distributed heating based on end-use heating technologies. Overall, the proposed modeling demonstrates that the integration of the heat and electricity system (when compared with the decoupled approach) can bring significant benefits by increasing the investment in the heating infrastructure in order to enhance the system flexibility that in turn can deliver larger cost savings in the electricity system, thus meeting the carbon target at a lower whole-system cost.

In Chapter 7, a cost-oriented representative-day-selection approach that can significantly reduce the computational burden of the whole-system integrated electricity and heat system model is proposed. Through a series of case studies, we demonstrated the superior performance of the proposed cost-oriented representative-day-selection approach against the widely used input-based approach. The tested case studies are characterised with increased complexity so

that we can demonstrate the improved advantages of the objective-based approach over the traditional input-based approach.

In Chapter 8, a series of key conclusions of the thesis are summarised while the most significant areas for future work are identified.

Chapter 2 District Heating Network Modelling

DHNs, potentially supplied by various low-carbon heat sources, can provide an alternative opportunity to decarbonise the heat system. There are more than 2,000 DHNs in various sizes in the UK, supplying heat demand for over 200,000 dwellings and 2,000 commercial and public buildings. Large DHNs are typically deployed in highly populated cities and university campuses. DHNs currently supply under 2% of the heat demand in the UK, covering residential, public sectors and commercial buildings.

Considerable benefits can be achieved through DHNs, as they can feed on renewable energy sources, geothermal energy, or waste heat from industrial processes. Meanwhile, increased energy efficiency can also be achieved by using high efficiency forms of heating technologies. Additionally, DHNs can provide significant flexibility to the electricity system through coordinated operation of different heating technologies. However, the huge investment cost of DHNs significantly restricts its large scale deployment.

In order to identify the optimal heating strategy to achieve the 80% carbon reduction target, it is important to investigate the potential role that DHNs will play in the low-carbon energy system. In this context, this chapter proposes a linear DHN investment model, covering infrastructure on both local district and national level. This linear DHN investment model will be integrated into a whole-system investment model of multi-energy system in Chapter 4.

2.1 Investment Model of Heat Network

2.1.1 Fractal Model for Network Generation

An algorithm to generate electricity distribution networks based on the fractal image science has been developed by S.A Smith and has been carried out by J.P. Green [22] and D. Melovic

[23]. The application of heat networks in the UK is still limited, but the design and construction of heat network should be very similar to that of the electricity distribution network, because the topology of both networks are decided by the location of consumers and the roads in the map which illustrate possible paths of both networks. Therefore, the fractal-based algorithm can also be used to generate the topology of different heat networks. There are two main steps for this algorithm, the first one is to locate of different consumers, the number if which is known in a given area. The second one is to establish the connections of all the consumers the locations of which have been determined in the first step.

2.1.2 Consumer Location Determination

According to the fractal-based algorithm, the distribution of consumers should follow the principles in the economic attraction model, which is drawn from the fractal image science. In this model, the availability of land and supply are two main factors that influence the settlement of consumers. In desert areas, the price of supply is very high, so new settlement is less likely to occur in this kind of areas. In densely populated areas, the price of land is very high, people don't tend to settle down in this kind of areas neither. The areas which are neither populous nor deserted are more attractive to new consumer settlement. This principle is reflected in (2.1) as a descriptive illustration (note that it is not a specific function),

$$k:\begin{cases} < 1, & if\ t_1 < l < t_2 \\ > 1, & if\ l < t_1\ or\ l > t_2 \end{cases}, l, t_1, t_2 > 0 \tag{2.1}$$

The variable k is introduced here to represent the attractiveness factor of a certain area. If k <1, then the area is attractive to consumer settlement. If k >1, then the area is repulsive to consumer settlement. k is a function of the typical length l of a given network. Figure 2.1 illustrates a specific example of k function when t_1=5, t_2=40. The parameter t_1 and t_2 are related to the fractal dimension which is determined by the geographical characteristics (e.g., urban, rural) in a given area. Table 2.1 demonstrates the value of t_1 and t_2 for 4 typical consumer layout and the corresponding fractal dimensions.

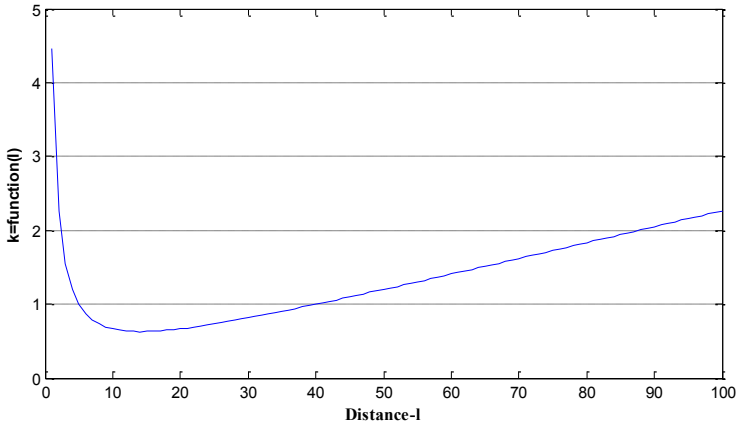

Figure 2.1– k function

Table 2.1 – t_1 and t_2 of typical consumer layout with its fractal dimensions

Type of area	t1	t2	Fractal dimension
Urban	0.01	5	1.81-1.98
Sub-urban	0.01	20	1.61-1.85
Sub-rural	0.01	50	1.44-1.67
rural	0.01	430	1.38-1.53

The procedures to determine the locations of different consumers in a network have been elaborated in [24]. In this section, we summarize the key points as follows:

1. Generate two initial nodes (x_1, y_1) and (x_2, y_2) randomly to form the primitive network (including 2 nodes and 1 branch). The centre of the primitive network is denoted as (x_c, y_c). All the other nodes will be integrated into the primitive network one by one.
2. The distance between node (x_1, y_1) and node (x_2, y_2) is denoted as l, which represents the typical length of the network. The angle between the initial branch and the horizontal direction is denoted as θ.
3. Generate a third node (x, y) randomly. Connect (x, y) with (x_c, y_c). Rotate (x, y) by the angle of θ counter-clockwise with (x_c, y_c) being the centre of the circle. (x, y) then becomes (x', y') after this transformation.

4. Calculate the attractiveness factor k basing on a chosen pair of t1 and t2. Contract or expand the vector $(x' - x_c, y' - y_c)$ with (x_c, y_c) fixed to get (x_3, y_3). (x_3, y_3) is the new generated node which is ready to integrate to the network.
5. The transformation process described in step 1 to step 4 can be expressed as Equation (2.2) and Figure 2.2,

$$\begin{bmatrix} x_3 \\ y_3 \end{bmatrix} = \begin{bmatrix} \cos\theta & -\sin\theta \\ \sin\theta & \cos\theta \end{bmatrix} \begin{bmatrix} k & 0 \\ 0 & k \end{bmatrix} \begin{bmatrix} x \\ y \end{bmatrix} + \begin{bmatrix} x_c \\ y_c \end{bmatrix} \tag{2.2}$$

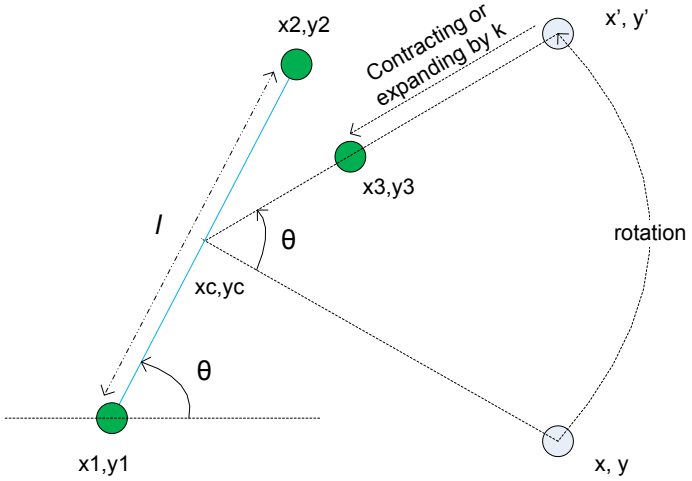

Figure 2.2– Transformation process of consumer location

The new primitive network includes 3 nodes and 3 potential branches (branches between every 2 nodes). Generate the next node randomly. Select the branch in the new primitive network which is closest to the new generated node, denote the centre of this branch as (x_c, y_c), repeat the procedures from step 1 to step 4.

Figure 2.3 shows the consumer distribution in urban areas and sub-urban areas respectively, based on the transformation procedures above.

It can be observed that in urban areas nodes tend to be evenly scattered, while in sub-rural areas nodes are scattered in cluster. This is because the gap between t_1 and t_2 in sub-rural areas is wider than that in urban areas, which makes new generated nodes more likely to be attracted to the existing network in sub-rural areas than in urban areas. Once a new generated node is repulsed by the existing network in sub-rural areas, it will be located further away from the

existing networking than that in urban areas. So the consumer distribution in sub-rural areas shows a clustered pattern. In urban areas, the possibility of a new node being attracted and being repulsed are close, so it forms an relatively even distribution.

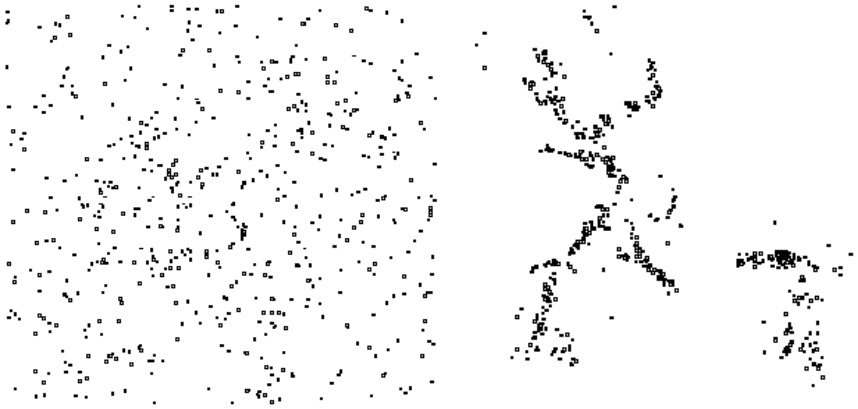

Figure 2.3– Consumer distribution in urban and sub-rural areas

2.1.3 Connection of Consumers

Basically, there are two situations when connecting a new node to the existing network, as shown in Figure 2.4. In situation (a), a T junction is constructed while in situation (b) an obtuse angle is formed. In each situation, the basic principle of connecting a new node to the existing network is to ensure that the length of the new branch is minimum. The ratio of the number of T junctions and the number of all consumers in the network is defined as branching rate [25].

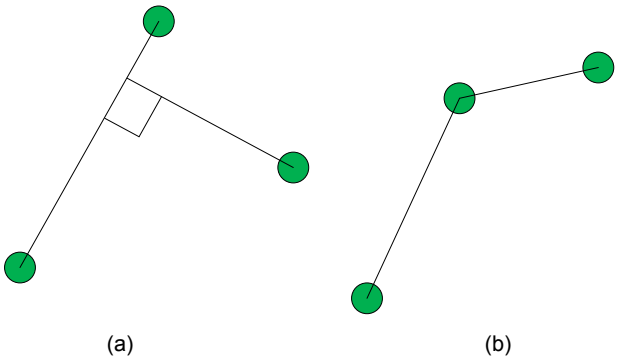

Figure 2.4– Situations of node connection

According to the fractal-based algorithm, there are two strategies to connect new consumers to the existing network.

1. The next node to be connected to the existing network is selected randomly. It turns out that the network formed in this way has a higher branching rate.
2. The next node to be connected to the existing network is the one which is closest to the last connected node. It turns out that the network generated in this way has a lower branching rate.

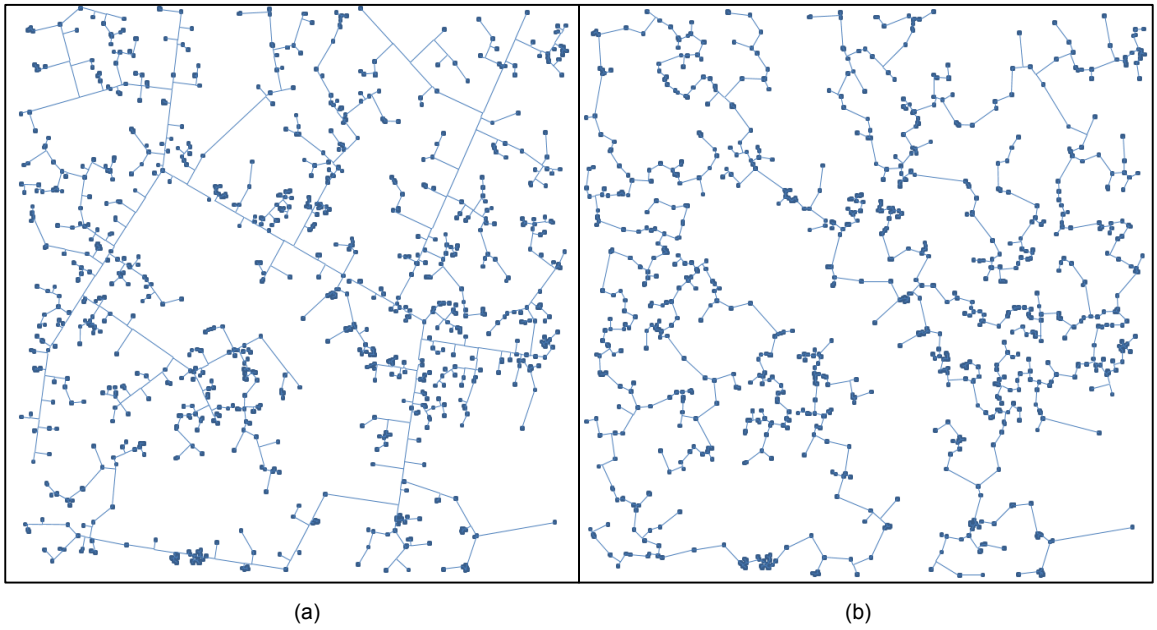

Figure 2.5– Consumer connection by different strategies

By using the first strategy only, the branching rate of the network is around 60%, as shown in Figure 2.5 (a), while by using the second strategy only, the branching rate is about 20%, as shown in Figure 2.5 (b). The branching rate of realistic networks are usually between 20% and 60%. A network with any branching rate between 20% and 60% can be generated by using both strategies together. By using the fractal-based algorithm, heat networks with different population density can be generated.

2.1.4 Heat Network Investment Model

There are two factors that can impact the capital cost of DHNs, including (i) the length of the pipelines, which is determined by the layout of consumers, and (ii) the size of the pipelines, which depends on the peak heat demand. At the planning stage, it is assumed that the pipelines of DHNs should be designed with adequate redundancy for the sake of potential expansion in the future, therefore, the length of pipelines becomes the key factor that drives the capital cost of DHNs. When the layout of consumers in a district has been determined, the potential capital cost of DHN in that district is also determined and will not be influenced by the variation of heat demand. The fractal-based algorithm introduced in 2.1.1 can calculate the length of heat networks given the relative parameters. Figure 2.6 shows the process to calculate the investment cost of heat networks in a given area with the help of this algorithm.

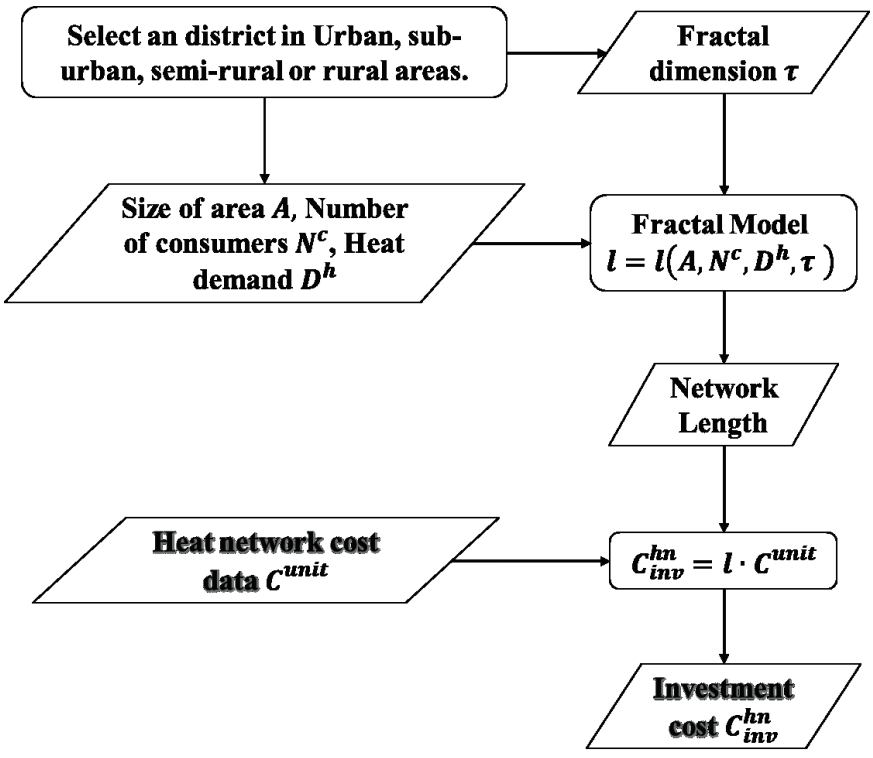

Figure 2.6– Flow chart of the calculation of heat network investment cost

The required input data in Figure 2.6 can be obtained by using National Heat Map. The National Heat Map is a free online tool which was commissioned by Department for Business, Energy & Industrial Strategy (BEIS) - and created by CSE in 2010. This tool can provide heat demand

information and heat consuming sector information of all areas in England. The purpose of National Heat Map is to support the planning and deployment of local low-carbon energy schemes in England through open accessible data and high-resolution maps of heat demand in different area. The uniqueness of the National Heat Map is characterised by its detailed address-level modelling of demand data and the tools for analysing the data. It combined a very detailed geographic model of energy use with a range of user-friendly visualisation and reporting tools, providing sophisticated GIS functionality to non-technical users via a standard web-browser [26]. As shown in Figure 2.7. With the help of the National Heat Map, we can access the statistics of the heat density (related to fractal dimension), the size of area and the number of consumers of a selected region, in respect with different sectors. These data can be applied as inputs of the heat network investment model.

Show 25 entries
Filter

Area: 106,000,000m²

Sector	Heat Demand (kWh)	Number of Addresses	Heat Density (kWh/m2)
Commercial Offices	1,270,000,000	24,045	12.0
Education	213,000,000	1,010	2.02
Government Buildings	278,000,000	394	2.64
Health	242,000,000	1,673	2.29
Hotels	450,000,000	3,727	4.26
Industrial	571,000,000	1,275	5.41
Other	46,400,000	847	0.439
Postal	15,400,000	883	0.146
Recreational	211,000,000	3,047	2.00
Residential	4,400,000,000	477,840	41.7
Retail	403,000,000	17,523	3.82
Science	1,650,000	46	0.0157
Transport	300,000,000	5,301	2.84
Total	**8,400,000,000**	**537,611**	**79.6**

Figure 2.7– National Heat Map and the data involved

Four representative districts covering urban, sub-urban, semi-rural and rural areas are selected on the National Heat Map and their corresponding heat networks are generated by using the fractal-based algorithm. Detailed parameters of these representative districts and the generated topology of the heat network that can be potentially deployed in these districts are given in Appendix A.1, based on the National Heat Map and the fractal model, respectively. Based on the data provided by DECC [27], the cost assumptions of the selected representative networks are presented in Appendix A.1.

The whole Great Britain (GB) can be represented by a combination of the representative areas. The number of each representative area are optimized to minimize the total error of area, population and heat demand between realistic data and calculated data, as in Equation (2.3),

$$\min_{N_i^{ra}} \left(\frac{\left| \sum_{i=1}^{R} N_i^{ra} \cdot A_i - A^{tot} \right|}{A^{tot}} + \frac{\left| \sum_{i=1}^{R} N_i^{ra} \cdot P_i - P^{tot} \right|}{P^{tot}} + \frac{\left| \sum_{i=1}^{R} N_i^{ra} \cdot D_i^h - D^{h,tot} \right|}{D^{h,tot}} \right) \quad (2.3)$$

where N^{ra} denotes the number of each representative areas; A denotes the area of representative areas; A^{tot} denotes the total geographic size of area of the GB; P denotes the population of representative areas; P^{tot} denotes the total population of the GB; D^h is the annual heat demand of representative areas; $D^{h,tot}$ is the annual total heat demand of the GB; R is the set of representative districts.

In summary, the investment cost of DHNs is basically decided by the length of pipework and the geographic features (e.g. urban, rural areas) in the deployed district. In this chapter, a fractal-based algorithm is applied to calculate the length of representative heat networks thus to determine the investment cost. Equation (2.4) presents the function of DHN investment cost,

$$C_{inv,i}^{hn}(\cdot) = \alpha_i^{hn} \cdot N_i^{ra} \cdot C_i^{unit} \cdot l\left(A_i, N_i^c, D_i^h, \tau_i\right) \quad \forall i \in R \quad (2.4)$$

Given that the investment cost of DHNs is dramatically influenced by the heat density in the supplied district, all GB regions are categorized into 4 different representative districts in this model in accordance with their heat density, including urban, sub-urban, rural and semi-rural areas. By using the National Heat Map, the size of area of representative districts, the number of consumers and annual heat demand within the representative districts can be accessed which are then provided as inputs into the fractal-based algorithm, thus the length of representative networks with different geographic features can be calculated. The whole GB area is then represented as a linear combination of representative areas (the coefficient of which is denoted as N^{ra}), with the errors of total consumer numbers, annual heat demand, and size of geographical areas minimized. By applying this approach, we can quantify the investment cost of DHNs driven by different user penetrations in different representative areas (α^{hn}) and

incorporate the linear DHN investment cost functions into the whole system investment model to optimize the penetration of DHNs.

2.2 Operation of District Heating

2.2.1 Heat Sources of District Heating

***Combined Heat and Power (CHP)*:**

CHP, also known as cogeneration, is a technology that can generate electricity and use the exhaust heat for heating process such as space heating and hot water heating. It has been proved to be a highly efficient way to convert primary energy into useful energy. CHP can be driven by both traditional fossil fuels (coal, gas and oil) and low carbon sources such as biomass and geothermal energy. Therefore, it is also seen as a promising way to decarbonise the energy system to meet the 2050 carbon reduction target [28]. Basically, three types of CHP are widely used for DHNs.

1. Gas-turbine-based CHP

Gas turbines can generate exhaust gases which are at 400-500°C [29]. These exhaust gases will enter a heat recovery boiler to heat water which will be injected into heat networks to meet heat demand. Gas turbines sacrifice some efficiency of electricity generation to upgrade the heat contained in exhaust gases so as to increase the overall energy efficiency. The ratio of heat to power for gas turbines is usually fixed, as expressed in Equation (2.5),

$$h_t^{CHP} = \lambda \cdot p_t^{CHP}, \forall t \in T \tag{2.5}$$

where p_t^{CHP} is the electricity generation at time t; h_t^{CHP} is the heat generation at time t; λ is ratio of heat to electricity for gas-turbine-based CHP; T is the set of time steps.

2. Steam-turbine-based CHP

Steam turbine CHP is characterised with increased suitability for the cold areas where heat demand accounts for the major part of the total energy consumption in winters. The amount of

heat generation depends on how far the steam can go through the turbine and the amount of steam which is extracted from turbine for heat generation [29].

In accordance with the operating modes, steam turbines can be categorised into back-pressure turbines and condensing turbines. For the latter category, a condenser is applied at the exit of the turbine to maximise the power output by expanding exhaust steam down to a vacuum which can improve the efficiency of power generation.

Figure 2.8 illustrates the operating area (known as the iron diagram) for a steam turbine CHP unit [30]. The upper and lower boundaries represent the maximum and minimum boiler load while the right boundary represents the back pressure operation mode. In the back pressure mode, all heat is extracted from the extraction point to maximize the heat generation under a certain fuel feeding rate.

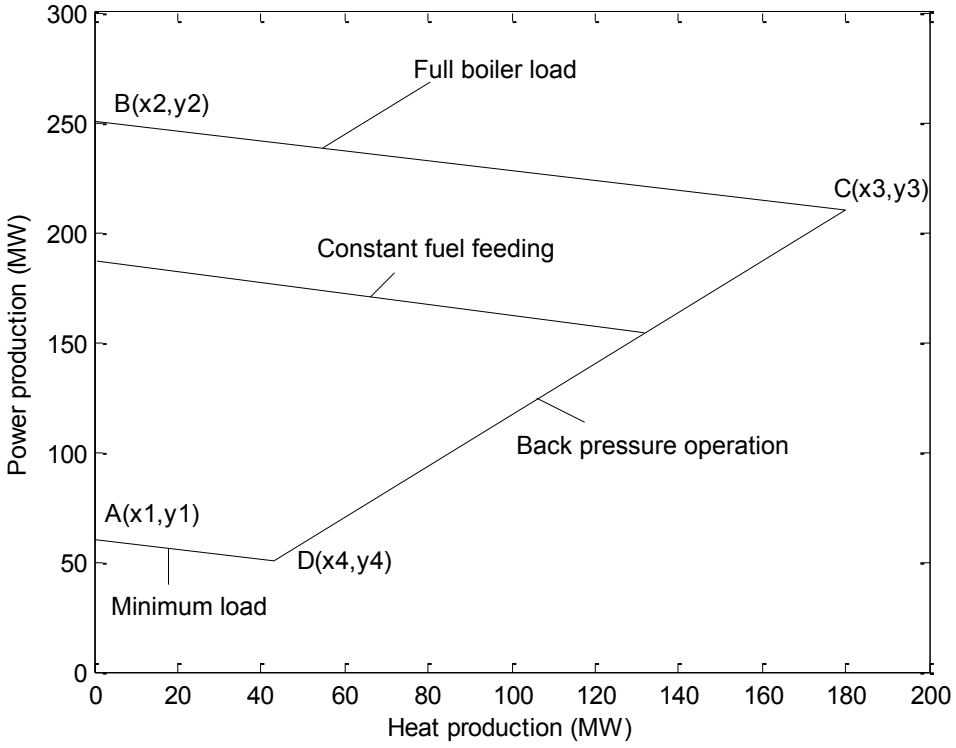

Figure 2.8– Operation area of a CHP unit

Point B shows that at the maximum fuel load, the power generation can reach 250MW, with no useful heat output. Keeping the same rate of fuel feeding, if the heat production is increased,

which means more steam is extracted from the extraction point, the power output will decrease correspondingly, the ratio of the change of heat and electricity is denoted as z. Eventually, the heat output reaches a maximum level because of the capacity limit of the heat exchanger. Keeping heat output maximum and reducing the boiler load, the operation point will move along the 'back pressure operation' line and finally reach point D. The slope of the 'back pressure operation' line is demoted as λ. At point D, if less heat is extracted from the low pressure turbine, the heat output will reduce while the power output will increase. When no heat is extracted, the operation point reaches A. From point A to point B, more fuel is needed.

A line paralleled with the upper and lower limit line represents the set of operating points under a certain fuel feeding rate, as shown in Figure 2.8. It demonstrates that in a constant fuel feeding rate, by adjusting the amount of heat extracted, how the operation point will move. So by controlling the fuel feeding rate, any point within the iron diagram can be reached [31].

3. Combined-cycle-gas-turbine-based CHP (CCGT CHP)

CCGT CHP is the most widely used type of CHP, as exhaust heat in higher grade can be acquired at the exit of the gas turbine, which can generate steam with higher pressure in the heat recovery boiler. Compared to steam turbines, more fuel is used for electricity generation in CCGT, because no heat is generated in gas turbine cycle. Therefore, CCGT is more suitable for areas where electricity demand is higher than heat demand.

Both steam turbine CHP and CCGT CHP extract heat from steam turbine, so they follow a similar operating principle. Their operational area is constrained by 4 boundaries, as illustrated in Figure 2.8, which is expressed in (2.6) and (2.7),

$$\left(\underline{p}^{CHP} - \frac{h_t^{CHP}}{z}\right) \leq p_t^{CHP} \leq \left(\overline{p}^{CHP} - \frac{h_t^{CHP}}{z}\right), \forall t \in T \tag{2.6}$$

$$0 \leq h_t^{CHP} \leq \lambda \cdot p_t^{CHP}, \forall t \in T \tag{2.7}$$

where $\overline{p}^{CHP}$ is the maximum electricity output; p^{CHP} is the electricity generation at time t; $\underline{p}^{CHP}$ is the minimum electricity output; h^{CHP} is the heat generation at time t; z is the conversion rate from electricity to heat for CHP plants; while λ is the maximum ratio of heat to electricity for

CHP plants. Note that the λ in (2.7) represents the same physical relationship between electricity and heat output as in (2.5).

***Heat Pump*:**

The industrial-sized HP is another favourable heat source for DHNs, due to its high efficiency of converting electric energy into thermal energy. Additionally, HP has the potential to provide low carbon heat with the decarbonisation of the electricity network.

For different district heating schemes, the temperature of supply water may vary significantly, as a consequence, the COP of HPs can be very different. This is because the temperature difference between the heat source (typically water source or ground source for industrial-sized HPs) and the heat sink (supply water) has a considerable impact on the COP of HPs. The lower the temperature of supply water is, the higher the COP of HPs becomes. In order to improve the energy efficiency while meeting the comfort requirement, underfloor heating system can be applied to work together with low temperature heat networks, due to its improve efficiency of thermal energy delivery.

***Thermal Energy Storage*:**

Hot-water-tank is the most commonly used TES for DHNs, which can provide flexibility for DHNs so as to reduce the infrastructure investment cost [32, 33]. Additionally, TES has the potential to provide flexibility to electricity network through coordinated operation with CHPs and HPs [34]. The mathematical model of TES can be formulated as Equation (2.8) – (2.12),

$$s_t^{out} \leq \overline{s}, \forall t \in T \tag{2.8}$$

$$s_t^{in} \leq \overline{s}, \forall t \in T \tag{2.9}$$

$$ec_t \leq \overline{s} \cdot \tau^s, \forall t \in T \tag{2.10}$$

$$ec_1 \leq ec_0 \cdot \eta^s + s_1^{in} \cdot \eta^{in} - \frac{s_1^{out}}{\eta^{out}} \tag{2.11}$$

$$ec_t \leq ec_{t-1} \cdot \eta^s + s_t^{in} \cdot \eta^{in} - \frac{s_t^{out}}{\eta^{out}}, \forall t \in T \tag{2.12}$$

where s^{out}/s^{in} represents the discharging/charging rate at time t; $\overline{s}$ represents the power rating of TES (for both charging and discharging); ec denotes the energy content stored in the water tank at time t; τ^s denotes the duration that storage can be fully charged/discharged from being empty at the rated power; ec_0 denotes the initial energy content stored in the tank; η^s denotes the static efficiency of storage; while η^{in}/η^{out} denotes the efficiency of energy charging/discharging.

2.2.2 Coordinated operation of CHP, HP and TES in DHN

Large-scale deployment of DHNs will introduce remarkable interactions between the electricity system and the heat system. The absence of the coordination between different components in DHNs would lead to inefficient operation in both electricity and heat system. As the most important heat source in DHNs, the operation of CHP is restricted by the iron diagram illustrated in Figure 2.8. In the case where the penetration of variable renewable energy sources is high, improved flexibility of the CHP operation is required to help alleviate the curtailment of RES by adjusting the electricity-to-heat ratio within a wider range. This section investigates the potential of increased flexibility in the operation of CHP through the coordinated operation with HP and TES.

HPs can generate heat by consuming electricity. When heat demand increases while electricity decreases, HPs can convert surplus electricity into heat, extending the lower bound and right bound of the iron diagram. The extended operating area of DHNs under coordinated operation of CHP and HP is constrained by (2.6) – (2.7) and (2.13) – (2.14),

$$p_t^{exd} \geq p_t^{CHP} - \overline{p}^{HP}, \forall t \in T \tag{2.13}$$

$$h_t^{exd} = h_t^{CHP} + COP^{HP} \cdot p_t^{HP} \leq h_t^{CHP} + COP^{HP} \cdot \overline{p}^{HP}, \forall t \in T \tag{2.14}$$

where p^{exd} and h^{exd} denote the extended electricity and heat output through coordinated operation of different components in DHNs; p^{CHP} and h^{CHP} denote electricity and heat output

of CHP; p^{HP} denotes electricity consumption of HPs; $\overline{p}^{HP}$ denotes the electric power rating of HPs; and COP^{HP} denotes the coefficient of performance of HPs.

Figure 2.9 illustrates the extended operating area of DHNs under coordinated operation of CHP and HP, compared to the original operating area of CHP (which is unified, the maximum electricity output of CHP is 1 p.u.). It is assumed that the electric power rating of HP is 0.1 p.u. and its COP is 2.5.

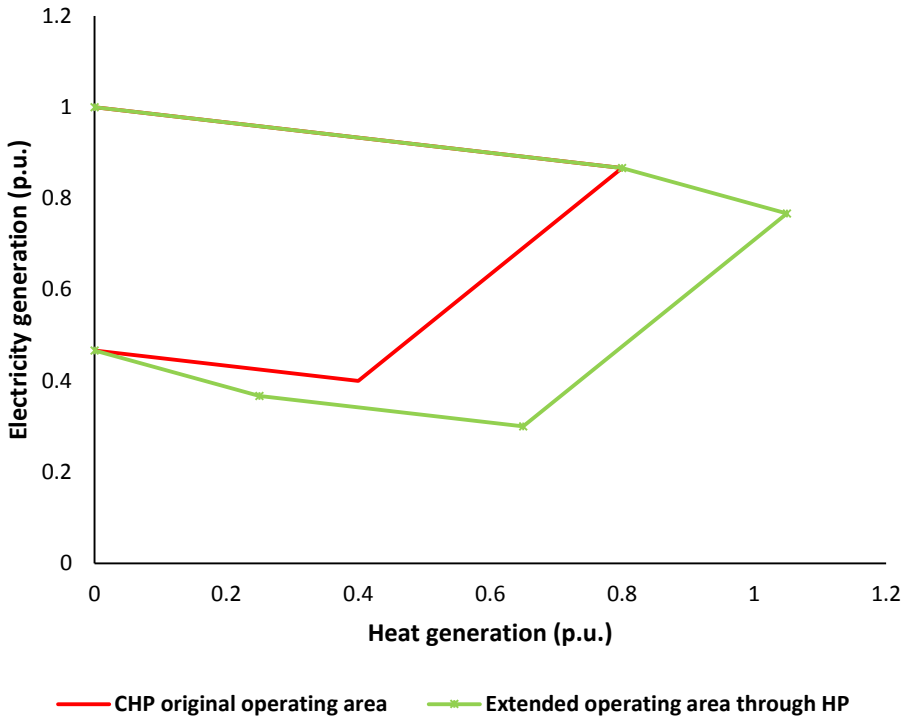

Figure 2.9– CHP working with HP

The TES can charge surplus heat generated by CHP and discharge heat when heat demand increases. Therefore, it can extend the range of heat generation for the all the operating points on the bound. The extended operating area of DHNs under coordinated operation of CHP and TES is constrained by (2.6) – (2.7) and (2.15) – (2.16),

$$h_t^{CHP} - \overline{s} \le h_t^{exd} = h_t^{CHP} + s_t^{out} - s_t^{in} \le h_t^{CHP} + \overline{s}, \forall t \in T \tag{2.15}$$

$$p_t^{exd} = p_t^{CHP}, \forall t \in T \tag{2.16}$$

where s^{in} and s^{out} denote charging and discharging rate of TES; and $\overline{s}$ denotes the power rating of TES.

Figure 2.10 illustrates the extended operating area of DHNs under coordinated operation of CHP and TES, compared to the original operating area of CHP. It is assumed that the power rating of TES is 0.2 p.u. for both charging and discharging.

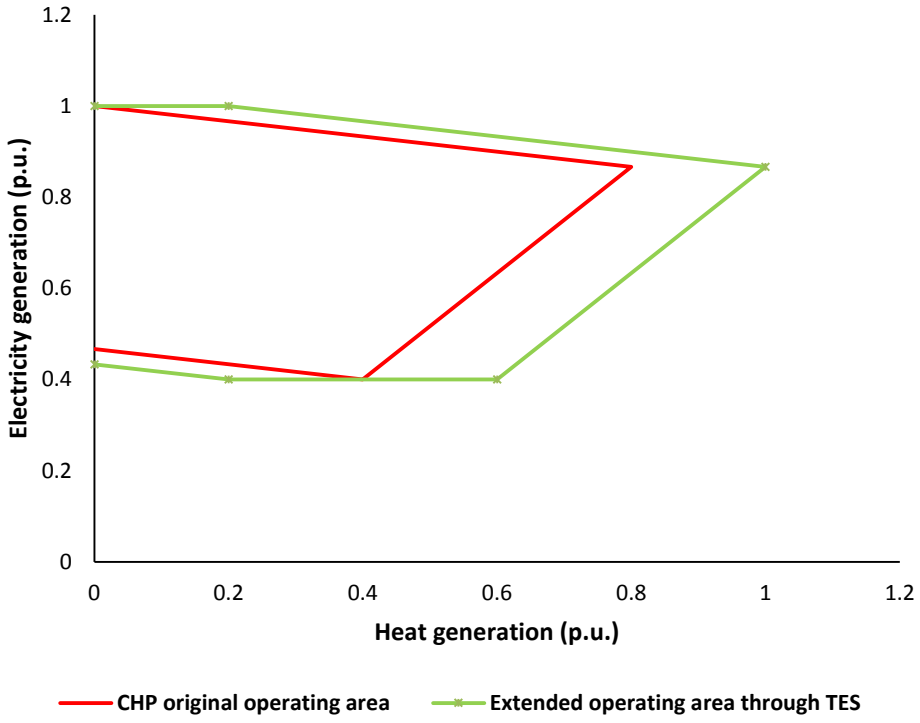

Figure 2.10– CHP working with TES

When both HP and TES support the operation of CHP, the extended operating area of DHNs, as constrained by (2.6) – (2.7) and (2.17) – (2.18), is enhanced by the combined contribution of HP and TES,

$$p_t^{exd} = p_t^{CHP} - p_t^{HP} \geq p_t^{CHP} - \overline{p}^{HP}, \forall t \in T \tag{2.17}$$

$$h_t^{CHP} + COP^{HP} \cdot \overline{p}^{HP} - \overline{s} \leq h_t^{exd} \leq h_t^{CHP} + COP^{HP} \cdot \overline{p}^{HP} + \overline{s}, \forall t \in T \tag{2.18}$$

Figure 2.11 illustrates the extended operating area of DHNs under coordinated operation of CHP, HP and TES, compared to the original operating area of CHP. The same assumptions are made as the cases demonstrated in Figure 2.10 and Figure 2.11.

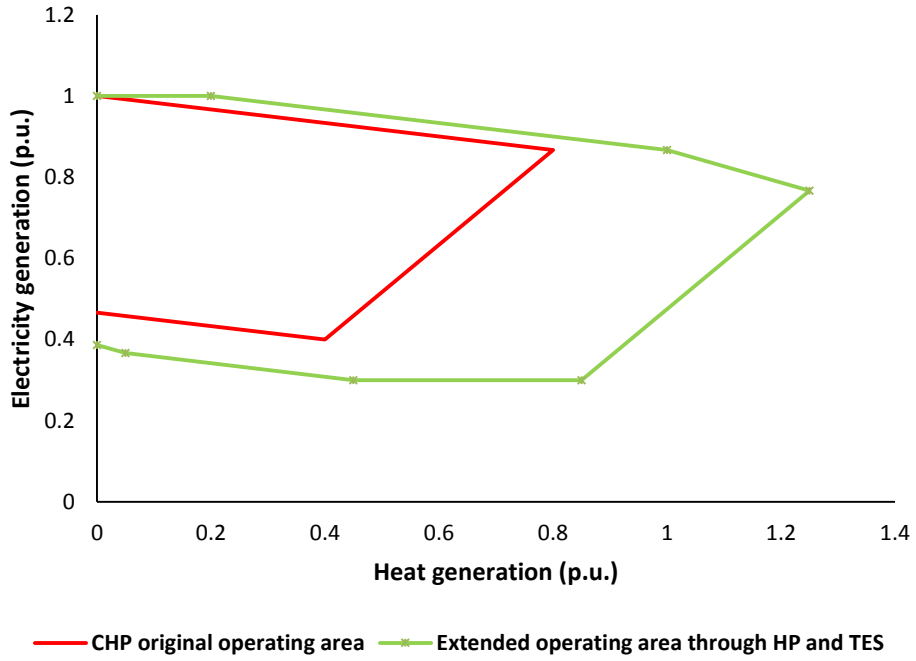

Figure 2.11– CHP working with HP and TES

From Figure 2.9 to Figure 2.11, we can see that HP and TES can both enhance the flexibility of CHP operation. For HP, all operating points in the extended operating area can be theoretically reached unconditionally. By contrast, the reachability of the points between the extended operating area through TES and the original operating area of CHP depends on the state of charge of TES. Specifically, the boundary of the extended area can be reached only when the stored heat in TES is enough to enable the maximum discharging or the headroom of TES is enough to enable the maximum charging.

2.3 Conclusions of the Chapter

DHNs is a potential heating method that can pave the pathway to a low-carbon future heat system. In order to identify the economically optimal heating technology portfolio to achieve the carbon reduction target, we cannot circumvent the potential contribution of DHNs.

Therefore, it is necessary to comprehensively model the investment cost of DHNs infrastructure on the national level.

This chapter proposes a novel linear DHN investment model by using the fractal-image-based algorithm, which can generate the potential topologies of DHN in different types of areas.

The length of pipelines, which determines the cost of excavation and the installation of pipes is the key factor that drives the capital cost of DHNs. When the layout of consumers in a district has been determined, the length of pipelines can be calculated with the help of the fractal-based algorithm, therefore, the potential capital cost of DHN in that district is also determined and will not be influenced by the variation of heat demand.

Given that the investment cost of DHNs is dramatically influenced by the heat density in the supplied district, all GB regions are categorized into 4 different representative districts in this model in accordance with their heat density, including urban, sub-urban, rural and semi-rural areas. By using the National Heat Map, the size of area of representative districts, the number of consumers and annual heat demand within the representative districts can be accessed which are then provided as inputs into the fractal-based algorithm, thus the length of representative networks with different geographic features can be calculated. The whole GB area is then represented as a linear combination of representative areas, with the errors of total consumer numbers, annual heat demand, and size of geographical areas minimized. By applying this approach, we can quantify the investment cost of DHNs driven by different user penetrations in different representative areas and incorporate the DHN investment cost functions into the whole system investment model to optimize the penetration of DHNs.

The operational principles of various heat sources in DHNs, including CHP plants, HPs and TESs are also investigated, following which, the coordinated operation of these heat sources to increase the flexibility of the energy system is explored. The results demonstrate that the synergy effects brought by integrating various heat sources can significantly improve the flexibility of DHN operation.

Chapter 3 Modeling of Flexibility through Building Thermal Characteristics

The application of advanced low-carbon heating technologies is crucial for paving the pathway to a decarbonised future heat system. For this purpose, the electrification of heat will play an important role in this background. However, the transition from the existing fossil-fuel-dominated system to a highly-electrified low-carbon system would require considerable investment in the assets and effective flexibility measures to support the electricity system operating properly. In this context, the building thermal characteristics can provide us an alternative perspective to alleviate the burden of new investment and provide flexibility to the electricity system. The improvement of the energy efficiency through the thermal characteristics of buildings can bring significant economic benefits to both the energy system and consumers [35].

Due to the inherent storage of buildings [36, 37], pre-heating can be taken advantaged to shift electricity demands and provide ancillary services according to the energy price signals, thus providing an opportunity to improve the efficiency of energy management of buildings and provide flexibility of the electricity system.

The dynamic thermal energy balancing process of pre-heating can be simplified as a storage model, however, it is not clear how much storage should be used to depict the capability of pre-heating given the thermal parameters of a building. Another concern is that the comfort requirement of consumers cannot be fully considered in a storage model. If we can find out the equivalent size of thermal storage to depict the capability of pre-heating while taking into account of the comfort requirement, then we can use the storage model to represent the functionality of pre-heating in more complex models.

This chapter investigates the utilisation of the inherent thermal storage of buildings as an alternative way to reduce the operational costs while taking into account the comfort conditions

in buildings. Pre-heating through building thermal storage is enabled by allowing temperature variations within a pre-defined comfort zone [38, 39]. Through pre-heating, energy consumption can be managed in an economic-benefit-oriented way [37, 40, 41]. By comparing the operational costs between the case where pre-heating is enabled and the case where additional TES is installed, we can evaluate the economic value of pre-heating and quantify the capability of the inherent storage of buildings under given thermal parameters of buildings. Linear programming is utilised to analyse the dynamic process of pre-heating and TES operation.

3.1 Thermal Dynamic Model of Buildings

As thermal energy can be stored in the air and the building structures, buildings are characterised with inherent thermal energy storage, thereby reducing the operational costs without the requirement of additional hot water tanks as TES.

The process of heat transfer is time dependent, the rate of thermal energy transferring into the building through the surface (e.g., walls, windows and roofs, etc.) equals the increase rate of the thermal energy inside the building. Figure 3.1 illustrates an equivalent electrical circuit to extract the key thermal characteristics of buildings. The air mass inside the building is equivalent to a thermal capacity C due to its intrinsic thermal energy storage, while the building envelop is seen as a quick response thermal conductance K to consider the heat exchange between the inside and outside of the building. The dynamic variation of the internal temperature T_i is determined by the thermal energy gains Q and the outside temperature T_o, as formulated in Equation (3.1) - (3.3),

$$C\frac{dT_i}{dt} + (T_i - T_o)K - Q = 0 \tag{3.1}$$

$$C = \rho \cdot C_p \cdot V \tag{3.2}$$

$$K = U \cdot A \tag{3.3}$$

where ρ denotes the density of the air in the building (kg/m^3), C_p denotes the specific heat of the air (J/kg·K), V represents the volume of the building (m^3), Q represents the heat supply (W), U is the heat transfer coefficient (U-value) of the building envelop (W/m^2·K), A is the surface area of the building envelope (m^2). Note that the time constant in this equivalent electrical circuit is $\tau = \frac{C}{K} = \frac{\rho C_p V}{hA}$.

It should be stressed that the internal temperature of the building is considered to be spatially uniform during the transient process, the temperature gradients inside the building are assumed to be negligible.

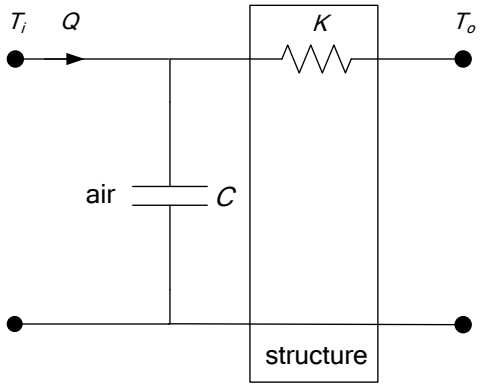

Figure 3.1– Equivalent electrical circuit of building thermal features

The thermal dynamic model of buildings shown in Figure 3.1 is simplified as a first-order model, which only considers the inherent storage of the internal air. Actually, the building structure (e.g., walls, floors) can also store thermal energy, therefore, a second-order model considering both the equivalent thermal capacity of air and building structure would be more precise. Considering the simplicity of the first-order thermal dynamic model and the fact that it has already been widely used in the past works (e.g., [42-44]) and proved to be accurate enough, we also adopt this simplified model to solve the energy management optimization problem in this section.

In order to integrate the thermal dynamic model into the energy management optimisation model under finite-length time intervals, the discretisation of the thermal energy balance

equation is imperative. By substituting dT_i/dt with $\Delta T_i/\Delta t$, Equation (3.1) can be re-written as the finite difference equation (3.4),

$$C\frac{\Delta T_i}{\Delta t} + (T_i - T_o)K - Q = 0 \tag{3.4}$$

According to [45], three basic approaches are commonly used to discretise differential equations into finite difference equations, namely Forward Euler, Backward Euler and Crank-Nicolson approach. In this section, we adopt the Forward Euler approach, considering its good performance for the first-order thermal dynamic model, the transformed finite difference equation is shown in (3.5),

$$C \cdot \left(T_{i,t+1} - T_{i,t}\right) + \Delta t \cdot \left[\left(T_{i,t} - T_{o,t}\right)K - Q\right] = 0, t, t+1 \in T \tag{3.5}$$

where T is the set of the whole time horizon. For second-order thermal dynamic model, the Crank-Nicolson approach is more suitable to obtain a higher accuracy, as demonstrated in [46].

3.2 Optimization of Energy Management in Buildings

3.2.1 Approach to Quantifying the Inherent Storage of Buildings

In this section, we adopt the thermal dynamic model of buildings in an energy management problem to evaluate the values of the inherent storage of buildings. As illustrated in Figure 3.2, the considered building is equipped with HVAC appliances supplying thermal energy (e.g., heat or cold) to keep the internal temperature within a desired zone. PV panels are deployed on the roof of the building to supply electricity load (i.e., HVAC-irrelevant load and HVAC-based load) within the building, or sell electricity to the grid. In this energy management problem, we consider the consumer can simultaneously provide multiple categories of demand response services. In the following, we consider two distinct categories of services [47]. The first category of service is energy arbitrage, which enables the consumers to arrange their energy consumption in response to the fluctuations of energy price for different time steps within a day. The second category of service is frequency response services. For the latter, we merely

take into account the frequency support for severe events, which do not occur on a frequent basis, in contrast to real-time frequency response services. Four types of frequency response services are considered in this section, namely primary response service, secondary response service, high-frequency response service, and flexible response service. According to the National Grid practice, primary and high-frequency response services require a decrease and increase in electricity consumption for a duration up to 30 seconds, respectively, while the secondary response service requires a constant consumption decrease for up to 30 minutes. The flexible response service is almost the same as the secondary response service, expect that it can only be called upon during specific pre-defined time.

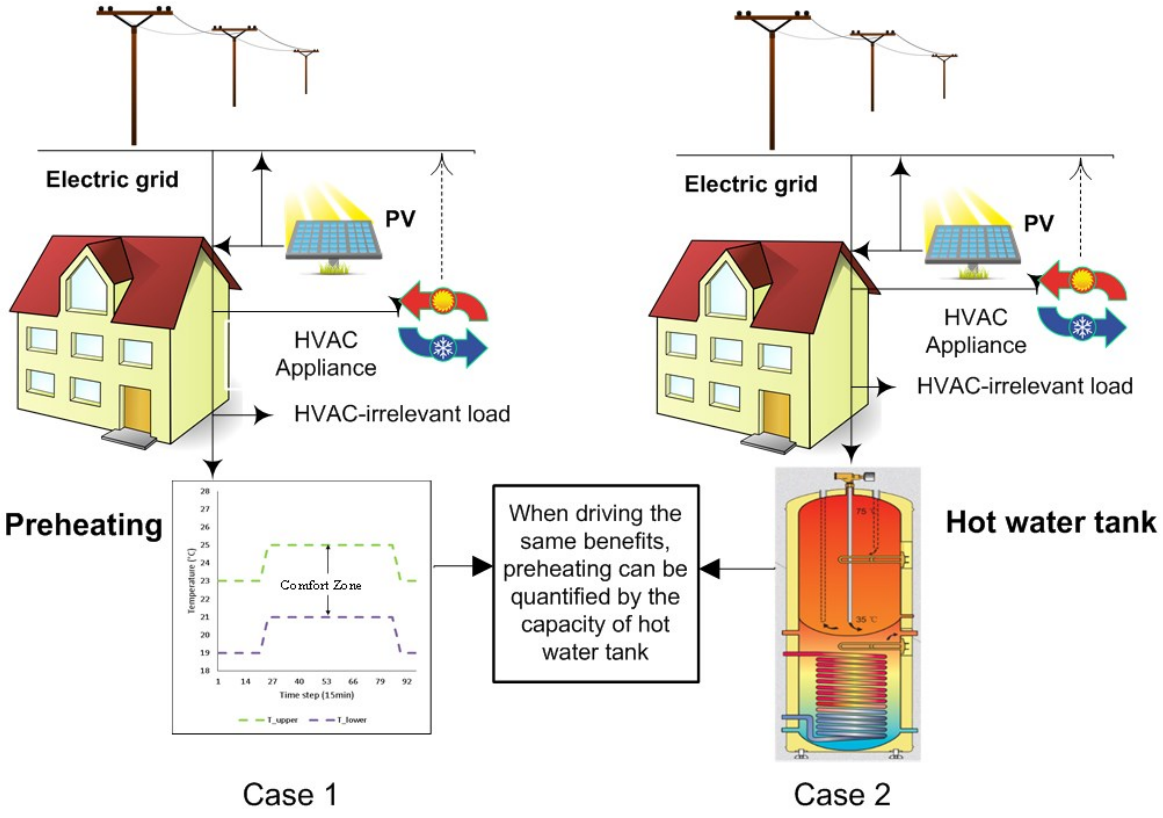

Figure 3.2– Quantifying the potential of pre-heating by comparing with hot water tanks

In order to quantify the values of pre-heating through the inherent thermal storage of the building, two cases are investigated.

In Case 1, pre-heating is enabled in the building by allowing a comfort zone of the indoor temperature, as shown in Figure 3.2. Through pre-heating, demand shift and the provision of

ancillary services can be delivered, thus reducing the total operational costs. The objective of this case is to calculate the minimum net energy cost $MinCost$ under given operational conditions. The obtained $MinCost$ then serves as an input in Case 2.

Case 2, the comfort zone of the indoor temperature is not allowed, in other words, the indoor temperature has to strictly follow the pre-defined comfortable temperature (set point). Meanwhile, hot-water-tank-based TES is installed in the building to provide flexibility to the electricity system, enabling demand shift and ancillary services. Given the net energy cost $MinCost$ [£], the objective of this case is to calculate the minimum size of TES [kWh], which is regarded as the equivalent size of TES of the inherent storage of the building.

3.2.2 Model of the Energy Management Optimization Problem in Buildings

3.2.2.1 Formulation of Case 1

This case is formulated as a linear programming problem. The objective function is to minimise the total operation cost, specifically, the net cost of electricity consumption (the cost of imported electricity minus the revenue of exported electricity) minus the revenue from balancing service provision. As describe in 3.2.1, primary response (P^{PR}), high-frequency response (P^{h}), secondary response (P^{SR}) and flexible response (P^{f}) are available for provision. Two pre-defined temporal windows w_1 and w_2 are considered to provide flexible response service, as formulated in Equation (3.6),

$$MinCost = \min \sum_{t=1}^{T} \left\{ \begin{matrix} \left(C_t^{im} \cdot P_t^{im} - C_t^{ex} \cdot P_t^{ex}\right) - \\ \left(C^{PR} \cdot P^{PR} + C^{h} \cdot P^{h} + C^{SR} \cdot P^{SR} \right. \\ \left. + C^{f} \cdot w_1 \cdot P^{f1} + C^{f} \cdot w_2 \cdot P^{f2} \right) \end{matrix} \right\} \cdot \Delta t \tag{3.6}$$

Power balance is formulated in (3.7). In this model, PV is considered to provide electricity to buildings, when the electricity provided by PV (P^{PV}) cannot satisfy the total demand, which includes HVAC-irrelevant electricity demand (P^{el}) and HVAC-driven electricity demand (P^{HVAC}), extra electricity has to be purchased from the grid (P^{im}). When PV-provided electricity is more than needed, the surplus part can be sold to the grid (P^{ex}).

$$P_t^{im} + P_t^{PV} - P_t^{ex} = P_t^{el} + P_t^{HVAC}, \forall t \in T \tag{3.7}$$

Equation (3.8) converts electric power P^{HVAC} (kW_{el}) to thermal power Q^{HVAC} (kW_{th}). The conversion rate from electricity to heat/cold for HVAC appliances is denoted as η^{HVAC}. Specifically for ASHP, which is adopted in this study, η^{HVAC} is the same with COP. The COP of ASHPs is formulated as a linear function of the ambient temperature (T_t^{am}) in this model, as shown in Equation (3.9),

$$Q_t^{HVAC} = \eta_t^{HVAC} \cdot P_t^{HVAC}, \forall t \in T \tag{3.8}$$

$$\eta_t^{HVAC} = a \cdot T_t^{am} + b, \forall t \in T \tag{3.9}$$

Constraint (3.10) limits the maximum output of HVAC appliances,

$$P_{min}^{HVAC} \leq P_t^{HVAC} \leq P_{max}^{HVAC}, \forall t \in T \tag{3.10}$$

where P_{max}^{HVAC} represents the corresponding power rating of HVAC appliances.

The first-order thermal dynamic model of buildings presented 3.1 is re-formulated as (3.11). The heat gains/losses come from heat transfer through walls and windows, the contribution of solar radiation through walls and windows, the internal heat gains (e.g., from people, appliances and lighting), and the output of HVAC appliance,

$$\begin{aligned} \Delta t \Bigg[\sum_{j \in J} U^{wall} \cdot A_j^{wall} \cdot (T_t^{am} - T_t) + \sum_{j \in J} U^{win} \cdot A_j^{win} \cdot (T_t^{am} - T_t) + \sum_{j \in J} \alpha^w \cdot R_j^{se} \\ \cdot U^{wall} \cdot A_j^{wall} \cdot I_{j,t}^T + \sum_{j \in J} \tau^{win} \cdot SC \cdot A_j^{win} \cdot I_{j,t}^T + Q_t^{in} + Q_t^{HVAC} \Bigg] \\ = \rho \cdot C \cdot V \cdot (T_{t+1} - T_t), \forall t \in T - \{NT\} \end{aligned} \tag{3.11}$$

where U^{wall} and U^{win} denote the heat transfer coefficient of the walls and windows [W/(m^2·K)]; A^{wall} and A^{win} denote the area of walls and windows surface [m^2]; α^w is the absorbance coefficient of the external surface of the wall [p.u.]; R^{se} is the external surface heat

resistance for convection and radiation [m^2·K/W]; I^T represents the total solar radiation on the walls/windows surface [kW/m^2]; τ^{win} represents the glass transmission coefficient of the windows [p.u.]; SC is the shading coefficient of the windows [p.u.]; Q^{in} is the internal heat gains [kW]; Q^{HVAC} is the output of HVAC appliances [kW]; T^{am} is the ambient temperature [°C]; T is the internal temperature [°C]; Δt is time intervals [h]. $j \in J$, which is the set of orientations; $t \in T$, which is the set of time horizon. Note that Δt is set 15 min (0.25 h) in the following studies of this chapter based on the time constant τ of the thermal dynamic process, as described in 3.1.

Constraint (3.12) defines the comfort zone of temperature $[\overline{T}, \underline{T}]$ that the consumers can tolerate. Pre-heating can be performed based on this zone of temperature to minimise the operational costs while considering the delivery of comfort.

$$\overline{T} \leq T_t \leq \underline{T}, \forall t \in T \tag{3.12}$$

In order to avoid the situation where the indoor temperature keeps following the upper or lower bound to minimise the operational cost at the cost of sacrificing the comfort, we enforce the average indoor temperature to be the same as the average temperature set points, as demonstrated in (3.13),

$$\frac{1}{NT}\sum_{t=1}^{NT} T_t = \frac{1}{NT}\sum_{t=1}^{NT} T_t^{set} \tag{3.13}$$

where *NT* is the number of time steps in T.

The allocation of various types of frequency response services is restricted in (3.14) – (3.20). Note that it is assumed the allocated response of all types should keep constant across the considered time horizon (i.e., 24 hours).

The primary and high frequency response services are limited as (3.14) and (3.15), where P_{min}^{HVAC} and P_{max}^{HVAC} denote the minimum and maximum output of HVAC appliances. It is worth noticing that we only consider the power balancing constraint for the primary and high-

frequency response service. Since their delivery time of these two types of services is no more than 30 seconds, so we assume that their impacts on energy levels in the building is negligible.

$$0 \leq P^{PR} \leq P_t^{HVAC} - P_{min}^{HVAC}, \forall t \in T \tag{3.14}$$

$$0 \leq P^{h} \leq P_{max}^{HVAC} - P_t^{HVAC}, \forall t \in T \tag{3.15}$$

The power restriction in terms of the provision of secondary and flexible response service inside and outside the two pre-defined temporal windows w_1 (for the delivery of P^{f1}) and w_2 (for the delivery of P^{f2}) is restricted in (3.16) – (3.18). The indicator $\mathbb{I}_A$ returns 1 if Statement A is true, while returns 0 if A is false. Since the secondary or flexible response service can be called at any time during a time interval, and the service delivery must be committed for 30 minutes from that moment it is called onward, therefore, we have to make sure that the level of response delivery agreed for time interval t can also cover time interval $t+1$, resulting in (3.18).

$$0 \leq P^{SR} \leq P_t^{HVAC} - P_{min}^{HVAC}, \forall t \in T \tag{3.16}$$

$$P^{SR} + P^{f1} \cdot \mathbb{I}_{t \in w_1} + P^{f2} \cdot \mathbb{I}_{t \in w_2} \leq P_t^{HVAC} - P_{min}^{HVAC}, \forall t \in T \tag{3.17}$$

$$P^{SR} + P^{f1} \cdot \mathbb{I}_{t \in w_1} + P^{f2} \cdot \mathbb{I}_{t \in w_2} \leq P_{t+1}^{HVAC} - P_{min}^{HVAC}, \forall t \in T - \{NT\} \tag{3.18}$$

In contrast to the primary and high-frequency response services, the provision of secondary and flexible response services would significantly influence the energy level inside the building due to 30 minutes' duration of the delivery. In order to make sure that calling the secondary/flexible response services will not conflict with the temperature limit in (3.12), the energy consumed by the delivery of these services should not exceed the maximum stored energy to maintain the internal temperature within the comfort zone, as shown in (3.19). Similar to the power restriction (3.18), the energy restriction has to satisfy the subsequent time interval $t+1$ as well, as presented in (3.20),

$$\rho \cdot C \cdot V \cdot \left(\overline{T} - T_t\right) \geq \Delta t \cdot \left(P^{SR} + P^{f1} \cdot \mathbb{I}_{t \in w_1} + P^{f2} \cdot \mathbb{I}_{t \in w_2}\right), \forall t \in T \tag{3.19}$$

$$\rho \cdot C \cdot V \cdot \left[\left(\overline{T} - T_{t+1}\right) + \left(\overline{T} - T_t\right)\right] \geq$$
$$2 \cdot \Delta t \cdot \left(P^{SR} + P^{f1} \cdot \mathbb{I}_{t \in w_1} + P^{f2} \cdot \mathbb{I}_{t \in w_2}\right), \forall t \in T - \{NT\} \tag{3.20}$$

3.2.2.2 Formulation of Case 2

By solving Case 1 as formulated in (3.6) – (3.20), the optimised operational cost $MinCost$ considering pre-heating through the inherent storage of the building can be obtained. In Case 2, we will calculate of equivalent size of TES of the inherent storage of the building based on $MinCost$ by using linear programming.

The objective (3.21) of Case 2 is to calculate the minimum size of additional TES that drives the same operational costs as in the case where the inherent storage of the building replace the functionality of TES. The result of (3.21), denoted as $EqSto$, is defined as the equivalent size of TES for the inherent storage of buildings,

$$EqSto = \min \max_{t \in T} s_t^{ec} \tag{3.21}$$

where s^{ec} represents the energy content in the TES at time step t, thereby $\max(s_t^{ec})$ can be perceived as the effective size of TES [kWh].

Equation (3.22) enforces the operational cost in Case 2 to be the equal to $MinCost$. The meaning of relevant symbols are the same as those in (3.6), except that the ancillary services are provided through the TES-based flexibility, instead of the building-inherent-storage-based flexibility.

$$\left(C_t^{im} \cdot P_t^{im} - C_t^{ex} \cdot P_t^{ex}\right) - \left(C^{PR} \cdot P^{PR} + C^{SR} \cdot P^{SR} + C^h \cdot P^h\right)$$
$$-C^f \cdot \left(w_1 \cdot P^{f1} - w_2 \cdot P^{f2}\right) = MinCost, \forall t \in T \tag{3.22}$$

As additional TES (hot water tank) is applied in Case 2 to replace the functionality of the intrinsic thermal storage of the building, the comfortable temperature zone is gone, leaving the indoor temperature to strictly follow the temperature set point, as shown in (3.23),

$$T_t = T_t^{set}, \forall t \in T \tag{3.23}$$

Constraint (3.24) and (3.25) limits the discharging rate s^{out} [kW] and charging rate s^{in} [kW] of the TES, while (3.26) shows the energy balance of TES. ε^s is defined as the minimum fully charged time of TES [hour], which is equal to the ratio of the energy capacity [kWh] to power rating of TES [kW]; η^s denotes the static efficiency of TES. To avoid the situation where both charging and discharging occur simultaneously, we consider the charging and discharging efficiency of TES which are denoted as η^{in} and η^{out}, respectively.

$$s_t^{in} \leq \frac{\max(s_t^{ec})}{\varepsilon^s}, \forall t \in T \tag{3.24}$$

$$s_t^{out} \leq \frac{\max(s_t^{ec})}{\varepsilon^s}, \forall t \in T \tag{3.25}$$

$$s_t^{ec} = s_{t-1}^{ec} \cdot \eta^s + s_t^{in} \cdot \eta^{in} - s_t^{out}/\eta^{out}, \forall t \in T \tag{3.26}$$

The first-order thermal dynamic model of buildings formulated in (3.11) is re-written as (3.27) to include the contribution of TES charging and discharging,

$$\begin{aligned} \Delta t[\sum_{j\in J} U^{wall} \cdot A_j^{wall} \cdot (T_t^{am} - T_t) + \sum_{j\in J} U^{win} \cdot A_j^{win} \cdot (T_t^{am} - T_t) + \sum_{j\in J} \alpha^w \cdot R_j^{se} \\ \cdot U^{wall} \cdot A_j^{wall} \cdot I_{j,t}^T + \sum_{j\in J} \tau^{win} \cdot SC \cdot A_j^{win} \cdot I_{j,t}^T + Q_t^{in} + Q_t^{HVAC} - s_t^{in} \\ + s_t^{out}] = \rho \cdot C \cdot V \cdot (T_{t+1} - T_t), \forall t \in T - \{NT\} \end{aligned} \tag{3.27}$$

Since ancillary services are provided through TES in Case 2, in order to ensure that there is enough energy in the TES to support the constant delivery of secondary/flexible response services in the calling period, the energy consumed by the delivery of these services should not exceed the maximum stored energy in TES, for both time interval t, as shown in (3.28), and $t+1$, as shown in (3.29),

$$s_t^{ec} \geq \Delta t \cdot \left(P^{SR} + P^{f1} \cdot \mathbb{I}_{t \in w_1} + P^{f2} \cdot \mathbb{I}_{t \in w_2}\right), \forall t \in T \tag{3.28}$$

$$s_t^{ec} + s_{t+1}^{ec} \geq 2 \cdot \Delta t \cdot \left(P^{SR} + P^{f1} \cdot \mathbb{I}_{t \in w_1} + P^{f2} \cdot \mathbb{I}_{t \in w_2}\right), \forall t \in T - \{NT\} \tag{3.29}$$

To summarise, Case 2 is formulated as (3.7) – (3.10), (3.14) – (3.18), (3.21) – (3.29), where (3.21) is the objective function while the others are the constraints. By solving this optimisation problem, we can obtain the equivalent size of TES for the inherent storage of buildings considered in Case 1.

3.3 Case Studies

In this section, a series of studies are performed based on Case 1 and Case 2 to investigate the values of the inherent thermal storage of buildings. A medium-sized residential house is selected as the baseline to illustrate the similarities and differences of operational patterns between the building thermal storage and hot-water-tank-based TES. Sensitivity studies are then carried out to explore the relationship between the value of building inherent storage and various factors.

3.3.1 Data Assumptions

Table 3.1 shows the parameters of a medium-sized residential house, which is investigated as the baseline in this section.

Table 3.1 – Building parameters of the baseline

heat transfer coefficient of the walls [W/(m2·K)]	Total area of walls (m2)	heat transfer coefficient of the windows [W/(m2·K)]	Window to wall ratio (%)	Long side (m)	Short side (m)	Height (m)
0.908	156	2.750	75	6	10	5

A winter day is selected to optimise the operational costs of the residential house in the baseline to investigate the impacts of building thermal storage on the pattern of heating. The ambient temperature is assumed as the yellow curve in Figure 3.3. For indoor temperature, the green dash curve demonstrates the temperature set points while the red and blue curves represent the upper and lower bound of the comfort zone. T^{up} and T^{dn} are defined as the temperature up and down deviation allowance, which in the base case are both set as 2 °C. A 5kW ASHP is assumed to be available in the house to provide heat, the linear coefficient term a and constant term b of COP formulated in (3.9) are assumed to be 0.07 and 2.07, respectively.

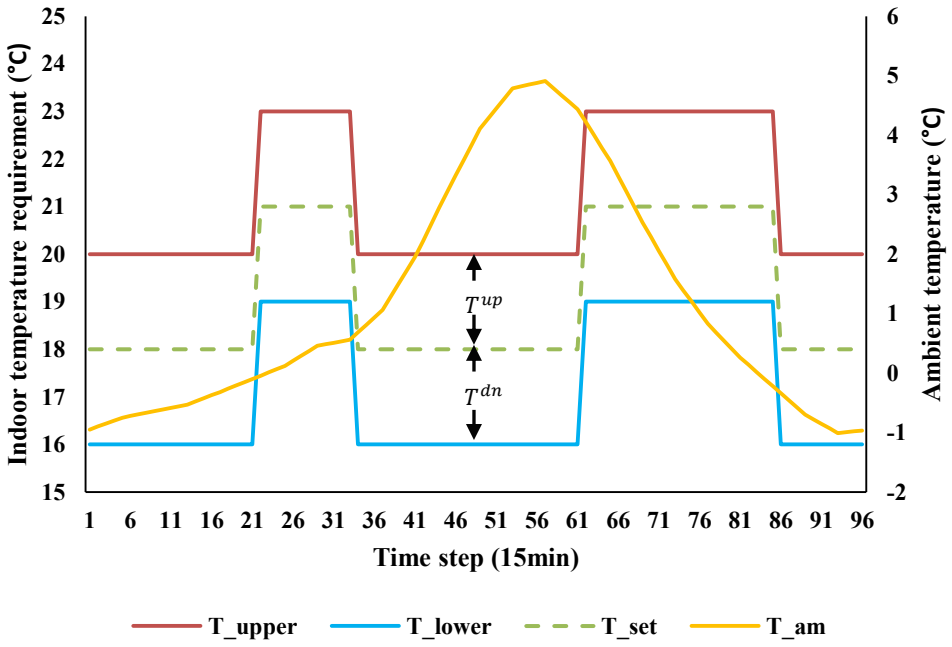

Figure 3.3– Indoor temperature requirement and ambient temperature assumption

The assumptions electricity price and HVAC-irrelevant electricity demand are illustrated in Figure 3.4. The green curve shows the price of importing electricity from the grid (C_im) while the purple curve shows the price of exporting electricity to the grid (C_ex).

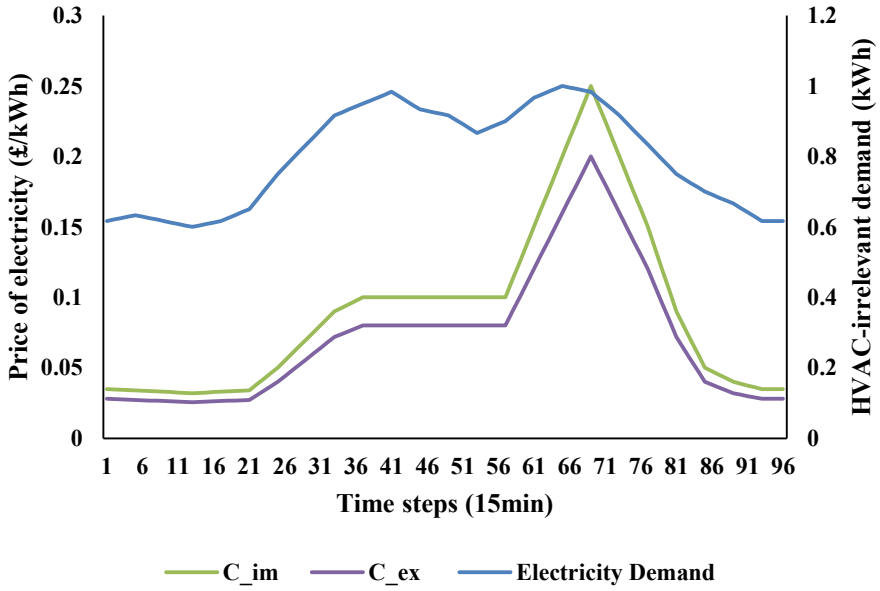

Figure 3.4– Price of importing/exporting electricity from/to the grid and HVAC-irrelevant demand

The power rating of the PV system is assumed to be 5kW. The internal heat gains and the solar radiation of the selected day are illustrated in Figure 3.5.

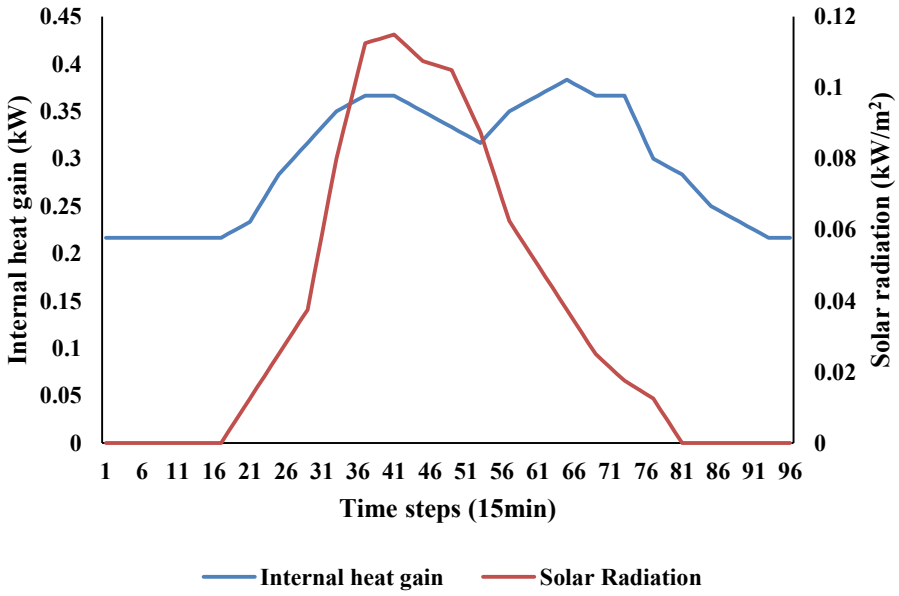

Figure 3.5– Internal heat gain and solar radiation

3.3.2 Quantification of Building Storage

Table 3.2 shows the results of the optimisation of Case 1 and Case 2. For Case 1, we investigate 2 scenarios to evaluate the benefits of pre-heating. In the first scenario, pre-heating is disabled by setting temperature deviation allowance (T^{up}/T^{dn}) 0, while in the second scenario, pre-heating is allowed by tuning T^{up}/T^{dn} up to 2 °C.

Table 3.2 – Operational costs and the corresponding size of storage in 2 Cases

Case 1	Energy cost (£)	Revenue (£)	Net cost (£)	T^{up}/T^{dn} (°C)
	8.41	0.31	8.10	0
	Energy cost (£)	Revenue (£)	Net cost (£)	T^{up}/T^{dn} (°C)
	8.06	0.44	7.63	2
Case 2	Energy cost (£)	Revenue (£)	Net cost (£)	TES (kWh)
	8.21	0.59	7.63	7.29

In Case 1, when T^{up}/T^{dn} is increased from 0 °C to 2 °C, 5.8% of net cost saving is driven by pre-heating. Through pre-heating, energy cost is reduced from 8.41£ to 8.06£ while the revenue from various response services is increased from 0.31£ to 0.44£. It can be inferred that the higher T^{up}/T^{dn} is set, the more benefits can be driven.

In Case 2, the net cost of Case 1 with pre-heating enabled is given as an input to minimise the size of TES. The result shows that when T^{up}/T^{dn} is set 2 °C, the equivalent size of TES for the inherent storage of the house is 7.29 kWh. Note that we assume that it takes the TES 3 hours to be fully charged from being empty by its rated power.

Further detailed results for Case 1 and Case 2 are given as follows to illustrate the similarities and differences of operational patterns between the building thermal storage and hot-water-tank-based TES.

Optimisation results for Case 1:

As described in 3.2.1, pre-heating is taken into account by allowing an indoor-temperature comfort zone. Through pre-heating, demand shift and the provision of ancillary services can be delivered, thus reducing the total operational costs.

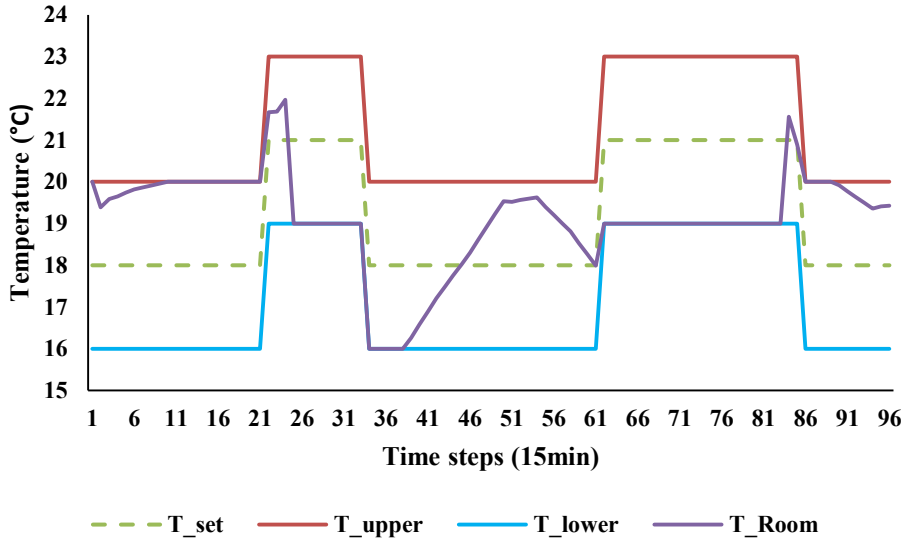

Figure 3.6– Indoor temperature variation in Case 1

The variation of indoor temperature is demonstrated in Figure 3.6. Based on the assumptions, the high-electricity-rate period covers time step 60 to 78. During this period, the indoor temperature virtually sticks to the lower bound of the temperature comfort zone to minimize the electricity consumption. During time steps 38 to 60, pre-heating is triggered, even though the heat demand over this period is lowest within the day (because the ambient temperature is high while the indoor temperature set point is low). Pre-heating also occurs between time step 1 to time step 25, to avoid high energy consumption during the next period characterised by relatively high electricity rate. In the night time, as the electricity rate is low, the indoor temperature tends to keep close to the upper bound, to fulfil the requirement in (3.13) that the average indoor temperature has to be the same as the average temperature set points (green dash curve).

Figure 3.7 illustrates the scheduled electricity consumption of HVAC appliance (i.e., HP) and the provision of various types of response services in Case 1. It can be observed that the lowest load factor of the HP (i.e., 40%) occurs between time step 38 to 60, which is higher than needed to satisfy the lowest temperature requirement due to the low heat demand in that period. The

surplus thermal energy is stored in the building and released gradually during the next few hours when the electricity price rises to keep the temperature sticking to the lower bound, thus avoiding high energy consumption during the peak-time of electricity price. Moreover, the increase of the lowest electricity consumption of HP allows additional primary response service in this case, driving more benefits.

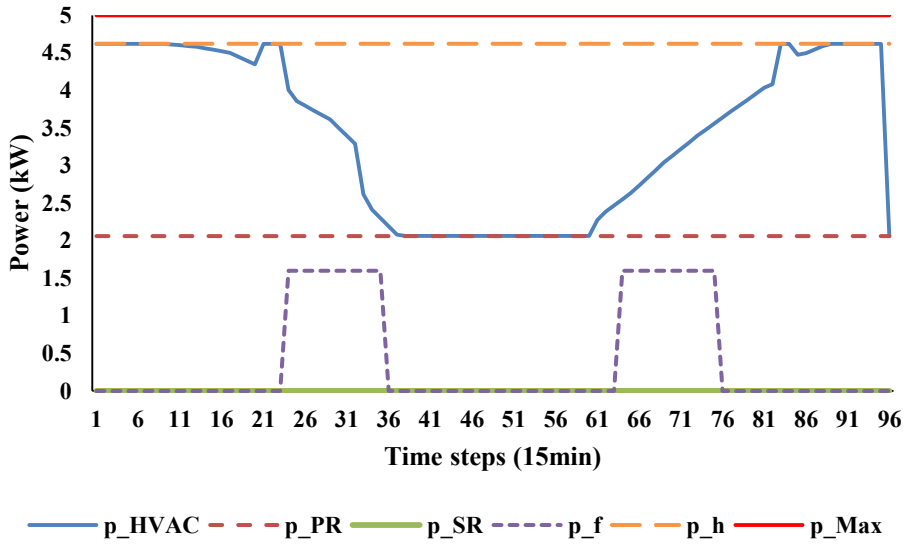

Figure 3.7– Electricity consumption and various response service of HP in Case 1

Optimisation results for Case 2:

As assumed in 3.2.1, the indoor temperature in this case has to stick to the pre-defined temperature set point. Meanwhile, hot water tank is deployed to shift demand and provide response services. The size of hot water tank drives the same net energy cost as in Case 1.

Figure 3.8 demonstrates the thermal energy variation in the hot-water-tank-based TES. As can be observed, TES keeps charging in two periods: time step 1 to 25 and time step 38 to 60, and discharges heat in the following periods until time step 38 and time step 78, respectively. The pattern of TES operation is very similar to the pattern of pre-heating demonstrated in Figure 3.6, if we consider the indoor temperature coinciding with the lower bound as TES discharging and otherwise as TES charging. This result indicates that the mechanisms of TES operation and pre-heating are basically the same, thus justifying the value of the quantifying pre-heating.

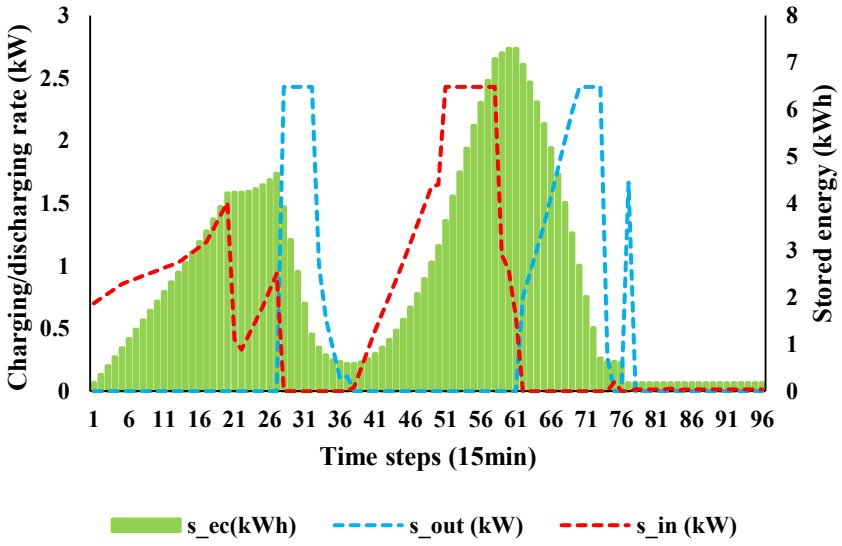

Figure 3.8– Operation dynamics of hot water tank in Case 2

Figure 3.9 illustrates the scheduled electricity consumption of HVAC appliance and the provision of various types of response services in Case 2. As can be seen, the overall variation trend of HP electricity consumption is similar to that in Case 1. However, there are two distinct differences that can be observed. The first difference is that in Case 2, the variation of HP electricity consumption is very steep while in Case 1, the consumption changes gradually. This reflects a slower response of pre-heating, as thermal energy stored in the building has to be released gradually, while TES can quickly discharge within the power rating. The second difference is that in Case 1, HP consistently operates at the lowest load factor between time step 38 to 60, and gradually tunes up its output in the following hours, while in Case 2, the output of HP fluctuates throughout the whole time. This indicates that the inherent storage of buildings cannot operate as flexibly as TES, because pre-heating can only shift demand to a few hours ago (fundamentally due to its high energy loss rate) while TES can shift demand over a wider range with a small amount of energy loss. Additionally, more response services is provided in Case 2, due to the increased flexibility of TES.

On the one hand, the analysis over Figure 3.8 and Figure 3.9 indicates that TES is characterised by improved operational performance compared to the inherent storage of buildings. On the other hand, the results demonstrate that the inherent storage of buildings alone can achieve the same economic benefits as TES, thus driving significant savings in the investment cost of TES.

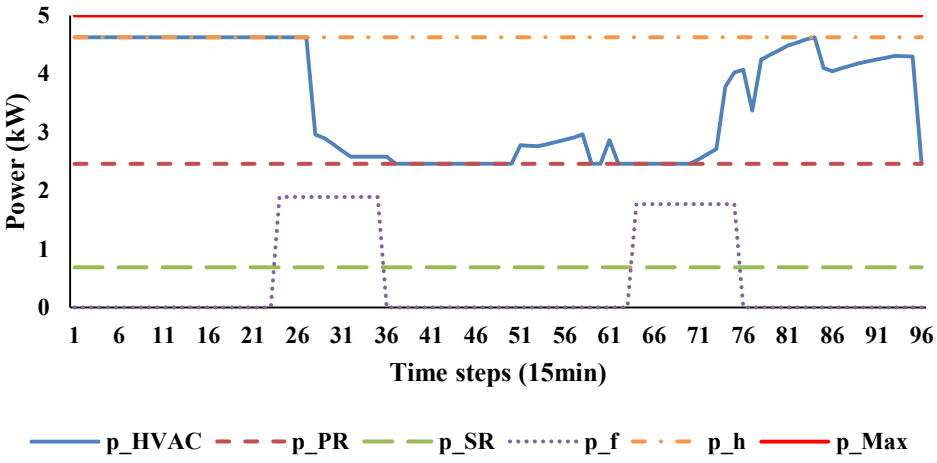

Figure 3.9– Electricity consumption and various response service of HP in Case 2

3.3.3 Sensitivity studies

The impact of building insulation condition on the equivalent size of its inherent storage

Figure 3.10 shows the relationship between the equivalent size of building storage and the building insulation condition. "1" on Axis x represents the insulation condition assumed in the baseline, as given in Table 3.1. For the other points on Axis x, the insulation parameters U^{wall} and U^{win} are multiplied by the corresponding values based on the baseline. The higher the value, the worse the insulation.

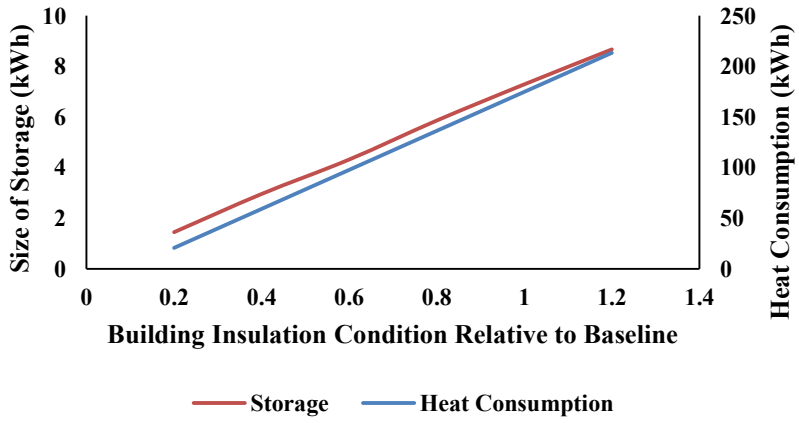

Figure 3.10– Relationship between equivalent size of building storage and building insulation condition

It can be observed that the equivalent size of building storage increases with the deterioration of the insulation condition linearly, which is a bit counter-intuitive. It should be stress that the benefits of building inherent storage is realised through pre-heating, in order to evaluate the values of pre-heating, we compare the economic benefits delivered through pre-heating and additional TES, when both cases achieve the same benefit, we quantify the value of pre-heating as the value of the corresponding size of TES. The core criteria in this quantification is economic benefits, instead of the physical capability of storage. When the insulation condition is improved, the decrease of indoor temperature will become slower, therefore, less heat supplement is required from the HPs, compressing the space of operational savings through pre-heating. Figure 3.10 also shows the impact of building insulation condition on the heat demand. As can be observed, heat demand increases linearly with the decrease of the building insulation level. For the extreme scenario where both U^{wall} and U^{win} are 0, there will be no heat exchange between the inside and outside of the building (when the curtain is off), pre-heating would be meaningless because no heat provision is needed. Therefore, pre-heating delivers more operational savings in buildings with a lower insulation level. However, when considering investment costs of different assets (e.g., HPs, generation), improved building insulation can significantly enhance the benefits of pre-heating, as reduced energy losses can introduce extra flexibility to pre-heating, making pre-heating more effective to shift peak load. This will be further demonstrated in 5.5.

The impact of building volume on the equivalent size of its inherent storage

Figure 3.11 demonstrates the relationship between the equivalent size of building storage and the building volume. As described in Equation (3.2), the thermal capacity of the building, which determines the capability of the building storage, is proportional to the building volume, therefore, the larger the building is, the more storage it can provide, as a result, the more benefits can be obtained from the inherent storage.

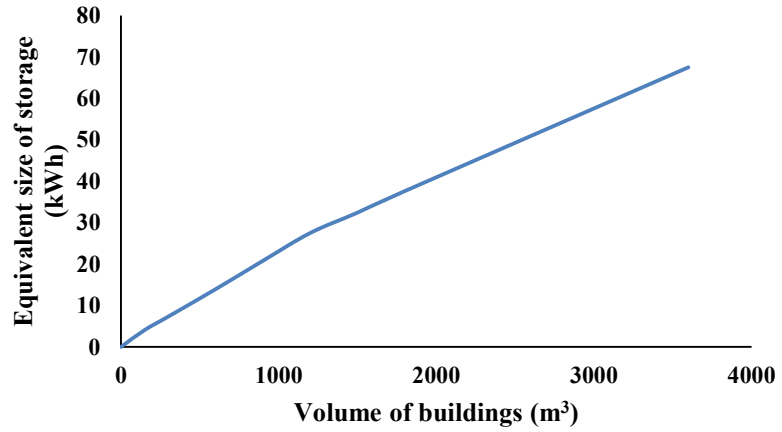

Figure 3.11– Electricity consumption and various response service of HP in Case 2

The impact of temperature deviation allowance on the equivalent size of its inherent storage

Figure 3.12 illustrates the relationship between the equivalent size of building inherent storage and the temperature deviation allowance. It can be observed that the equivalent size of building storage highly depends on the width of the temperature comfort zone. However, there is a cap of the benefits through increasing the size of TES in Case 2.

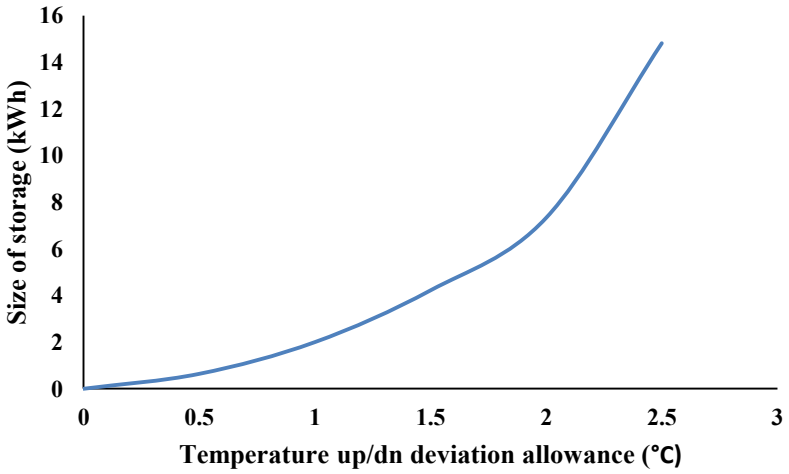

Figure 3.12– Relationship between the equivalent size of storage and the temperature deviation allowance

The result of the simulation indicates that when the size of TES is higher than 23.2 kWh, the net operational cost in Case 2 will not change with the increase of TES size. On the other hand, the increase of temperature deviation allowance in Case 1 will keep bringing added benefits

until the indoor temperature can freely drift without the need of any heat provision. It should be emphasised that the temperature deviation allowance depends on the customers' acceptance, it can vary significantly across different households. This case provides a conclusion of how the value of building inherent storage corresponds to the temperature deviation allowance.

3.4 Conclusions of the Chapter

The benefits of the intrinsic storage of buildings can be realised through pre-heating. Pre-heating offers a cost-effective way to alleviate the burden of additional investment at the end-side and provide flexibility to the electricity system. Additionally, it can shift electricity demands in response to the energy price signals and offer various ancillary services for extra revenue, thus providing an alternative opportunity to improve the efficiency of energy management of buildings.

The dynamic thermal energy balancing process of pre-heating can be simplified as a storage model, however, it is not clear how much storage should be used to depict the capability of pre-heating given the thermal parameters of a building. Another concern is that the comfort requirement of consumers cannot be fully considered in a storage model.

In this chapter, the first-order building thermal dynamic model is integrated into an energy management problem to investigate the utilisation of pre-heating as an alternative way to reduce the operational costs while taking into account the comfort conditions in buildings. Pre-heating through building thermal storage is enabled by allowing temperature variations within a pre-defined comfort zone. Through pre-heating, energy consumption can be managed in an economic-benefit-oriented way. By using linear programming, we are able to compare the operational costs between the case where pre-heating is enabled and the case where additional TES is installed, and thus evaluate the economic value of pre-heating and quantify the capability of the inherent storage of buildings under given thermal parameters of buildings.

The results show that the mechanisms of TES operation and pre-heating are basically the same, except that pre-heating is characterised with higher heat loss rate, thus justifying the simplification of the pre-heating process as a TES model.

A series of sensitivity studies are performed to investigate the limiting factors of the value of building inherent storage. Results show that (i) the equivalent storage of preheating is almost proportional to the volume of buildings and the insulation level of buildings; (ii) When the insulation condition is improved, the heat demand decreases accordingly, compressing the space of operational savings through pre-heating. Therefore, pre-heating can deliver more operational savings in buildings with a lower insulation level. However, when considering investment costs of different assets (e.g., HPs, generation), improved building insulation can significantly enhance the benefits of pre-heating, as reduced energy losses can introduce extra flexibility to pre-heating, making pre-heating more effective to shift peak load; (iii) Additionally, the equivalent size of building storage highly depends on the width of the temperature comfort zone. However, there is a cap of the benefits through increasing the size of TES. The result indicates that when the size of TES is higher than a certain amount, the net operational cost in Case 2 will not change with the increase of TES size. On the other hand, the increase of temperature deviation allowance in Case 1 will keep bringing added benefits until the indoor temperature can freely drift without the need of any heat provision. It should be emphasised that the temperature deviation allowance depends on the customers' acceptance, it can vary significantly across different households. This case provides a conclusion of how the value of building inherent storage corresponds to the temperature deviation allowance.

Chapter 4 Integrated Electricity and Heat System Investment Model

Decarbonisation of energy sectors is one of the key challenges in achieving the 80% carbon reduction target by 2050. There is growing evidence that the interaction between heat and electricity systems will be critical in facilitating cost effective transition to lower carbon system. In this context, this chapter proposes a novel modelling framework for the whole system optimisation of the integrated heat and electricity systems, considering operation and investment timescales and covering both local and national level infrastructure. This approach can be applied to optimize the heating technology portfolio to decarbonise the integrated heat and electricity systems. Main heating strategies considered in this chapter include (i) electrification of heat sector through the application of heat networks, supplied by CHP plant, industrial size HPs as well as gas boilers, and (ii) electrified heat at the consumer end through the application of hybrid HPs.

The proposed optimization model can simultaneously optimize, for the first time, the investment in electricity generation (including conventional and low carbon generation as well as CHP), heating devices, heat networks, reinforcement of electricity transmission and distribution networks while minimizing the system operation cost, taking into account frequency response and operating reserve requirements. The impact of integrated systems reducing system inertia on the frequency response requirement is explicitly modelled in the constraints. Carbon emission and security constraints are also included.

Previous works or similar tools can consider the integrated electricity and heat system on a local level or just optimize the integrated operation without investment planning. Some recent work studied the integrated operation and investment planning of the integrated energy system, but cannot consider the information of local districts. The proposed integrated electricity and heat system model applies a fractal-based algorithm which can create representative local networks that capture statistical properties of typical network topologies that range from high-

load density city/town networks to low-density rural networks. The national system is represented by a combination of the representative local networks so that the local district and national level infrastructure can be considered together.

4.1 The Framework of the Integrated Electricity and Heat Model

Various interactions exist between electricity and heat systems, as illustrated in Figure 4.1. Specifically, CHP can generate electricity and heat simultaneously. Through adjusting its power-to-heat ratio, it can convert surplus electricity into storable heat, and increase the generation of electricity during peak time by reducing heat output. As analysed in 2.2.2, the physical interaction bridged by CHP between electricity and heat systems can be further strengthened through the coordinated operation of CHP, HP and TES. For distributed heating, end-use HP also links electricity and heat systems by converting electricity into heat. This link is improved with the existence of end-use TES, since electricity cannot be cost-effectively stored at the end-use side, the coordination of TES and HP can indirectly achieve so.

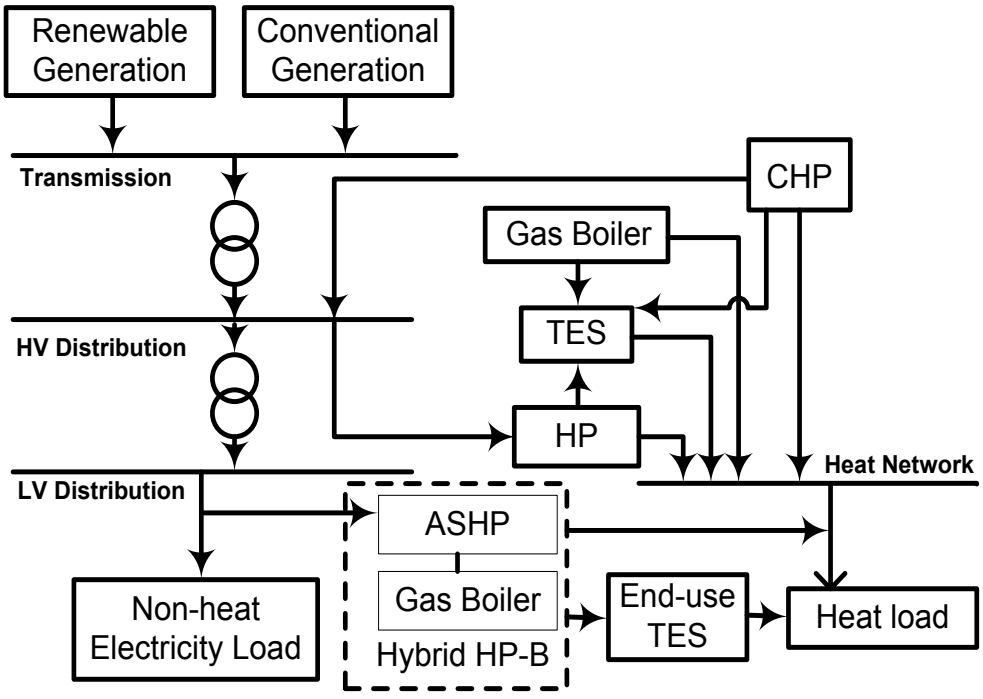

Figure 4.1– Interactions between the integrated electricity and heat system

Due to these operational links between electricity and heat systems, significant benefits can potentially be achieved through adequately considering the services that the heat system can provide to the electricity system. It is important to emphasize that the impact of cooling system on the whole system operation and investment can also investigated by using the model presented in Chapter. However, due to a lack of cooling demand data on the national level, the cooling system is not analyzed in this thesis. The role cooling system can potentially play in the multi-energy system will be investigated in the future work as mentioned in Chapter 8.

The proposed integrated electricity and heat system investment model is formulated as a mixed integer linear programming problem (MILP) with hourly time resolution across a whole year, while also considering sub-hourly frequency regulation and reserve constraints. The framework of this model is illustrated in Figure 4.2.

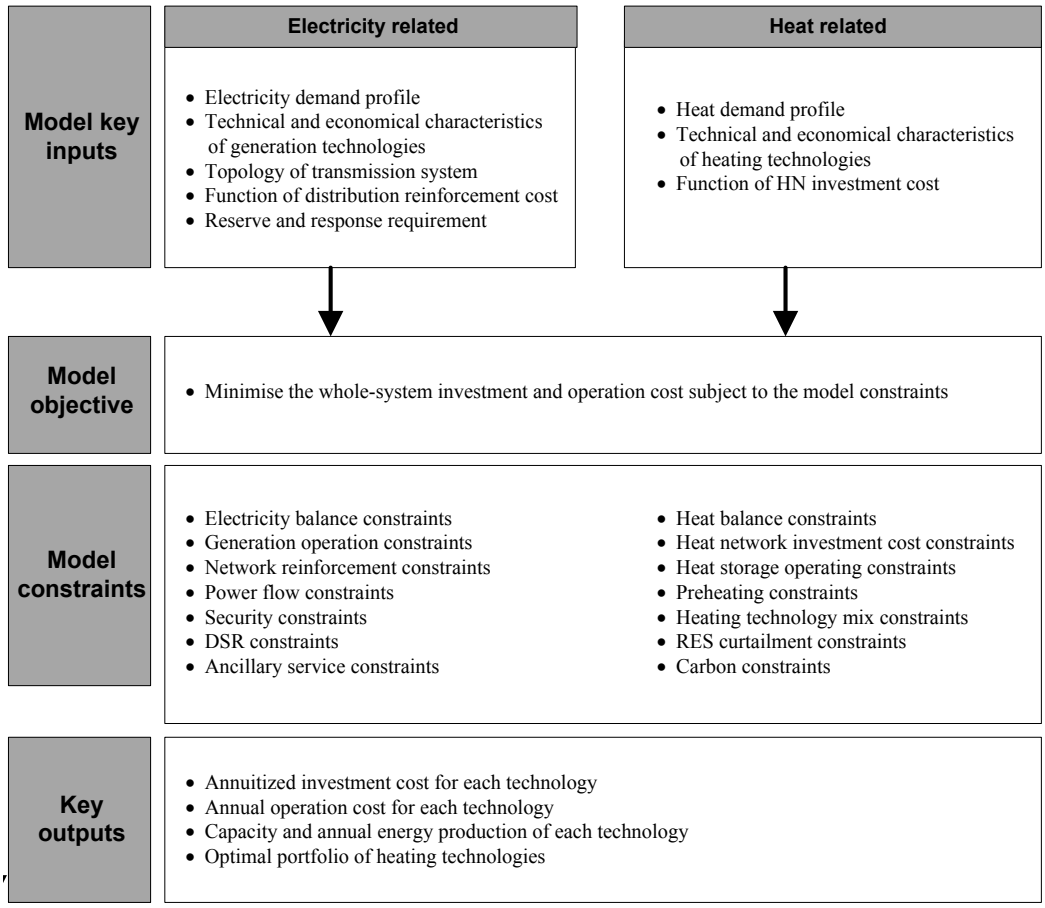

Figure 4.2– Framework of the integrated heat and electricity system investment model

The objective function (4.1) is to minimize the whole system cost which includes the annual operation costs and the annuitized investment costs related to different types of generation, heating plants/appliances, energy storage as well as electricity and heat networks:

The constraints associated with the electricity system are based on the whole-system analysis of the electricity system planning presented in [48], including: (i) generator operating constraints (specifically, the CHP operating constraints are categorized into generator operating constraints while the approach of CHP modelling presented in [22] is applied to determine the operating boundary of CHP in this model), (ii) Demand-side response constraints, (iii) power flow constraints, (iv) distribution network reinforcement constraints and (v) DC power flow constraints (used for the expansion of the transmission system).

4.2 Formulation of the Integrated Electricity and Heat Model

4.2.1 Objective Function

The objective function (4.1) is to minimize the whole system cost, comprising annual operation costs of both electricity and heat sectors and annuitized investment costs associated with different assets. The operation cost includes electricity generation cost and fuel cost for gas boilers. The investment cost includes capital cost of generators, heating assets, district heating networks, and reinforcement cost of transmission and distribution networks,

$$\begin{aligned}\min\varphi = &\sum_{t=1}^{T}\sum_{i=1}^{G}\sum_{j=1}^{L} C_{op}^{g}\left(p_{t,i,j}^{g}, \mu_{t,i,j}\right) + \sum_{t=1}^{T}\sum_{i=1}^{B}\sum_{j=1}^{L} C_{op}^{b}\left(h_{t,i,j}^{b}\right) + \sum_{i=1}^{G}\sum_{j=1}^{L} C_{inv}^{g}\left(cap_{i,j}^{g}\right) \\ &+ \sum_{i=1}^{H_d \cup H_e}\sum_{j=1}^{L} C_{inv}^{h}\left(cap_{i,j}^{h}\right) + \sum_{i=1}^{HN} C_{inv}^{hn}\left(\alpha_{i}^{hn}\right) + \sum_{i=1}^{F} C_{inv}^{f}\left(cap_{i}^{f}\right) \\ &+ \sum_{i=1}^{DN} C_{inv}^{dn}\left(cap_{i}^{DN}\right)\end{aligned} \tag{4.1}$$

where T, G, L, B, H_d, H_e, DHN, F and DN are sets of operating time steps, generation types, locations (nodes), boiler types, district heating assets, end-use heating assets, district heating networks, transmission networks and distribution networks, respectively; C_{op}^{g} represents the function of generation operation cost, which is associated with generation output p^g and synchronised units μ; C_{op}^{b} represents the function of boiler operation cost, which is associated with boiler output h^b; C_{inv}^{g} represents the function of generation investment cost, which is determined by the capacity of different generation cap^g; C_{inv}^{h} represents the function of heating asset investment, which is determined by the capacity of different heating assets cap^h; C_{inv}^{hn} is the function of heat network investment cost, which is associated with the penetration of heat networks in different types of areas α^{hn}; C_{inv}^{f} represents the reinforcement cost of electricity transmission lines, which is determined by the expanded capacity of transmission line cap^f; and C_{inv}^{dn} is the function of electricity distribution network reinforcement cost, which is associated with the expended capacity of distribution network capacity cap^{DN}.

Details about the formulation of operation costs are given as following (note that Carbon price is included in the fuel cost):

1) The operation costs of generators/CHPs consist of variable cost, no-load cost and start-up cost. The piecewise linear approximation of the generation operation cost proposed in [49] is applied in this model. The operation cost of generators is approximated as the summation of (i) variable cost which is a function of generation output (p^g), (ii) no-load cost which is determined by the number of online units (μ) and (iii) start-up cost which is determined by the number of starting-up units (μ^{st}). Equation (4.2) – (4.4) gives the single-segment linear approximation of the generation cost,

$$\sum_{t=1}^{T}\sum_{i=1}^{G}\sum_{j=1}^{L} C_{op}^{g}\left(p_{t,i,j}^{g}, \mu_{t,i,j}\right) = \sum_{t=1}^{T}\sum_{i=1}^{G}\sum_{j=1}^{L}\left(p_{t,i,j}^{g} \cdot OC_i^{var} + \mu_{t,i,j} \cdot OC_i^{nl} + \mu_{t,i,j}^{st} \cdot OC_i^{st}\right) \quad (4.2)$$

$$\mu_{t,i,j}^{st} \geq \mu_{t,i,j} - \mu_{t-1,i,j} \quad (4.3)$$

$$\mu_{t,i,j}^{st} \geq 0 \quad (4.4)$$

where OC^{var} is the incremental fuel cost; OC^{nl} is the no-load operation cost of generators; μ^{st} is the number of units started up; while OC^{st} is the start-up cost.

2) Gas boilers serve as supplementary heating devices that are used to reduce the capacity of electrification-based heating plants/appliances (e.g. CHPs and HPs) and electricity infrastructure reinforcement. In this model, both industrial size gas boilers (applied in district heating) and end-use gas boilers (working as a part of hybrid HP-Bs) are taken into consideration, as formulated in (4.5),

$$\sum_{t=1}^{T}\sum_{i=1}^{B}\sum_{j=1}^{L} C_{op}^{b}\left(h_{t,i,j}^{b}\right) = \sum_{t=1}^{T}\sum_{j=1}^{L} h_{t,j}^{gb,d}\cdot OC^{gb,d} + \sum_{t=1}^{T}\sum_{j=1}^{L} h_{t,j}^{gb,e}\cdot OC^{gb,e} \tag{4.5}$$

where $h^{gb,d}$ and $OC^{gb,d}$ represent the heat output and variable operation cost of industrial size gas boilers applied in district heating networks, while $h^{gb,e}$ and $OC^{gb,d}$ represent the heat output and variable operation cost of end-use gas boilers.

The annuitized infrastructure investment costs (Annuity factors for different assets are considered given corresponding discount rates and life spans) include:

1) Capital costs of different types of generators.

The capital cost of generation is formulated in (4.6),

$$\sum_{i=1}^{G}\sum_{j=1}^{L} C_{inv}^{g}\left(cap_{i,j}^{g}\right) = \sum_{i=1}^{G}\sum_{j=1}^{L}\left(C_{i}^{g}\cdot AF_{i}^{g} + C_{i}^{fix,g}\right)\cdot cap_{i,j}^{g} \tag{4.6}$$

where C^{g} is the capital cost of various generation; AF^{g} is the annuity factor of generators; $C^{fix,g}$ is the fixed O&M cost of generation;

2) Capital costs of different district heating plants/devices (superscripted by d), which may include CHPs, industrial size HPs, industrial size TESs and industrial size gas boilers,

$$\sum_{i=1}^{H_d}\sum_{j=1}^{L} C_{inv}^{h}\left(cap_{i,j}^{h}\right) = \sum_{i=1}^{H_d}\sum_{j=1}^{L}\left(C_{i}^{d}\cdot AF_{i}^{d} + C_{i}^{fix,d}\right)\cdot cap_{i,j}^{d} \tag{4.7}$$

where C^d is the capital cost of various district heating plants/devices (subject to the set of H_d); AF^d is the corresponding annuity factor; $C^{fix,d}$ is the fixed O&M cost of district heating plants/devices, while cap^d is the capacity of different district heating plants/devices.

3) Capital costs of end-use heating appliances (superscripted by e), which may potentially include hybrid HP-Bs and end-use TESs,

$$\sum_{i=1}^{H_e}\sum_{j=1}^{L} C_{inv}^{h}\left(cap_{i,j}^{h}\right) = \sum_{i=1}^{H_e}\sum_{j=1}^{L}\left(\left(C_i^e \cdot AF_i^e + C_i^{fix,e}\right)\cdot cap_{i,j}^{e} + N_j^h \cdot \omega_j^e \cdot C_i^{ins,e} \cdot AF_i^e\right) \quad (4.8)$$

where C^e is the capital cost of various end-use heating appliances (subject to the set of H_e); AF^e is the annuity factor; $C^{fix,e}$ is the fixed O&M cost; cap^e is the capacity of different heat appliances; N^h is the number of households; ω^e is the percentage of households using end-use heating technologies; and $C^{ins,e}$ is the installation cost of different end-use heating appliances.

4) Heat network investment cost

The investment costs for the reinforcement of distribution network is shown in (4.9),

$$\sum_{i=1}^{D} C_{inv}^{hn}\left(\alpha_i^{hn}\right) = \sum_{i=1}^{HN} \omega_i^{HN} \cdot N_i^{HN} \cdot IC_i^{HN} \quad (4.9)$$

where ω^{HN} is the penetration of heat networks in each representative areas; N^{HN} is the number of representative heat networks; IC^{HN} is the investment cost of representative heat networks. Note that when HN appears as a superscript, it is just used to characterize a symbol, not an index. It is the same for the superscript of DN in (4.11).

5) Electricity transmission line reinforcement

The investment costs for the reinforcement of transmission network is shown in (4.10),

$$\sum_{i=1}^{F} C_{inv}^{f}\left(cap_i^f\right) = \sum_{i=1}^{F} C^f \cdot AF_i^f \cdot cap_i^f \quad (4.10)$$

where C^f is the capital cost of transmission networks; AF^f is the annuity factor of electricity transmission lines.

6) Electricity distribution network reinforcement. A schematic function of the distribution network reinforcement cost has been illustrated in Figure 4.3, while a linear approximation of this function is applied in this model as formulated in (4.11),

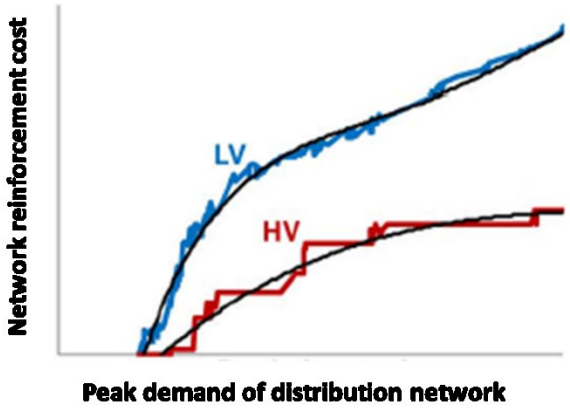

Figure 4.3– Distribution network reinforcement function

$$\sum_{i=1}^{DN} C_{inv}^{dn}(cap_i^{DN}) = \sum_{i=1}^{DN} C_i^{DN} \cdot cap_i^{DN} \tag{4.11}$$

where C^{DN} is the reinforcement cost of different types of representative distribution networks.

This model takes account of a variety of operation constraints while minimizing the whole system cost as well as meeting the carbon target. All these constraints are applied on hourly time resolution ($\forall t \in T$) across all locations ($\forall j \in L$).

4.2.2 Various Constraints

4.2.2.1 Energy Balance

1) Electricity balance

Constraint (4.12) ensures that electricity supply (p^g) and demand (p) are balanced in each time interval within the entire electricity system. Different types of electricity generation including nuclear power, CCGT, gas CCS, OCGT, GGCT CHP, wind and PV are considered,

$$\sum_{i=1}^{G}\sum_{j=1}^{L} p_{t,i,j}^{g} = \sum_{j=1}^{L} p_{t,j} \tag{4.12}$$

Electricity demand consists of non-heat based demand (p^{ele}), which can be redistributed through DSR (p^{ele+} and p^{ele-}), and heat-driven electricity demand (p^{heat}), which particularly refers to the demand of end-use HPs ($h^{hp,e}$) and industrial size HPs ($h^{hp,d}$), as shown in (4.13) and (4.14). COP^{a} and COP^{w} denote the COP of air source HPs and water source HPs, respectively,

$$p_{t,j} = \left(p_{t,j}^{ele} + p_{t,j}^{ele+} - p_{t,j}^{ele-}\right) + p_{t,j}^{heat} \tag{4.13}$$

$$p_{t,j}^{heat} = h_{t,j}^{hp,e}/COP_{t}^{a} + h_{t,j}^{hp,d}/COP^{w} \tag{4.14}$$

In this modelling, air source HPs (ASHP) are applied for end-use heating. For district heating systems, water source HPs (WSHP) are applied due to their high efficiency. As the ambient temperature varies significantly, the COP of ASHPs will change accordingly. The COP of ASHPs is formulated as a linear function of the ambient temperature (T^{a}) in this model, as given in (4.15),

$$COP_{t}^{a} = a^{HP} \cdot T_{t}^{a} + b^{HP} \tag{4.15}$$

The industrial-size HP (for DHN) is typically sourced from temperature-stable heat sources, so its COP is much more stable than that of ASHPs, for the sake of simplification, we assume that the COP of industrial HPs is constant in this model.

2) Heat balance

Constraint (4.16) shows the energy balance for the heat system. On the supply side, both district and end-use heating systems are considered. Due to the inherent thermal storage in heat networks and buildings, heat demand can be shifted through preheating for both district heating and end-use heating, which is considered in (4.16),

$$\sum_{i=1}^{H_d} h_{t,i,j}^{d} - h_{t,j}^{d+} + h_{t,j}^{d-} + \sum_{i=1}^{H_e} h_{t,i,j}^{e} - h_{t,j}^{e+} + h_{t,j}^{e-} = h_{t,j} \tag{4.16}$$

$$\sum_{i=1}^{H_d} h_{t,i,j}^{d} = h_{t,j}^{chp} + h_{t,j}^{hp,d} + h_{t,j}^{gb,d} + s_{t,j}^{+,d} - s_{t,j}^{-,d} \tag{4.17}$$

$$\sum_{i=1}^{H_e} h_{t,i,j}^{e} = h_{t,j}^{hp,e} + h_{t,j}^{gb,e} + s_{t,j}^{+,e} - s_{t,j}^{-,e} \tag{4.18}$$

where h represents the total heat demand. h^d denotes the heat provided by district heating which is supplied by CHPs (h^{chp}), industrial-sized HPs ($h^{hp,d}$), TES ($s^{+,d}$ and $s^{-,d}$) and gas boilers ($h^{gb,d}$), while h^e denotes the heat provided by end-use heating appliances including end-use HPs ($h^{hp,e}$), gas boilers ($h^{gb,e}$), end-use heat storage ($s^{+,e}$ and $s^{-,e}$). h^{d+} and h^{d-} denote the district heat shifted through preheating while h^{e+} and h^{e-} denote the end-use heat shifted through preheating. Note that we assume in this model that end-use heating technologies are only used to supply a single household.

3) Power flow constraint

For the sake of decarbonization, it is essential to electrify the heat sector which may require the reinforcement of the transmission network. In this modeling, DCOPF is performed to optimize the capacity and the location of reinforcement of transmission networks. Constraint (4.19) is applied for all transmission lines ($\forall m \in F$), where G, D and θ represent electricity generation, electricity demand and voltage angle at each location,

$$-cap_m^f \leq F(G, D, \theta)_{t,m} \leq cap_m^f \tag{4.19}$$

Equation (4.20) – (4.22) gives the explicit form of Equation (4.19). The DCOPF here is crucial to determine the additional size of the transmission lines,

$$g_{t,i} - d_{t,i} = \sum_{j=1}^{D} B_{i,j} \cdot \theta_{t,j} \ , t \in T, i \in D \tag{4.20}$$

$$p_{t,m} = \frac{\theta_{t,N_m^{st}} - \theta_{t,N_m^{en}}}{X_m}, t \in T, m \in F \tag{4.21}$$

$$-(f_m^{ex} + f_m^{ad}) \leq p_{t,m} \leq (f_m^{ex} + f_m^{ad}), \ \ t \in T, m \in F \tag{4.22}$$

where g is the electricity generation; d is the electricity demand; p is the power flow in transmission lines; f^{ex} is the existing capacity of transmission lines; f^{ad} is the additional capacity (reinforcement) of transmission lines; T is the set of operating steps; D is the set of nodes; F is the set of transmission lines; N^{st} and N^{en} denote the number of the start node and end node of the mth transmission corridor.

4) Heating technology mix constraints

Both district heating and end-use heating are considered in this model. For a single household, it is assumed that heat demand is supplied by either district heating system or end-use system. The percentage of households supplied by district heating system (ω^d) and end-use system (ω^e) are to be optimized.

The heat demand supplied by district heating technologies and end-use heating technologies are as stated in constraint (4.23) and (4.24), while (4.25) ensures that all heat demand is satisfied,

$$\sum_{i=1}^{H_d} h_{t,i,j}^{d} - h_{t,j}^{d+} + h_{t,j}^{d-} = \omega_j^d \cdot h_{t,j}, \forall t \in T, \forall j \in L \tag{4.23}$$

$$\sum_{i=1}^{H_e} h_{t,i,j}^{e} - h_{t,j}^{e+} + h_{t,j}^{e-} = \omega_j^e \cdot h_{t,j}, \forall t \in T, \forall j \in L \tag{4.24}$$

$$\omega_j^d + \omega_j^e = 1, \forall j \in L \tag{4.25}$$

Different heat plants/devices can be utilised in both district heating and end-use heating. To be more specific, CHP, industrial-size HP, gas boiler and hot water tank (TES) can potentially supply district heat demand, while HP, gas boiler and TES are considered to as options to supply end-use heating. This model can determine the investment portfolio of different heating technologies in district heating and end-use heating. The size of each heating plant/device is optimized subject to the cost trade-off and carbon limit, based on a series of cost assumptions as following.

In this model, we take into account the installation costs and O&M costs of HPs. Gas boilers are already present in most of the households so only O&M costs of gas boilers are considered (these are the assumptions in particular study of the UK case, although this model can consider investment and installation cost of gas boilers and other technologies as appropriate). Costs of smart control devices that are required to switch the operation of hybrid HP-B between ASHPs and gas boilers according to their real-time energy efficiency are also considered. The operational cost of the HP is temperature-dependant (as shown in Equation (4.15), the hourly temperature data is given as input) instead of a constant cost function, which means the HP may not be able to supply the heat load in cold days. Also, the operational cost of the HP may be higher than that of the gas boiler due to reduced COP. Furthermore, operation of HP with reduced COP may drive network reinforcement and increased investment in peaking generation capacity, which is the core advantage of hybrid HP-B in scenarios with low carbon emissions.

4.2.2.2 Energy Shifting

1) Thermal Energy Storage

TES is an important component in the integrated electricity and heat system as it can store the thermal energy that is converted from electricity via HPs or CHP, thus provide a series of balancing services for the electricity system. TES can be potentially applied in both district heating and end-use heating. In this model, TES specifically refers to the hot water tank. The maximum discharging and charging rate is restricted by (4.26) and (4.27),

$$s_{t,j}^{+} \leq s_{j}^{cap}, \forall t \in T, \forall j \in L \tag{4.26}$$

$$s_{t,j}^{-} \leq s_j^{cap}, \forall t \in T, \forall j \in L \tag{4.27}$$

where s^+ and s^- denote the charging rate (in kWh) of TES while s^{cap} represents the power capacity of TES. Both the charging rate and discharging rate are limited by the power capacity.

Energy capacity of TES (s^{ec}) is limited by (4.28), where ε^s is defined as the ratio of the energy capacity to the power rating of TES, as formulated in (4.29). To be more specific, ε^s is the time hot water tank (TES) consumes to be fully charged from being empty with the maximum charging rate (or fully discharged from being full charged with the maximum discharging rate). Typically, the size of TES is measured by the maximum energy content (kWh) and there is a limit of the charging/discharging rate (power rating, kW). For convenience, we use ε^s to measure the size of TES,

$$s_{t,j}^{ec} \leq s_j^{cap} \cdot \varepsilon^s, \forall t \in T, \forall j \in L \tag{4.28}$$

$$\varepsilon^s(h) = \frac{\text{Energy capacity } (kWh)}{\text{Power rating } (kW)} \tag{4.29}$$

The energy balance constraint is presented as (4.30), where η^s is the static efficiency of TES. There might also be a tiny portion of heat loss in the process of charging and discharging, for simplicity, we omit it here,

$$s_{t,j}^{ec} = s_{t-1}^{ec} \cdot \eta^s + s_{t,j}^{-} - s_{t,j}^{+}, \forall t \in T, \forall j \in L \tag{4.30}$$

Constraints (4.26) – (4.30) are applied for both industrial size TES and end-use TES.

2) DSR constraints

The flexibility provided by flexible electricity load and ancillary service provision through short-term interruption of operation of end-use HPs are included in the model. Based on the DSR model presented in in Reference [48], (4.31) limits the amount of shiftable load,

$$p_{t,j}^{ele-} \leq \alpha^{dsr} \cdot p_{t,j}^{ele}, \forall t \in T, \forall j \in L \tag{4.31}$$

In this model, only some specific types of flexible loads are considered to provide domestic DSR, including electric vehicles, smart appliances (e.g. smart dishwashers, smart fridge) and peak reduction from industry and commercial sectors, which have broad consumer acceptance of DSR [50].

The use of demand response in this modelling is limited by α^{dsr} which is the Ratio of the flexible electricity demand to the total demand. Note that α^{dsr} depends on the consumers' willingness to shift load, which can change with time. For simplicity, we assumed that it is not time-dependent.

It should be stressed that in the proposed model, no additional cost is incurred due to the provision of demand response. However, the constraints on consumer flexibility are based on the data in [51], which gives the proportion of different smart appliance users that are willing to provide demand response (α^{dsr}), so there is barely compromise on services delivered to consumers.. Based on [51], it is assumed that 80% of the EV can be charged flexibly and 41% of the smart appliances are flexible, while respecting the constraints related to the service delivery. The rest of demand, including industrial and commercial sectors can provide 10% peak reduction and load shifting within the same day.

Constraint (4.32) gives the demand balance of DSR, where D_x denotes the set of time steps in the xth day. In this model, it is assumed that most of the residential flexible demand can be shifted within a day,

$$\sum_{t \in D_x} p_{t,j}^{ele-} \leq \sum_{t \in D_x} p_{t,j}^{ele+}, \forall j \in L \tag{4.32}$$

Note that Equation (4.32) does not fit all types load. In this section, we assume that the load decrease has to be lower than the increase over the day only for the flexible loads considered in this model. This model can also consider load shifting in longer time, but we made a simplification by assuming that most of residential demand can be shifted within a day or only in a few hours, based on [51]. Take smart dishwasher as an example, we can optimise its operation over night, but it should finish washing up by the following morning; the same argument is applied for charging of EVs.

The contribution of end-use HPs in providing frequency response service and operating reserve service for the electricity system is shown in (4.33) and (4.34),

$$rsp_{t,j}^{hp,e} \leq h_{t,j}^{hp,e} / COP_t^a \,, \forall t \in T, \forall j \in L \tag{4.33}$$

$$res_{t,j}^{hp,e} \leq \alpha_j^{hp,res} \cdot h_{t,j}^{hp,e} / COP_t^a \,, \forall t \in T, \forall j \in L \tag{4.34}$$

where $rsp^{hp,e}$ and $res^{hp,e}$ denote the response and reserve that end-use HP can provide. More specifically, the operation of HPs can be interrupted for a short term to provide primary response, while the temperature comfort compromise can be neglect due to the thermal inertia in buildings [52]. Additionally, the operation of HPs can be turned down by a maximum percentage of $\alpha^{hp,res}$ for the required period to provide RES.

3) Pre-heating constraints:

Pre-heating can be applied in both district heating (through the inherent storage in DHN pipelines [53]) and end-use heating systems (through the thermal insulation of buildings). Constraints (4.35) – (4.37) present a generic pre-heating model for both district and end-use heating systems. Constraint (4.35) presents the amount of heat demand that can be shifted, which depends on the flexibility of heat systems. In district heating systems, the flexibility is driven by the capacity of the inherent storage of DHN pipelines as the proportion of heat demand can be redistributed ($\alpha^{PH,d}$). It is worth noticing that the storable energy in DHN pipelines is typically limited (one or two hours' worth of heat content) due to the constant flow of heat in the pipelines. In end-use heating systems, the flexibility is measured by the percentage of residential buildings ($\alpha^{PH,e}$) that have the potential to participate in pre-heating (with good insulation and a large mass of envelope which can provide a meaningful amount of storage). Constraint (4.36) ensures that the increased load for pre-heating is limited by the capacity of the heating devices. The energy balancing process of pre-heating is simplified as a storage model (4.37),

$$h_{t,j}^{x-} \leq \alpha^{PH,x} \cdot \sum_{i=1}^{H_x} h_{t,i,j}^{x} \,, \forall t \in T, \forall j \in L, x \in \{d, e\} \tag{4.35}$$

$$h_{t,j}^{x+} \leq \alpha^{PH,x} \cdot \sum_{i=1}^{H_x} cap_{i,j}^{x}, \forall t \in T, \forall j \in L, x \in \{d, e\} \tag{4.36}$$

$$h_{t,j}^{PH,x} = h_{t-1}^{PH,x} \cdot \eta^{PH,x} + h_{t,j}^{x+} - h_{t,j}^{x-}, \forall t \in T, \forall j \in L, x \in \{d, e\} \tag{4.37}$$

In this modeling it is assumed that the average heat loss rate is proportional to the stored heat.

Given that the 'pre-heating' in district heating pipelines is simplified as a storage model as given in Equation (4.37), which means that the thermal energy in the pipelines can be kept as long as needed while considering heat losses. It should be emphasised that this may lead to inaccuracy compared to realistic cases. As the water in the pipelines keep flowing all the time, it can be pre-heated, but it cannot be stored indefinitely. In any case the storable energy in the pipelines is not considerable, about one or two hours' worth of heat consumption. On the other hand, the district heating connected buildings also have a thermal storage in their envelopes just like 'end-use heating systems'. In both cases, only houses with a large mass have a meaningful amount of storage (without a dedicated thermal storage). In this model, we use "The share of participating houses" ($\alpha^{PH,x}$) to represent the houses that have the potential to do pre-heating, or with good insulation and a large mass of envelope which can provide a meaningful amount of storage. By doing sensitivity studies, we can investigate the impact of preheating with different contribution on the investment and operation of the integrated electricity and heat system.

The storage loss is actually not in relation to amount of stored heat in buildings. It is a function of the temperature difference between the building and the ambient. The higher the temperature difference, the faster the pre-heated thermal energy will dissipate from the building envelope. This is of course a bit rough, since buildings have a complicated envelope and the heat loss is also affected by the ground temperature, solar gains and wind speed, etc. In this thesis, we make the simplification that the average heat loss of the considered buildings (with good insulation to do pre-heating) is proportional to the stored heat. Since there are significant uncertainties about the average heat loss rate, we have performed sensitivity studies to investigate the benefits through pre-heating under different heat loss rate, which are presented in the later sections.

4.2.2.3 Energy Production

1) Generation unit constraints:

The constraints associated with generation unit operation are based on the whole-system analysis of the electricity system planning presented in [48], as presented as following:

Minimum stable generation and maximum output. As formulated in (4.38), generation plant of different categories are modelled individually, with identical thermal plants being clustered into groups. This model requires one set of integer variables (μ) for each group of plants,

$$\mu_{t,i,j} \cdot \underline{p}_j^g \leq p_{t,i,j}^g \leq \mu_{t,i,j} \cdot \overline{p}_j^g, \forall t \in T, \forall i \in G, \forall j \in L \tag{4.38}$$

where μ denotes the number of synchronized generation units; p^g denotes the electricity output of generators; $\underline{p}^g$ and $\overline{p}^g$ represent the minimum stable and maximum generation, respectively.

Ramp-up and ramp-down constraint. As formulated in (4.39) and (4.40), this model considers the restriction of ramping rate of generation units,

$$p_{t,i,j}^g - p_{t-1,i,j}^g \leq \mu_{t,i,j} \cdot r_i^{up}, \forall t \in T, \forall i \in G, \forall j \in L \tag{4.39}$$

$$p_{t-1,i,j}^g - p_{t,i,j}^g \leq \mu_{t,i,j} \cdot r_i^{dn}, \forall t \in T, \forall i \in G, \forall j \in L \tag{4.40}$$

where r^{up} denotes the limit of ramp-up rate while r^{dn} denotes the limit of ramp-down rate.

Start-up and shut down constraints. The number of starting-up and shutting-down units are determined by (4.41) – (4.44),

$$\mu_{t,i,j}^{st} \geq \mu_{t,i,j} - \mu_{t-1,i,j}, \forall t \in T, \forall i \in G, \forall j \in L \tag{4.41}$$

$$\mu_{t,i,j}^{st} \geq 0\ , \forall t \in T, \forall i \in G, \forall j \in L \tag{4.42}$$

$$\mu_{t,i,j}^{dn} \geq \mu_{t-1,i,j} - \mu_{t,i,j}, \forall t \in T, \forall i \in G, \forall j \in L \tag{4.43}$$

$$\mu_{t,i,j}^{dn} \geq 0, \forall t \in T, \forall i \in G, \forall j \in L \tag{4.44}$$

where μ^{st} and μ^{dn} denote the number of starting-up and shutting down generation units, respectively.

Minimum on-line and off-line time. As presented in (4.45) – (4.47), the minimum on-line and off-line time of generation units are restricted into a given length of time,

$$\sum_{k=t-\underline{Up}_i}^{t-1} \mu_{k,i,j}^{st} \leq \mu_{t,i,j}, \forall t \in T, \forall i \in G, \forall j \in L \tag{4.45}$$

$$\mu_{t,i,j} \leq \overline{\mu}_{t,i,j} - \sum_{k=t-\underline{Dn}_i}^{t-1} \mu_{k,i,j}^{dn}, \forall t \in T, \forall i \in G, \forall j \in L \tag{4.46}$$

$$\mu_{t,i,j} \leq \overline{\mu}_{t,i,j}, \forall t \in T, \forall i \in G, \forall j \in L \tag{4.47}$$

where $\underline{Up}$ denotes the minimum on-line time; $\underline{Dn}$ denotes the minimum off-line time; while $\overline{\mu}$ represents the total number of the *i*th type of generation units, which is determined by Constraint (4.47).

The availability of ancillary service. Constraint (4.48) ensures that generation units leave some room for the provision of frequency response and operating reserve,

$$\mu_{t,i,j} \cdot \underline{p}_j^g \leq p_{t,i,j}^g + rsp_{t,i,j}^g + res_{t,i,j}^g \leq \mu_{t,i,j} \cdot \overline{p}_j^g, \forall t \in T, \forall i \in G, \forall j \in L \tag{4.48}$$

where rsp^g and res^g denote the frequency response and operating reserve that can be provided by the generation units.

Maximum reserve and response provided by each generation technology. Constraints (4.49) and (4.50) limit of the availability of reserve and response service, which may significant vary with the type of generation,

$$res_{t,i,j}^{g} \le \mu_{t,i,j} \cdot \overline{res}_{i,j}^{g}, \forall t \in T, \forall i \in G, \forall j \in L \tag{4.49}$$

$$rsp_{t,i,j}^{g} \le \mu_{t,i,j} \cdot \overline{rsp}_{i,j}^{g}, \forall t \in T, \forall i \in G, \forall j \in L \tag{4.50}$$

where $\overline{res}^{g}$ and $\overline{rsp}^{g}$ are given as a percentage of the maximum output of generation units, representing the upper limit of the provision of reserve and response service.

Annual energy production of generation limits. As formulated in (4.51), we take into account the annual availability of thermal generation associated with scheduled inspection and maintenance,

$$\sum_{t=1}^{T} p_{t,i,j}^{g} \le \overline{AAF}_{i} \cdot \tau \cdot cap_{i,j}^{g}, \forall i \in G, \forall j \in L \tag{4.51}$$

where $\overline{AAF}_{i}$ denotes the annual availability factor of different generation, given as a percentage of the maximum operating hours τ.

Total capacity of different generation technologies. Constraint (4.52) determines the total capacity of different generation (cap^{g}),

$$\mu_{t,i,j} \cdot \overline{p}_{j}^{g} \le cap_{i,j}^{g}, \forall t \in T, \forall i \in G, \forall j \in L \tag{4.52}$$

2) CHP operating constraints:

The operating area of CHP is illustrated in Figure 4.4, which is modelled by (4.53) and (4.54). CHP can change its heat and electricity ratio by adjusting the amount of steam extracted from the turbine, the slope of the upper bound (equal to $-1/z$) gives the ratio of the change of electricity output to the corresponding change of heat output. For a given fuel feeding rate, if the steam extraction changes, operating points will move along the lines which are parallel with the upper bound. For any point (A) within the operating area, there is a corresponding point (A') on the y-axis which is characterized by the same fuel feeding rate as A ($\overline{AA'}$ is parallel with the upper bound) [30]. In order to apply the generation model which is formulated in

(4.38) – (4.52) to CHP, all the operating points of CHP are converted into the corresponding points on the y-axis (electricity-only mode), as shown in (4.55),

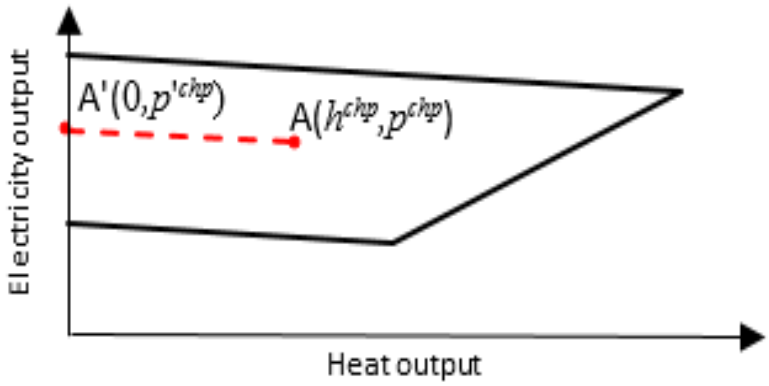

Figure 4.4– Operating area of CHP

$$\mu_{t,i,j} \cdot \underline{p}_j^{chp} \le p_{t,j}^{chp} + h_{t,j}^{chp}/z_j \le \mu_{t,i,j} \cdot \overline{p}_j^{chp}, \forall t \in T, \forall i \in G, \forall j \in L \quad (4.53)$$

$$h_{t,j}^{chp} \le \lambda_j \cdot p_{t,j}^{chp}, \forall t \in T, \forall j \in L \quad (4.54)$$

$$p_{t,i=CHP,j}^{g} = p'^{chp}_{t,j} = p_{t,j}^{chp} + h_{t,j}^{chp}/z\,, \forall t \in T, \forall j \in L \quad (4.55)$$

1. RES curtailment:

The deployment of variable renewable energy sources is crucial for decarbonizing the energy system. In this study, wind and PV generation are taken into consideration. Due to the mismatch between the energy demand and the availability of RES, curtailment will constantly occur without the support of various ancillary services, leading to significant energy losses. The curtailment of RES is formulated as the difference between the available RES power (vre^{ava}) in (4.56) and the actual output of RES (vre) in (4.57),

$$vre_{t,i,j}^{ava} = vre_{t,i,j}^{af} \cdot cap_{i,j}^{g}\ , \forall t \in T, \forall j \in L, i \in \{wind, solar\} \quad (4.56)$$

$$vre_{t,i,j} \le vre_{t,i,j}^{ava}\ , \forall t \in T, \forall j \in L\ , i \in \{wind, solar\} \quad (4.57)$$

4.2.2.4 Ancillary Service

This model takes into account the requirement of frequency response for the electricity system, which is typically driven by the effect of reduced system inertia with high penetrations of RES. To be more specific, the expected trend that intermittent renewable energy will gradually substitute conventional generation will lead to a decrease in the inertia of the electricity system provided by rotating synchronous units. As a consequence, more frequency response will be required to maintain the frequency within the regulatory bounds, driving an increase in the part-load rate of generators, leading to reduced efficiencies of generation. In this context, the supplementary frequency response provided by the heat system will significantly enhance the operational performance of conventional generation, reducing the integration cost of RES. The requirement of frequency response which covers delivery time frame from secondly to hourly scale for different levels of electricity load and RES output in the UK system is determined exogenously in [54] and applied as input.

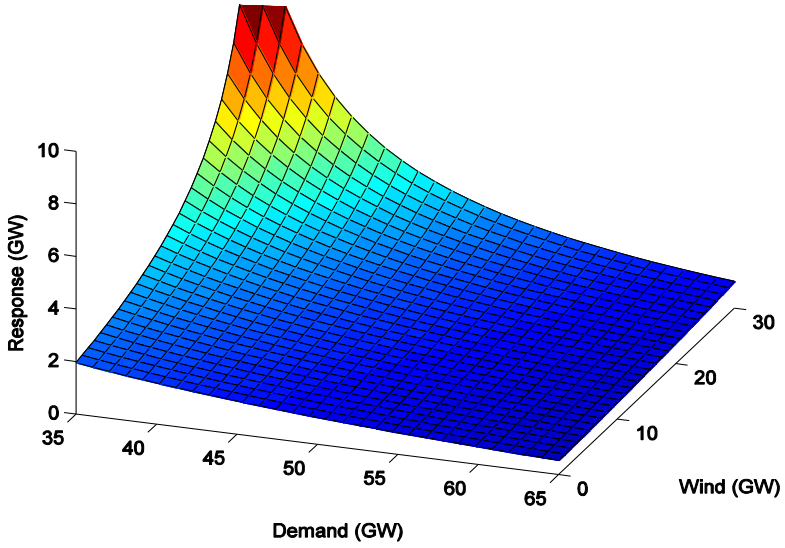

Figure 4.5– Requirement of frequency response for different levels of electricity load and RES output in the UK system

Two key categories of balancing services are considered in this model, including frequency response, which is delivered in a few minutes to half an hour; and operating reserve, which is typically sub-categorized into spinning and standing reserve, with the delivery time of half an

hour to several hours [48]. Multiple sources of uncertainty (including renewables output and generation outage) need to be considered in order to adequately capture the challenges on the operation of future low carbon power system, which has been investigated in our previous work regarding the electricity system [48]. In this model, we follow the frequency response modelling in our previous work [54] which tackles sudden generation or transmission loss. As presented in [54], the frequency response is required to limit the frequency nadir above the limits (49.2Hz in this case) after sudden generation outage, which is becoming harder to fulfil due to declining system inertia and reduced responsive generating units. The increasing operating reserve driven by the forecasting error of renewable and load as well as the replacement of primary response is also incorporated as constraint for each time interval.

The frequency response constraint and operating reserve constraint are formulated as (4.58) and (4.59), respectively. Hence technologies in district heating (through CHPs and HPs) as well as end-use heating systems could provide ancillary services for the electricity system based on these constraints,

$$\sum_{i=1}^{G}\sum_{j=1}^{L} rsp_{t,i,j}^{g} + \sum_{i=1}^{H_d}\sum_{j=1}^{L} rsp_{t,i,j}^{d} + \sum_{i=1}^{H_e}\sum_{j=1}^{L} rsp_{t,i,j}^{e} \geq \underline{FR}_t, \forall t \in T \tag{4.58}$$

$$\sum_{i=1}^{G}\sum_{j=1}^{L} res_{t,i,j}^{g} + \sum_{i=1}^{H_d}\sum_{j=1}^{L} res_{t,i,j}^{d} + \sum_{i=1}^{H_e}\sum_{j=1}^{L} res_{t,i,j}^{e} \geq \underline{OR}_t, \forall t \in T \tag{4.59}$$

The frequency response requirement is directly linked with the level of system inertia in each time interval, which is critical in the future low inertia system. This requirement is derived based on our previous work in [54]. Although a complete MILP formulation (4.60) was proposed in [55], which uses a piecewise linear version of the constraint to reduce the computational burden of the proposed large-scale model,

$$R \geq \frac{\Delta P_L \cdot \Delta P_L \cdot T_d}{4 \cdot \Delta f_{max} \cdot H} \tag{4.60}$$

where H is the system inertia from thermal plants, ΔP_L is the largest generation loss, T_d is delivery time of response, Δf_{max} is the maximum frequency deviation at nadir. The online capacity of synchronous generators is linear to the level of system inertia. The piecewise function of frequency response is demonstrated in Figure 4.6.

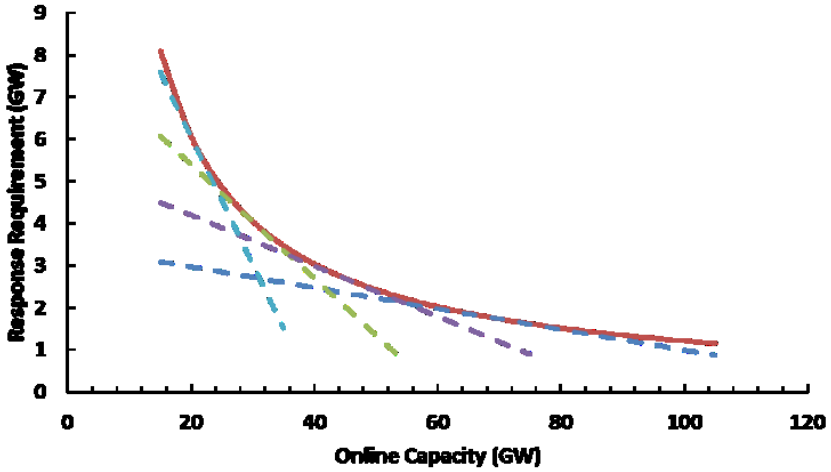

Figure 4.6– Piecewise linear function of frequency requirement of the system

Operating reserve requirement ($\underline{OR}$) is determined by forecasting errors of wind output, PV output, electricity load and the capacity of the largest generator, as formulated in (4.61),

$$\underline{OR}_t = \varsigma^W \cdot vre_t^W + \varsigma^{PV} \cdot vre_t^{PV} + \varsigma^D \cdot p_t + Cap^L, \forall t \in T \tag{4.61}$$

where ς^W, ς^{PV} and ς^D denote the forecasting errors of wind output, PV output and electricity load; vre^W, vre^{PV} and p denote wind output, PV output and electricity load, Cap^L denotes the capacity of the largest generator. Note that, in this model, we take into account the availability of operating reserve to cover the worst case of generation shortage, but the delivery of reserve is not modelled. Therefore, forecasting errors cannot be mitigated by the reserve in our model. A two stage model considering realization is more suitable for the consideration of reserves addressing forecasting errors. However, limited by the complexity of our model, we only consider the reserves required to deal with the uncertainty of the system generation. Similar simplification is commonly made in previous research (e.g., [48] and [56]).

It should be noted that there is no direct constraint on the share of non-synchronous generation, but this is actually considered by the inertia-dependant frequency response requirement. According to [54], the more non-synchronous generators are online, the lower inertia the system has. Meanwhile, only synchronous generators can provide inertia to the system. Therefore, there must be adequate synchronous generators to provide enough inertia to keep the system operation stable. Constraint (4.58) exactly ensures that adequate amount of synchronous generation is scheduled to operate in order to provide sufficient level of inertia.

4.2.2.5 Network Investment Constraints

1) Distribution network reinforcement constraint:

Based on the distribution network reinforcement model presented in [48], the cost of reinforcing distribution networks is formulated as a function of the expanded capacity of the distribution network (cap^{DN}). A schematic function of the distribution network reinforcement cost has been illustrated in [48], while a linear approximation of this function is applied in this section as shown in (4.2). $cap^{DN}$is determined by the net increase of peak demand within the distribution network, as shown in (4.62),

$$-cap_i^{DN} \leq \alpha_i^p \cdot p_t - \sum_{j \in DN_i} p_{t,j}^g - \overline{cap}_i^{DN} \leq cap_i^{DN}, \forall t \in T, \forall i \in DN \tag{4.62}$$

It is assumed that CHP and PV are deployed in the distribution network. The cost coefficient (C^{DN} in the objective function) is derived through the analysis of the network reinforcement cost driven by the increase in peak demand by applying the fractal-based algorithm proposed by [22]. The created representative distribution networks based on this algorithm have been calibrated by the analysis of the corresponding real distribution networks. Although the parameters of real networks are very case-specific and vary significantly, the analysis of the large regions characterised by the representative networks provides an estimate of the real network reinforcement cost. The design parameters of the representative networks represent those of real distribution networks of similar topologies, for instance with regards to the number and type of consumers and load density (e.g. high-load density city/town networks to low-density rural networks), associated network lengths and costs, etc. As described in [57], key

typical representative distribution networks, covering urban, sub-urban, semi-rural, or rural areas, are created by using the fractal-based algorithm and are incorporated into this model. Figure 4.7 gives examples of the distribution networks created by using the fractal-based algorithm.

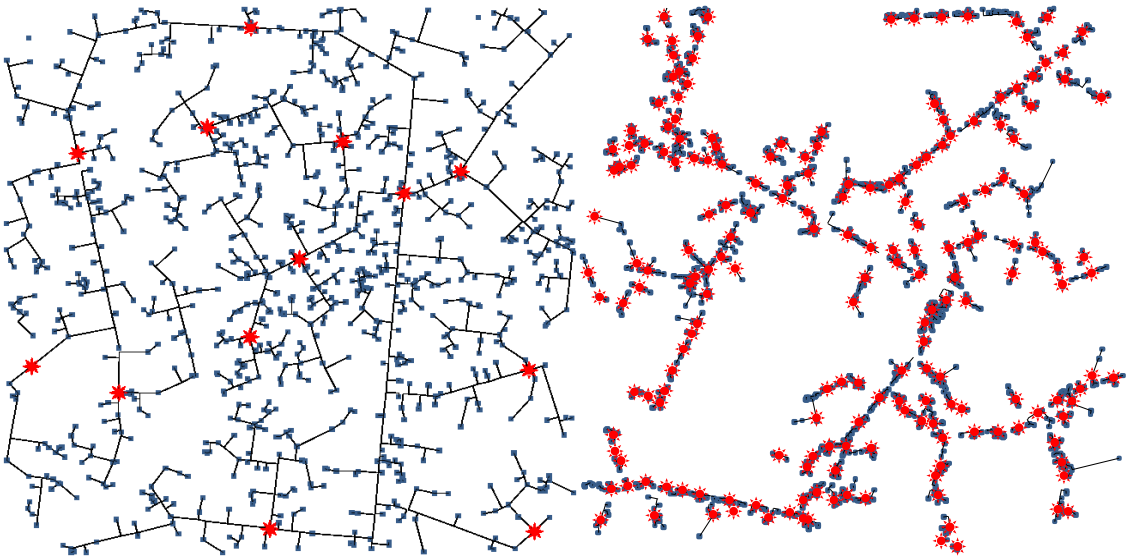

Figure 4.7– Representative networks of (a) urban area and (b) rural area

2) Heat network investment cost:

As the key indicator of DHN investment cost, heat density is used to compartmentalize the whole GB area into different district types covering urban, suburban, semirural and rural areas. By using the fractal-based algorithm proposed in [22], generic heat networks are created covering representative districts with different heat densities. The number of consumers and heat demand in representative districts are obtained from the National Heat Map [26] and applied as inputs into the fractal-based algorithm to establish the topologies and further calculate the length of the representative heat networks which drives their investment costs. Equation (4.63) determines the capital cost of representative HNs,

$$IC_i^{HN} = C_i^{DN} \cdot F_L^{HN}\left(A_i, N_i^h, \sum_{t\in T} h_{t,i}\right) \ , \forall i \in HN \tag{4.63}$$

where C^{DN} denotes the capital cost (per unit length) of HNs while $F_L^{HN}(\cdot)$ calculates the length of representative HNs based on the fractal-based algorithm, given the size of area, number of consumers and heat demand in the representative districts. Appendix Table A.5 demonstrates the length of different representative HNs.

By applying the approach proposed in [57, 58], the whole GB area is represented by a combination of different types of representative districts, while minimizing the errors of the total heat demand, the number of households and the size of geographical areas between the calculated data and the realistic data. The number of different representative HNs, denoted as N^{HN} in (4.9), has been optimized exogenously, as given in Table A.5. By applying this concept, the investment cost associated with different penetrations of DHN (ω^{HN} in (4.9)) in each representative district can be quantified and then incorporated into the whole system investment model to optimize the share of DHN.

In summary, there are three steps to calculate the DHN cost, the first two steps are carried out exogenously while the third step is a part of the optimization.

Step 1: We choose four representative districts, characterised by urban, suburban, semirural and rural areas. DHN is a potential heating technology for these representative districts. If DHN is deployed in a district (the whole district uses DHN), then the length of pipelines can be calculated based on the fractal-based algorithm proposed in [22] (a more detailed description about this algorithm is demonstrated in Section 2.1). This algorithm can generate the topology of a network given the size of areas (A in km^2), number of consumers (N^h) and heat demand ($\sum_{t\in T} h_{t,j}$). A, N^h and $\sum_{t\in T} h_{t,j}$ can be acquired by National Heat Map (a free online tool, as shown in the left figure). An example of the topology of an urban district is illustrated in the right figure.

The investment cost that is incurred if DHN is deployed in a district can be calculated based on (4.64). Thus, the investment cost for deploying DHN in a representative district is determined.

Step 2: The whole GB area is represented by a combination of these four representative districts, in other words, each representative district is replicated by a number (combination coefficient) to represent all the districts with the same characteristics. The number of each

representative district (N^{HN}) is optimized by minimizing the errors of the total heat demand, the number of households and the size of geographical areas between the calculated data and the realistic data.

Step 3: Equation (4.23) – (4.25) optimize the total penetration of DHNs covering all types of representative districts. The investment cost associated with different penetrations of DHN in each representative district can be then incorporated into the whole system investment model to optimize the share of DHN in each representative district. In (4.9), the total investment cost of DHNs is determined by (4.64),

$$\sum_{i=1}^{HN} \omega_i^{HN} \cdot N_i^{HN} \cdot IC_i^{HN} \tag{4.64}$$

4.2.2.6 Other Constraints:

1) Security requirement

Constraint (4.65) ensures that the model will propose a sufficient generating capacity to achieve a given level of security specified by LOLE. To achieve this, LOLP is estimated as a function of the capacity margin (which is defined as the ratio of the surplus generating capacity to the peak demand, as formulated in (4.66) and is built exogenously through the standard reliability approach by applying generation availability data [48],

$$\sum_{t=1}^{T} F^{LOLP}(CM_t) \leq \overline{LOLE} \tag{4.65}$$

$$CM_t = \frac{\sum_i^G \sum_j^L (\mu_{t,i,j} \cdot \overline{p}_j^g - p_j^g)}{\max\limits_{t \in T} (\sum_{j=1}^L p_{t,j})}, \forall t \in T \tag{4.66}$$

A piecewise linear approximation of the LOLP function was presented in [48], as shown in Figure 4.8. In this model, we apply the linear approximation of the LOLP function as security requirement to optimize the capacity of generation, as formulated in (4.67),

$$F^{LOLP}(CM_t) \geq \alpha_{L,1} \cdot CM_t + \beta_{L,1}$$
$$\vdots \tag{4.67}$$
$$F^{LOLP}(CM_t) \geq \alpha_{L,n} \cdot CM_t + \beta_{L,n}$$

where a^L denotes the linear coefficient term while b^L denote the constant term of the LOLP function.

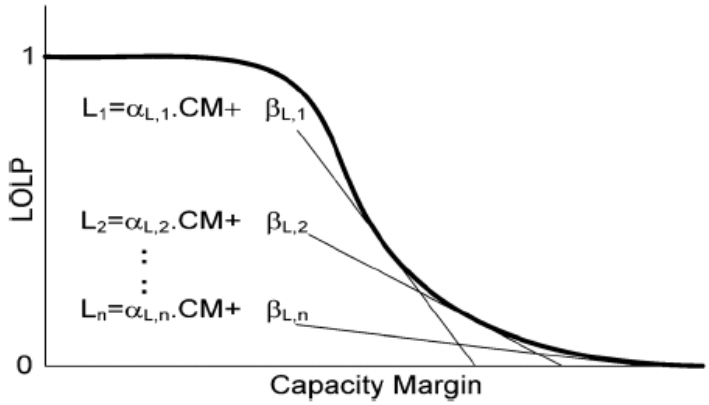

Figure 4.8– Piecewise linear approximation of LOLP function

2) Carbon limit:

The total carbon emission (t/year) is defined as the product of the given overall carbon target (g/kWh) and the annual energy consumption (GWh/year), covering both electricity and heat sectors. In this model, CO2 mainly comes from the conventional generation (CCGT, OCGT) on the electricity side and by CHP and gas boilers on the heat side. In order to meet given carbon targets, low-carbon generations (including nuclear, wind, PV and gas CCS) have to be invested in to alleviate the carbon emission, although these low-carbon generations are characterised by higher capital cost. Constraint (4.68) ensures that the total carbon emissions do not exceed the regulated amount of carbon emissions,

$$\sum_{t=1}^{T}\sum_{i=1}^{G}\sum_{j=1}^{L} CO2_{t,i,j}^{g} + \sum_{t=1}^{T}\sum_{j=1}^{L} CO2_{t,j}^{gb} \leq \overline{CO2} \cdot \sum_{t=1}^{T}\sum_{j=1}^{L}\left(h_{t,j} + p_{t,j}^{heat}\right) \tag{4.68}$$

where $CO2^{g}$ denotes the CO2 emission from various generation; $CO2^{gb}$ denotes the CO2 emission from gas boilers; $\overline{CO2}$ denotes the overall carbon target.

4.3 Conclusions of the Chapter

This chapter proposes a novel modelling framework for the whole system optimisation of the integrated heat and electricity systems, considering operation and investment timescales and covering both local and national level infrastructure.

The proposed MILP optimization model can simultaneously optimize, for the first time, the investment in electricity generation (including conventional and low carbon generation as well as CHP), heating devices, heat networks, reinforcement of electricity transmission and distribution networks while minimizing the system operation cost, taking into account frequency response and operating reserve requirements. The impact of integrated systems reducing system inertia on the frequency response requirement is explicitly modelled in the constraints. Carbon emission and security constraints are also included.

A variety of operation constraints are taken into account, including: electricity and heat balance constraints, heating technology mix constraints, power flow constraint, DSR constraints, TES operating constraints, pre-heating constraints, generation unit constraints, RES curtailment constraints, ancillary service constraints, CHP operating constraints, distribution network reinforcement constraint, heat network investment cost constraints, system security constraints, and carbon constraint. Specifically for ancillary service constraints, this model takes into account the requirement of frequency response for the electricity system, which has been modelled exogenously and applied as input in this model.

This proposed integrated heat and electricity system investment model can be applied to optimize the heating technology portfolio to decarbonise the integrated heat and electricity systems, and assess the values of the integration of electricity and heat system and revealing trade-offs between electrification of heat sector through HNs and through electrified heat at the consumer end side.

Chapter 5 Evaluation of Alternative Heating Decarbonisation Strategies

To achieve the goal of Climate Change Act 2008, almost all the heat for domestic usage should be decarbonised by 2050, as a result, the low-carbon technologies for heating must be adopted in the future heating system. Attractive low-carbon heating technologies including district heating, HP, and thermal storage are not applied in the UK on a large scale. What the benefits and problems they may bring about to the system; how the heat network can interact with the electricity network; what heating technology mix can maximize the economic and operational benefits of the system are the main points of this chapter.

The heat sector accounts for approximately half of the total energy consumption in the UK. In order to meet the target of 80% carbon reduction by 2050, alternative heating technologies are required to replace gas boilers that currently predominate in the UK. Electric HPs, hybrid heating technologies, DHNs and hydrogen boilers are promising low-carbon heating technologies that can potentially deliver the carbon target [9, 59-61], whereas the comparison of their economic competitiveness, which is crucial for their large-scale deployment, remains unknown. Due to the interactions between heat system and electricity system, the investment strategy of various heating technologies can bring significant impacts to electricity sectors. This leads to the need of the joint optimisation of heat and electricity system investment. Given that the lack of flexibility in the electricity system is a key factor that limits the integration of RES [62-64], heat systems can potentially deliver substantial amount of flexibility by providing various balancing services and support peak demand management [65]. As presented in [33] and [56], district heating can alleviate the curtailment of RES through coordinated operation of multiple components in heat networks (e.g. CHP, TES, electric boilers, etc.). Reference [66] demonstrates an operating model of multiple heat plants feeding heat to DHNs, while the advantages of the deployment of industrial-sized HPs in DHNs are presented in [67-69]. In regard to end-use heating technologies with low-carbon potentials, research [70-74] are

focused on the analysis of hybrid heating technologies on the consumer side, with the potential to connect HPs, gas boilers and resistive heating devices through smart control. The economic and operational performances of different hybrid heating technologies are elaborated in [71], manifesting significant economic advantages through the deployment of hybrid electric HPs and gas boilers (Hybrid HP-B). The authors in [75] demonstrate the potential benefits of hydrogen for the operation of the electricity system. Due to the thermal inertia of pipework, DHNs can provide flexibility to the electricity system [76]. Moreover, supported by TES which is characterized with significantly lower capital cost than electricity storage, the value of DHNs can be further enhanced through coordinated operation with electricity systems [77]. Similarly, the performance of TES supporting end-use heating appliances is discussed in [71]. Previous research regarding the planning of DHNs is mainly focused on the local level [78-80], while the national level infrastructure is barely considered. A whole-system approach is presented in [48] to optimize the investment of the electricity system where only electric HP is considered for decarbonizing the heat sector. In this context, this chapter applies the integrated electricity and heat system investment model proposed in Chapter 4 for assessing the economic performance of various heat decarbonisation strategies. Compared to the previous developed model for multi-energy system planning (e.g., Balmoral model), this model can cover both local district and national level infrastructures while taking account of the impact of reduced electricity system inertia on the frequency response requirements. Moreover, carbon emission restrictions can also be considered to investigate the economic performance of alternative heating strategies under specific carbon scenarios.

This chapter firstly describes the testing system and relative assumptions, and then applies the proposed integrated electricity and heat system investment model to assess the economic characteristics of different heating technologies for decarbonizing the heat sector and the consequential impacts on the investment and operation of the electricity system. Specifically, a set of comprehensive case studies are carried out to 1) compare the annual system cost coving multiple sectors under the heating strategies of HP-only (electric HP is the only option of heat provision), hybrid HP-Bs, DHNs and hydrogen boilers; 2) analyse the impact of different heating strategies on the electricity system; 3) present the optimized portfolio of heating technologies to achieve the decarbonisation; and 4) demonstrate the impact of building energy efficiency on the economic performance of the optimal heating strategy.

5.1 System Description and Assumptions

5.1.1 Simplified Topology of the GB System

In this chapter, the impacts of different heating technologies on the whole system is evaluated on a simplified GB system in which the transmission system is represented by five key regions, including 1) Scotland, 2) North England and Wales, 3) Middle England and Wales, 4) South England and Wales and 5) London (embedded within the South England and Wales region), characterised by a dramatic north to south power flow. Figure 5.1 illustrates the topology of the simplified network together with the length and existing capacity of the transmission corridors connecting the key regions. In each of the regions, appropriate combinations of representative networks characterised by different load density are taken into account to represent the aggregated DHNs and electricity distribution networks, following the approach proposed in [57].

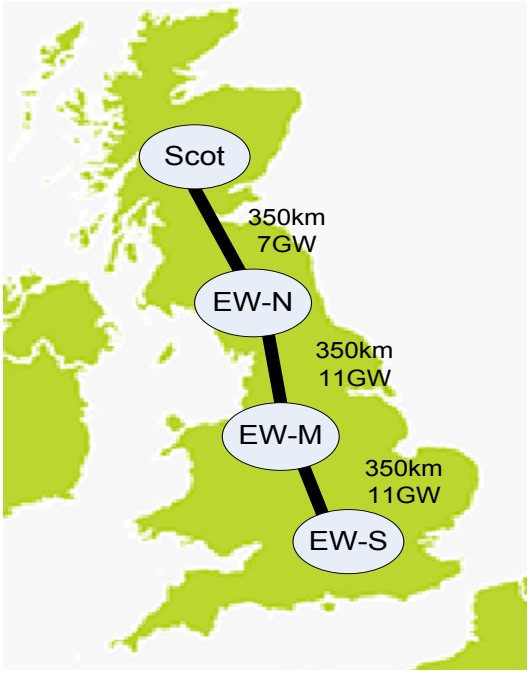

Figure 5.1– Schematic topology and the existing capacity of the GB transmission links between the key regions

The investment cost of electricity distribution and heat networks are represented as functions of electricity and heat demand (these functions are created through exogenous modelling) and

incorporated into the system optimization model. The penetration of different heating technologies (e.g., heat networks, end-use HPs) can be optimized for each region. Distribution networks in different voltage levels are considered. The impact of CHP and industrial HP on the reinforcement of HV distribution networks is also taken into account.

For electricity generation, conventional technologies (including CCGT and OCGT) and low-carbon technologies (potentially including wind, PV, nuclear and CCS) are considered in the investment optimization. The availability factor of wind and solar generation are illustrated in Fig. A.1 and Fig. A.2. Generation plant of different categories are modelled individually, with identical thermal plants being clustered into groups. The proposed model requires one set of integer variables for each group of plants. Since a large amount of existing fossil fuel based generators have to be decommissioned to achieve the significant progression to a low-carbon system, it would not be straightforward to compare the generation mix across different scenarios based on the existing generation system. Therefore, we applied a simplified electricity system model without taking account of the existing generation capacity in the UK. The key point of this work is to provide general comparisons among different types of heating strategies, which can be potentially applied in different countries. For heat generation, the comparisons of economic performance across DHN, HP-only and hybrid heating are the focus of this chapter.

5.1.2 Energy Demand Assumptions

Heat demand has a key influence on the investment of assets in terms of supply, delivery and end-use appliance. However, there is a lack of national-level heat demand profile on an hourly basis. This chapter applies the heat demand model constructed in [59], which is derived from actual heat profiles covering different types of properties and adjusted by the temperature and daily gas consumptions with the diversity of load considered. Heat profiles under three temperature scenarios (mild, normal and cold) in different future years are created. In this chapter, we select the “normal” scenario in 2030 to simulate the annual operation cost. Since the life span of generation and heating assets is usually more than 20 years, the investment planning has to guarantee that the size of all assets is always adequate to cover the peak demand over their life span. As the peak demand is a key driver of the investment cost, we add 3 extreme

days (where the demand is 20% higher than the 3 days with the highest demand in the "cold" scenario) at the end of the time series of the "normal" scenario) to achieve the redundancy of the planning. Additionally, it is assumed that 77% of annual heat demand is for space heating while 23% for water heating [71]. The final peak heat demand is estimated at 247 GW and the minimum demand is 4GW, with total annual heat energy consumption of 371 TWh, as shown in Figure 5.2.

The electricity demand is divided into non-heat electricity demand and heat-driven electricity demand. The maximum non-heat electricity demand is estimated at 72GW while the minimum demand at 19GW, with annual energy of 325TWh, as shown in Figure 5.2. The heat-driven electricity demand depends on the optimized electrification rate of heat demand.

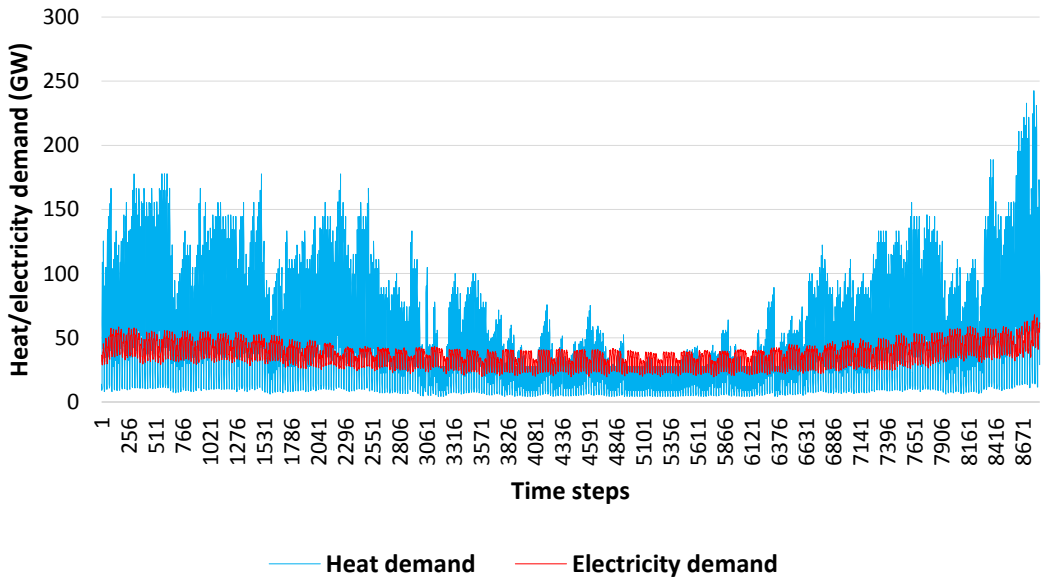

Figure 5.2– UK heat and electricity demand

5.1.3 Economic and Operational Parameters of Different Technologies

Cost and operation data for different types of generation are listed in Appendix Table. A.7 [81, 82], Table. A.8 [62, 81] and Table. A.9 [62], while the data for heating technologies are given in Table. A.10 [71, 83]. It is worth noticing that: (i) the efficiency of ASHP is temperature-dependant, a linear cost model for ASHP is applied as shown in Figure 5.3, considering a constant instalation cost for any size of ASHP; (ii) the capital cost of industrial HP includes

both equipment and installation (more details about the technical and economic data of industrial HP can be accessed in [84]); (iii) as gas boilers have already been installed in most residential houses in the UK, we assume that the deployment of hybrid HP-B does not incur investment cost of gas boilers. On the other hand, the cost of the smart control device that is required to optimize the operation of hybrid HP-B between ASHPs and gas boilers is considered (80£/household according to [71]).

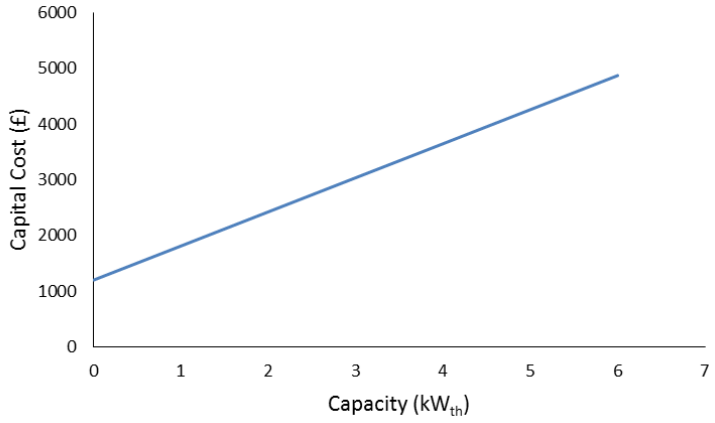

Figure 5.3– Capital cost of HPs

In terms of the deployment of hydrogen, the capital cost of electrolysis is 586£/kW while the hydrogen storage 15£/kW [17]. It is also assumed that the present NG boilers can be upgraded to fit hydrogen with a cost of 80£.

TES can be deployed for both end-use heating and district heating, the prices of which are estimated at 2.4£/litre and 80£/m3, respectively [84] (installation, O&M costs, etc., are included), with the same stationary loss rate of 1% per hour [71]. It is also assumed that the ratio of the energy capacity to the power rating of TES (ε^s) is 3 hours for end-use TES and 6 hours for industrial-sized TES, as given in Table. A.11. Relative parameters of representative heat networks and distributed networks are estimated in Table. A.5 [27] and Table. A.12 [57]. Since the annual energy consumption of circulation pumps in DHN is much lower than the annual heat losses under the variable flow operating mode [8], it is considered as additional heat losses. The total heat loss in DHN is thus estimated at around 5% of the total heat distribution [85, 86]. It should be stressed that different results can be obtained based on different cost assumptions, but the model can be applied in different scenarios.

Two carbon scenarios, 100g/kWh and 50g/kWh, are analysed in which the total carbon emission is quantified from all generation sources covering both electricity and heat sector. It is assumed that the gas price is projected at 68p/therm in the 2030 scenario while a carbon price of 78£/t is added to the fuel price of generation for the sake of facilitating the deployment of low-carbon technologies.

5.2 Economic Performance of Different Heating Technologies

This section quantifies the economic performance of different heating strategies (as listed in Table 5.1) under the given carbon scenarios by analysing the decoupled whole system costs of full deployment of each technology, demonstrating their unique characteristics and giving the optimal portfolio of heating technologies [87, 88].

Table 5.1 – Description of different heating strategies

Case of Heating strategy	Description
Hybrid HP-B	All residential heat demand is supplied by hybrid HP-B. The size of HP and gas boiler is optimized by the methodology presented in Chapter 4.
HP-only	All residential heat demand is supplied exclusively by ASHP. The size of a single ASHP can cover the peak demand of individual households.
DHN	All residential heat demand is supplied by DHN. The size of each heat plant applied in DHN is optimized by the methodology presented in Chapter 4.
Hydrogen Boiler	All residential heat demand is supplied by hydrogen Boilers. The size of a single hydrogen Boiler can cover the peak demand of individual households.
Optimal portfolio	Residential heat demand can be potentially supplied by hybrid HP-B, ASHP and DHN, the penetrations of which are optimized by the methodology presented in Chapter 4.

In order to avoid the confusion caused by the comparison across multiple heating strategies, we choose hybrid HP-B as the baseline due to its significant economic advantage [71] and compare the other cases with the baseline.

5.2.1 Full Deployment of Different Heating Technologies

Comparison of economic performance between hybrid HP-B and HP-only

Figure 5.4 demonstrates the decoupled annual system costs under full deployment of hybrid HP-B and HP-only in the two given carbon scenarios. Overall, the annual system cost for the deployment of hybrid HP-Bs is about 20.1% lower than for the deployment of HP-only under the carbon target of 100g/kWh and 19.1% lower under the carbon target of 50g/kWh.

To be more specific, the application of hybrid HP-B leads to higher OPEX (represented by red blocks, potentially covering CCGT, OCGT, CHP, gas boilers and gas CCS) against HP-only, due to a significant investment switch from ASHPs to EGB. Since gas boilers require no further investment cost, significant savings are achieved when the hybrid HP-B is fully deployed. A decreased investment in ETES is delivered in the case of hybrid-HP-Bs as the improved flexibility provided by gas boilers weakens the system dependence on ETES. It is worth noticing that most of the benefits through the deployment of hybrid HP-Bs against HP-only is driven by the reduced investment in end-use heating appliance (indicated by blue blocks), while further savings are achieved in 1) distribution networks reinforcement (DN CAPEX) due to significant reduction in peak electricity demand which is compensated by gas-based heat, and 2) OCGT CAPEX, which is also driven by the reduced peak electricity demand. A noticeable increase in LG CAPEX (represented by green blocks) can be observed in the case of hybrid HP-Bs, as a compensation for the extra consumption of fossil fuels (increase in OPEX) in order to meet the carbon limit. Carbon target has a crucial influence on the investment in low carbon generation, consequently impacting the system OPEX.

When improving the carbon intensity target from 100g/kWh to 50g/kWh, it can be observed that the CAPEX of low carbon generation significantly rises while the OPEX remarkably reduces, leading to a minor net increase in the total system cost.

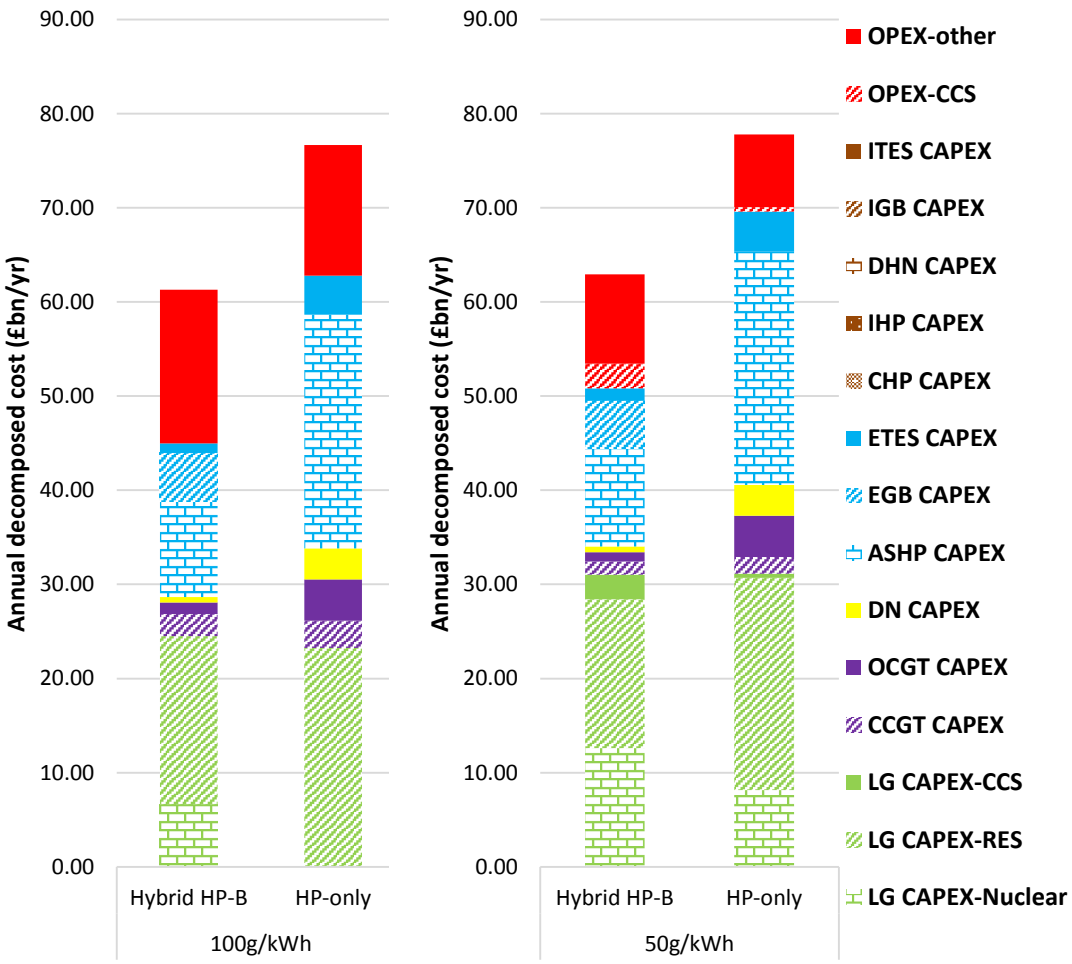

Figure 5.4– Annual decoupled system cost of full deployment of Hybrid HP-B and HP-only

Comparison of economic benefits between hybrid HP-B and DHN

In spite of a low penetration in the present UK system, district heating is a potential alternative of end-use heating (represented by hybrid HP-B) to deliver the ambitious carbon target. Figure 5.5 compares the annual system costs under full deployment of hybrid HP-Bs and DHN in the two given carbon scenarios. Overall, the annual system cost for the deployment of hybrid HP-Bs is about 16.8% (16%) lower than for the deployment of DHN under the carbon target of 100g/kWh (50g/kWh).

It can be further observed that large savings are achieved in OPEX for the case of DHN due to the improved efficiency of district heating plants/devices; A relatively slight reduction in DN CAPEX is achieved when DHN is deployed, as a consequence of the electricity consumption

shift from low voltage distribution network (driven by EHP) to high voltage distribution network (driven by IHP). It is also demonstrated that the application of DHN reduces the investment in CCGT due to the deployment of CHP. Further savings are achieved in LG CAPEX, indicating that the DHN has a higher carbon efficiency which can alleviate the requirement of decarbonizing electricity sectors. In spite of the multiple benefits brought by DHN as analysed above, the huge investment in DHN CAPEX which accounts for approximately 80% of the investment of district heating (represented by brown blocks) dramatically jeopardizes the competitiveness of large-scale deployment of DHNs against hybrid HP-Bs.

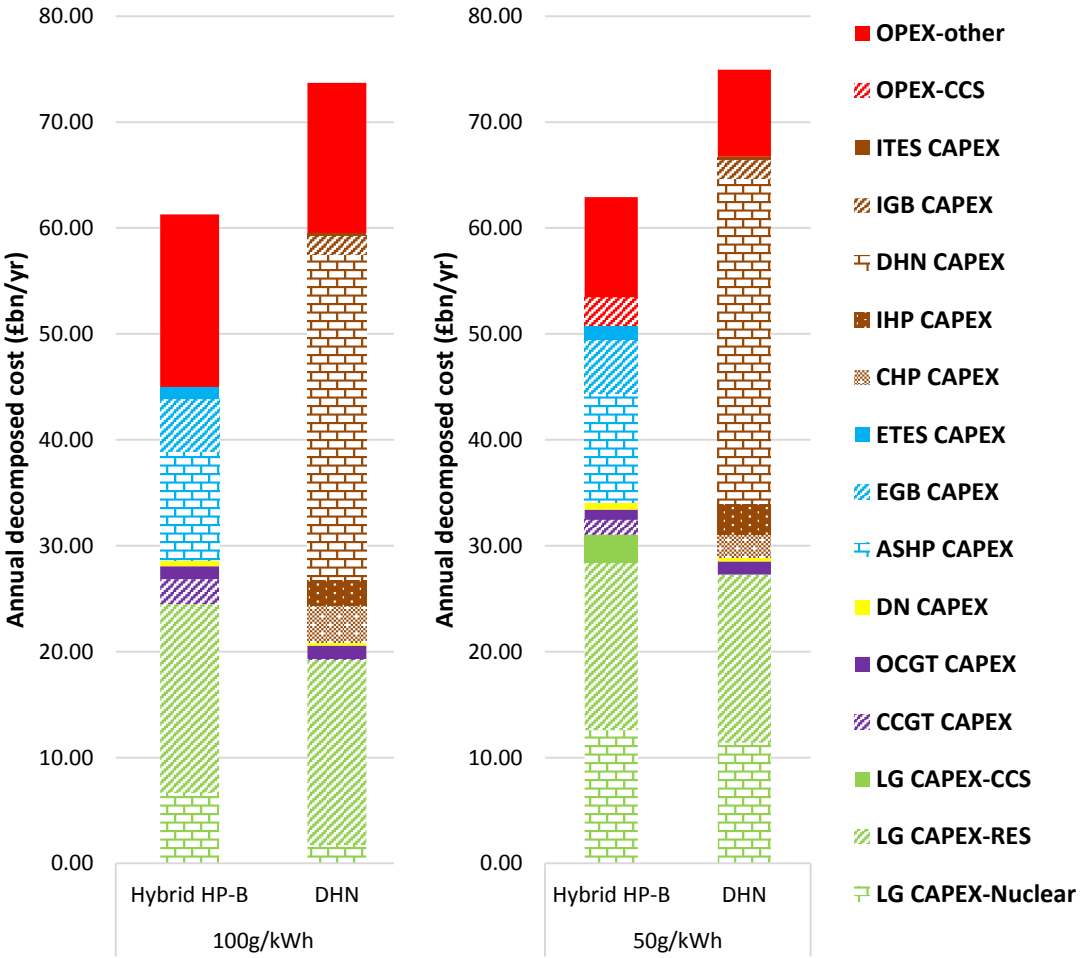

Figure 5.5– Annual decoupled system cost of full deployment of Hybrid HP-B and DHN

However, unlike hybrid HP-Bs whose economical characteristics are virtually geographically independent, the competitiveness of DHN highly depends on the heat density of the deployed

area. Figure 5.5 indicates that it is not advantageous to deploy DHN on the whole scale, but DHN can be more economic than hybrid HP-B in highly populous areas. Therefore, it is essential to give an optimal portfolio of heating technologies while indicating their penetration in different geographical type of areas (e.g. urban and rural).

Comparison of economic benefits between hybrid HP-B and hydrogen boiler

Hydrogen boiler is another potential low-carbon heating technology that can effectively decarbonise the heat sector. SMR and electrolysis of water are regarded as two main methods for industrial bulk production of hydrogen. This section is focused on the investigation of the economic potential of using electrolysis to produce hydrogen, due to its major interactions with the electricity system.

Figure 5.6 demonstrates the decoupled annual system costs under full deployment of hybrid HP-B and hydrogen boilers in the two given carbon scenarios. Overall, the annual system cost for the deployment of hybrid HP-Bs is about 30.4% lower than for the deployment of hydrogen boilers under the carbon target of 100g/kWh and 28.4% lower under the carbon target of 50g/kWh. Therefore, full deployment of hydrogen boilers is the least economic heating strategy to decarbonise the heat sector compared to the other three investigated strategies. Specifically, dramatic increase in the investment of generation can be observed in the case of hydrogen boiler than the other cases, due to increased electricity demand driven by the production of hydrogen and reduced heat efficiency of hydrogen boilers (compared to HPs). Additionally, extra investment in the infrastructure of hydrogen production (i.e., electrolysis plants and hydrogen storage) and end-use appliances (i.e., the upgrade of natural gas boilers to fit hydrogen) are required, further jeopardising the competitiveness of hydrogen boilers. Moreover, it should be emphasised that the cost of upgrading the current gas network to fit the delivery of hydrogen or the investment of new hydrogen network is not taken into account, which can potentially be a major limiting factor of large-scale application of hydrogen. All these results indicate that the application of hydrogen boilers is highly capital-intensive compared to the other heating technologies.

However, it can be noticed that considerable amounts of RES is deployed together with the application of hydrogen boilers, which significantly increases the requirement of OCGT to

serve as back-up capacities. Meanwhile, nuclear and CCS are no longer needed. This is because the coordinated operation of the electrolysis and hydrogen storage can provide remarkable flexibility to the electricity system, thus boosting the integration of RES. This result demonstrates the environmental advantage of electrolysis-based hydrogen in decarbonising the energy system.

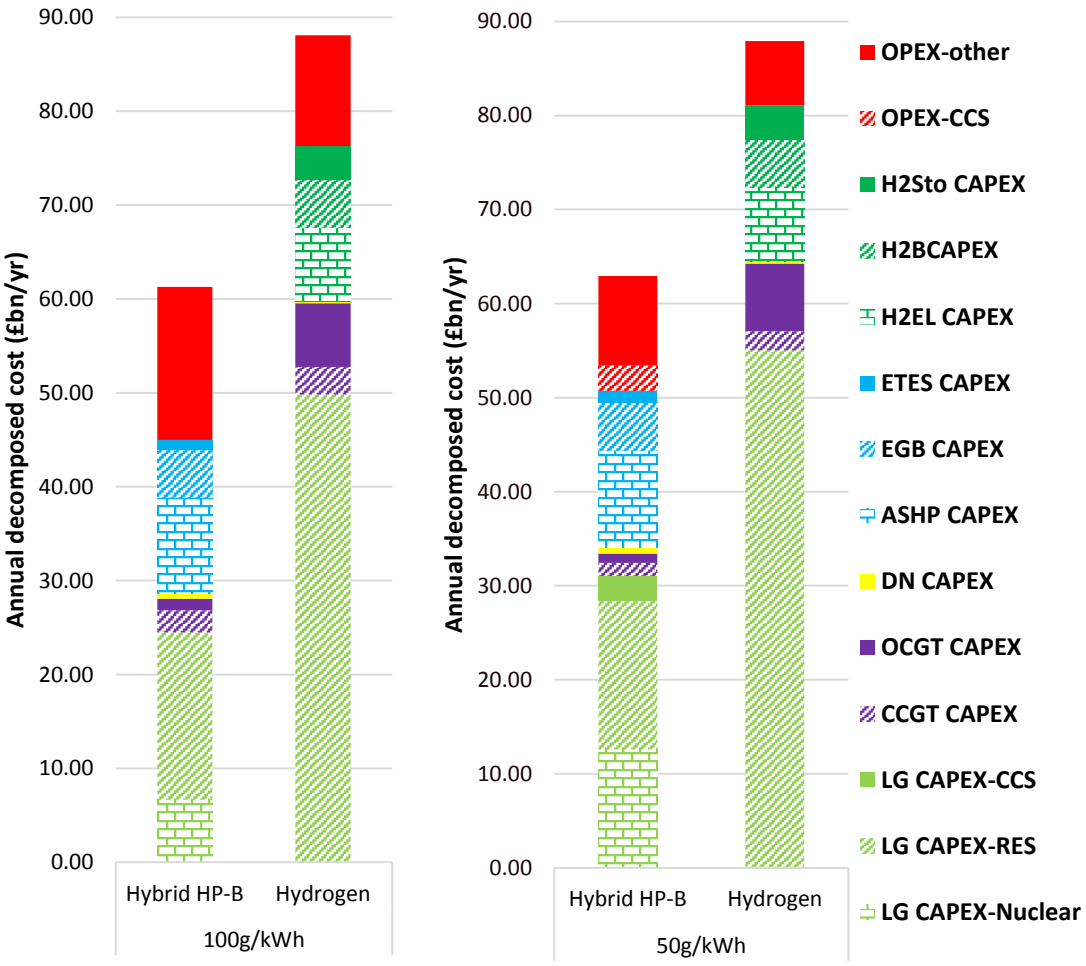

Figure 5.6– Annual decoupled system cost of full deployment of Hybrid HP-B and DHN

5.2.2 The Optimal Portfolio of Heating Technologies

This section optimizes heating technology mix by considering geographic factors that can influence the economic characteristics of DHN and compares the whole system costs of full deployment of hybrid HP-Bs against the economically optimal portfolio of different heating technologies in given carbon targets, as demonstrated in Figure 5.7.

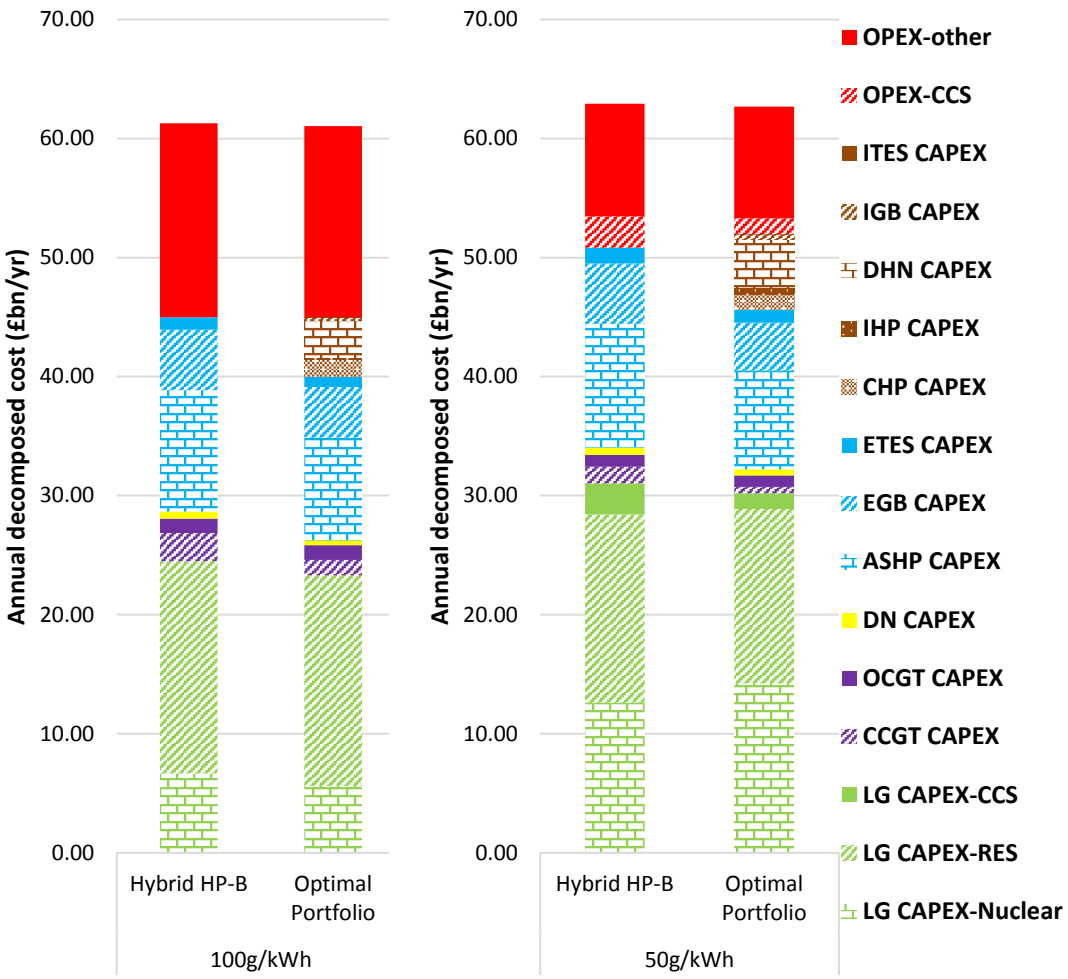

Figure 5.7– Annual decoupled system cost of optimal portfolio and full deployment of Hybrid HP-B

Overall, there is only a minor difference (about 0.4% for both carbon targets) between the total system costs of hybrid HP-B and the optimal portfolio, indicating that limited benefits can be brought in through optimized deployment of DHN and hybrid HP-B based on the assumptions for the UK case.

It is further observed in Figure 5.8 that 16% (21%) of total heat demand is supplied by DHN under the carbon target of 100g/kWh (50g/kWh), where all DHN are deployed in urban areas. DHN covers 41% and 54% of heat provision in urban areas in two given carbon scenarios, manifesting the improved competitiveness of DHN in populous regions. It is worth noticing that the competitiveness of DHN is further enhanced in a more demanding carbon scenario, due to its better performance in decarbonisation.

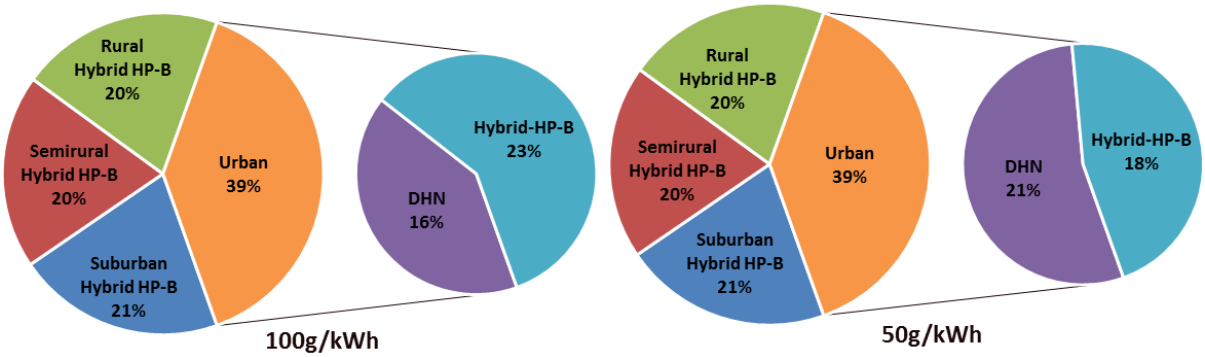

Figure 5.8– Heating technology distribution in each type of areas for the optimal portfolio

HP-only and hydrogen boilers are not used in the optimal portfolio due to their diseconomy under the assumptions in this chapter. However, further simulations show that if the carbon target is tightened to 10g/kWh, 3.22% of heat demand will be supplied by electrolysis-based hydrogen, due to its environmental advantage of boosting the integration of RES.

5.2.3 Sensitivity Studies

The conclusions on the economic performance of different heating strategies drawn from Section 5.2.1 and 5.2.2 are based on the cost assumptions from existing references. However there are significant uncertainties in the cost for these heating technologies which may fundamentally change their competitiveness. This section conducts sensitivity analyses on the cost of ASHP and heat networks which have crucial impacts on the economic performance of different heating strategies.

5.2.3.1 Sensitivity analysis on ASHP cost

Figure 5.9 (a) illustrates the annual whole system cost of different heating strategies in a series of ASHP capital cost scenarios under the carbon target of 100g/kWh (the conclusions are similar for 50g/kWh).

As the system cost of DHN is not related to the cost of ASHP, it keeps stable in the whole cost range. It can be seen that the competitiveness of HP-only is highly sensitive to the variation of ASHP capital cost while the economic performance of hybrid HP-B and the optimal portfolio are much more robust. Figure 5.9 (b) demonstrates the impact of ASHP installation cost on the

annual whole system cost of different heating strategies under the carbon target of 100g/kWh, indicating HP-only and hybrid HP-B have similar sensitivity to the installation cost of ASHP.

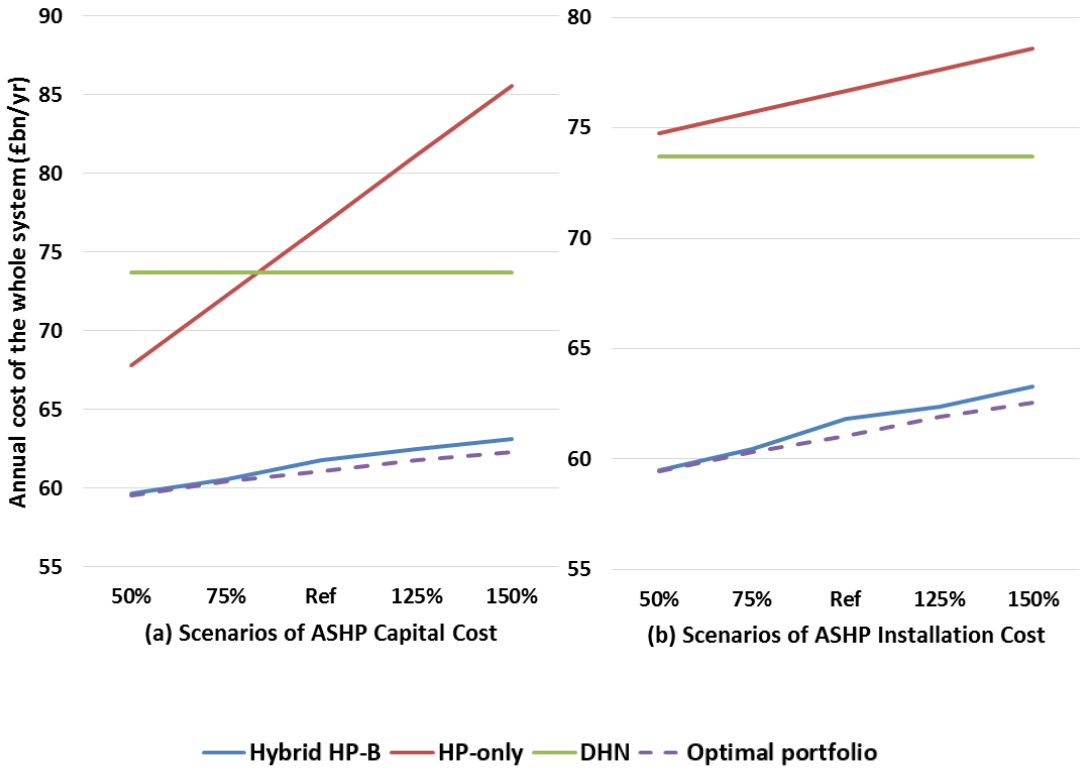

Figure 5.9– Sensitivity study on ASHP capital cost

5.2.3.2 Sensitivity analysis on heat network capital cost

The capital cost of heat networks can be influenced by many factors, e.g. the geological condition of the excavation, the level of existing utility congestion, etc., leading to a significant uncertainty. Figure 5.10 (a) illustrates the sensitivity of different heating strategies to the variation of heat network capital cost. As can be seen, the whole system cost of DHN is dramatically sensitive to the variation of heat network capital cost. When the cost is increased by 15%, the economic advantage for the full deployment of DHN over HP-only is gone. It can be further observed from Figure 5.10 (b) that the optimal penetration of DHN drops rapidly with the increase of heat network capital cost. When the cost climbs by 30%, only 1% of heat demand is supplied by DHN, leaving hybrid HP-B virtually the optimal heating strategy.

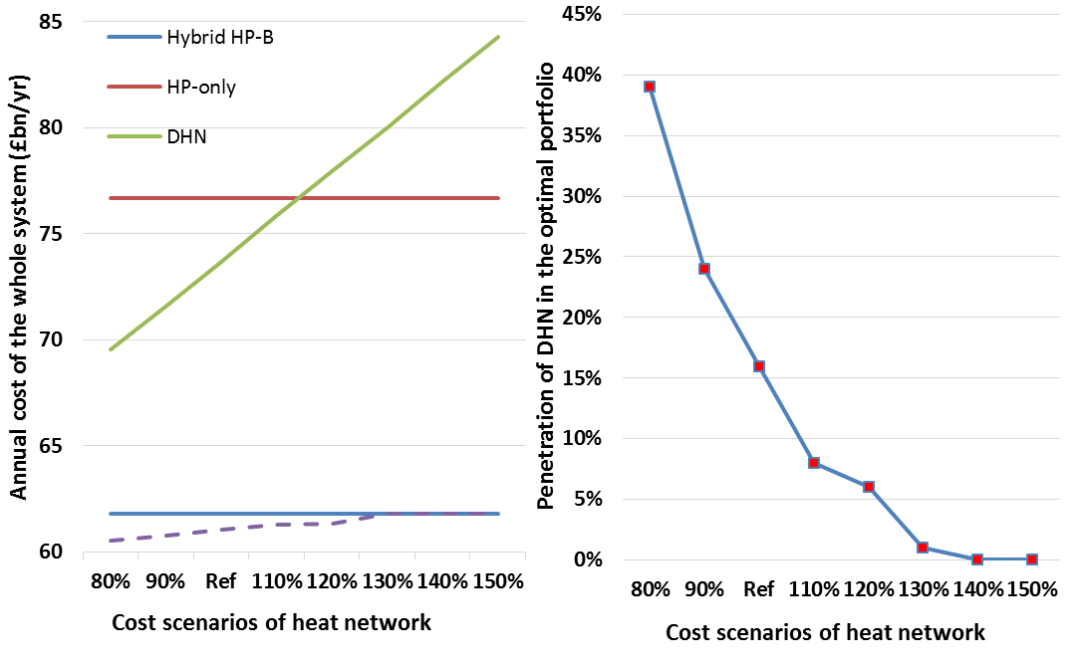

Figure 5.10– Sensitivity study on the capital cost of heat network

5.3 The Impact of Heating Strategy on Electricity System

As a crucial way to fulfil the decarbonisation target, the electrification of heat sectors builds a strong connection between electricity and heat systems. As a result, the investment and operation of electricity system will highly depend on the prospective heating strategies. This section compares how different heating technologies shape the electricity system and gives the generation mix where optimal heating strategy is applied.

5.3.1 Full Deployment of Different Heating Technologies

Comparison of electricity systems under full deployment of hybrid HP-B and HP-only

By using gas boiler as a supplementary heat source during peak time, hybrid HP-B requires less expansion of electricity system than HP-only. Figure 5.11 compares the generation mix and decomposed annual electricity production between cases where hybrid HP-B and HP-only are fully deployed under given carbon targets.

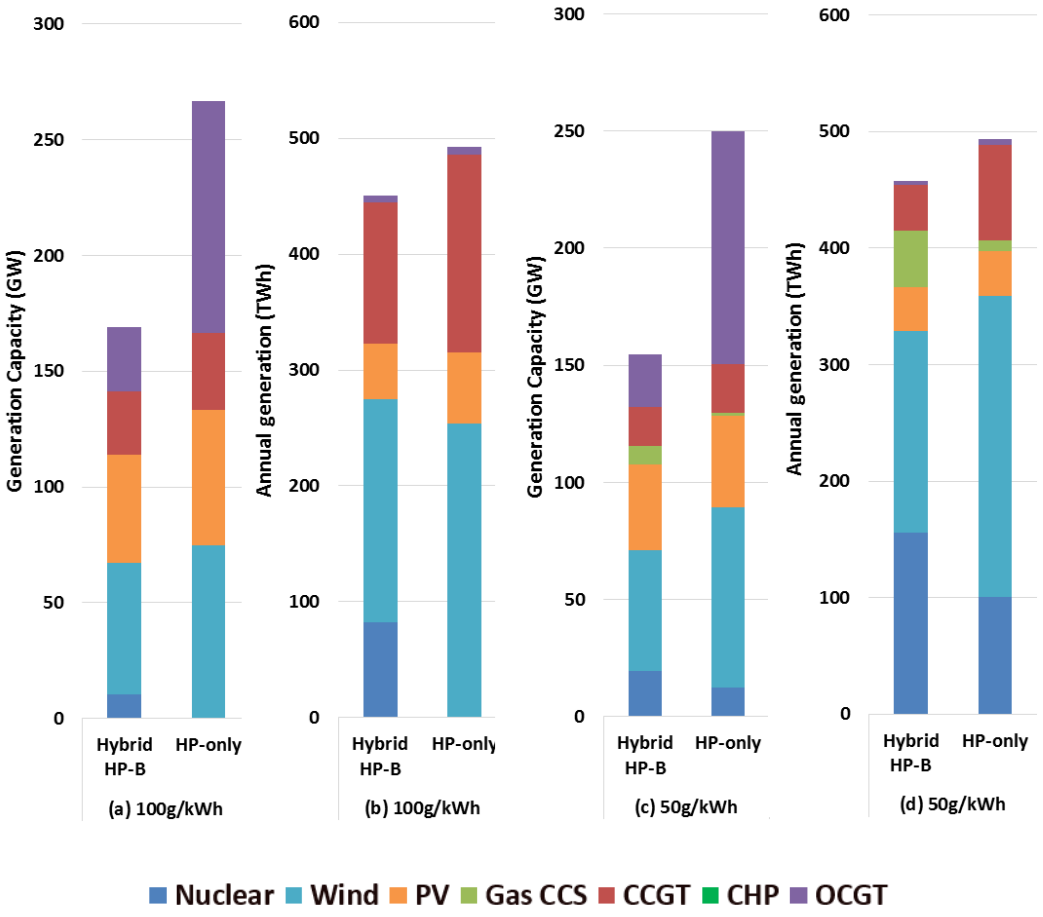

Figure 5.11– Generation mix and annual electricity production under full deployment of hybrid HP-B and HP-only under different carbon targets

From Figure 5.11 (a), it can be observed that part of RES (wind and PV) is replaced by nuclear power in the case of hybrid HP-B (compared to the case of HP-only), due to a decrease in the flexibility provided by heat sector, driven by reduced investment in ETES and ASHP (which can provide ancillary services through interrupted operation). Substantial amount of OCGT that serves as back-up capacity is saved in the case of hybrid HP-B, on account of a significant reduction in peak electricity demand through gas supplying the peak heat demand. In terms of annual electricity generation, it can be seen from Figure 5.11 (b) that 42TWh of annual electricity generation is saved when heating technology is switched from HP-only to hybrid HP-B, mainly due to the shift of electricity-based heat generation to gas-based heat generation and reduced heat losses in ETES. The difference in annual generation is further reflected on the decreased operation efficiency of CCGT where the annual generation of CCGT in the case

of hybrid HP-B is notably lower than in the case of HP-only while the installed capacities in both cases are almost the same.

When the carbon target is set at 50g/kWh (compared to 100g/kWh), as shown in Figure 5.11 (c) and Figure 5.11 (d), less RES and more nuclear is invested, as a result of increased integration costs of RES in more demanding carbon scenarios. NG CCS is also required to assist in accommodating RES while keeping the carbon emission within limits. Since hybrid HP-B can provide less flexibility for the electricity system compared with HP-only, more NG CCS is invested for the sake of RES integration.

Comparison of electricity systems under full deployment of hybrid HP-B and DHN

The deployment of DHN enables the application of CHP which can potentially reshape the electricity system. Figure 5.12 compares the generation mix and annual electricity production between cases where hybrid HP-B and DHN are applied.

It can be seen from Figure 5.12 (a) that almost all CCGT in the case of hybrid HP-B is replaced by CHP in the case of DHN as CHP can provide similar services to the electricity system with a higher overall energy efficiency. A considerable difference in nuclear generation can be observed from Figure 5.12 (b), indicating that the system with hybrid HP-B is less flexible than that with DHN. Given that the investment cost of industrial-sized TES is significantly lower than that of end-use TES, it is more economic to deploy TES in DHN, granting DHN the advantage of providing more flexibility to the electricity system. As a consequence, more RES is accommodated in the case of DHN. A gap of 39.4TWh in the annual generation between these 2 cases (100g/kWh) is noteworthy, which manifests the high energy efficiency of DHN due to the high COP of industrial-sized HP (3.8) over ASHP (3) and the high overall efficiency of CHP. When carbon target is tightened to 50g/kWh, a remarkable decrease in CHP capacity is observed due to its carbon intensity. As a consequence, less RES can be accommodated while more nuclear is installed. It is interesting to notice that no NG CCS is invested in the case of DHN in contrast to the case of hybrid HP-B, as sufficient flexibility can be provided from DHN so that CCS, as the most expensive source of flexibility in this model, is not necessary.

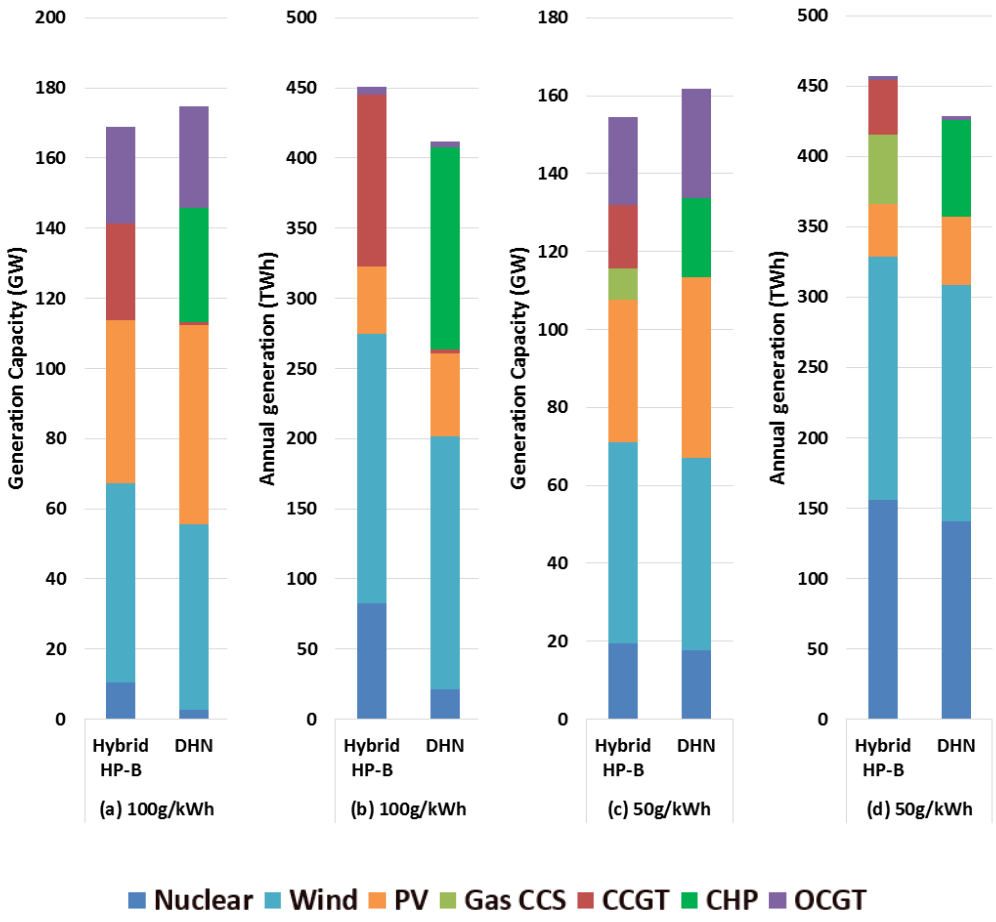

Figure 5.12– Generation mix and annual electricity production under full deployment of hybrid HP-B and DHN under different carbon targets

Comparison of electricity systems under full deployment of hybrid HP-B and hydrogen boiler

The application of hydrogen boilers requires mass deployment of electrolysis and hydrogen storage. The coordinated operation of the electrolysis and hydrogen storage can potentially provide huge flexibility to the electricity system. For example, electrolysis can use surplus RES which will otherwise be curtailed to produce hydrogen. This hydrogen is then stored for later use; additionally, ancillary services can be delivered by reducing the production of electrolysis without compromising the energy requirement due to the existence of hydrogen storage, thus boosting the integration of RES. Therefore, environmental benefits driven by the shift from nuclear to RES for the decarbonisation of the energy system can be potentially delivered by electrolysis-based hydrogen.

Figure 5.13 compares the generation mix and decomposed annual electricity production between cases where hybrid HP-B and hydrogen boilers are fully deployed under given carbon targets. It can be observed that full deployment of hydrogen requires a dramatic increase in the generation capacity compared to the other cases. As all the heat demand is supplied by electrolysis-based hydrogen, the energy covered by natural gas in the case of Hybrid HP-B and DHN is shifted to electricity, thus increasing the requirement of generation capacity. Additionally, the reduced heat efficiency of hydrogen boilers compared to HPs further enhance the electricity demand.

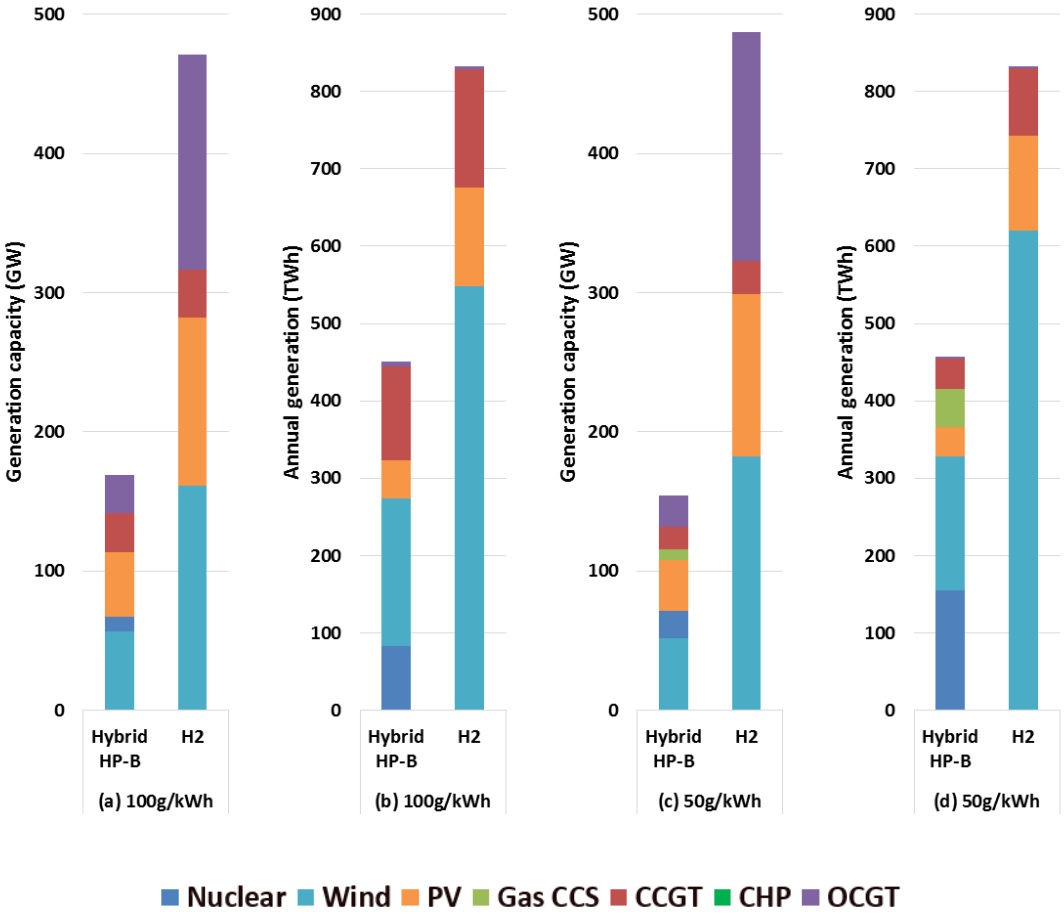

Figure 5.13– Annual decoupled system cost of full deployment of Hybrid HP-B and DHN

A dramatic boost of RES and OCGT can be further observed with the application of hydrogen boilers. Meanwhile, nuclear and CCS are not seen economic in this case. This results indicate the boosting effect of electrolysis-based hydrogen on the integration of RES.

5.3.2 Optimal Heating Technology Portfolio

The generation mix and decomposed annual electricity production in the scenario where heating technologies are fully optimized are given in Figure 5.14.

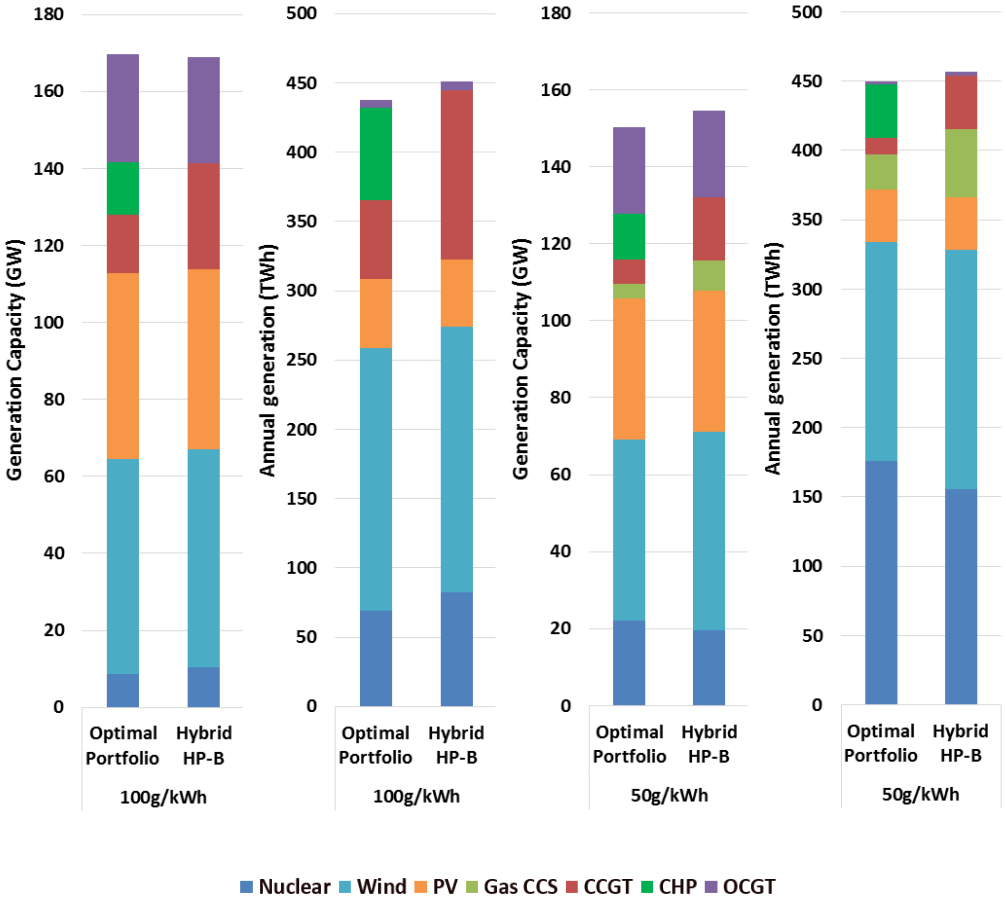

Figure 5.14– Generation mix and annual electricity production under optimal portfolio and full deployment of hybrid HP-B

As can be seen, the most distinct difference between the cases of optimal portfolio and hybrid HP-B is the role CHP plays in the electricity system. About half of the CCGT in the case of hybrid HP-B is substituted by CHP in the case of optimal portfolio under the carbon target of 100g/kWh while a large portion of both NG CCS and CCGT are switched to CHP when the carbon target is tightened to 50g/kWh. It can be further observed that 13.19TWh and 7.29TWh of annual generation is saved under carbon target of 100g/kWh and 50g/kWh, due to the improved efficiency of the heat sources deployed in DHN. However, a higher penetration of

DHN is deployed in the carbon scenario of 50g/kWh (21%) than that in the carbon scenario of 100g/kWh (16%), as analysed in 5.2.1, indicating that the overall energy efficiency of DHN is reduced with the tightening of carbon restriction. This is because increased capacity of industrial-sized HPs is installed in DHNs as a compensation for diminished scale deployment of CHP when the carbon target is tightened, lowering the overall efficiency of DHN.

5.4 The Impact of Heating Strategy on Heat System

As different heating strategies source from different heat plants/appliances, it is necessary to find out the optimized technology combination of each heating strategy.

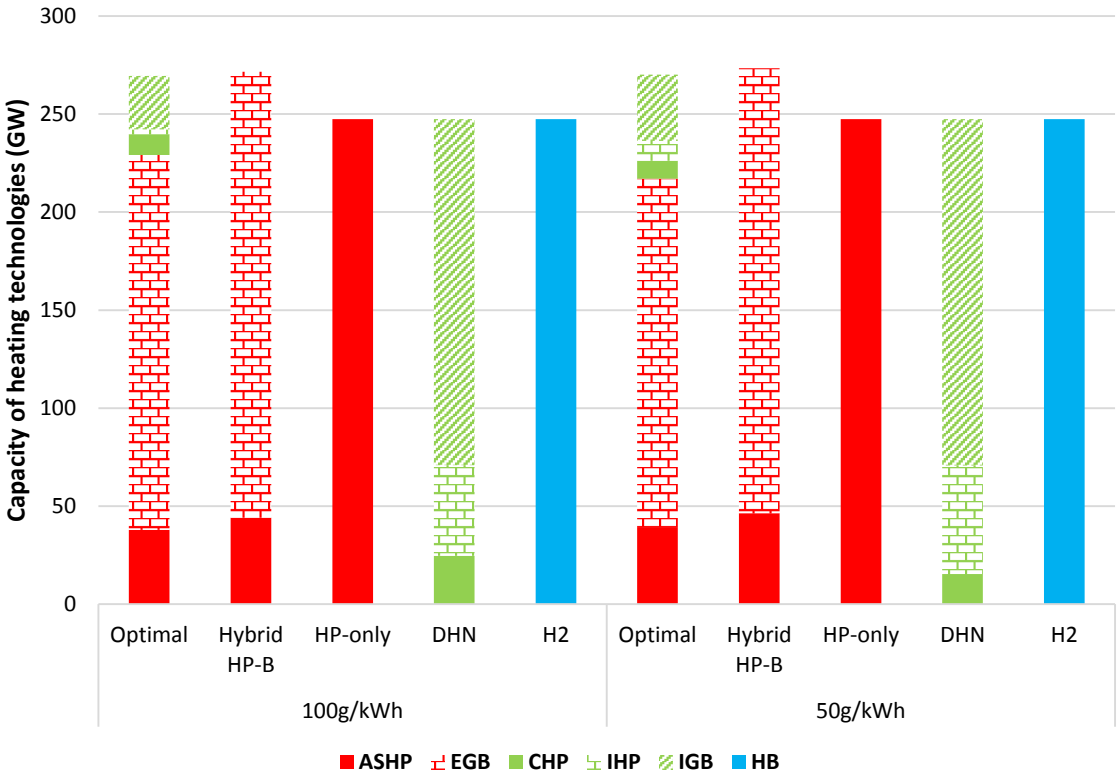

Figure 5.15– Heating technology mix of different heating strategies under different carbon targets

Figure 5.15 demonstrates the heating technology mix when different heating strategies are deployed, where green blocks represent district heating technologies, red blocks represent end-use ASHP and NG boilers, while blue blocks represent hydrogen boilers.

Compared to the case of HP-only, 82.2% (100g/kWh) and 81.2% (50g/kWh) of ASHP is saved while gas boilers are used to fill the gap of heat supply in the case of hybrid HP-B. A surplus of total capacity can be observed in “hybrid HP-B” and “optimal portfolio” (peak heat demand is 247GW), which is because the COP of ASHP is sensitive to the ambient temperature, as a result of which the efficiency of EGB is higher than that of ASHP in extremely cold days, therefore, only a part of ASHP is in operation while the rest of demand is covered by EGB in these days, leading to a deployment of over-sized EGB. Basically, the optimized capacity of EGB in “hybrid HP-B” is a balance between reduced energy efficiency due to temperature variation and the increased investment cost of EGB (O&M cost).

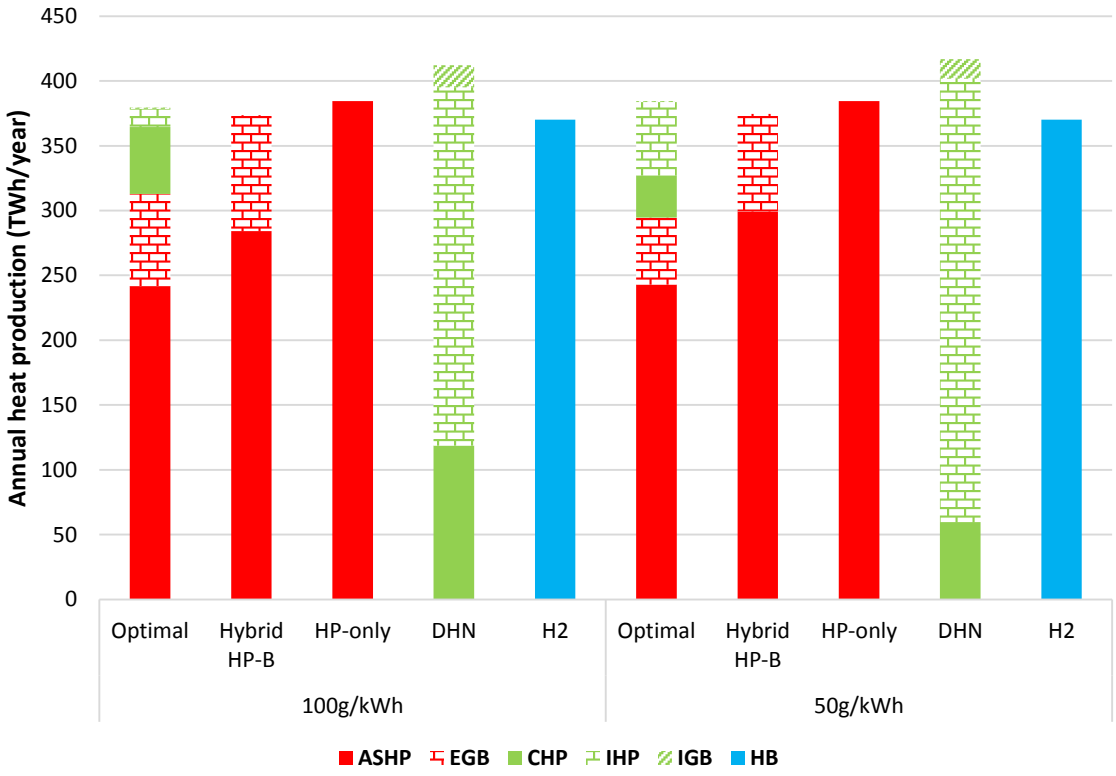

Figure 5.16– Annual heat production of different heating strategies

In the case of DHN, CHP and IHP supply the base load while IGB covers the peak load. Since the COP of IHP is not dependant on the ambient temperature, investment of over-sized heat plants is not incurred. When carbon target is tightened from 100g/kWh to 50g/kWh, a switch of heat plants from CHP to HP occurs. Meanwhile the load factor of CHP decreases from 55.0% to 44.3% while the load factor of HP increases from 68.1% to 70.6%, indicating that

CHP operates in part-load more frequently due to an increased requirement in ancillary services in a more demanding carbon scenario.

The annual heat production from different heat sources in each heating strategy is given in Figure 5.16. From the bar of "Hybrid HP-B", it can be observed that ASHP, which accounts for 16.2% (100g/kWh) and 17.0% (50g/kWh) of heat appliances in capacity, covers 76.0% (100g/kWh) and 79.9% (50g/kWh) of annual heat production.

Table 5.2 gives the aggregated size (in GWh) of TES for each heating strategy. As can be seen, "DHN" has the largest size of TES due to reduced investment cost of ITES while "Hybrid HP-B" has the lowest requirement of TES, thanks to the flexibility of gas. Comparing the three individual heating technologies, "DHN" incurs the highest heat generation, followed by "HP-only", with "Hybrid HP-B" producing the least thermal energy. The difference in heat generation is mainly attributed to the difference in the penetration of TES in which heat loss (1% per hour for both ITES and ETES) constantly occurs. Another reason accounting for the increased heat production for "DHN" is that heat loss also occurs in heat networks which is associated with the insulation level of pipework. In the case of tighter carbon target, more TES is installed to provide flexibility to the system, leading to increased heat losses (reflected in Figure 5.16 as increased heat production).

Table 5.2 – Aggregated size of TES for each heating strategy

Carbon scenario	Size of TES	Optimal	Hybrid HP-B	HP-only	DHN
100g/kWh	ITES (GWh)	73.2	NA	NA	431.1
	ETES (GWh)	71.3	86.1	346.4	NA
50g/kWh	ITES (GWh)	133.1	NA	NA	484.9
	ETES (GWh)	91.1	111.2	350.0	NA

5.5 The impact of building energy efficiency on the performance of the optimal heating strategy

5.5.1 The impact of building energy efficiency on whole system costs

The building energy efficiency has a significant impact on the heat demand level. The improvement of building energy efficiency provides an alternative perspective to decarbonise the energy system in a cost-effective way. As investigated in Section 3.3.3, when the building insulation is improved, thermal energy consumption for space heating decreases linearly, which may drive savings across different sectors.

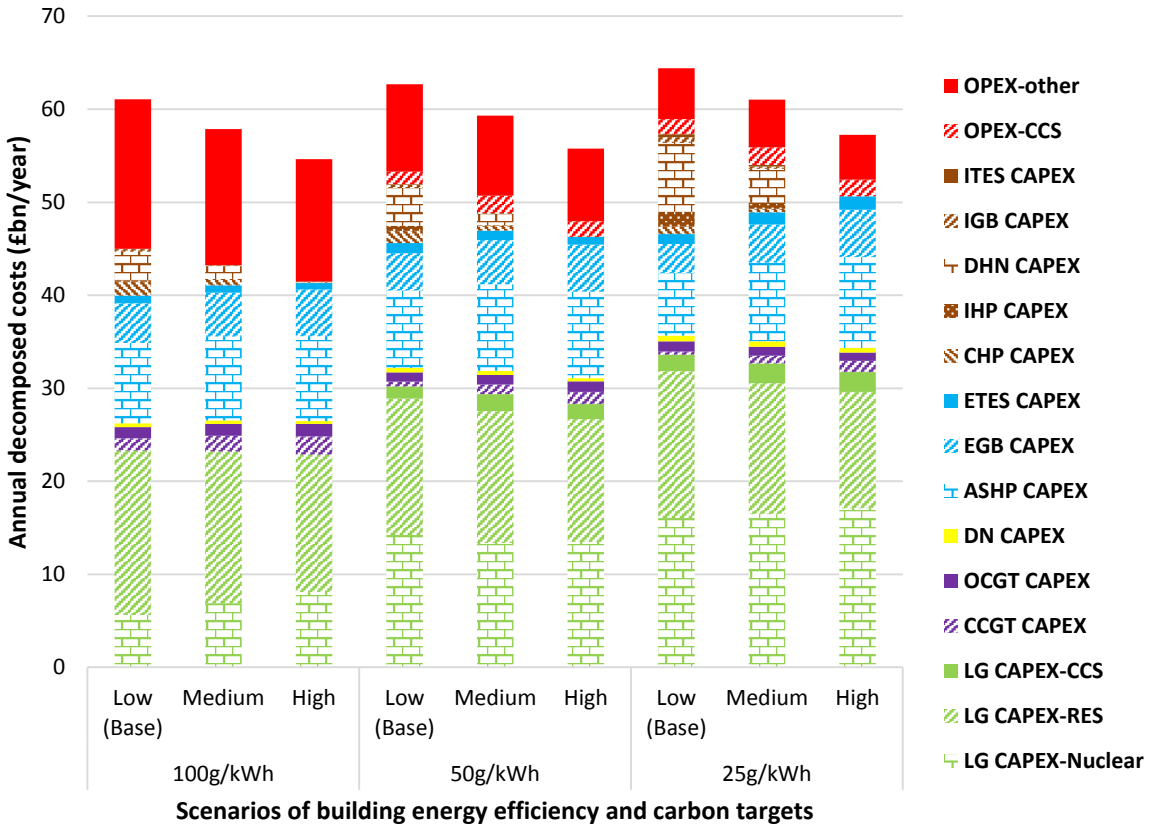

Figure 5.17– Impact of building energy efficiency on the system cost under different carbon targets

Figure 5.17 demonstrates the relationship between the level of building energy efficiency and decomposed system costs in the case of the optimal heating technology portfolio under different carbon targets. For each carbon target, three scenarios with improved building energy efficiency (e.g., Low, Medium and High) are tested. The "Low" scenario is the baseline which has been described in 5.1. For the scenarios of "Medium" and "High", it is assumed that 25% and 50% reduction in heat consumption per household is achieved, respectively. It can be observed that when the building energy efficiency improves, the total system cost decreases. Specifically, the investment in district-heating technologies (brown blocks) is gradually shifted to distributed-heating technologies (blue blocks), meanwhile, large savings are achieved in the total investment of heat sectors (e.g., both district heating and distributed heating).

It is interesting to observe that significant decrease in the investment of district heating occurs with the improvement of building energy efficiency, while the increase in the investment of distributed heating is minor. This is because DHN CAPEX mainly depends on the length of the pipeline. When the layout of consumers in a district has been determined, the potential capital cost of DHN in that district is also determined and will not be influenced by the variation of heat demand. Therefore, the lower the heat demand (kW), the higher the unit investment (£/kW) of DHN. As a consequence, the penetration of DHNs decreases with the improvement of building energy efficiency. In contrast, the investment of distributed-heating technologies (i.e., Hybrid HP-B) is influenced by two factors, the first factor is its penetration, which is increased to compensate the decrease in DHNs; the second one is the heat demand (kW) per household, which is decreased with the improvement of building energy efficiency. Therefore, the change of investment in distributed-heating technologies is minor across different building energy efficiency scenarios, due to two opposite contributors. This result indicates that the competitiveness of DHNs reduces when building energy efficiency improves.

Additionally, it is noticeable that the investment of RES decreases with improved building energy efficiency. There are limiting factors: firstly, reduced heat demand requires less generation; secondly, decreased availability of flexibility from heat sectors (due to reduced investment) limits the integration of RES. The first factor also leads to investment savings in the other types of generation, but the second factor will boost the investment in nuclear or CCS

to deliver the carbon target. As a consequence, the variation in nuclear and CCS is not consistent in different scenarios.

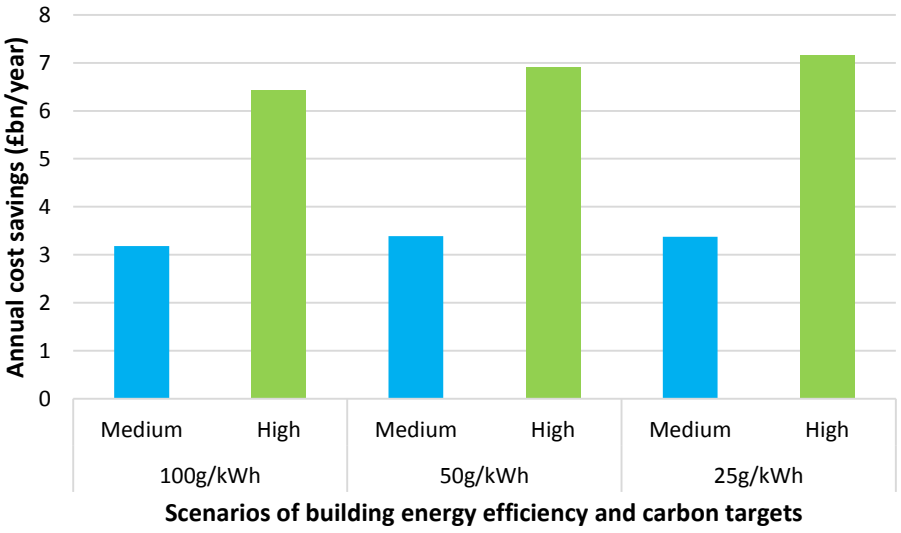

Figure 5.18– Savings through improved energy efficiency under different carbon targets

Moreover, the impact of carbon target on the value of building energy efficiency improvement is demonstrated in Figure 5.18. It can be observed that the more demanding the carbon target is required, the more savings can be achieved through the improved building energy efficiency. This result is more apparent in the "High" scenario.

5.5.2 The impact of building energy efficiency on the value of pre-heating

In Section 3.2.2.2, pre-heating was investigated in the context of building energy management, the results indicate that when the building energy efficiency is increased, less benefits can be achieved through pre-heating, since the reduction of heat demand will compress the space of operational savings.

However, when considering the investment cost of different assets, the benefits of pre-heating can be significantly enhanced through the improvement of the building insulation condition. Figure 5.19 demonstrates the savings through pre-heating under different building energy efficiency and carbon targets, the results are obtained by comparing the case when pre-heating

is enabled in all the households and the case where pre-heating is not allowed. It can be observed that the system savings consistently increase with the improvement of the building energy efficiency in different carbon scenarios. Additionally, the more demanding the carbon target is required, the more savings can be achieved. This is because reduced building energy losses driven by the improvement of energy efficiency can introduce extra flexibility to pre-heating, thus driving savings in the investment costs. The value of this flexibility is increased in more demanding carbon scenarios.

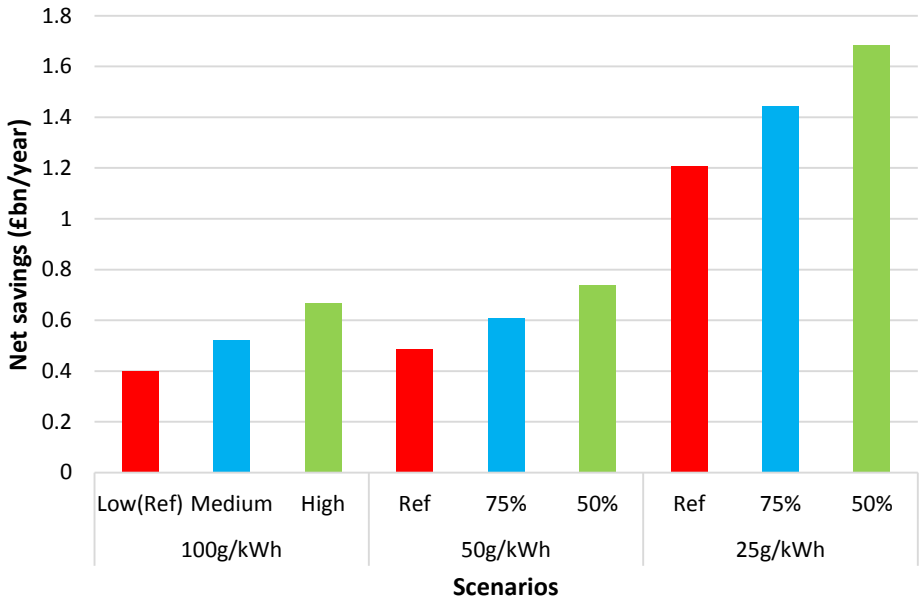

Figure 5.19– Savings through pre-heating under different building energy efficiency and carbon targets

5.6 Conclusions of the Chapter

This chapter applies a whole-system approach to assess the economic performance of various heating strategies in the decarbonisation of the heat sector through coordinated operation with the electricity system. A set of comprehensive case studies are carried out to compare the economic performance of different heating strategies from multiple perspectives and analyse the associated impacts on the electricity system.

The case studies on the full deployment of individual heating technologies suggest that hybrid HP-B has a significant overall economic advantage over HP-only, DHN and the hydrogen boiler, mainly due to investment savings from the presence of residential gas boilers. To be more specific, the comparison of hybrid HP-B over HP-only indicates that hybrid HP-B can drive savings over HP-only through the reduced requirement of distribution network reinforcement and OCGT as back-ups, due to the significant reduction of peak electricity demand which is compensated by gas-based heat, however, the operation cost increases as a result of reduced level of electrification in the heat sector, while more low-carbon generation is invested to compensate for the extra carbon emission from the gas consumption. The comparison of hybrid HP-B over DHN indicates that the main advantage of hybrid HP-B is the saved investment in the construction of the pipework. However, the investment cost of DHN highly depends on the heat density of the deployed area and hence grants DHN the economic advantages to be deployed in highly populous areas. Among all the investigated heating technologies, hydrogen boilers is the most capital-intensive, making it not suitable for large-scale deployment yet. However, since it can boost the integration of RES, its competitiveness can be improved under a more demanding carbon scenario.

The economic assessment for the optimal portfolio of heating technologies is performed given the cost assumptions, demonstrating that under the carbon target of 100g/kWh, 16% of the total heat demand is covered by DHN (all deployed in urban areas) while the rest supplied by hybrid HP-B. When the carbon target is tightened to 50g/kWh, a 5% increase in the penetration of DHN is deployed (21% in total), manifesting its enhanced competitiveness in a more demanding carbon scenario.

A series of sensitivity studies are performed to illustrate the robustness of the heating strategies to the cost uncertainty of heating technologies. The results also clearly demonstrate the changes on the electricity side driven by the different decarbonisation strategies in the heating system.

The building energy efficiency has a significant impact on the whole system cost. When the building energy efficiency improves, the investment in district-heating technologies is gradually shifted to distributed-heating technologies, meanwhile, large savings are achieved in the total investment of heat sectors.

The capital cost of DHN mainly depends on the length of the pipeline. When the layout of consumers in a district has been determined, the potential capital cost of DHN in that district is also determined and will not be influenced by the variation of heat demand. Therefore, the lower the heat demand (kW), the higher the unit investment (£/kW) of DHN. As a consequence, the competitiveness of DHNs reduces when building energy efficiency improves. Additionally, the investment of RES decreases with improved building energy efficiency due to reduced heat demand and decreased availability of flexibility from heat sectors.

The value of building energy efficiency improvement is also impacted by carbon targets, the more demanding the carbon target is required, the more savings can be achieved through the improved building energy efficiency. Additionally, the whole system benefits through pre-heating increase with the improvement of the building energy efficiency in different carbon scenarios. The more demanding the carbon target is required, the more savings can be achieved. This is because reduced building energy losses driven by the improvement of energy efficiency can introduce extra flexibility to pre-heating, thus driving savings in the investment costs. The value of this flexibility is increased in more demanding carbon scenarios.

The conclusions in this section can provide guidance of future heating strategy planning for the transition to a decarbonised energy system.

Chapter 6 Assessment of Benefits of Integrated Heat and Electricity Systems

The interaction between electricity and heat systems will play an important role in facilitating the cost effective transition to a low carbon energy system with high penetration of renewable generation. This section presents a novel integrated electricity and heat system model in which, for the first time, operation and investment timescales are considered while covering both the local district and national level infrastructures. This model is applied to optimize decarbonization strategies of the UK integrated electricity and heat system, while quantifying the benefits of the interactions across the whole multi-energy system, and revealing the trade-offs between portfolios of (a) low carbon generation technologies (renewable energy, nuclear, CCS) and (b) district heating systems based on heat networks and distributed heating based on end-use heating technologies. Overall, the proposed modeling demonstrates that the integration of the heat and electricity system (when compared with the decoupled approach) can bring significant benefits by increasing the investment in the heating infrastructure in order to enhance the system flexibility that in turn can deliver larger cost savings in the electricity system, thus meeting the carbon target at a lower whole-system cost.

Heating accounts for approximately half of the total energy consumption and is responsible for over 25% of carbon emissions in the UK. Therefore, decarbonization of the heat sector is one of the key challenges in achieving the 80% carbon reduction target by 2050 [59]. There is growing evidence that the interaction between electricity and heat systems will be important in facilitating cost effective transition to a lower carbon system by efficiently accommodating RES. The lack of flexibility in the electricity system is a key limiting factor for effectively integrating RES [62, 89-91], whereas the heat system and the electrified transport sector can potentially provide considerable amount of flexibility by delivering a range of balancing services and support the management of peak demand [33, 65, 92]. Both district (DHNs) and

end-use heating technologies (e.g. end-use HPs) are potential options for the decarbonization of the heat sector. As presented in [33] and [56], HNs can alleviate wind curtailment through coordinated operation of CHP with thermal energy storage (TES). The potential role of DHNs in a 100% renewable energy sources based energy system is investigated in [93]. CHP generation supplying heat to DHNs is modelled in [30, 33, 94, 95], while the benefits of the application of industrial size HPs in DHNs are outlined in [68, 69, 96]. In terms of end-use heating, the impacts of HPs on wind power integration have been investigated in [97, 98] while [70-72, 99] focuses on the analysis of hybrid heating technologies at consumer premises, which can potentially link electrical HPs, gas boilers and resistive heating devices. The economic and operational advantages of different combinations of end-use heating technologies are analyzed in [71, 99], demonstrating the cost-effectiveness of hybrid electrical HPs and gas boilers (Hybrid HP-B). The authors in [100] proposed a decomposed algorithm to calculate the combined heat and electricity system based on a real system. Integrated heat and electricity dispatch considering thermal inertia of buildings has been analyzed in [36]. DHNs can also improve the efficiency of energy supply through pre-heating [53, 101]. TES, characterized with significantly lower capital cost than electricity storage, can further enhance the value of DHNs in integrated electricity and heat systems [77, 102]. Similarly, benefits of end-use TES supporting hybrid HP-B are demonstrated in [71].

Previous research on the investment and operation optimization of DHNs mostly focuses on the local level infrastructure [78-80]. The authors in [48] proposed a whole-system investment model for the electricity system where HPs are assumed to be the only option for the decarbonization of the heat sector. In this context, a novel modeling framework for the whole system optimization of the combined electricity and heat system is proposed in this section. In the context of the previous work, the proposed model for the first time considers operation and investment timescales while covering both local and national level of heat and electricity infrastructures. Furthermore, the impact of reduced system inertia on the frequency response requirements is explicitly modelled while security constraints and carbon emission targets are also included in the proposed framework. This approach is applied to optimize the decarbonization strategy of the combined electricity and heat system, selecting the cost effective portfolio of heating technologies, including DHNs (supplied by CHP plants, industrial size HPs, gas boilers as well as TES), and consumer end hybrid HP-Bs. The proposed model

simultaneously optimizes, for the first time, the investment in electricity generation (including conventional and low carbon generation), heating plants/appliances, DHNs, reinforcement of electricity transmission and distribution networks while considering system operation cost and taking into account frequency regulation and operating reserve requirements.

Through several case studies, we demonstrate the interaction between electricity and heat systems across operation and investment timescale while simultaneously managing conflicts and synergies between local and national level objectives. Key contributions of this section can be summarized as:

1) Presenting a novel combined electricity and heat system modeling framework considering both operation and investment timescales with spatial granularity including local and national level infrastructure.

2) Quantifying the benefits of the integrated planning of electricity and heat systems and demonstrating the impact on the technology mixes in both electricity and heat sectors.

6.1 Interactions between Electricity and Heat Systems

As shown in Figure 6.1, the electricity and heat systems are coupled through end-use hybrid HP-Bs as well as district based CHPs and HPs. The absence of coordination would drive inefficient investments in both electricity and heat systems (at both local and national level). On the other hand, inherent flexibility in the heat system can be used to alleviate these challenges through coordinated operation and investment with the electricity system. For instance, inherent storage in DHN (the pipework) enhanced by TES and the CHP that adjusts power-to-heat ratio, can provide balancing service needed to support efficient integration of RES, while reducing peak demand and the investment in back-up generation [103]. Furthermore, if demand side response (DSR) is enabled, flexible end-use hybrid HP-Bs could bring benefits across all sectors of the electricity system. The developed model considers all these potential interactions so that the whole system benefits of the integrated electricity and heat system can be quantified.

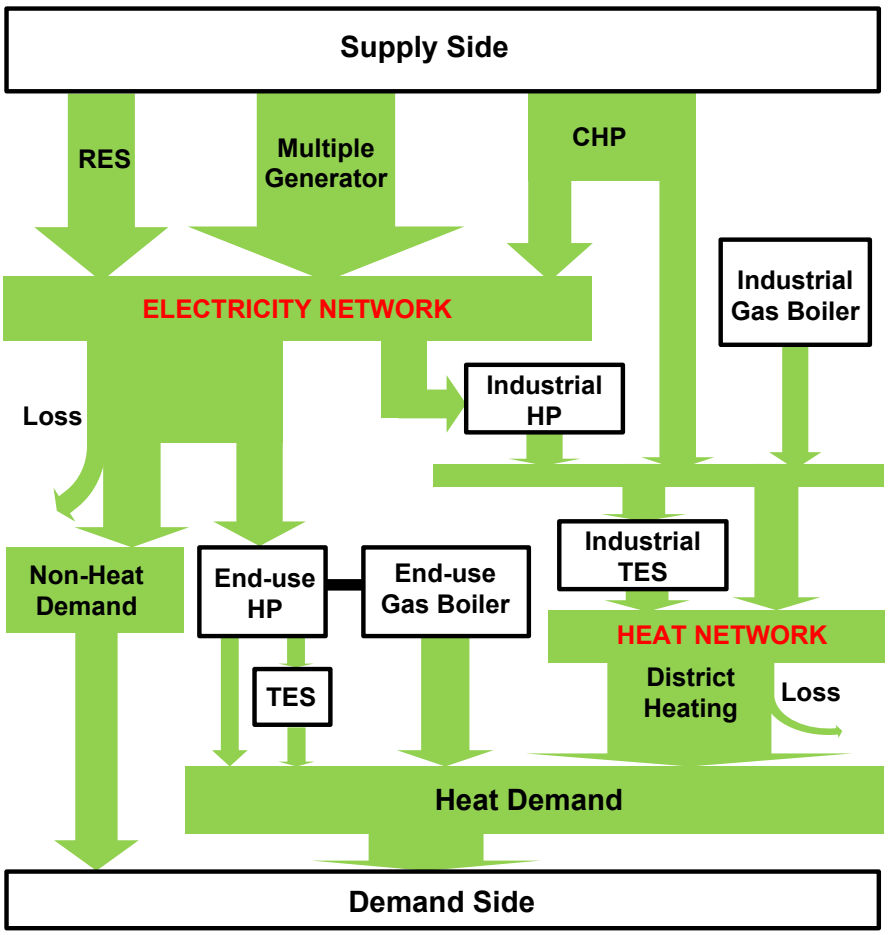

Figure 6.1– Interaction and energy balance of integrated electricity and heat system

The heat system can potentially provide substantial flexibility for the electricity system. Given that there are different understandings in the concept of flexibility in different reseach, it is worth stressing that the flexibility in this chapter particularly refers to 3 aspects: 1) the ability to shift demand, 2) the ability to provide frequency response service and 3) the ability to provide operating reserve. To be more specific, the coordinated operation of CHP, HP and TES can shift heat-driven electricity demand and provide frequencey response as well as operating reserve; End-use HPs, through temporarily turning down their output (which will not compromise the comfort due to the thermal inertia of buildings), can achieve the same purpose with the support of end-use TES. Moreover, preheating can further enhance the flexibility of the electricity system by shifting demand. All these heat system based flexibility measures have been modelled in Chapter 4 explicitly.

6.2 Analysis of Benefits through System Integration

In this section, the integrated electricity and heat system model proposed in Chapter 4 is applied to two GB 2030 scenarios, with different carbon targets, involving different mixes of low carbon generation, as shown in Table 6.1. In both scenarios, CCS plants are allowed to be added to the mix if the carbon targets cannot otherwise be satisfied. In the integrated electricity and heat system, the overall carbon emissions are quantified from all sources involved in meeting both electrical and thermal demand [104].

Table 6.1 – GB 2030 scenarios of low carbon generation

Tested scenarios	Wind (GW)	PV (GW)	Nuclear (GW)
100g/kWh	50	20	8
50g/kWh	80	35	10

Regarding decarbonization of heat sector, it is assumed that HNs and hybrid HP-Bs are two main technologies delivering low-carbon heat in 2030, based on the conclusions of Chapter 5. The tested system and relative parameters are same as described in 5.1.

6.2.1 Overall Benefits of Integrated Electricity and Heat System

In order to quantify the benefits through the integration of electricity and heat systems, the whole system costs of the integrated and decoupled systems are compared. Figure 6.2 presents the annual savings in different system segments enabled by the integration of electricity and heat systems in two carbon scenarios considered.

As shown in Figure 6.2, the integration of electricity and heat systems delivers significant savings in operation costs (OPEX), represented by red blocks, comprising operation costs of NG CCS, NG CHP, CCGT, OCGT and gas boilers, driven by significantly enhanced flexibility and efficiency of system operation through application of more efficient CHP and reduced renewable curtailment; Blue blocks indicate savings in capital costs (CAPEX) related to end-use heating technologies, including ASHP, end-use gas boilers (EGB), as a proportion of heat

demand is supplied by HNs; Relatively minor investment savings are achieved in reducing capital expenditure associated with conventional generation (including CCGT and OCGT) and distribution networks (DN), as change in peak demand is not significant given that end-use heating is supplied by hybrid HPs (i.e. gas boilers are used to supply heat demand during peaks). Significant system integration driven savings are made by reducing the capacity of low-carbon generation (LG CAPEX), particularly referring to NG CCS (shown in green), as renewable generation is curtailed much less (particularly in 50g/kWh carbon scenario), so the carbon targets can be met by reducing NG CCS capacity. Brown blocks present additional integration driven capital expenditure (negative savings) in district heating, including heat network pipelines (DHN), NG CHP plants, industrial HPs (IHP), industrial gas boilers (IGB), and industrial thermal energy storage (ITES). Additional investment in end-use thermal energy storage (ETES) is also driven by the system integration.

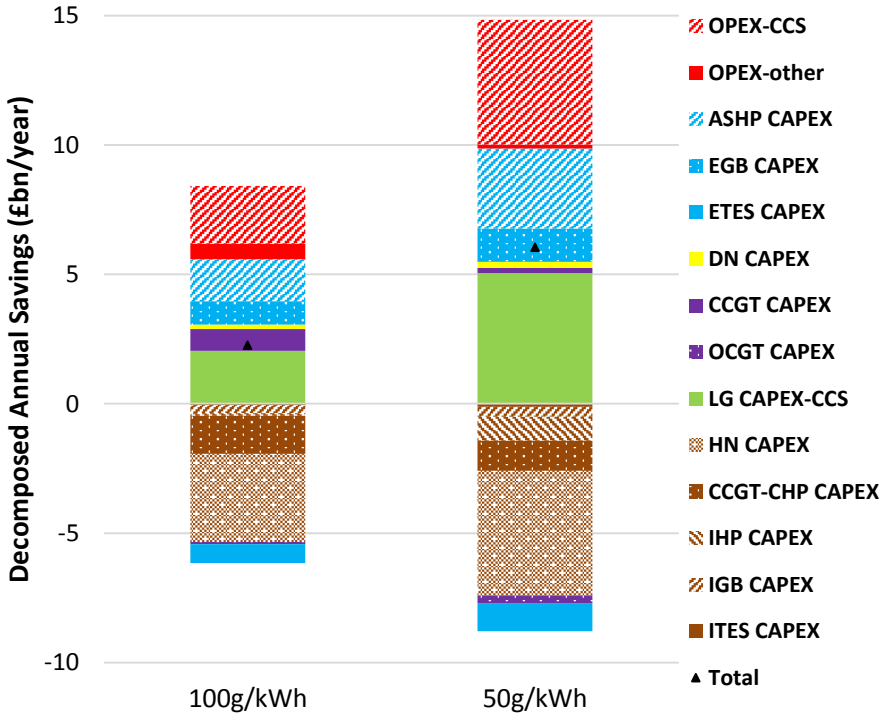

Figure 6.2– Savings from the integration of electricity and heat systems

The objective of the model proposed in Chapter 4 is to minimise combined system investment costs and operation costs while meeting the given carbon targets. Hence the interactions between electricity systems and heat systems are crucial for both investment and operation

cost. According to Figure 6.2, there are indeed significant savings in both investment and operation costs.

As shown in Table 6.1, this case study is performed with fixed amount of nuclear, wind and PV, while additional CCS will be added if the carbon target cannot be met by the given amount of low-carbon generation, and the capacity of CCS is determined by the optimization.

Through Figure 6.2, we demonstrated that when the infrastructure is determined by the investment planning without considering the operational interaction between electricity and heat systems, the carbon target cannot be fulfilled and hence more CCS is needed, driving large extra cost in both investment and operation.

The total annual saving through the system integration (denoted as "Total") is influenced by the carbon target. Figure 6.2 shows that the annual saving is about £2.3bn/year (3.53% of the total annual system cost of the decoupled system) under the overall carbon target of 100g/kWh while the saving increases to £6bn/year (8.69% of the total annual system cost of the decoupled system) under the overall carbon target of 50g/kWh. Further simulations have been performed to investigate the relationship between the annual saving through the system integration and the intensity of the carbon target. When the carbon constraint is above 266g/kWh, the total system cost of both integrated and decoupled case is no longer influenced by the carbon constraint.

There is inherent interaction between electricity and heat system, both in operation and investment context, e.g. application of CHP will provide heat to heat networks but also electricity to the electricity system; similarly, HPs use electricity to provide heat. This interaction is indeed taken into account, but the key point of the integrated investment planning and operation in this section, is that we take into account the balancing services that the heat system can provide to the electricity system which can enhance the ability of the system to accommodate variable renewables and significantly reduce the total investment and operation cost in electricity system compared to the decoupled, in which the balancing services that the heat system can potentially provide for the electricity system are not considered, while still meeting the specified carbon targets. Fundamentally, the benefits of the integrated investment planning come from the flexibility that the heat system provides to the electricity system which

significantly reduces both investment and operation cost of electricity system, while increasing investment in heat system. To be more specific, CHP and industrial size HPs and thermal energy storage, typically deployed in heat networks, can provide ancillary services for the electricity system. End-use HPs, through temporarily turning down their output (which will not compromise the comfort due to the thermal inertia of buildings), can also provide ancillary services. In the planning stage, if we consider the flexibility which heat systems can potentially provide for the electricity systems, significant savings can be achieved in the electricity side on the cost of increasing the investment on the heat side, but the overall system costs are reduced significantly. If the heat system and electricity system are planned separately, the requirement of flexibility in the electricity system has to be met by the components within the electricity system, incurring dramatic flexibility associated cost, which will otherwise incur little extra costs with the flexibility provision from the heat systems.

It should be emphasised that when the electricity system itself is flexible enough, or in other words, other sources of flexibility are already available in the electricity system, (e.g. thermal generators with higher flexibility and efficiency, electrical energy storage and demand side response, etc.) the value of the integrated planning of the electricity and heat systems would be significantly reduced. The impact of the flexibility of electricity system on the value of the system integration will be further investigated in Section 6.2.7.

6.2.2 Impact of Integration on Electricity System

Figure 6.3 presents the generation mix and annual electricity production in different scenarios. It is important to note that the total amount of generation capacity is very similar in integrated and decoupled scenarios (as peak demands are broadly the same in both scenarios). We can also observe that the reduction in CCGT and NG CCS capacity, which is driven by the enhanced flexibility and reduced RES curtailment (as presented in Figure 6.3 (b) and Table 6.2) through the system integration, requires increase in firm generation capacity to meet the security supply, which is achieved by NG CHP and OCGT plant. It is worth stressing that the model selects the economically optimal portfolio of electricity generation. In other words, given the cost assumptions, large-scale deployment of other types of generation (e.g. biogas-

based, biomass-based, etc.) is not seen to be economic compared to the generation types selected by the model, from the whole-system point of view.

It should be stressed that the case study illustrated in Figure 6.3 is performed under the given GB 2030 scenarios proposed by the UK government with fixed amount of nuclear, wind and PV (as in Table 6.1). If the carbon targets cannot be met by the given amount of low-carbon generation, additional NG CCS would be added to deliver the carbon target.

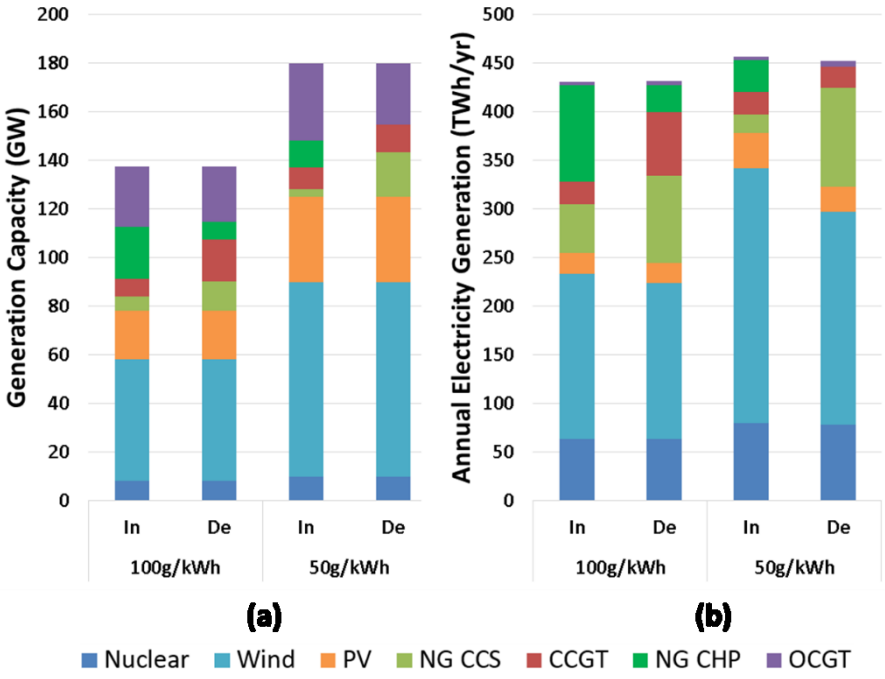

Figure 6.3– (a) Generation mix and (b) annual electricity generation of integrated and decoupled cases under different carbon scenarios

Table 6.2 – Annual Curtailment of RES in Different Scenarios

Carbon target (g/kWh)	System	Wind curtailment (TWh/year)	Solar curtailment (TWh/year)
100	Integrated	0.62	0.00
	Decoupled	10.55	0.05
50	Integrated	10.07	1.13
	Decoupled	53.72	10.42

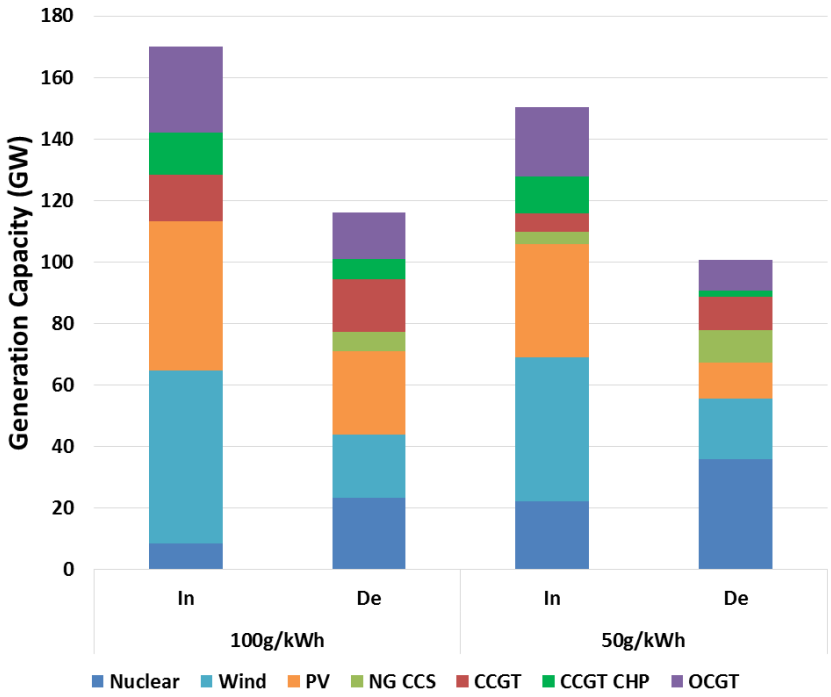

Figure 6.4– Cost optimal generation mix for different scenarios

Figure 6.3 demonstrates the impact of the system integration on the curtailment of RES. Due to the lack of flexibility in the decoupled system, significant amount of RES is curtailed, and hence additional capacity of NG CCS is required to deliver the carbon target, which significantly increases the cost. To further reveal the impact of system integration on the overall electricity generation mix, we perform the case study (presented in Figure 6.4) in which the capacities of all types of low carbon generation are optimized while meeting the same carbon targets. Instead of demonstrating the impact of the system integration on the curtailment of RES, Figure 6.4 focuses on the optimal generation portfolios.

It can be observed in Figure 6.4 that considerable capacity of wind and PV generation is installed in the integrated system while in the decoupled scenarios more nuclear and NG CCS is required due to the inability of the system to effectively utilize RES. This is because the additional costs that are incurred due to the integration of RES (e.g. increased balancing cost) can be significantly reduced by the increased flexibility provided by the integration of the electricity and heat system. This case study indicates that coupling the energy sectors can significantly increase the utilization of RES.

It is important to emphasise that we assume RES cannot provide frequency response in this section, although our previous work [105] has clearly shown the potential value of RES providing inertia and frequency response for the electricity system. However, on the technology side, the measurement of rate of change of frequency and coordination among large number of wind turbines still need to be resolved. On the economy side, the recovery effect of inertia provision and curtailment of RES for frequency response provision may prevent its large-scale deployment. Of course, as the technology development goes ahead, all these issues may be resolved and RES can efficiently provide inertia and frequency response, leading to less benefit from energy system integration.

6.2.3 Impact of Integration on Heat System

The heating technology mix and annual thermal energy production in different scenarios are shown in Figure 6.5. Blue blocks represent end-use heating technologies (hybrid HP-Bs) while red blocks represent district heating technologies (HNs). It is interesting to observe that all HNs are deployed in urban areas (the penetration of which is given in Table 6.3) while only hybrid HP-B are applied in suburban, semirural and rural areas, demonstrating that heat density is the key driving/limiting factor for the application of HNs.

Table 6.3 – Penetration of HNs in Urban Area

Carbon target (g/kWh)	System	Penetration of HNs in urban areas (%)
100	Integrated	61.4%
	Decoupled	15.4%
50	Integrated	64.0%
	Decoupled	0%

As shown in Figure 6.5 (a), when integration is enabled, heating technology is shifted from hybrid HP-Bs to HNs. This drives larger investment in the heat sector as can be derived from Figure 6.2; capital investment in the heat sector under the integrated scenario are £3.54bn and £4.12bn larger under 100g/kWh and 50g/kWh respectively when compared with decoupled

scenarios, due to the higher capital cost associated with district heating infrastructure (dominated by investments in HNs). On the other hand, large reduction in system operation costs and investment in NG CCS capacity, driven by enhanced system flexibility, drives considerable overall net savings. Overall, this analysis demonstrates that the integration of electricity and heat systems will drive increase in investment in heat infrastructure in order to reduce significantly operation and investment cost of the electricity system and ensure that the carbon target are met at the minimum whole-system cost.

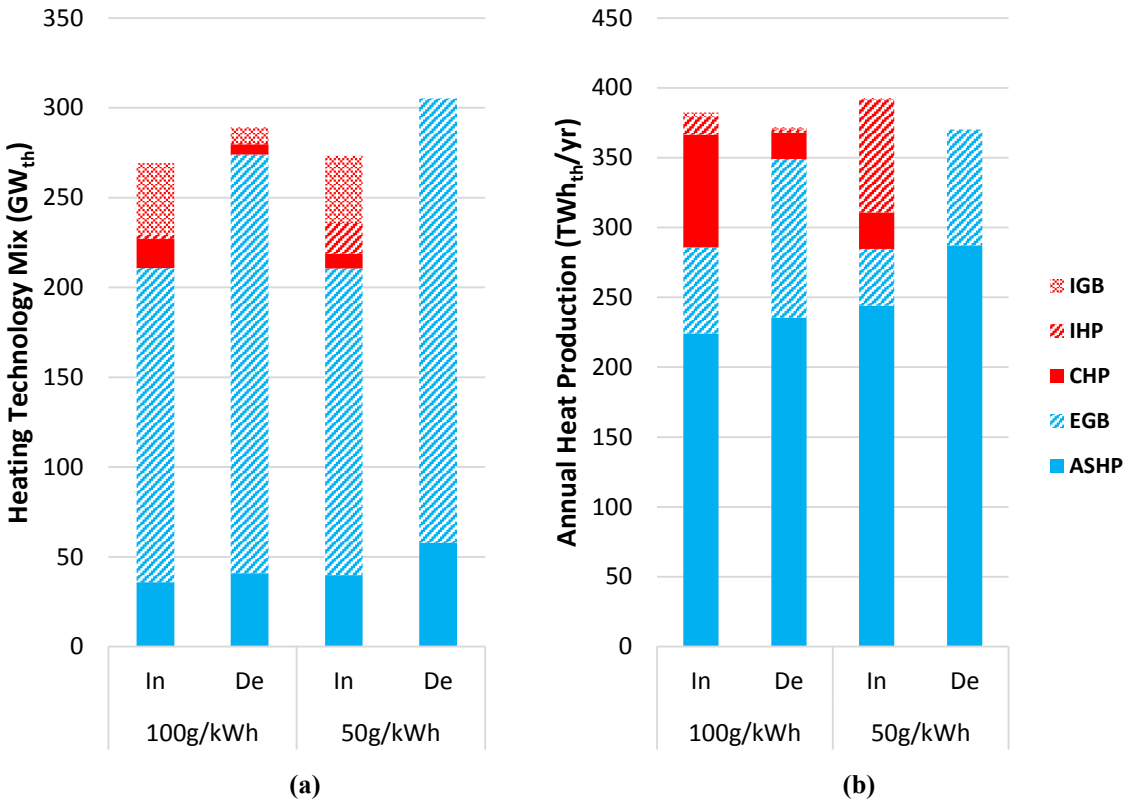

Figure 6.5– (a) Heating technology mix and (b) annual heat production of integrated and decoupled cases under different carbon scenarios

In the light of Figure 6.5 (b), the system integration also has a notable impact on the composition of annual heat production from different heating technologies. It can be observed that the integration increases heat production of NG CHP from 5% to 21%, under the carbon target of 100g/kWh. When the carbon target is 50g/kWh, increase in heat production of NG CHP is lower (from 0% to 7%), which is driven by the relatively high carbon intensity of NG CHP (CHP CCS is a potential low-carbon heat source, but according to the results of the

simulation, it is not economic to deploy CHP CCS on a large scale based on the proposed carbon scenarios and the cost assumptions taken). Therefore, heat provided by IHPs increases from 0% to 21%, demonstrating that this technology may potentially play a significant role in decarbonizing heat (given its high COP) in the longer term.

6.2.4 Impact of Integration on Carbon Emissions

The integration of the electricity and heat system can influence the decarbonization strategies in different sectors. Table 6.4 presents the optimized carbon intensities in electricity and heat sectors under given overall carbon targets. The carbon intensity of the heat sector represents CO2 emissions associated with total heat production (including electrified heat). Basically, the carbon emissions are driven by the conventional generation (e.g. CCGT, OCGT) on the electricity side and NG CHP together with gas boilers on the heat side.

As shown in Table 6.4, the system integration increases the carbon intensity in the electricity sector and reduces the carbon emissions in the heat sector, while achieving the same overall carbon target. For the electricity sector, we observe from Figure 6.3 (b) that when the integration is enabled, more electricity is generated by NG CHP, causing an overall increase in carbon emissions in the electricity sector. For the heat sector on the other hand, Figure 6.5 (b) demonstrates that less gas-boiler-based heat and more electrified heat from HPs and NG CHPs (CHP is considered as a virtual HP [106]) is produced, thus reducing the carbon emissions in the heat sector.

Table 6.4 – Carbon intensity in electricity and heat sector

Overall carbon target (g/kWh)	System	Carbon intensity in electricity sector (g/kWh_{el})	Carbon intensity in heat sector (g/kWh_{th})
100	Integrated	124.6	77.9
	Decoupled	105.6	95.3
50	Integrated	55.8	43.4
	Decoupled	38.8	60.3

As assumed in Table 6.1, capacities of nuclear, wind and PV are specified, while NG CCS can be further added to the generation mix if the carbon targets cannot be satisfied. Therefore, the curtailment of RES in the decoupled system is much higher than that in the integrated system, and hence more NG CCS is deployed to compensate the curtailment and meet the carbon target. On the one hand, although the curtailment of RES is significantly alleviated through the system integration, the overall carbon intensity on the electricity side is still increased due to the significant reduction in generation from NG CCS. On the other hand, the system integration drives the electrification of the heat sector, thus reducing the carbon intensity on the heat side. The overall carbon intensities of both integrated system and decoupled system are the same. To summarize, higher carbon emissions in electricity sectors are allowed given lower carbon emissions in heat sectors, as the total carbon emissions are constant (meeting the same carbon target). This will lead to higher costs in heat sectors and lower costs in electricity sectors, but the overall system costs are reduced significantly.

This study indicates that the system integration can deliver the shift in carbon emissions from the heat sector to the electricity sector, driven by the shift in heat production from gas-boilers to NG CHPs while facilitating the electrification of the heat sector, which leads to significant cost savings in the electricity sector through the replacement of some NG CCS capacity by NG CHP (fundamentally enabled by the flexibility that significantly reduces RES curtailment).

6.2.5 Value of TES

As TES plays an important role in facilitating the interaction between the electricity and the heat system, we specifically calculate the potential savings through the application of TES in the integrated electricity and heat system. In order to quantify the value of TES, we compare the costs of the integrated electricity and heat system with (main case) and without (counterfactual) TES. Table 6.5 summaries the annual savings in OPEX and CAPEX of the electricity sector and CAPEX of the heat sector through the application of TES under given carbon scenarios. Note that the CAPEX of TES for the main case is £0.78bn/year and £1.21bn/year under the carbon target of 100g/kWh and 50g/kWh respectively, while no TES is installed in the counterfactual.

Table 6.5 – Savings from TES in integrated electricity and heat system

Carbon target	OPEX	CAPEX of electricity Sector	CAPEX of heat sector	Total
(g/kWh)	(£bn/yr)	(£bn/yr)	(£bn/yr)	(£bn/yr)
100	1.84	0.78	-1.81	0.81
50	2.73	2.41	-3.10	2.05

It can be seen that TES plays an important role in reducing the whole system operation and investment costs in the electricity sector at the cost of increasing the investment in the heat sector. Specifically, TES enables: a) delivery of operation savings through alleviating the curtailment of RES, b) reduction of NG CCS capacity by supporting provision of ancillary services leading to an increase in RES production and c) the shift in heat delivery from end-use to district based technologies, driven by the flexibility requirements (supported by the relatively low capital cost of industrial size TES).

6.2.6 Benefits from Pre-heating

Due to the improved insulation of buildings, pre-heating through heat-driven electricity devices can enable further reduction in the operation cost of the integrated system although overall energy consumption increases.

Figure 6.6 illustrates the impact of preheating on the operation of hybrid HP-Bs spanning 3 days in winter. To highlight the impact of pre-heating, it is assumed in this case that all hybrid HP-B users participate in pre-heating. The results demonstrate that the level of pre-heating will be influenced by the amount of RES production. Savings in the operation cost is achieved by shifting heat-load to the hours when RES production is significant, which reduces RES curtailment. On the other hand, during the hours when the availability of RES is low, pre-heating is not extensively used. It should be noted that this analysis has been simplified by assuming that the flexibility enabled by preheating would not compromise the consumer comfort.

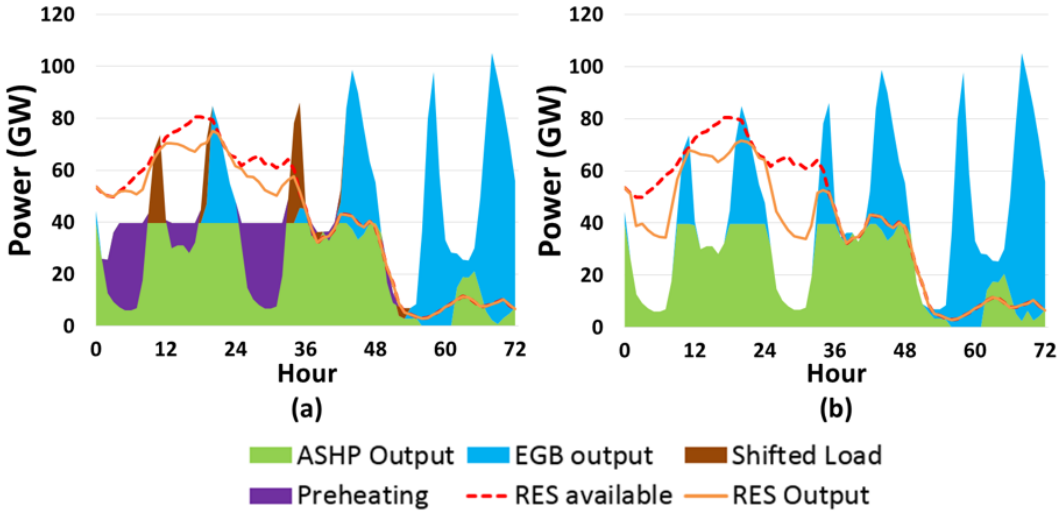

Figure 6.6– Operating patterns of hybrid HP-Bs without (b) preheating

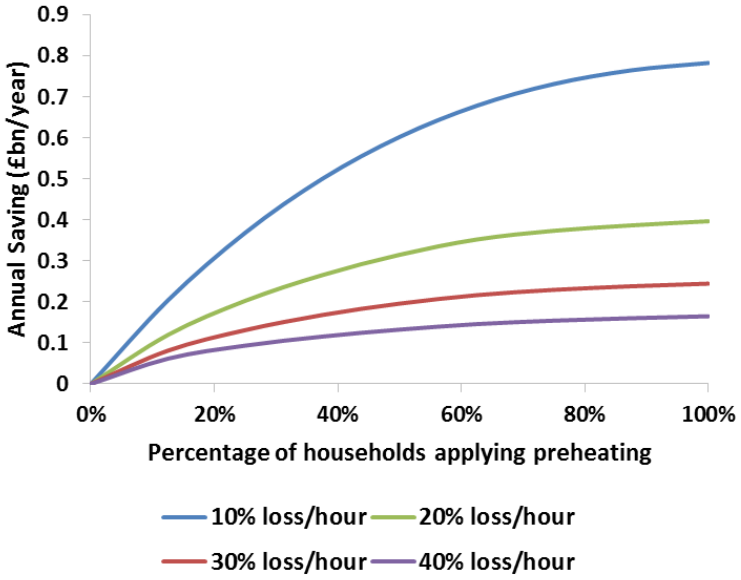

Figure 6.7– Annual Savings of the Whole System through preheating

The insulation levels of buildings as well as the percentage of households contributing to pre-heating are potential factors that may influence the value of pre-heating. In this context, Figure 6.7 shows the annual savings associated with pre-heating considering (i) different insulation levels of buildings and (ii) different percentage of households participating in pre-heating. In addition to the savings in operation cost (driven by increased utilization of RES), the

application of pre-heating can also substitute a considerable amount of TES, driving further savings. From the results, it can be concluded that a) the value of pre-heating is intensely affected by the buildings insulation levels (energy efficiency); b) as expected, the marginal value of pre-heating declines with the increase of percentage of households providing this service.

It is worth noticing that the improvement of building insulation level can effectively reduce heat demand, thus compressing the space of operational savings through pre-heating, as demonstrated in Section 3.3.3. However, when considering investment costs of different assets, improved building insulation can introduce extra flexibility to pre-heating, as thermal energy can be stored for a longer time. Therefore, pre-heating can shift peak load in a more flexible way, thus increasing investments savings.

6.2.7 Impact of Electricity Based Flexibility Measures

Considerable potential savings can be achieved through the integration of the heat and electricity system according to Section 6.2.1. However, the value of the integrated electricity and heat system may be significantly influenced by the availability of flexibility options in the electricity system. This section investigates the benefits through the integration of the heat system with a more flexible electricity system, compared to Section 6.2.1, revealing the impact of the electricity-based flexibility measures on the value of the integration. For the illustrative purpose, this case study is carried out by enhancing the flexibility of the electricity system through:

1) Applying more efficient and more flexible thermal generation. The comparison of the operating parameters between generators with low and high flexibility and efficiency are presented in Table. A.13.

2) Assuming that 15GW of electrical energy storage have already deployed in the electricity system and can provide all ancillary services.

3) Assuming that 20% of the non-heat driven electricity load is flexible to provide demand side response.

The aggregated OPEX savings and CAPEX savings in electricity and heat sectors through the integration of the heat system and the electricity system with increased flexibility are given in Table 6.6, while more detailed information is demonstrated in Figure 6.8.

Table 6.6 – Savings from the system integration with increased flexibility

Carbon target (g/kWh)	OPEX (£bn/yr)	CAPEX of electricity sector (£bn/yr)	CAPEX of heat Sector (£bn/yr)	Total (£bn/yr)
100	1.24	0.66	-1.44	0.46
50	1.21	1.29	-1.34	1.15

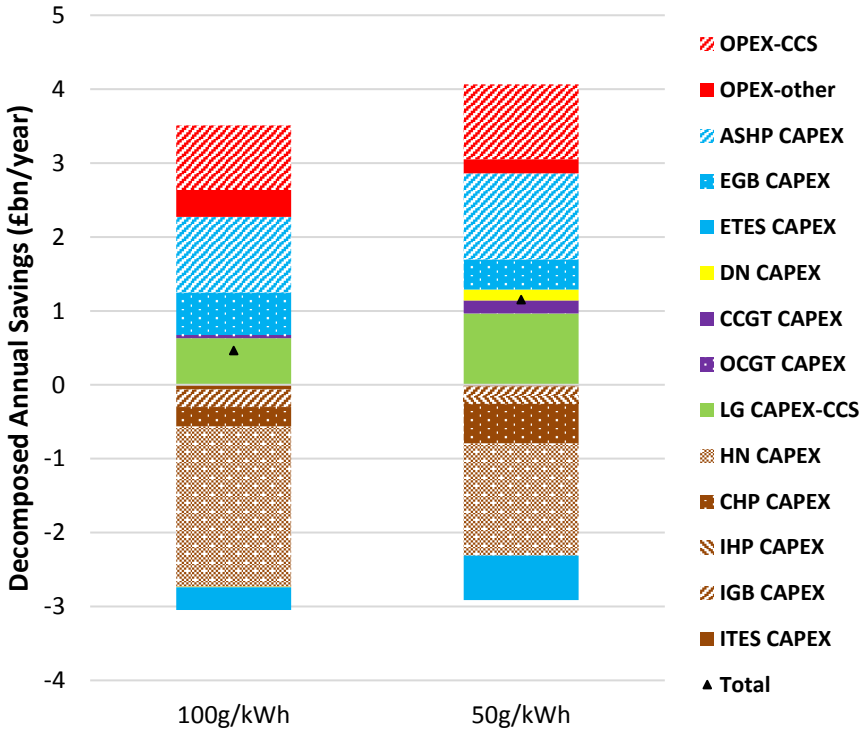

Figure 6.8– Savings from the integration of electricity and heat systems when different flexibility measures are available in the electricity system

Compared with Section 6.2.1, the total saving of the integrated electricity and heat system in this case reduces significantly, from £2.3bn/year to £0.46bn/year under the carbon target of 100g/kWh, and from £6bn/year to £1.15bn/year under the carbon target of 50g/kWh. This demonstrates that the benefits driven by the integration of the electricity and heat system may

reduce accordingly if the flexibility within the electricity system increases. It is however important to note that the additional cost associated with enhancing the flexibility of the electricity system is not taken into account. To be specific, it is assumed that flexible thermal generators, electrical storage are already deployed in the electricity system while DSR can be dispatched without incurring miscellaneous costs. In fact, it can be very capital-intensive to improve the flexibility of thermal generation and deploy electrical energy storage on a large scale. The potential cost that DSR can incur depends on consumers' willingness and behaviour, which have significant uncertainty. Meanwhile, the heat system can provide substantial flexibility for the electricity system through system integration which otherwise will not be put into any use. If we consider the additional cost associated with flexible generators, electrical storage and DSR, the model will choose the system integration as the prioritised flexibility source.

To summarise, flexibility (particularly referring to energy arbitrage, response and reserve provision) is crucial for the integration of renewable sources so that facilitating the transition to a low-carbon energy system. There are many ways to improve the flexibility of the electricity system, system integration is a very cost-effective one.

6.2.8 Impact of Balancing Service Requirements on the Value of System Integration

The level of balancing services required has a significant impact on the value of system integration. The average and maximum amounts of reserve and response services in different scenarios are presented in Table 6.7, that correspond to the generation scenarios presented in Figure 6.3 (a). It can be observed that reduction in carbon emissions significantly increases the amount of balancing services.

Table 6.8 presents the cost savings associated with system integration under two carbon targets in two cases. In the first case, the volumes of reserve and response required are modelled as described in Section 4.2.2.4, while in the second case, the assumption is made that no balancing services would be required. It can be observed that the benefits of system integration

significantly decrease when there is no need for the provision of balancing services. Moreover, as expected, the benefits of system integration are larger under the lower carbon target.

Table 6.7 – Savings from System Integration in Different Scenarios

	100g/kWh		50g/kWh	
	Reserve (GW)	Response (GW)	Reserve (GW)	Response (GW)
Maximum	9.8	5.9	14.9	9.3
Average	4.9	2.7	7.0	5.1

Table 6.8 – Level of Ancillary Service Requirement in Different Scenarios

		100g/kWh	50g/kWh
Savings from system integration (£billion/year)	Reserve and response considered	2.3	6
	No reserve and response requirement	0.8	2.2

6.3 Conclusions of the Chapter

This chapter investigates the potential benefits of taking advantage of the interactions between the electricity system and heat system at the planning stage.

A series of case studies are carried out to quantify the benefits driven by the integration of the electricity and heat systems based on the cost assumptions. Results show that the annual saving by considering the system integration is up to 3.53% of the total annual system cost in the case where system integration is disregarded under the overall carbon target of 100g/kWh, while that saving can increase to 8.69% under the overall carbon target of 50g/kWh. Decomposed savings across different sectors through considering the system integration are also demonstrated. The analysis shows that increased investment in district heating infrastructure will enhance system flexibility that will in turn deliver larger cost savings in the operation and

investment of the electricity system, ensuring that the carbon target is met at the minimum whole-system cost.

Additionally, system integration can deliver the shift in carbon emissions from the heat sector to the electricity sector, driven by the shift in heat production from gas-boilers to NG CHPs, while facilitating the electrification of the heat sector, which leads to significant cost savings in the electricity sector through the replacement of some NG CCS capacity by NG CHP (fundamentally enabled by the flexibility that significantly reduces RES curtailment).

TES also plays an important role in reducing the whole system operation and investment costs in the electricity sector at the cost of increasing the investment in the heat sector. Specifically, TES enables: a) delivery of operation savings through alleviating the curtailment of RES, b) reduction of NG CCS capacity by supporting provision of ancillary services leading to an increase in RES production and c) the shift in heat delivery from end-use to district based technologies, driven by the flexibility requirements (supported by the relatively low capital cost of industrial size TES).

Moreover, the application of pre-heating can substitute a considerable amount of TES, driving further savings. Based on the results, the value of pre-heating is intensely affected by the building insulation levels (energy efficiency); and the marginal value of pre-heating declines with the increase of percentage of households providing this service. It is worth noticing that the improvement of building insulation level can effectively reduce heat demand, thus compressing the space of operational savings through pre-heating. However, when considering investment costs of different assets, improved building insulation can introduce extra flexibility to pre-heating, thus increasing investments savings.

In the end, this chapter also demonstrates that the level of balancing service requirements would have a major impact on the value of the system integration. In this context, provision of balancing services by different technologies, including the contribution of RES, nuclear generation, emerging flexibility technologies, etc., would potentially have a considerable impact on the value of the system integration.

Chapter 7 Computational Complexity Reduction

7.1 Computational Complexity of the Integrated Heat and Electricity System Model

As introduced in Section in 4.1, the integrated electricity and heat system model is formulated as an MILP with hourly time resolution across a whole year, while also considering sub-hourly frequency regulation and reserve constraints. This model simultaneously optimizes the operation and investment costs of the integrated energy system while covering both the local district and national level infrastructures. The whole GB transmission network is represented by four regions, including 1) Scotland, 2) North England and Wales, 3) Middle England and Wales, and 4) South England and Wales. In each region, the penetration of different heating technologies (e.g. district heating, supplied by CHP, HP, hot water tank based TES and gas boilers, as well as end-use heating, supplied by HPs, TES and gas boilers) is to be determined. The reinforcement of four categories of electricity distribution networks and the investment of four categories of heat networks characterised by different load density are also to be optimized in each region. The investment cost functions of electricity distribution and heat networks are established exogenously incorporated into the whole system optimization model. Distribution networks in different voltage levels are considered. The impact of CHP and industrial HP on the reinforcement of HV distribution networks is taken into account. Different types of generation plants are modelled individually, with identical categories of thermal plants being clustered into groups. The proposed model requires one set of integer variables for each group of plants. Moreover, the start-up & shut-down constraints as well as the minimum online & offline constraints of generators introduce more integer variables, further increase the complexity to solve this model.

The complexity of investment planning models while taking into account a large number of operational conditions directly leads to dramatic computational burdens. The proposed integrated electricity and heat model is implemented by using FICO® Xpress as a solver on a

computer with two 2.7GHz processors and 512GB RAM. FICO Xpress optimizer is a commercial optimization solver which can be used to solve linear programming, mixed integer linear programming, and a series of non-linear programming problems (e.g., QP, QCQP, SOCP, etc.). It uses the modelling language Xpress Mosel and works under the integrated development environment Xpress Workbench. In FICO Xpress, linear programming can be solved through the primal simplex method, the dual simplex method or the barrier interior point method, while mixed integer programming are solved by a combination of the branch and bound method and the cutting-plane method. It takes approximately 7.32×10^5 s (8.47 days) to solve the full-size model.

As running the proposed model over a whole year with hourly resolution is very time-consuming, it is crucial to simplify the calculation so that this model can be solved within a reasonable time. One research direction to find the solution to this challenge is to reduce the size of input data by selecting a set of representative periods from the total number of operating snapshots. The selected periods have to retain most of the characteristics of the original data while ensuring that the investment decisions made based on them are near-optimal [107-109].

7.2 Previous Work of Data Selection

Different algorithms have been investigated for the selection of representative periods. In the early research, heuristic approaches was applied by experts to manually select the representative operating scenarios that can best describe the statistical characteristics of the input data, particularly based on the variations of electricity or heat demand and RES availability. For instance, in [110], 17 time snapshots are selected from the data covering a 2-year period (i.e., 16 time snapshots representing different seasons and one snapshot capturing the summer super-peak moment) to describe the diurnal and seasonal fluctuation in electricity demand and generation output. However, approaches based on heuristic selection lack the criteria of systematic selection. Additionally, the increased deployment of renewables may give rise to improved diversity in the patterns of operating conditions, leading to the inadequacy of performing the heuristic selection approaches manually.

Lately, a couple of clustering-based algorithms have been presented to fully describe the statistical characteristics and correlations between the electricity demand and RES data. In [111], a k-means-based clustering approach was applied to capture the inter-spatial correlation between the electricity demand and wind generation in an investment planning problem. The authors in [112] also use the k-means clustering approach to implement the selection of representative operating snapshots for wind generation investment.

However, only using the selected representative operating snapshots to solve the energy-system investment problem will miss out the inter-temporal information of system operation due to the break in the chronological data sequences. As the ignorance of inter-temporal information may lead to unreasonable results, it is crucial to select representative periods (e.g., days) instead of representative time snapshots, which can simultaneously describe (i) the correlation among different input vectors, such as energy demand and RES availability, (ii) the inter-spatial correlations among various regions, and (iii) the temporal auto-correlation of each variable. To this end, reference [108] proposed an optimization-oriented approach of representative day selection to investigate the impacts of the integration of variable and intermittent renewables on electricity system investment problems, and presented the metrics of representativeness evaluation. Meanwhile, two hierarchical-clustering-based selection approaches was proposed in [113] electricity system expansion in the long run, taking into consideration the inter-temporal operational restrictions. Additionally, critical statistical characteristics of the operational information included in the input data (i.e., temporal autocorrelations and spatial correlations) can be captured through this approach.

The aforementioned selection methods are all performed according to the operational information in the input domain (e.g. load profile, wind availability factor, etc.), which is convenient and straightforward for the implementation of the selection. However, since the investment decisions can be significantly non-linear to the input variables for the long-term investment planning problems, the input domain may not be the most appropriate domain to do the clustering. To this end, the work presented in [114] applied a moment-matching based approach to cluster operating snapshots according to the optimal power flow (OPF) patterns, pointing out that power flow patterns are crucial drivers for the reinforcement of the transmission networks. Many other researches also indicated that the OPF-based approach

could lead to a reduction in the number of selected scenarios required to optimize the transmission network expansion problems, while improving the accuracy of the selection. Furthermore, authors in [115] proposed an operating-state-aggregation algorithm to select representative scenarios based on the benefit of transmission lines, while the work presented in [116] considered the expected electricity transmission corridors as the clustering variables, and particularly investigated the crucial operating conditions that may lead to the compromise in the system security. Additionally, scenario reduction is performed in the context of risk-averse electricity trading in [117], based on the distance between two scenarios using an auxiliary variable, which captures the Conditional Value at Risk (CVaR) of profits. Particularly, there are some other references that cluster scenarios based on the objective domain, which can effectively address the nonlinear relationship between the investment decisions and the input variables. An objective-domain-based scenario selection framework was recently proposed in [109], taking account of the investment decisions of transmission network expansion, clustering every single scenario. In [118], an objective-function-based algorithm was proposed to reduce scenarios for electricity trading decision making in a stochastic programming model. The clustering of scenarios considers the distance between the optimal objective function values of the corresponding single-scenario optimisation problems when fixing the first-stage decisions.

Although various clustering domains have already been explored to effectively perform the operational snapshots selection, few studies have considered the inter-temporal information in the operation constraints by performing representative periods (e.g., day) selection to simplify the calculation of energy system planning problems. In this context, it is highly meaningful to investigate a more advanced method for the selection of representative days to further enhance the efficiency of calculation without compromising the accuracy.

7.3 Representative-day Selection Based on a Cost-oriented Approach

In this section, a data selection framework is investigated to select a couple of days that can accurately represent the original data, according to the investment decisions that are determined

by every single day. While this framework conducts data clustering in the objective domain, it is not only based on the optimal value of the objective function, as the case in [118]. Instead, the scenario reduction is performed by clustering the values of all the decision variables, which can capture more information than the value of objective function. Moreover, this framework can take into account the inter-temporal characteristics of different scenarios by grouping time snapshots in a period (24 time snapshots grouped as a day in this section), and further reduce the dimension of the period-based vectors (decision variables), thus keeping the intra-period information.

7.3.1 Problem Statement

Given the multi-dimensional input dataset $X = \{\vec{x}_d^1, \vec{x}_d^2, \dots \vec{x}_d^N | d = 1, \dots D\}$, including N chronological sequences covering D time steps that represent the given operational conditions (e.g. electricity and heat demand, RES availability factor), the target of the integrated-electricity-and-heat-system investment model is to find the optimal set of investment decisions Γ^* (e.g., capacity of different generation, heating plants/appliances, etc.) that can minimize the whole-system cost C_{tot}, while simultaneously considering both the investment cost C_{inv}, which is merely determined by Γ^*, and the operation cost C_{op}, which is jointly driven by Γ^* and X. Thus, the minimum system cost can be express as Equation (7.1),

$$C^* = C_{tot}(X, \Gamma^*) = C_{inv}(\Gamma^*) + C_{op}(X, \Gamma^*) \tag{7.1}$$

Considering the complexity of the proposed integrated-electricity-and-heat-system investment model, it is intractable to run the optimization program with the full-size of the input dataset X (across the whole time horizon). Therefore, selecting a subset $X^\dagger$ from X as representative data while calculating their probabilities of occurrence $\Psi^\dagger$, and using $X^\dagger$ and $\Psi^\dagger$ to simulate the optimization problem, can be a potential solution to the challenge of the computational burden regarding the original problem driven by the full-size input data. However, how to effectively choose $X^\dagger$ that can lead to a near-optimal result, as demonstrated in (7.2), need to be addressed,

$$C_{inv}(\Gamma^\dagger) + C_{op}(X, \Gamma^\dagger) = C_{tot}(X, \Gamma^\dagger) \approx C^* \tag{7.2}$$

where $\Gamma^{\dagger}$ represents the investment decisions obtained by solving the optimization problem based on $X^{\dagger}$ and $\Psi^{\dagger}$.

Given that the clustering-based approach has already been validated to be effective for the selection of representative subset $X^{\dagger}$ from the original dataset X, we will also apply this approach as the basis. As the proposed model comprises a series of inter-temporal constraints, such as generator ramping, minimum online-offline time, etc. it is essential to select sets of consecutive snapshots (e.g. days) as representative periods to make sure that inter-temporal information is captured, thus introducing further challenges:

(i) Dimension increase of the clustering domain: Representative snapshots selection is implemented in a dataset with two dimensions, comprising $d1$ (Dimension 1) - sets of variables and $d2$ – sets of time steps. In contrast, representative period selection needs to be performed based on a three-dimensional dataset, consisting of $d1$ - sets of variables, $d2$ - sets of time steps included in an operational period and $d3$ – sets of operational periods. Therefore, it increases the dimension of the clustering domain, thus makes it more challenging for the calculation.

(ii) Nonlinearity between the operational conditions and the investment decisions: Increased nonlinearity will be introduced between the input data and output results, with the rise of the complexity of the optimization problem. Therefore, it is inadequate just to capture the crucial statistical features, such as variability, distribution and correlation, of the input dataset.

(iii) Curse of dimensionality: The more time steps an operational period includes, the higher dimensional the clustered data will be regarding $d2$. Moreover, the considerable size of $d1$ in a large-scale system, as modelled in Chapter 4, can also result in significant challenges in clustering. These aspects will lead to the curse of dimensionality.

It is worth noticing that, in terms of the operational periods, this section will be dedicated to representative day selection in the context of the energy system investment problem. However, this approach can be further extended to the selection of periods in any length (e.g. several hours or a month) by changing the size of $d2$, to meet the requirement in different contexts.

7.3.2 Cost-oriented Representative Day Selection Framework

In order to handle to challenges described in 7.3.1, this section presents a cost-oriented representative-day-selection framework under the collaboration with Mingyang Sun, Fei Teng, etc., as published in [119], which includes four steps:

1) Clustering Domain Transformation

Perform simulation for each individual day to acquire the results of the investment decisions (e.g. the capacity of different generation), which are used as clustering variables in the next steps.

2) Dimensionality Reduction

As the clustering variables include all the decision variables that drive the investment cost, which can incur the curse of dimensionality, it is essential to perform dimensionality reduction of the clustering variables to extract the main statistical characteristics.

3) Cluster Assignment

Cluster the lower-dimensional variables based on the extracted statistical characteristics.

4) Representative Day Selection

Select one representative day from each cluster. The chronologically corresponding data in the input domain is then selected to perform the simulation of the optimization problem.

A detailed description of this approach, which elaborates the implementation of these steps is presented as following:

Step 1: Clustering Domain Transformation

Traditionally, the representative scenario clustering is performed in the input domain, which is straightforward and effective in many situations. However, to deal with the increased nonlinearity between the input data and the output brought by the complexity rise in the proposed multi-energy system investment model, it will be imperative to consider clustering in other domains. This problem can be defined as the mathematical form as below:

Let Set X denotes the multivariate input data in chronological sequences (specifically including the availability profile RES, the demand profile of electricity & heat, and ambient temperature in different locations), as formulated in Equation (7.3),

$$X = \left\{\vec{x}_d^1, \vec{x}_d^2, \dots \vec{x}_d^{N_L \times (N_{RES}+N_{DE}+N_{AT})} | d = 1, \dots D\right\} \in \mathbb{R}^{D \times [N_L \times (N_{RES}+N_{DE}+N_{AT})] \times N_d} \quad (7.3)$$

where D represents the number of days in the studied time horizon; N_L represents the number of locations; N_{RES} represents the number of RES generation types; N_{DE} represents the number of demand; N_d represents the number of time steps in a day; and N_{AT} represents the number of ambient temperature.

As introduced earlier, there are concerns related to (i) the dimension increase of the clustering domain when selecting representative days, and (ii) the nonlinearity between the operational conditions and the investment decisions. The key challenge to address these concerns is to find a nonlinear mapping function $f: X \to Z$ that transforms the dataset X in the input domain into a dataset Z in an effective domain, while ensuring that the clusters $[X^1, X^2, \dots, X^K] \subseteq X$ established according to the cluster index $y = cluster(Z)$ eventually leads to near-optimal investment decisions $\Gamma^{\dagger}$, based on the representative periods $X^{\dagger} = \left[x_1^{\dagger}, x_2^{\dagger}, \dots, x_K^{\dagger}\right]$ (where $x_1^{\dagger} \in X^1, x_2^{\dagger} \in X^2, \dots, x_K^{\dagger} \in X^K$) and their corresponding probability of occurrence $\Psi^{\dagger} = \left\{\psi_k^{\dagger}, k = 1,2, \dots, K\right\}$. Note that K is the number of clusters while $cluster(\cdot)$ denotes the function of clustering method.

Most of the previous research determines cluster index y according to the dataset X in the input domain while ensuring that the selected periods $X^{\dagger}$ can capture most of the important statistical information associated with X, thus resulting in a similar outcome to the case in which the results are obtained based on the original input data X (e.g., [108], [113]). However, the input-based clustering approach can sometimes be off the track, leading to an inappropriate scenario reduction due to the following reasons: (i) Operating periods with completely different statistical patterns in the input domain can result in similar or even identical investment decisions; (ii) Meanwhile, operating periods with similar statistical patterns in the input domain can sometimes lead to highly different results; (iii) Since the capacities of RES generation are to be optimized, it is impossible to pre-define the impact of RES output in the process of

clustering; iv) The statistical features related to the ancillary service requirements cannot be effectively captured in the input domain.

To address the aforementioned drawbacks, we propose a cost-oriented algorithm in this section to map the clustering domain from the input dataset X to decomposed investment costs (Set Z), by running the optimization problem for each individual day and further performing the clustering according to the cluster index determined through grouping the investment costs.

The input dataset is given as $X = [X^W, X^{PV}, X^E, X^H, X^T] = \{\vec{x}_d^W, \vec{x}_d^{PV}, \vec{x}_d^E, \vec{x}_d^H, \vec{x}_d^T | d = 1, \dots D\} \in \mathbb{R}^{D\times[N_L\times(N_{RES}+N_{DE}+N_{AT})]\times N_d}$, where X^W and X^{PV} denote the availability factor of wind and PV output, X^E and X^Hrepresent electricity and heat load, while X^T is the ambient temperature. In the first step of the cost-oriented representative day selection framework, the investment optimization problem is simulated based on the input data of each individual day d. Note that the input data of day d is repeated across the whole year to ensure that all simulations are performed under the same time horizon. The output data in this step is the investment cost of each technology at each location, which can be expressed as $\Gamma = [\Gamma_1, \Gamma_2, \dots, \Gamma_D] \in \mathbb{R}^{D\times[N_L\times N_T]}$, $\Gamma_d = \left\{\gamma_d^{l,tech}, b = 1,2, \dots, N_L, tech = 1,2, \dots, N_T, d \in D\right\}$, where $\gamma_d^{l,tech}$denotes the investment costs of technology type $tech$ at location l, driven by the input data of day d.

Step 2: Dimensionality Reduction

As introduced in Section 7.3.1, there are two crucial challenges associated with dimensionality when selecting representative days. The first challenge is that representative day selection will switch the input data from a two-dimensional dataset ($d1$: $N_L \times (N_{RES} + N_{DE} + N_{AT})$ variables and $d2$: $N_d \times D$ time snapshots) to three-dimensional dataset ($d1$: $N_L \times (N_{RES} + N_{DE} + N_{AT})$ variables, $d2$ - N_d time steps included in a day and $d3 - D$ days). The second challenge is that the number of operating days for clustering is very limited. In terms of the first challenge, the first step has provided a solution by mapping the clustering domain from input dataset $X \in \mathbb{R}^{D\times[N_L\times(N_{RES}+N_{DE}+N_{AT})]\times N_d}$ to investment cost dataset $\Gamma \in \mathbb{R}^{D\times[N_L\times N_T]}$, thus reducing the dimension of $d2$. However, regarding the second challenge, the consideration of various technology types and different location for deployment in the national-level system will

introduce the curse of dimensionality, which refers to the problem that linear increase in dimensions will lead to exponential increase in volume, in the Euclidean space [120]. Therefore, it is necessary to further reduce the dimension of the investment cost domain, even though its dimension has already been lowered through the clustering domain transformation in the first step.

Basically, two approaches, namely feature extraction and feature selection, are commonly used to realize dimensionality reduction. In the cost-oriented representative-day-selection framework, the investment costs of each technology deployed at each location are taken as the clustering variables, making it more suitable to capture key characteristics of clustering variables through an automatic way or quasi-automatic way, as it is difficult to manually determine which variables exert higher impacts on the optimal results merely according to sets of investment costs.

Classical linear dimensionality reduction such as linear discriminant analysis and principle component analysis have been widely applied but with a limited performance in many cases. A bunch of nonlinear dimensionality reduction algorithms have been investigated to improve the performance, (e.g., kernel principal component analysis, and Laplacian Eigenmaps [121], etc.. Since the size of the clustering data in our study is very limited (there are only 365 days), those algorithms that require a huge number of clustering statistics (e.g., neural-network-based approaches and data-driven high-dimensional scaling) are not suitable. Therefore, we apply Laplacian Eigenmaps, which is a geometry-based algorithm characterized by locality-preserving and natural connection for data grouping. The inherent geometric features of the manifold based on the clustering data can be reflected by the dimension-reduced data.

The procedures of LEM to reduce the dimension of the investment cost dataset Γ can be expressed as following mathematical problem.

Given that $\Gamma = \{\Gamma_d\}_{d=1}^{D} \in \mathbb{R}^{D\times[N_L\times N_T]}$ is the investment cost driven by each individual day, while γ denotes the target dimension after being reduced, we firstly establish an adjacency graph, denoted as $Q = (N, E)$, in which N is the set of nodes while E is the set of edges in this graph. Note that nodes in N ($n_i \in N$) are linked to sets of investment costs $\Gamma_i, i \in [1,2,\dots,D]$, thus the number of nodes in N is equal to the number of days D. If the statistical distance of a

pair set of investment cost (Γ_i, Γ_j) is close enough, according to the measurement through the k-nearest neighbour (KNN) approach, their corresponding pair of nodes n_i and n_j will be connected by an edge $E_{i,j} \in E$.

Secondly, the weights $W = \{w_{i,j}, i,j = 1,2,\dots,D\}$ of each edge $E = \{E_{i,j}, i,j = 1,2,\dots,D\}$ are determined through the approach presented in Equation (7.4),

$$w_{i,j} = \begin{cases} 1, \text{if } n_i \text{ and } n_j \text{ are connected via edge } E_{i,j} \\ 0, \text{if } n_i \text{ and } n_j \text{ are not connected} \end{cases} \tag{7.4}$$

Next, we will find the solution to the eigenvector problem: $L\alpha = \lambda D\alpha$. Note that D in this equation denotes the diagonal weight matrix, which is calculated as $D = \{D_{i,i} = \sum_j w_{i,j}, \forall i,j \in 1,2,\dots,D\}$, while $L = D - W$ represents the Laplacian matrix. Then, the solution $A = [\alpha_0, \alpha_1, \dots, \alpha_{\gamma-1}] \in \mathbb{R}^{D\times\gamma}$ is calculated based on the target dimension γ, the order of which is consistent with the order of their eigenvalues $0 = \lambda_0 \le \lambda_1 \le \cdots \le \lambda_{\gamma-1}$. Finally, the investment cost dataset after dimensionality reduction can be expressed as $\Gamma^{DR} = \{\tilde{\Gamma}_i, \forall i \in 1,2,\dots,D\} \in \mathbb{R}^{D\times\gamma}$, where $\tilde{\Gamma}_i = \left(\alpha_0(i), \alpha_1(i), \dots, \alpha_\gamma(i)\right) \in \mathbb{R}^{\gamma}$.

Step 3: Cluster Assignment

In this step, we will group the data of the dimension-reduced investment cost dataset $\tilde{\Gamma}$ into K clusters, namely $\tilde{\Gamma}^k \subset \tilde{\Gamma}$, $k = 1,2,\dots,K$. The main point is to differentiate various investment costs. The objective of the clustering is to obtain the index of each cluster $y \in \mathbb{R}^D$, which will then be used to distribute the input data $\vec{x}_d$. $d = 1,2,\dots,D$ into different clusters, as shown in Equation (7.5),

$$X_{cls} = \{X_k\}_{k=1}^{K}, X_k \in \mathbb{R}^{N_k\times[N_L\times(N_{RES}+N_{DE}+N_{AT})]\times N_d} \tag{7.5}$$

Hierarchical clustering is a commonly used approach to establish a series of hierarchical clusters based on the similarity of the data in different clusters [122]. In this framework, both agglomerative hierarchical clustering and Ward's linkage are applied to construct clusters of

investment costs and select the final operating days from each individual group as representatives. The advantages of this approach include:

1) Regarding the geometry of established clusters, the applied hierarchical clustering approach can deal with non-spherical cases.

2) Clusters established through hierarchical clustering are independent of the original assignment of data, so they are characterized with a deterministic instinct to avoid repeatability.

3) Hierarchical clustering does not require prior information about the cluster number, so the agglomeration can be finalised with any required number of clusters.

4) Ward's minimum variance criterion [123] has an advantage over the other types of linkages (e.g., single-linkage, complete-linkage, etc.) for the minimization of the overall inner-cluster variance. For the day selection approach proposed here, it is significant to make sure the variance of clustered investment costs of different groups is minimum for corresponding to the input dataset that lead to close investment costs.

Basically, hierarchical clustering could be carried out through the following procedures according to the clustering variables $\tilde{\Gamma} \in \mathbb{R}^{D\times\gamma}$. Firstly, each individual point in $\tilde{\Gamma}$ is allocated to its own singleton group. Through the measurement of Euclidean distance, the similarity matrix can be established for $\tilde{\Gamma}$, as in Equation (7.6),

$$S = \left\{s_{i,j}, \forall i,j \in 1,2,\dots,D\right\} \in \mathbb{R}^{D\times D} \tag{7.6}$$

In this way, any two clusters with the shortest distance will be combined into one based on their similarity. It is worth noticing that, the similarities across different clusters are measured according to the Ward's linkage criterion. For any two clusters k_1 and k_2, their distance d_{k_1,k_2} is obtained according to Equation (7.7),

$$d_{k_1,k_2} = \left\|\tilde{\Gamma}_c^{k_1}\tilde{\Gamma}_c^{k_2}\right\|_2 \sqrt{\frac{n_{k_1}n_{k_2}}{n_{k_1}+n_{k_2}}} \tag{7.7}$$

where $\|\cdot\|_2$ represents Euclidean distance, $\tilde{\Gamma}_c^{k_1}$ and $\tilde{\Gamma}_c^{k_2}$ denote the centroids of clusters k_1 and k_2, while n_{k_1} and n_{k_2} denote the operating day counts of cluster k_1 and k_2.

Step 4: Representative Day Selection

In the last step, we will choose one typical day from each individual cluster as the representative of all days in the same cluster, and determine their weights.

Representative day identification: The mean point or the medoid point is commonly adopted to represent the overall statistical information of the cluster. However, the mean point is not suitable to play as the representative in this case because it may not be able to correspond back to any real operating day in the input domain. Therefore, we use the medoid point $\vec{\gamma}_k^{\dagger} \in \mathbb{R}^{|L|\times|T|}$ of cluster k in the investment cost domain $\tilde{\Gamma}$ as the representative and then correspond it back to the operating day with the same day label in the input domain of X, which is the selected representative day. The data in the representative day is denoted as $\vec{x}_k^{\dagger} \in \mathbb{R}^{|L|\times(|RES|+|DE|+|AT|)}$.

Determination of the weight for each representative day: As all the operating days in have identical probability of occurrence, it is rational to adopt the day count in a cluster as the weight of the representative day selected from that cluster. The outputs of the representative day selection framework include the data in the selected days, denoted as $X^{\dagger} = \{\vec{x}_k^{\dagger}, k = 1,2,\dots,K\}$, and their weight of occurrence, denoted as $\Psi^{\dagger} = \{\psi_k^{\dagger}, k = 1,2,\dots,K\}$.

7.3.3 Evaluation of the Proposed Representative Day Selection Approach

In this section, we will evaluate the performance of the proposed cost-oriented representative-day-selection approach by comparing it with the state-of-the-art input-based approach, which has been widely used for scenario reduction.

The summary of these two tested approaches are presented as following. Note that as the input-based approach is not the focus in our work, we just described it briefly. More details about this approach has been elaborated in a recent paper [113].

Tested Approach 1: Cost-oriented Representative Day Selection Approach

---

Input:

1. Multidimensional dataset of wind and PV availability factor, and electricity and heat load and ambient temperature across the whole time horizon $X = [X^W, X^{PV}, X^E, X^H, X^T]$;
2. Target dimension after dimensionality reduction γ;
3. Target number of representative days K;

Mathematical model of the energy system planning problem $Planning(\cdot)$.

Procedures:

Step 1: Group the input data by days (7.8). Run the model for each individual day, obtaining the decomposed investment costs driven by each day, as formulated in (7.9).

$$X = [X^W, X^{PV}, X^E, X^H, X^T] = \{\vec{x}_d^W, \vec{x}_d^{PV}, \vec{x}_d^E, \vec{x}_d^H, \vec{x}_d^T | d = 1, \dots D\} \tag{7.8}$$

$$\Gamma_d = Planning(\vec{x}_d), d = 1,2, \dots, D \tag{7.9}$$

Step 2: Perform dimensionality reduction by using the method of LEM, as shown in (7.10). After this step, the dimension of $\tilde{\Gamma}$ becomes γ.

$$\tilde{\Gamma} = LEM(\Gamma) \tag{7.10}$$

Step 3: Cluster $\tilde{\Gamma}$ into K groups by using hierarchical clustering, as given in (7.11). Then correspond each individual cluster from the investment cost domain $\tilde{\Gamma}^k$to the input domain X_k, as shown in (7.12).

$$\left[\tilde{\Gamma}^k|_{k=1}^K, \Lambda_{D,k}|_{k=1}^K\right] = HierachicalClustering\left(\tilde{\Gamma}, K\right) \tag{7.11}$$

$$X_k = \left\{\vec{X}_d, \forall d \in \Lambda_{D,k}\right\}, k = 1,2, \dots, K \tag{7.12}$$

Step 4: Adopt the index of the medoid point of each cluster as the index of representative days (7.13) and (7.14). Select representative days (7.15) based on the adopted day index and calculate the probability of occurrence of each representative day based on (7.16). It is worth noticing that idx_k^{med} denotes the day index that corresponds to the medoid point of a cluster.

$$idx_k^{med} = medoid\left(\tilde{\Gamma}^k\right), k = 1,2,\dots,K \tag{7.13}$$

$$\vec{x}_k^{\mathrm{f}} = X_k\left(idx_k^{med}\right), k = 1,2,\dots,K \tag{7.14}$$

$$X^{\mathrm{f}} = \left\{\vec{x}_k^{\mathrm{f}}, k = 1,2,\dots,K\right\} \tag{7.15}$$

$$\Psi^{\mathrm{f}} = \left\{\psi_k^{\mathrm{f}} = \left|\Lambda_{D,k}\right|/\Lambda_D, k = 1,2,\dots,K\right\} \tag{7.16}$$

Output:

1. Set of input data of representative days: $X^{\mathrm{f}} = \left\{\vec{x}_k^{\mathrm{f}}, k = 1,2,\dots,K\right\}$;

2. Set of probabilities of representative days: $\Psi^{\mathrm{f}} = \left\{\psi_k^{\mathrm{f}}, k = 1,2,\dots,K\right\}$.

Tested Approach 2: Input-based Representative Day Selection Approach

---

Input:

1. Multidimensional dataset of wind and PV availability factor, and electricity load across the whole time horizon $X = [X^W, X^{PV}, X^E, X^H, X^T]$;

Target number of representative days K;

Procedures:

Step 1: Re-arrange the input operating condition data, grouping them by days, as $X = [X^W, X^{PV}, X^E, X^H, X^T] = \{\vec{x}_d^W, \vec{x}_d^{PV}, \vec{x}_d^E, \vec{x}_d^H, \vec{x}_d^T | d = 1, \dots D\}$.

Step 2: Adopt hierarchical clustering approach to cluster days according to X;

Step 3: Select the medoid point of each individual cluster as the representative day and calculate their corresponding probability of occurrence.

Output:

1. Set of input data of representative days: $X^{\dagger} = \{\vec{x}_k^{\dagger}, k = 1,2, \dots, K\}$;

2. Set of probabilities of representative days: $\Psi^{\dagger} = \{\psi_k^{\dagger}, k = 1,2, \dots, K\}$.

It is important to stress that the aim of proposing the cost-oriented representative-day-selection approach is to simplify the calculation of the energy-system-investment-planning problem with improved accuracy, as the widely used input-based approach has some limitations:

1) Due to the potential nonlinearity between the input domain and output domain in complex cases, operational days characterized by significantly different statistical features may lead to similar investment results. Meanwhile, operational days characterized by similar statistical features can give rise to very different results. Therefore, clustering directly based on the investment cost can avoid the mismatch caused by the nonlinearity.

2) The input data is given as $X = [X^W, X^{PV}, X^E, X^H, X^T]$, where X^W and X^{PV} are the availability factor of Wind and PV. In the cases where the capacities of Wind and PV are decision variables, the impact of Wind and PV generation on the system operation cannot be predefined. This can result in an irrational day selection if clustering is performed directly on the input dataset X, because the optimized results of the capacities of Wind and PV can influence the weight of X^W and X^{PV} in X.

3) As modelled in Section 4.2.2.4, the requirement of ancillary services (i.e., operating reserve and frequency response) can only be determined when the optimization problem has been solved, therefore, their influence on optimization results would not be adequately taken into account if clustering is only based on the input dataset X.

In order to demonstrate that the proposed cost-oriented approach can effectively address the aforementioned three limitations faced by the input-based approach, we test both approaches in three simplified cases with increased complexity. Note that we only consider the investment planning on the electricity side in the three testing cases for simplicity.

In the first case, a fixed amount of RES is given, while no inter-temporal constraints are taken into consideration. The aim of this case is to demonstrate that even in the simplest scenario, the proposed cost-oriented approach still has some advantage over the input-based approach.

In the second case, we consider the capacity of RES as decision variable (to be optimized), while inter-temporal constraints are still not considered. The aim of this case is to show that the proposed cost-oriented approach can effectively address the second limitation faced by the input-based approach.

In the third case, we take into account inter-temporal constraints and ancillary service requirement on the top of the second case. The aim of this case is to show that the cost-oriented approach can effectively tackle the third limitation.

Finally, we adopt the proposed approach to solve the integrated-electricity-and-heat-system investment model presented in Chapter 4.

In each case, the accuracy and computational time of the two tested approaches are compared with the benchmark (i.e., the simulation performed under the whole time horizon) to investigate the benefits of the proposed cost-oriented approach. Both of the proposed cost-oriented approach and the input-based approach are tested by using MATLAB 2017a and FICO® Xpress, on an Intel Xeon E5-2690 PC with 8 cores.

Case 1: As the simplest case, inter-temporal constraints are not considered, while a fixed amount of wind and PV is given as input, as listed in Table 7.1. The benchmark solution of Case 1 is presented in Table 7.2, in which the optimization is simulated based on the whole time horizon (i.e., 365 days).

Table 7.1 – Planned deployment of Wind and PV in each region

	Scot (GW)	North E&W (GW)	Mid E&W (GW)	South E&W (GW)
Wind	18	0	0	10
PV	0	0	2	9

Table 7.2 – Benchmark solution and CPU time in Case 1

Operation cost (£m/year)	Investment cost (£m/year)	Total cost (£m/year)	CPU time (s)
2340.07	1230.86	3570.94	899.62

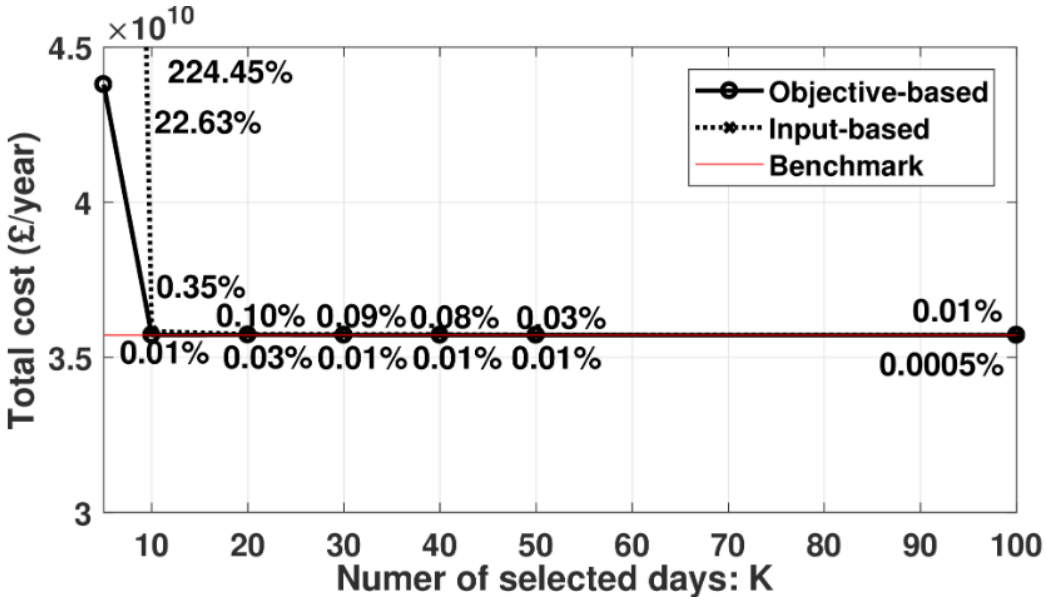

Figure 7.1– Performance of tested approaches against the number of representative days in Case 1

Figure 7.1 presents the results obtained through the objective-based approach and the input-based approach based on different numbers of representative days (K). The performance of each approach can be compared by the error of the total cost between the tested approaches and the benchmark. As can be observed, both approaches converge to the benchmark since K

reaches 10, but the cost-oriented approach consistently shows higher accuracy than the input-based approach.

Case 2: In this case, the availability of Wind and PV are given as input, but their capacities are decision variables, which are to be optimized. As the RES availability alone cannot describe the full RES-related operating conditions, clustering based on the input data may lead to significant inaccuracy since the impact of RES on the system operation is not captured sufficiently. Meanwhile, the investment costs is considered to be a more rational domain for clustering because it directly indicates the investment requirements driven by all input data. Therefore, it is expected that the performance of the proposed cost-oriented approach will be better than the input-based approach.

Both approaches are tested against K in this case. Table 7.3 gives the optimization results as well as the computational time of the benchmark obtained based on the full-size of input data, while Figure 7.2 demonstrates the total costs of tested approaches and shows their errors over the benchmark results. For both approaches, the estimated total costs keep approaching the benchmark with the increase of K. However, the cost-oriented approach consistently shows superior accuracy under the same K. As observed, the cost-oriented approach tends to converge faster to the benchmark. Specifically, when K reaches 30, the error of the estimated cost reduces to 0.02%, whereas the error driven by the input-based approach is still 0.50% even when K reaches 50.

Furthermore, Table 7.4 shows the CPU time under different K. As can be seen, remarkable reduction in CPU time against the benchmark (i.e., 4325.83s) is achieved for both approaches, while preserving high accuracy. For example, by using the cost-oriented approach, the computational cost can be reduced by 99.7% to achieve a result with an accuracy as high as 99.98% in this case.

Table 7.3 – Benchmark solution and CPU time in Case 2

Operation cost (£m/year)	Investment cost (£m/year)	Total cost (£m/year)	CPU time (s)
1666.95	1712.44	3379.39	4325.83

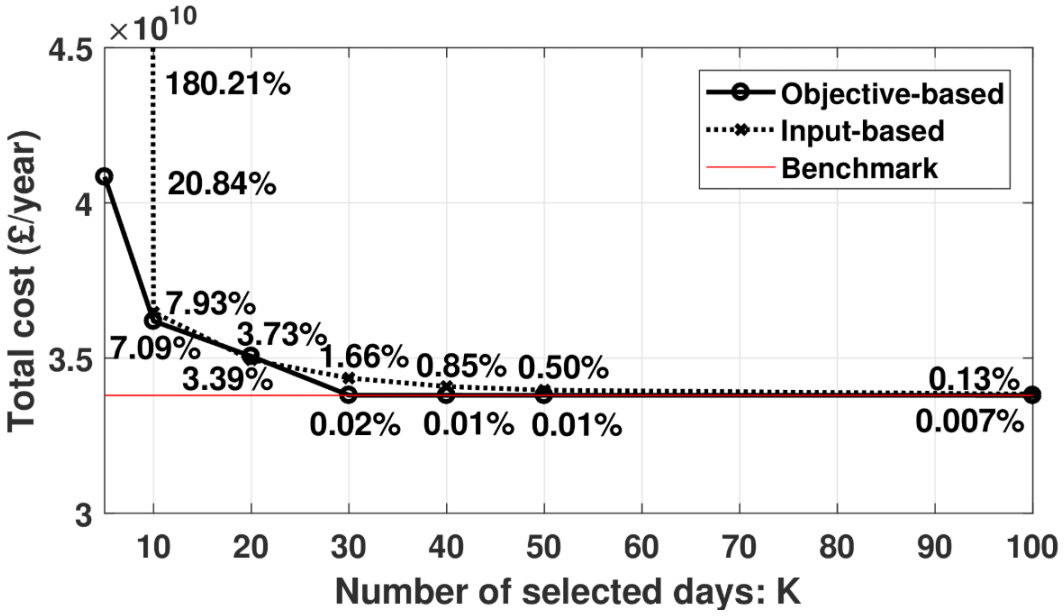

Figure 7.2– Performance of tested approaches against the number of representative days in Case 2

Table 7.4 – CPU time against number of representative days in Case 2

	K=10	K=20	K=30	K=40	K=50	K=100
Cost-oriented	14.26	25.40	40.26	60.72	92.92	368.01
Input-based	13.84	25.58	35.69	55.57	83.47	353.12

Case 3: In this case, the intertemporal constraints, including generator ramp, minimum online/offline time, and the requirement of ancillary services are considered. This will significantly increase the complexity of the calculation. Table 7.5 presents the optimization results and computational time of the benchmark in this case.

Table 7.5 – Benchmark solution and CPU time in Case 3

Operation cost (£m/year)	Investment cost (£m/year)	Total cost (£m/year)	CPU time (s)
2179.79	1320.61	3500.40	95460.13

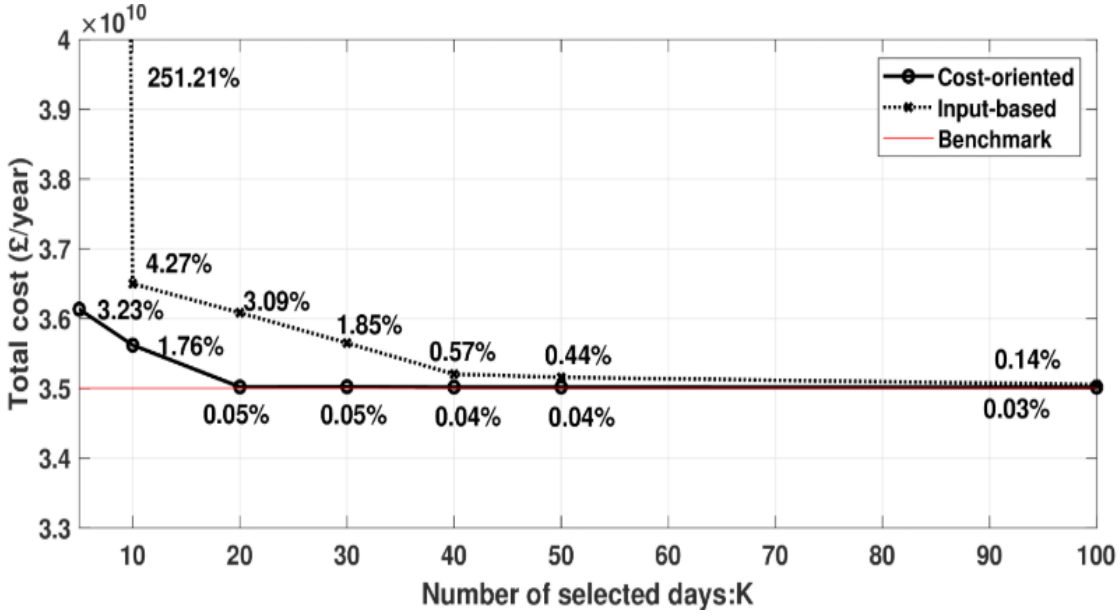

Figure 7.3– Performance of tested approaches against the number of representative days in Case 3

Figure 7.3 demonstrates the total costs calculated by using the tested approaches and their errors against the benchmark under different K. It can be observed that the cost-oriented approach shows improved performance over the input-based approach in Case 3 compared to Case 2. It is worth noticing that, the cost-oriented approach only requires 20 representative days to achieve an accuracy of 99.95%. Meanwhile, it takes the input-based approach 40 representative days to converge to a high accuracy (99.52%).

Table 7.6 – CPU time against number of representative days in Case 3

	K=10	K=20	K=30	K=40	K=50	K=100
Cost-oriented	47.73	141.42	369.92	684.61	1098.3	8419.3
Input-based	48.31	136.39	357.62	659.24	997.45	8143.58

Table 7.6 gives the CPU time of the cost-oriented approach under different K in Case 3. As can be seen, the cost-oriented approach only requires 20 representative days to achieve a highly accurate result, reducing the computational time from 95,460.13s in the benchmark to 141.42s. It is significant to stress that, the computational burden rises exponentially with the increase of the model complexity. Therefore, the benefits of proposed cost-oriented representative-day-

selection approach will increase when solving investment-planning problems with higher complexity.

We now employ the proposed cost-oriented representative-day-selection approach to solve the integrated-electricity-and-heat-system investment model presented in Chapter 4, under the scenario described in Section 6.2.2, where the capacities of all generation are optimized under the carbon target of 100g/kWh.

Table 7.7 shows the performance of the cost-oriented approach with different K, while the last column gives the benchmark result. It can be observed that the CPU time and the calculating error rise significantly compared to the three simplified cases, due to the increased complexity of the tested model. When K reaches 50, the error is lower than 1%. More accurate results can be achieved by increasing K, but the corresponding increase in computational time would be much more dramatic, thus jeopardising the overall benefits.

Table 7.7 – CPU time and error of proposed approach against number of selected days

K	10	20	30	40	50	100	365
CPU Time (s)	162	832	1822	3254	7523	67036	732604
Error (%)	23.68	6.34	4.21	2.56	0.94	0.58	0

7.4 Conclusions of the Chapter

This chapter proposes a cost-oriented representative-day-selection approach that can significantly reduce the computational burden of the integrated-electricity-and-heat-system investment-model proposed in Chapter 4, while ensuring that the investment decisions made based on the selected days are near-optimal.

The proposed representative-day-selection approach comprises 4 key steps: (1) transfer of the clustering domain, (2) dimensionality reduction, (3) cluster allocation, and (4) representative day identification. In the first step, the purpose is to map the original dataset in the operational domain to the objective domain, which is characterised with the investment costs of various technologies covering different regions based on the simulation of each individual day, because

the objective domain is more rational for performing data clustering in the investigated context. In the second step. The aim of performing dimensionality reduction is to handle the issue of high-dimensionality while allowing the data clustering to be carried out in a more effective domain that retains the key features of the original domain. In the third step, a hierarchical clustering approach under Ward's linkage criterion is adopted to cluster the operating days according to the corresponding investment costs. In the final step, the medoid point of each established group is identified as the representative day.

Three factors limit the performance of the widely used input-based approach, including: (i) the potential nonlinearity between the input domain and output domain in complex cases may lead to mismatch in data clustering; (ii) the impact of RES generation on the system operation cannot be predefined in the cases where the capacities of Wind and PV are decision variables; and (iii) the impact of ancillary services requirements on the optimization result cannot be adequately taken into account if clustering is only based on the input dataset. In order to demonstrate the effectiveness of the proposed cost-oriented approach in terms of addressing the limitations faced by the input-based approach, three simplified cases with increased complexity were tested. In the first case, a fixed amount of RES is given, while no inter-temporal constraints are taken into consideration. In the second case, the capacity of RES is considered as decision variable, while inter-temporal constraints are still not considered. In the third case, the inter-temporal constraints and ancillary service requirement are taken into account on the top of the second case. Results demonstrate that the proposed cost-oriented approach consistently shows advantages over the input-based approach throughout the three cases.

Chapter 8 Conclusions and Future Work

This thesis has investigated a series of decarbonisation strategies in order to support the 2050 carbon reduction target. By using the proposed integrated electricity and heat system investment model, it evaluated the economic performance of different promising low-carbon heating technologies and identified the optimal heating technology portfolio for delivering a low-carbon future energy system in different scenarios. This thesis also demonstrated the significance of considering various interactions among different energy sectors at the planning stage and the synergy effect through the coordinated operation of different components of the multi-energy system.

This final chapter summarises the conclusions drawn from the previous chapters and addresses the research questions 1 to 4, before listing further work.

8.1 Summary of Conclusions

8.1.1 District Heating Network Modelling

In Chapter 2, a novel DHN investment model is proposed to address RQ1.

In this model, the length of pipelines, which determines the cost of excavation and the installation of pipes is the key factor that drives the capital cost of DHNs. When the layout of consumers in a district has been determined, the length of pipelines can be calculated with the help of the fractal-based algorithm, the potential capital cost of DHN in that district is then determined and will not be influenced by the variation of heat demand. Therefore, the lower the heat demand (kW) in this district, the higher the unit investment (£/kW) of DHN.

As the investment cost of DHNs is dramatically influenced by the heat density in the supplied district, all GB regions are categorized into these 4 different representative districts in

accordance with their heat density. Based on the fractal-based algorithm, the length of representative networks with different geographic features can be calculated. The whole GB area is then represented as a linear combination of representative areas. By applying this approach, the investment cost of DHNs driven by different user penetrations in different representative areas can be quantified and incorporated into the national level energy system investment model to optimize the penetration of DHNs.

This chapter also investigated the operational principles of various heat sources in DHNs, including CHP plants, HPs and TESs and analyzed the coordinated operation of these heat sources to increase the flexibility of DHN operation. The results demonstrate that the synergy effects brought by integrating various heat sources can significantly improve the flexibility of DHN operation. HP and TES can both enhance the flexibility of CHP operation. All operating points in the extended operating area through HP can be theoretically reached unconditionally, while the reachability of the points between the extended operating area through TES and the original operating area of CHP depends on the state of charge of TES. Specifically, the boundary of the extended area can be reached only when the stored heat in TES is enough to enable the maximum discharging or the headroom of TES is enough to enable the maximum charging. When both HP and TES support the operation of CHP, the extended operating area of DHNs is enhanced by the combined contribution of HP and TES.

8.1.2 Modeling of Flexibility through Building Thermal Characteristics

In Chapter 3, the dynamic thermal process of pre-heating is investigated to address RQ2.

The first-order building thermal dynamic model is integrated into an energy management problem to investigate the utilisation of pre-heating as an alternative way to reduce the operational costs while taking into account the comfort conditions in buildings. Pre-heating through building thermal storage is enabled by allowing temperature variations within a pre-defined comfort zone. Through pre-heating, energy consumption can be managed in an economic-benefit-oriented way. By comparing the operational costs between the case where pre-heating is enabled and the case where additional TES is installed, the economic value of pre-heating can be evaluated and the capability of the inherent storage of buildings can be quantified under given thermal parameters of buildings.

A series of sensitivity studies are performed to investigate the limiting factors of the value of building inherent storage. Results show that (i) the equivalent storage of preheating is almost proportional to the volume of buildings and the insulation level of buildings; (ii) When the insulation condition is improved, the heat demand decreases accordingly, compressing the space of operational savings through pre-heating. Therefore, pre-heating can deliver more operational savings in buildings with a lower insulation level. However, when considering investment costs of different assets (e.g., HPs, generation), improved building insulation can significantly enhance the benefits of pre-heating, as reduced energy losses can introduce extra flexibility to pre-heating, making pre-heating more effective to shift peak load; (iii) Additionally, the equivalent size of building storage highly depends on the width of the temperature comfort zone. However, there is a cap of the benefits through increasing the size of TES, while the increase of temperature deviation allowance will keep bringing added benefits until the indoor temperature can freely drift without the need of any heat provision.

8.1.3 Integrated Electricity and Heat System Investment Model

In Chapter 4, a novel modelling framework for the whole system optimisation of the integrated heat and electricity systems investment is proposed to address RQ3.

The proposed optimization model can simultaneously optimize the investment in electricity generation (including RES and traditional generation), heating assets (including district heating plants and distributed heating appliances), the construction of heat networks, reinforcement of electricity transmission networks and distribution networks, while minimizing the system operational cost, taking into account frequency response and operating reserve requirements. The impact of integrated systems reducing system inertia on the frequency response requirement is explicitly modelled in the constraints. Carbon emission and security constraints are also included. The investment model of DHNs proposed in Chapter 2 is integrated into this combined heat and electricity system investment model to optimize the penetration of DHNs in different representative areas.

A variety of operation constraints are taken into account, including: electricity and heat balance constraints, heating technology mix constraints, power flow constraint, DSR constraints, TES operating constraints, pre-heating constraints, generation unit constraints, RES curtailment

constraints, ancillary service constraints, CHP operating constraints, distribution network reinforcement constraint, heat network investment cost constraints, system security constraints, and carbon constraint.

To further address RQ3, a set of comprehensive cases studies are carried out by applying the integrated heat and electricity system investment model in Chapter 5 and 6.

8.1.4 Evaluation of Alternative Heating Decarbonisation Strategies

In Chapter 5, the economic performance of various heating strategies in the decarbonisation of the heat sector through coordinated operation with the electricity system is assessed. A set of comprehensive case studies are carried out to compare the economic performance of different heating strategies from multiple perspectives and analyse the associated impacts on the electricity system.

The results suggest that hybrid HP-B has a significant overall economic advantage over HP-only and DHN, mainly due to investment savings from the presence of residential gas boilers. To be more specific, the comparison of hybrid HP-B over HP-only indicates that hybrid HP-B can drive savings over HP-only through the reduced requirement of distribution network reinforcement and OCGT as back-ups, due to the significant reduction of peak electricity demand which is compensated by gas-based heat, however, the operation cost increases as a result of reduced level of electrification in the heat sector, while more low-carbon generation is invested to compensate for the extra carbon emission from the gas consumption. The comparison of hybrid HP-B over DHN indicates that the main advantage of hybrid HP-B is the saved investment in the construction of the pipework. However, the investment cost of DHN highly depends on the heat density of the deployed area and hence grants DHN the economic advantages to be deployed in highly populous areas. Among all the investigated heating technologies, hydrogen boilers is the most capital-intensive, making it not suitable for large-scale deployment yet. However, since it can boost the integration of RES, its competitiveness can be improved under a more demanding carbon scenario.

The economic assessment for the optimal portfolio of heating technologies is performed given the cost assumptions, demonstrating that under the carbon target of 100g/kWh, 16% of the total

heat demand is covered by DHN (all deployed in urban areas) while the rest supplied by hybrid HP-B. When the carbon target is tightened to 50g/kWh, a 5% increase in the penetration of DHN is deployed (21% in total), manifesting its enhanced competitiveness in a more demanding carbon scenario. A series of sensitivity studies are performed to illustrate the robustness of the heating strategies to the cost uncertainty of heating technologies. The results also clearly demonstrate the changes on the electricity side driven by the different decarbonisation strategies in the heating system. The building energy efficiency has a significant impact on the whole system cost. When the building energy efficiency improves, the investment in district-heating technologies is gradually shifted to distributed-heating technologies, meanwhile, large savings are achieved in the total investment of heat sectors.

The capital cost of DHN mainly depends on the length of the pipeline. When the layout of consumers in a district has been determined, the potential capital cost of DHN in that district is also determined and will not be influenced by the variation of heat demand. Therefore, the lower the heat demand (kW), the higher the unit investment (£/kW) of DHN. As a consequence, the competitiveness of DHNs reduces when building energy efficiency improves. Additionally, the investment of RES decreases with improved building energy efficiency due to reduced heat demand and decreased availability of flexibility from heat sectors.

The value of building energy efficiency improvement is also impacted by carbon targets, the more demanding the carbon target is required, the more savings can be achieved through the improved building energy efficiency. Additionally, the whole system benefits through pre-heating increase with the improvement of the building energy efficiency in different carbon scenarios. The more demanding the carbon target is required, the more savings can be achieved.

8.1.5 Assessment of Benefits of Integrated Heat and Electricity Systems

In Chapter 6, the benefits through considering the interactions between the heat system and the electricity system at the planning stage were quantified across different sectors of the whole multi-energy system.

The results demonstrated that the integration of the heat and electricity system can bring significant benefits by increasing the investment in the heating infrastructure in order to

enhance the system flexibility that in turn can deliver larger cost savings in the electricity system, thus meeting the carbon target at a lower whole-system cost. System integration can deliver the shift in carbon emissions from the heat sector to the electricity sector, driven by the shift in heat production from gas-boilers to NG CHPs, while facilitating the electrification of the heat sector, which leads to significant cost savings in the electricity sector through the replacement of some NG CCS capacity by NG CHP (fundamentally enabled by the flexibility that significantly reduces RES curtailment).

TES can also make a great contribution to the reduction of the whole system operational and investment costs in the electricity sector at the cost of increasing the investment in the heat sector. Specifically, TES enables: (i) delivery of operation savings through alleviating the curtailment of RES, (ii) reduction of NG CCS capacity by supporting provision of ancillary services leading to an increase in RES production and (iii) the shift in heat delivery from end-use to district based technologies, driven by the flexibility requirements.

The benefits of pre-heating were also investigated. Based on the results, the application of pre-heating can substitute a considerable amount of TES, but the value of pre-heating is intensely affected by the building insulation levels. Additionally the marginal value of pre-heating declines with the increase of percentage of households providing this service. It is worth noticing that the improvement of building insulation level can effectively reduce heat demand, thus compressing the space of operational savings through pre-heating. However, when considering investment costs of different assets, improved building insulation can introduce extra flexibility to pre-heating, thus increasing investments savings.

In the end, this chapter investigated the role that balancing service requirement plays in the benefits of system integration. The results indicated that the level of balancing service requirements would have a significant impact on the value of the system integration. In this context, the benefits through system integration may vary with the development of different balancing-service-provision technologies, including the contribution of RES, nuclear generation, and emerging flexibility technologies, etc.

8.1.6 Computational Complexity Reduction

In Chapter 7, a cost-oriented representative-day-selection approach is proposed to reduce the computational burden of the integrated-electricity-and-heat-system investment-model, while ensuring that the results are near-optimal, thus addressing RQ4.

The proposed representative-day-selection approach comprises 4 key steps: (1) transfer of the clustering domain, (2) dimensionality reduction, (3) cluster allocation, and (4) representative day identification. By using this approach, the computational burden of the integrated electricity and heat system investment model can be significantly reduced. Additionally, the investment decisions made based on this approach can reach a high accuracy.

This chapter also demonstrates the superior performance of the proposed cost-oriented representative-day-selection approach against the widely used input-based approach. Based on our analysis, there are three factors that can potentially limit the performance of the input-based approach, including: (i) the potential nonlinearity between the input domain and output domain in complex cases may lead to mismatch in data clustering; (ii) the impact of RES generation on the system operation cannot be predefined in the cases where the capacities of Wind and PV are decision variables; and (iii) the impact of ancillary services requirements on the optimization result cannot be adequately taken into account if clustering is only based on the input dataset. In order to demonstrate the effectiveness of the proposed cost-oriented approach in terms of addressing the limitations faced by the input-based approach, three cases with increased complexity were tested. The results of all case studies indicate consistent improvement of accuracy when using the proposed cost-oriented approach compared to the input-based approach.

8.2 Future Work

Based on the conclusions of this thesis, a number of significant areas are identified for improvement in future work:

- It will be useful to further improve this thesis by getting a detailed understanding of the local effects of different categories of buildings which may potentially have significant

impacts on the suitability of different heating technologies and develop more detailed understanding of the impact of building efficiency and HNs.

- The gas network is an important component of the multi-energy system, especially when natural gas still dominates the heat sector and supplies a considerable proportion of the electricity generation in the UK. Therefore, it will be important to integrate the gas network into the proposed integrated electricity and heat system investment model to enable a more comprehensive analysis of the potential development direction of multi-energy system towards a low-carbon future.
- There is growing evidence that hydrogen may play an important role in the decarbonisation of the future energy system. Additionally, recent research indicates that the present distribution-level gas network can be adopted to deliver hydrogen without much update, therefore, the potential investment cost of adopting hydrogen will be significantly reduced, increasing the competitiveness of hydrogen. In this context, it will be important to further enhance the model by investigating the potential role and value of hydrogen technologies.
- Electric vehicles can significantly enhance the impact of DSR on the electricity system while fuel cells can effectively decarbonise the energy system by feeding on hydrogen. Therefore, it is also significant to consider the importance of the transport sector in the integrated energy system, including the impact of large scale application of electric vehicles and fuel cells on the electricity system.
- The cooling system is an important component of the multi-energy system, it will have significant impacts on the future energy system operation and investment decision, especially in the context that improved building insulation is required to reduce the heat demand in winter, which will bring about the issues of overheating in summer. Therefore, it will be necessary to investigate the role cooling system plays in the future multi-energy system planning.
- It will be interesting to investigate the potential role of end-side-used micro-CHP and the season heat storage in the future energy system.
- In order to identify robust strategies for the decarbonization of the integrated electricity and heat sectors, it is essential to understand the impact of considerable uncertainties in

future cost of different technologies and expand the proposed integrated electricity and heat system investment model into a multi-stage model.

- In terms of the representative-day-selection approach, it will be helpful to further develop the proposed cost-oriented approach for the selection of longer operating periods to address the investment planning problem considering inter-day or seasonal energy storage. Additionally, it will be helpful to expand of the proposed approach for the multi-stage investment planning problems.

References

[1] C. C. Committee, "Building a low-carbon economy-the UK's contribution to tackling climate change," *The Stationery Office, London,* 2008.

[2] DECC, "Annual Statement of Emissions for 2012," DECC, London, 2014.

[3] R. Sansom, "Decarbonising low grade heat for low carbon future," 2014.

[4] D. Energy, "2050 pathways for domestic heat, final report," 2012.

[5] B. Rezaie and M. A. Rosen, "District heating and cooling: Review of technology and potential enhancements," *Applied Energy,* vol. 93, pp. 2-10, 2012/05/01/ 2012.

[6] S. Frederiksen and S. Werner, *District heating and cooling*: Studentlitteratur, 2013.

[7] D. Connolly, H. Lund, B. V. Mathiesen, S. Werner, B. Möller, U. Persson*, et al.*, "Heat Roadmap Europe: Combining district heating with heat savings to decarbonise the EU energy system," *Energy Policy,* vol. 65, pp. 475-489, 2014/02/01/ 2014.

[8] M. Pirouti, A. Bagdanavicius, J. Ekanayake, J. Wu, and N. Jenkins, "Energy consumption and economic analyses of a district heating network," *Energy,* vol. 57, pp. 149-159, 2013/08/01/ 2013.

[9] U. Persson and S. Werner, "Heat distribution and the future competitiveness of district heating," *Applied Energy,* vol. 88, pp. 568-576, 2011/03/01/ 2011.

[10] P. A. Østergaard and H. Lund, "A renewable energy system in Frederikshavn using low-temperature geothermal energy for district heating," *Applied Energy,* vol. 88, pp. 479-487, 2011/02/01/ 2011.

[11] V. Verda and F. Colella, "Primary energy savings through thermal storage in district heating networks," *Energy,* vol. 36, pp. 4278-4286, 2011/07/01/ 2011.

[12] A. Arteconi and F. Polonara, "Assessing the Demand Side Management Potential and the Energy Flexibility of Heat Pumps in Buildings," *Energies,* vol. 11, p. 1846, 2018.

[13] D. Vanhoudt, D. Geysen, B. Claessens, F. Leemans, L. Jespers, and J. Van Bael, "An actively controlled residential heat pump: Potential on peak shaving and maximization of self-consumption of renewable energy," *Renewable Energy,* vol. 63, pp. 531-543, 2014.

[14] K. MacLean, R. Sansom, T. Watson, and R. Gross, "Managing Heat System Decarbonisation," *Comparing the impacts and costs of transitions in heat infrastructure,"Imperial College-Centre for Energy Policy and Technology,* 2016.

[15] P. E. Dodds, P. Ekins, A. Hawkes, F. Li, I. Staffell, W. McDowall*, et al.*, "The role of hydrogen and fuel cells in providing affordable, secure low-carbon heat," 2014.

[16] E. R. Partnership, "Potential Role of Hydrogen in the UK Energy System," Energy Research Partnership, London, 2016.

[17] J. Speirs, P. Balcombe, E. Johnson, J. Martin, N. Brandon, and A. Hawkes, "A greener gas grid: What are the options," *Energy Policy,* vol. 118, pp. 291-297, 2018/07/01/ 2018.

[18] K. Damen, M. v. Troost, A. Faaij, and W. Turkenburg, "A comparison of electricity and hydrogen production systems with CO2 capture and storage. Part A: Review and selection of promising conversion and capture technologies," *Progress in Energy and Combustion Science,* vol. 32, pp. 215-246, 2006/01/01/ 2006.

[19] K. Damen, M. van Troost, A. Faaij, and W. Turkenburg, "A comparison of electricity and hydrogen production systems with CO2 capture and storage—Part B: Chain analysis of promising CCS options," *Progress in Energy and Combustion Science,* vol. 33, pp. 580-609, 2007/12/01/ 2007.

[20] A. Almansoori and N. Shah, "Design and Operation of a Future Hydrogen Supply Chain: Snapshot Model," *Chemical Engineering Research and Design,* vol. 84, pp. 423-438, 2006/06/01/ 2006.

[21] S. Samsatli, I. Staffell, and N. J. Samsatli, "Optimal design and operation of integrated wind-hydrogen-electricity networks for decarbonising the domestic transport sector in Great Britain," *International Journal of Hydrogen Energy,* vol. 41, pp. 447-475, 2016/01/05/ 2016.

[22] J. Green, S. Smith, and G. Strbac, "Evaluation of electricity distribution system design strategies," *IEE Proceedings-Generation, Transmission and Distribution,* vol. 146, pp. 53-60, 1999.

[23] D. Melovic and G. Strbac, "Statistical model for design of distribution network," in *2003 IEEE Bologna Power Tech Conference Proceedings*, 2003, p. 5 pp. Vol.3.

[24] C. K. Gan, "Strategies for Design of Future Distribution Networks," Ph.D, Imperial College London, 2011.

[25] D. Melovic, "Optimal Distribution Network Design Policy," Ph.D, Imperial College London, 2005.

[26] DECC. *National Heat Map*.

[27] DECC, "Assessment of the Costs, Performance, and Characteristics of UK Heat Networks," DECC, London, UK, 2015.

[28] "London Heat Network Manual," Mayor of London, 2014.

[29] DECC, "CHP Technology – A detailed guide for CHP developers – Part 2," London, UK2008.

[30] D. D. Andrews, A. Krook-Riekkola, E. Tzimas, J. Serpa, J. Carlsson, N. Pardo-Garcia*, et al.*, "Background report on EU-27 district heating and cooling potentials, barriers, best practice and measures of promotion," ed: Publications Office of the European Union, 2012.

[31] W. Haichao, J. Wenling, and Z. Chuanzhi, "Design and Operation Regulation of Combined Heating System with Gas-fired Boilers as Peak-load Heat Sources in Secondary Heating Network," in *Intelligent Computation Technology and Automation (ICICTA), 2011 International Conference on*, 2011, pp. 813-817.

[32] J. Xu, R. Wang, and Y. Li, "A review of available technologies for seasonal thermal energy storage," *Solar Energy,* vol. 103, pp. 610-638, 2014.

[33] X. Chen, C. Kang, M. O. Malley, Q. Xia, J. Bai, C. Liu*, et al.*, "Increasing the Flexibility of Combined Heat and Power for Wind Power Integration in China: Modeling and Implications," *IEEE Transactions on Power Systems,* vol. 30, pp. 1848-1857, 2015.

[34] Y. Kitapbayev, J. Moriarty, and P. Mancarella, "Stochastic control and real options valuation of thermal storage-enabled demand response from flexible district energy systems," *Applied Energy,* vol. 137, pp. 823-831, 2015.

[35] S. R. Griful, U. Welling, and R. H. Jacobsen, "Multi-modal Building Energy Management System for Residential Demand Response," in *Digital System Design (DSD), 2016 Euromicro Conference on*, 2016, pp. 252-259.

[36] Z. Pan, Q. Guo, and H. Sun, "Feasible region method based integrated heat and electricity dispatch considering building thermal inertia," *Applied Energy,* vol. 192, pp. 395-407, 2017/04/15/ 2017.

[37] J. E. Braun, "Reducing energy costs and peak electrical demand through optimal control of building thermal storage," *ASHRAE transactions,* vol. 96, pp. 876-888, 1990.

[38] K. Konis and L. Zhang, "Occupant-aware energy management: simulated energy savings achievable through application of temperature setpoints learned through end-user feedback," *Proceedings of SimBuild,* vol. 6, 2016.

[39] S. R. Bull, "Renewable energy today and tomorrow," *Proceedings of the IEEE,* vol. 89, pp. 1216-1226, 2001.

[40] T. T. Chow, A. Chan, K. Fong, Z. Lin, W. He, and J. Ji, "Annual performance of building-integrated photovoltaic/water-heating system for warm climate application," *Applied Energy,* vol. 86, pp. 689-696, 2009.

[41] A. D. Carvalho, P. Moura, G. C. Vaz, and A. T. de Almeida, "Ground source heat pumps as high efficient solutions for building space conditioning and for integration in smart grids," *Energy conversion and management,* vol. 103, pp. 991-1007, 2015.

[42] X. Jin, Y. Mu, H. Jia, J. Wu, T. Jiang, and X. Yu, "Dynamic economic dispatch of a hybrid energy microgrid considering building based virtual energy storage system," *Applied energy,* vol. 194, pp. 386-398, 2017.

[43] X. Jin, J. Wu, Y. Mu, M. Wang, X. Xu, and H. Jia, "Hierarchical microgrid energy management in an office building," *Applied Energy,* vol. 208, pp. 480-494, 2017.

[44] L. Yu, D. Xie, C. Huang, T. Jiang, and Y. Zou, "Energy Optimization of HVAC Systems in Commercial Buildings Considering Indoor Air Quality Management," *IEEE Transactions on Smart Grid,* 2018.

[45] R. J. LeVeque, *Finite difference methods for ordinary and partial differential equations: steady-state and time-dependent problems* vol. 98: Siam, 2007.

[46] M. Aunedi, "Value of flexible demand-side technologies in future low-carbon systems," 2013.

[47] V. Trovato, S. H. Tindemans, and G. Strbac, "Leaky storage model for optimal multi-service allocation of thermostatic loads," *IET Generation, Transmission & Distribution,* vol. 10, pp. 585-593, 2016.

[48] D. Pudjianto, M. Aunedi, P. Djapic, and G. Strbac, "Whole-systems assessment of the value of energy storage in low-carbon electricity systems," *IEEE Transactions on Smart Grid,* vol. 5, pp. 1098-1109, 2014.

[49] M. Carrion and J. M. Arroyo, "A computationally efficient mixed-integer linear formulation for the thermal unit commitment problem," *IEEE Transactions on Power Systems,* vol. 21, pp. 1371-1378, 2006.

[50] R. D'hulst, W. Labeeuw, B. Beusen, S. Claessens, G. Deconinck, and K. Vanthournout, "Demand response flexibility and flexibility potential of residential smart appliances: Experiences from large pilot test in Belgium," *Applied Energy,* vol. 155, pp. 79-90, 2015.

[51] W. Mert, "Consumer acceptance of smart appliances," Inter-university Research Centre for Technology, Work and Culture, 2008.

[52] J. Bode, "Measuring short-term air conditioner demand reductions for operations and settlement," 2012.

[53] Z. Li, W. Wu, M. Shahidehpour, J. Wang, and B. Zhang, "Combined heat and power dispatch considering pipeline energy storage of district heating network," *IEEE Transactions on Sustainable Energy,* vol. 7, pp. 12-22, 2016.

[54] F. Teng, V. Trovato, and G. Strbac, "Stochastic scheduling with inertia-dependent fast frequency response requirements," *IEEE Transactions on Power Systems,* vol. 31, pp. 1557-1566, 2016.

[55] F. Teng and G. Strbac, "Full Stochastic Scheduling for Low-Carbon Electricity Systems," *IEEE Transactions on Automation Science and Engineering,* vol. 14, pp. 461-470, 2017.

[56] G. Li, R. Zhang, T. Jiang, H. Chen, L. Bai, H. Cui*, et al.*, "Optimal dispatch strategy for integrated energy systems with CCHP and wind power," *Applied Energy,* vol. 192, pp. 408-419, 2017/04/15/ 2017.

[57] G. Strbac, M. Aunedi, D. Pudjianto, P. Djapic, F. Teng, A. Sturt*, et al.*, "Strategic assessment of the role and value of energy storage systems in the UK low carbon energy future," *Report for Carbon Trust,* 2012.

[58] C. K. Gan, P. Mancarella, D. Pudjianto, and G. Strbac, "Statistical appraisal of economic design strategies of LV distribution networks," *Electric Power Systems Research,* vol. 81, pp. 1363-1372, 2011.

[59] R. Sansom and G. Strbac, "The impact of future heat demand pathways on the economics of low carbon heating systems," in *BIEE–9th Academic Conf*, 2012, pp. 19-20.

[60] Q. Zhang, L. Zhang, J. Nie, and Y. Li, "Techno-economic analysis of air source heat pump applied for space heating in northern China," *Applied Energy,* vol. 207, pp. 533-542, 2017/12/01/ 2017.

[61] M. Münster, P. E. Morthorst, H. V. Larsen, L. Bregnbæk, J. Werling, H. H. Lindboe*, et al.*, "The role of district heating in the future Danish energy system," *Energy,* vol. 48, pp. 47-55, 2012/12/01/ 2012.

[62] G. Strbac, M. Aunedi, D. Pudjianto, F. Teng, P. Djapic, R. Druce*, et al.*, "Value of Flexibility in a Decarbonised Grid and System Externalities of Low-Carbon Generation Technologies," *Imperial College London, NERA Economic Consulting,* 2015.

[63] W. Zappa, M. Junginger, and M. van den Broek, "Is a 100% renewable European power system feasible by 2050?," *Applied Energy,* vol. 233-234, pp. 1027-1050, 2019/01/01/ 2019.

[64] P. D. Lund, J. Lindgren, J. Mikkola, and J. Salpakari, "Review of energy system flexibility measures to enable high levels of variable renewable electricity," *Renewable and Sustainable Energy Reviews,* vol. 45, pp. 785-807, 2015.

[65] P. Mancarella and G. Chicco, "Integrated energy and ancillary services provision in multi-energy systems," in *2013 IREP Symposium Bulk Power System Dynamics and Control - IX Optimization, Security and Control of the Emerging Power Grid*, 2013, pp. 1-19.

[66] T. Fang and R. Lahdelma, "Genetic optimization of multi-plant heat production in district heating networks," *Applied Energy,* vol. 159, pp. 610-619, 2015/12/01/ 2015.

[67] P. A. Østergaard and A. N. Andersen, "Booster heat pumps and central heat pumps in district heating," *Applied Energy,* vol. 184, pp. 1374-1388, 2016/12/15/ 2016.

[68] M. B. Blarke and H. Lund, "Large-scale heat pumps in sustainable energy systems: system and project perspectives," in *Sustainable Development Of Energy, Water And Environment Systems*, ed: World Scientific, 2007, pp. 69-78.

[69] P. Mancarella, "Cogeneration systems with electric heat pumps: Energy-shifting properties and equivalent plant modelling," *Energy Conversion and Management,* vol. 50, pp. 1991-1999, 2009/08/01/ 2009.

[70] P. Mancarella, "MES (multi-energy systems): An overview of concepts and evaluation models," *Energy,* vol. 65, pp. 1-17, 2014.

[71] S. Heinen, D. Burke, and M. O'Malley, "Electricity, gas, heat integration via residential hybrid heating technologies–An investment model assessment," *Energy,* vol. 109, pp. 906-919, 2016.

[72] K. Klein, K. Huchtemann, and D. Müller, "Numerical study on hybrid heat pump systems in existing buildings," *Energy and buildings,* vol. 69, pp. 193-201, 2014.

[73] K. J. Chua, S. K. Chou, and W. Yang, "Advances in heat pump systems: A review," *Applied energy,* vol. 87, pp. 3611-3624, 2010.

[74] C. Vuillecard, C. E. Hubert, R. Contreau, P. Stabat, and J. Adnot, "Small scale impact of gas technologies on electric load management–μCHP & hybrid heat pump," *Energy,* vol. 36, pp. 2912-2923, 2011.

[75] S. Clegg and P. Mancarella, "Integrated modeling and assessment of the operational impact of power-to-gas (P2G) on electrical and gas transmission networks," *IEEE Transactions on Sustainable Energy,* vol. 6, pp. 1234-1244, 2015.

[76] J. Zheng, Z. Zhou, J. Zhao, and J. Wang, "Integrated heat and power dispatch truly utilizing thermal inertia of district heating network for wind power integration," *Applied Energy,* vol. 211, pp. 865-874, 2018/02/01/ 2018.

[77] A. Hast, S. Rinne, S. Syri, and J. Kiviluoma, "The role of heat storages in facilitating the adaptation of district heating systems to large amount of variable renewable electricity," *Energy,* 2017.

[78] X. Liu and P. Mancarella, "Modelling, assessment and Sankey diagrams of integrated electricity-heat-gas networks in multi-vector district energy systems," *Applied Energy,* vol. 167, pp. 336-352, 2016/04/01/ 2016.

[79] A. Ahmed and P. Mancarella, "Strategic techno-economic assessment of heat network options for distributed energy systems in the UK," *Energy,* vol. 75, pp. 182-193, 2014.

[80] C. Bordin, A. Gordini, and D. Vigo, "An optimization approach for district heating strategic network design," *European Journal of Operational Research,* vol. 252, pp. 296-307, 2016.

[81] BEIS, "Electricity Generation Costs," BEIS, London, UK,Nov. 2016.

[82] V. Black, "Cost and performance data for power generation technologies," *Prepared for the National Renewable Energy Laboratory,* 2012.

[83] E. Styrelsen, "Technology Data for Energy Plants—Generation of Electricity and District Heating, Energy Storage and Energy Carrier Generation and Conversion," *Energinet. dk, Energi Styrelsen, Denmark,* 2012.

[84] Danish Energy Agency, "Technology Data for Energy Plants for Electricity and District heating generation," Danish Energy Agency, Copenhagen, 2016.

[85] R. Abdurafikov, E. Grahn, L. Kannari, J. Ypyä, S. Kaukonen, I. Heimonen*, et al.*, "An analysis of heating energy scenarios of a Finnish case district," *Sustainable Cities and Society,* vol. 32, pp. 56-66, 2017/07/01/ 2017.

[86] K. Çomaklı, B. Yüksel, and Ö. Çomaklı, "Evaluation of energy and exergy losses in district heating network," *Applied Thermal Engineering,* vol. 24, pp. 1009-1017, 2004/05/01/ 2004.

[87] X. Zhang, G. Strbac, F. Teng, and P. Djapic, "Economic assessment of alternative heat decarbonisation strategies through coordinated operation with electricity system – UK case study," *Applied Energy,* vol. 222, pp. 79-91, 2018/07/15/ 2018.

[88] X. Zhang, G. Strbac, P. Djapic, and F. Teng, "Optimization of Heat Sector Decarbonization Strategy through Coordinated Operation with Electricity System," *Energy Procedia,* vol. 142, pp. 2858-2863, 2017/12/01/ 2017.

[89] E. Lannoye, P. Daly, A. Tuohy, D. Flynn, and M. O'Malley, "Assessing Power System Flexibility for Variable Renewable Integration: A Flexibility Metric for Long-Term System Planning," 2015.

[90] G. Strbac, M. Aunedi, D. Pudjianto, P. Djapic, S. Gammons, and R. Druce, "Understanding the Balancing Challenge, Report for the Department of Energy and Climate Change," *London, UK, August,* 2012.

[91] E. Lannoye, D. Flynn, and M. O. Malley, "Evaluation of Power System Flexibility," *IEEE Transactions on Power Systems,* vol. 27, pp. 922-931, 2012.

[92] J. Kiviluoma and P. Meibom, "Influence of wind power, plug-in electric vehicles, and heat storages on power system investments," *Energy,* vol. 35, pp. 1244-1255, 2010/03/01/ 2010.

[93] H. Lund, B. Möller, B. V. Mathiesen, and A. Dyrelund, "The role of district heating in future renewable energy systems," *Energy,* vol. 35, pp. 1381-1390, 2010/03/01/ 2010.

[94] F. Fang, Q. H. Wang, and Y. Shi, "A Novel Optimal Operational Strategy for the CCHP System Based on Two Operating Modes," *IEEE Transactions on Power Systems,* vol. 27, pp. 1032-1041, 2012.

[95] H. Wang, W. Yin, E. Abdollahi, R. Lahdelma, and W. Jiao, "Modelling and optimization of CHP based district heating system with renewable energy production and energy storage," *Applied Energy,* vol. 159, pp. 401-421, 2015/12/01/ 2015.

[96] DECC, "Heat Pumps in District Heating," DECC, London UK. 2016.

[97] K. Hedegaard and M. Münster, "Influence of individual heat pumps on wind power integration – Energy system investments and operation," *Energy Conversion and Management,* vol. 75, pp. 673-684, 2013/11/01/ 2013.

[98] K. Hedegaard, B. V. Mathiesen, H. Lund, and P. Heiselberg, "Wind power integration using individual heat pumps – Analysis of different heat storage options," *Energy,* vol. 47, pp. 284-293, 2012/11/01/ 2012.

[99] S. Heinen and M. O'Malley, "Power system planning benefits of hybrid heating technologies," in *PowerTech, 2015 IEEE Eindhoven*, 2015, pp. 1-6.

[100] X. Liu, J. Wu, N. Jenkins, and A. Bagdanavicius, "Combined analysis of electricity and heat networks," *Applied Energy,* vol. 162, pp. 1238-1250, 2016/01/15/ 2016.

[101] C. Lin, W. Wu, B. Zhang, and Y. Sun, "Decentralized Solution for Combined Heat and Power Dispatch through Benders Decomposition," *IEEE Transactions on Sustainable Energy,* 2017.

[102] T. Nuytten, B. Claessens, K. Paredis, J. Van Bael, and D. Six, "Flexibility of a combined heat and power system with thermal energy storage for district heating," *Applied Energy,* vol. 104, pp. 583-591, 2013/04/01/ 2013.

[103] J. Mikkola and P. D. Lund, "Modeling flexibility and optimal use of existing power plants with large-scale variable renewable power schemes," *Energy,* vol. 112, pp. 364-375, 2016.

[104] X. Zhang, G. Strbac, N. Shah, F. Teng, and D. Pudjianto, "Whole-System Assessment of the Benefits of Integrated Electricity and Heat System," *IEEE Transactions on Smart Grid,* pp. 1-1, 2018.

[105] F. Teng and G. Strbac, "Assessment of the Role and Value of Frequency Response Support From Wind Plants," *IEEE Transactions on Sustainable Energy,* vol. 7, pp. 586-595, 2016.

[106] R. Lowe, "Combined heat and power considered as a virtual steam cycle heat pump," *Energy Policy,* vol. 39, pp. 5528-5534, 2011/09/01/ 2011.

[107] J. Ma, V. Silva, R. Belhomme, D. S. Kirschen, and L. F. Ochoa, "Evaluating and Planning Flexibility in Sustainable Power Systems," *IEEE Transactions on Sustainable Energy,* vol. 4, pp. 200-209, 2013.

[108] K. Poncelet, H. Höschle, E. Delarue, A. Virag, and W. D'haeseleer, "Selecting Representative Days for Capturing the Implications of Integrating Intermittent Renewables in Generation Expansion Planning Problems," *IEEE Transactions on Power Systems,* vol. 32, pp. 1936-1948, 2017.

[109] M. Sun, F. Teng, I. Konstantelos, and G. Strbac, "An objective-based scenario selection method for transmission network expansion planning with multivariate stochasticity in load and renewable energy sources," *Energy,* 2018/01/05/ 2018.

[110] W. Short, P. Sullivan, T. Mai, M. Mowers, C. Uriarte, N. Blair*, et al.*, "Regional energy deployment system (ReEDS)," *Contract,* vol. 303, pp. 275-3000, 2011.

[111] L. Baringo and A. J. Conejo, "Correlated wind-power production and electric load scenarios for investment decisions," *Applied Energy,* vol. 101, pp. 475-482, 2013/01/01/ 2013.

[112] R. Domínguez, A. J. Conejo, and M. Carrión, "Toward Fully Renewable Electric Energy Systems," *IEEE Transactions on Power Systems,* vol. 30, pp. 316-326, 2015.

[113] Y. Liu, R. Sioshansi, and A. J. Conejo, "Hierarchical Clustering to Find Representative Operating Periods for Capacity-Expansion Modeling," *IEEE Transactions on Power Systems,* vol. 33, pp. 3029-3039, 2018.

[114] D. Z. Fitiwi, F. de Cuadra, L. Olmos, and M. Rivier, "A new approach of clustering operational states for power network expansion planning problems dealing with RES (renewable energy source) generation operational variability and uncertainty," *Energy,* vol. 90, pp. 1360-1376, 2015/10/01/ 2015.

[115] Q. Ploussard, L. Olmos, and A. Ramos, "An Operational State Aggregation Technique for Transmission Expansion Planning Based on Line Benefits," *IEEE Transactions on Power Systems,* vol. 32, pp. 2744-2755, 2017.

[116] R. Alvarez, A. Moser, and C. A. Rahmann, "Novel Methodology for Selecting Representative Operating Points for the TNEP," *IEEE Transactions on Power Systems,* vol. 32, pp. 2234-2242, 2017.

[117] S. Pineda and A. J. Conejo, "Scenario reduction for risk-averse electricity trading," *IET Generation, Transmission & Distribution,* vol. 4, pp. 694-705, 2010.

[118] J. M. Morales, S. Pineda, A. J. Conejo, and M. Carrion, "Scenario Reduction for Futures Market Trading in Electricity Markets," *IEEE Transactions on Power Systems,* vol. 24, pp. 878-888, 2009.

[119] M. Sun, F. Teng, X. Zhang, G. Strbac, and D. Pudjianto, "Data-Driven Representative Day Selection for Investment Decisions: A Cost-Oriented Approach," *IEEE Transactions on Power Systems,* pp. 1-1, 2019.

[120] E. Keogh and A. Mueen, "Curse of dimensionality," in *Encyclopedia of machine learning*, ed: Springer, 2011, pp. 257-258.

[121] M. Belkin and P. Niyogi, "Laplacian Eigenmaps for Dimensionality Reduction and Data Representation," *Neural Computation,* vol. 15, pp. 1373-1396, 2003.

[122] S. C. Johnson, "Hierarchical clustering schemes," *Psychometrika,* vol. 32, pp. 241-254, 1967.

[123] J. H. Ward Jr, "Hierarchical grouping to optimize an objective function," *Journal of the American statistical association,* vol. 58, pp. 236-244, 1963.

Appendix A Data and Parameters

A.1 Parameters and Images of Representative Districts

Representative area 1 is selected from an urban area characterised by a high heat density. Detailed parameters of this area acquired from the National Heat Map and the fractal model are listed in Table. A.1, while the generated topology of heat network that can be potentially deployed in this area illustrated in Fig. A.1. According to the economic attraction model described in 2.1.2, the consumers are highly evenly distributed within the given area (compared to the other representative areas as follows).

Table. A.1 – Parameters of representative area 1

Area (km2)	0.864
Heat density (kWh/km2/yr)	61.7
Area category	Urban
Consumer count	836
Length of network (km)	16.82

Representative area 2 is selected from an area with a relatively low heat density compared to representative area 1 and categorised as sub-urban area in this thesis. Detailed parameters of this area acquired from the National Heat Map and the fractal model are listed in Table. A.2, while the generated topology of heat network that can be potentially deployed in this area is illustrated in Fig. A.2. As can be seen, the consumer distribution is less even than that in representative area 1.

Table. A.2 – Table Parameter of representative area 2

Area (km2)	0.912
Heat density (kWh/km2/yr)	25.1
Area category	Suburban
Consumer count	651
Length of network (km)	12.94

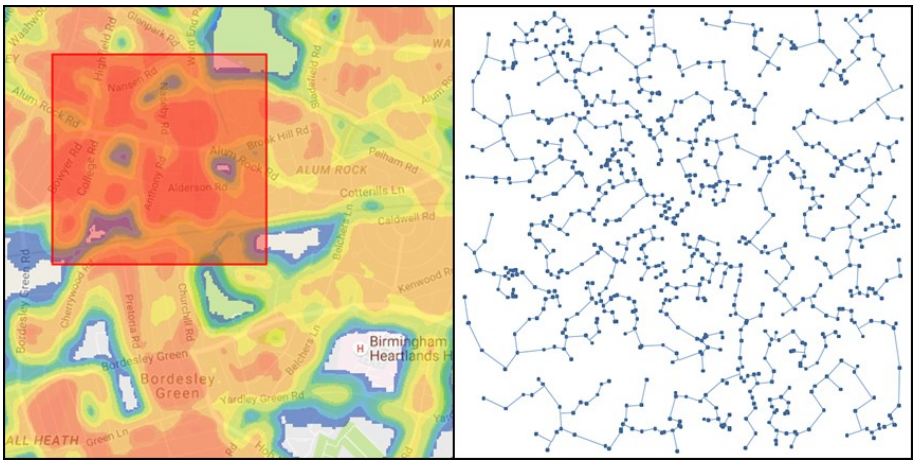

Fig. A.1 – Topology of heat network that can be potentially deployed in representative network 1

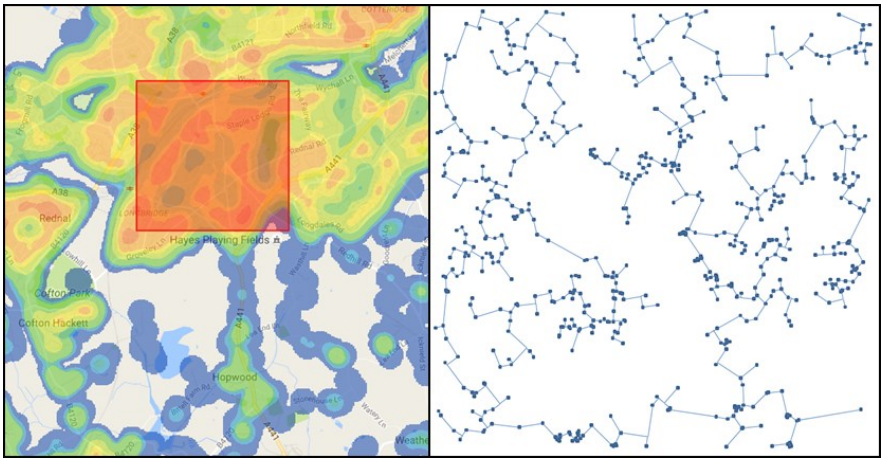

Fig. A.2 – Topology of heat network that can be potentially deployed in representative network 2

Representative area 3 is selected from an area with a much lower heat density than the previous representative areas and categorised as semi-rural area in this thesis. Detailed parameters of

this area acquired from the National Heat Map and the fractal model are listed in Table. A.3, while the generated topology of heat network that can be potentially deployed in this area is illustrated in Fig. A.3.

Table. A.3 – Table Parameter of representative area 3

Area (km2)	4.36
Heat density (kWh/km2/yr)	3.05
Area category	Semirural
Consumer count	956
Length of network (km)	20.43

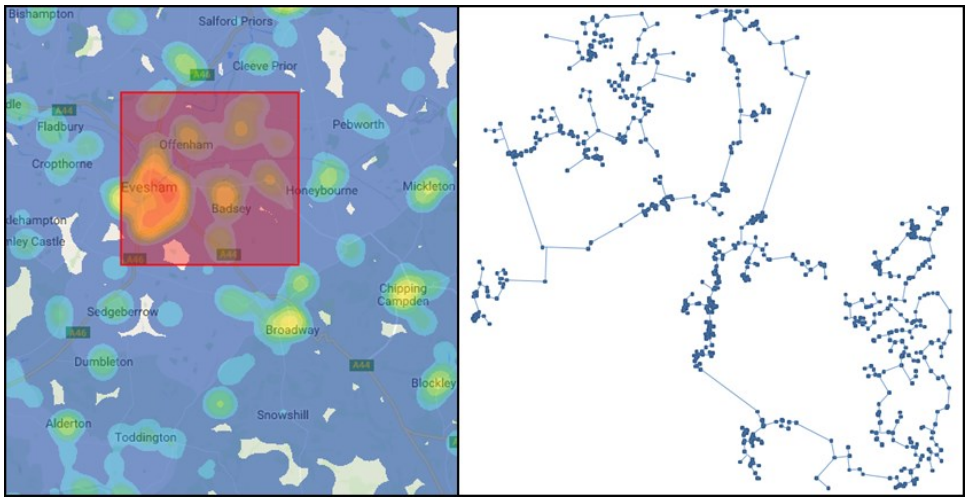

Fig. A.3 – Topology of heat network that can be potentially deployed in representative network 3

Representative area 4 is selected from an area with the lowest heat density compared to the other representative areas and categorised as rural area in this thesis. Detailed parameters of this area acquired from the National Heat Map and the fractal model are listed in Table. A.4, while the generated topology of heat network that can be potentially deployed in this area is illustrated in Fig. A.4.

Table. A.4 – Table Parameter of representative area 4

Area (km2)	19.11
Heat density (kWh/km2/yr)	0.89
Area category	Rural
Consumer count	1632
Length of network (km)	39.62

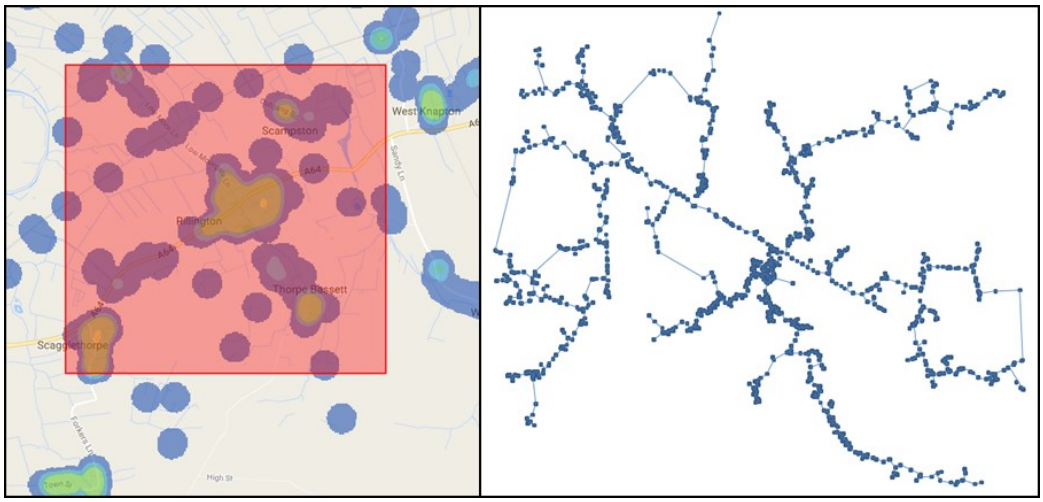

Fig. A.4 – Topology of heat network that can be potentially deployed in representative network 4

The cost assumptions of DHNs, length of pipelines under full deployment of DHNs, and the number of representative districts are presented in Table. A.5 and Table. A.6 [27].

Table. A.5 – Parameters of different representative DHNs

Type of areas	Capital cost of DHN (£/km)	Length of pipelines under full deployment of DHN (km)	Number of representative districts
Urban	1122	16.8	3632
Suburban	772	12.9	4536
Semirural	597	20.4	7300
Rural	468	39.6	5992

Table. A.6 – Economic parameters of DHNs

Parameter of DHNs	Values
Life span (year)	40
Cost of capital (%)	6%

A.2 Profiles of RES Availability Factor

The availability factor of wind and solar generation are illustrated in Fig. A.5 and Fig. A.6. The maximum and average availability factor for wind are 1 and 0.39 while for solar are 0.78 and 0.12. The potential output of wind/solar generation is equal to the product of the capacity of wind turbine/PV panel and their availability factor, while the actual output is the difference between the potential output and the curtailment.

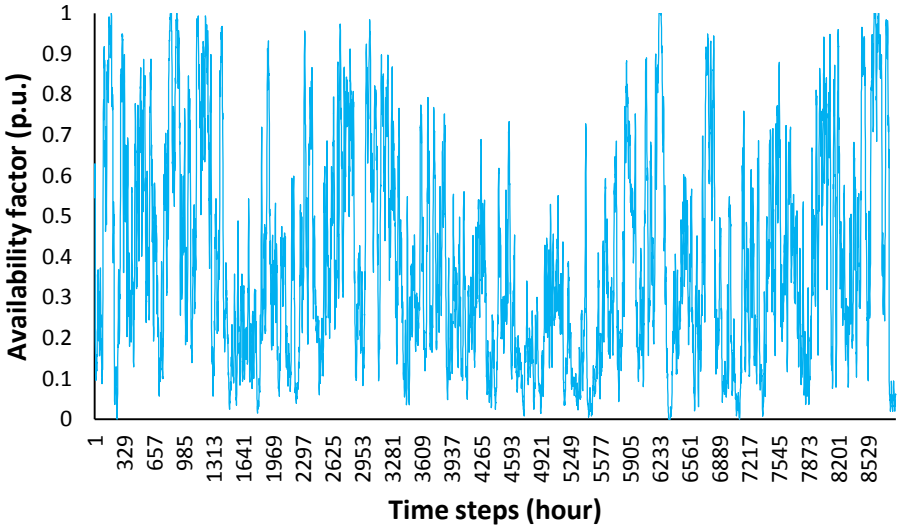

Fig. A.7 – Profile of wind availability factor

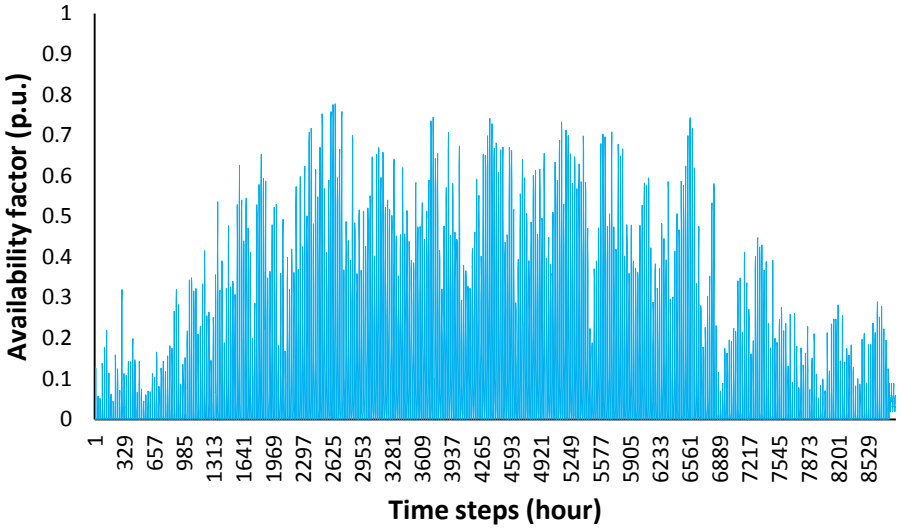

Fig. A.8 – Profile of solar energy availability factor

A.3 Operation & Economic Parameters of Different Technologies

Table. A.7 shows the cost parameters of various generation technologies.

Table. A.7 – Cost Parameters of Generation Plants

Generation	Capital cost (£m/MW)	Fixed O&M (£/kW/year)	Variable O&M (£/MWh)	Discount Rate (%)	Lifetime (year)
Nuclear	4.34	83.4	5	8.90%	60
CCGT	0.51	16.6	3	7.80%	25
OCGT	0.32	8.2	3	7.80%	25
NG CCS	2.15	41.6	3	9.20%	25
Coal CCS	2.43	92.7	3	8.20%	15
NG CHP	0.76	34.4	5	7.80%	25
Biomass CHP	5.17	304.7	11	12.20%	24
Wind	1.52	30.9	5	8.90%	23
PV	0.67	6.2	0	6.50%	25

Table. A.8 and Table. A.9 give the operational parameters of different generation technologies.

Table. A.8 – Operation parameters of Generation Plants

Generation	Min stable generation	Ramp rates	Annual Availability Factor	Max Response provision	Max Reserve provision
Nuclear	80%	10%	0.91	0%	0%
CCGT	50%	60%	0.93	10%	50%
OCGT	40%	100%	0.93	10%	60%
NG CCS	50%	50%	0.93	10%	50%
Coal CCS	40%	50%	0.93	5%	60%
NG CHP	50%	60%	0.93	10%	50%
Biomass CHP	50%	60%	0.93	10%	50%
Wind	N/A	N/A	0.39	0%	0%
PV	N/A	N/A	0.12	0%	0%

Table. A.9 – Carbon and operating cost parameters of thermal generators

Generation technology	Average cost (£/kWh)		Efficiency		Average CO2 emissions (g/kWh)	
	MSG	Full	MSG	Full	MSG	Full
Coal CCS	54.4	39.5	25.4%	35.0%	116	80
CCGT	84.7	74.1	51.5%	58.8%	422	368
CCGT CCS	63.4	55.9	45.2%	51.3%	39	34
OCGT	139.7	124.5	31.2%	35.0%	689	613
NG CHP	84.7	74.1	51.5%	58.8%	422	368
Biomass CHP	42.9	37.5	34.8%	39.8%	0	0

Table. A.10 and Table. A.11 give the economic and operational parameters of different heating technologies and TES.

Table. A.10 – Parameters of Heating Technologies in 2030

End-use heating	Capital cost (£/kWth)	Installation (£)	O&M fixed (£/kWth /yr)	Efficiency (%)
ASHP	612	1200	20	1.6-3.6
Gas boiler	N/A	N/A	32	95%
District heating	Capital cost (£m/MWth)		O&M fixed (£/MWth/yr)	Efficiency (%)
HP	0.48		3200	380%
Gas boiler	0.08		2960	98%

Table. A.11 – Parameters of TES

Storage	CAPEX	ε^s (h)	Static eff	Charging eff
ITES	80 £/m3	6	99%	99%
ETES	2.4 £/litre	3	99%	99%

Table. A.12 shows the parameters of 4 types of representative distribution networks.

Table. A.12 –Parameters of distribution networks in 2030

	Percentage of demand supplied	Unit Reinforcement cost (£/kVA/year)	Peak load that can be accommodated without reinforcement (GW)
Urban	33.3%	37	5
Suburban	41.2%	62	4.8
Semirural	17.8%	26	2.1
Rural	7.7%	19	1

Table. A.13 shows the parameters of different types of generation with low and high flexibility.

Table. A.13 – Operating parameters of generators in different scenarios

Flexibility & efficiency	Generation	MSG	Maximum response (% rating)	Efficiency (%)	
				MSG	FULL
Low	CCGT	50%	12%	51.5%	58.8%
	Gas CCS	50%	7%	45.2%	51.3%
	Nuclear	60%	0	-	-
	OCGT	40%	30%	31.2%	35.0%
	Coal CCS	40%	5%	25.4%	35.0%
High	CCGT	40%	17%	55.1%	58.8%
	Gas CCS	40%	10%	48.1%	51.3%
	Nuclear	80%	0	-	-
	OCGT	40%	40%	33.0%	35.0%
	Coal CCS	40%	5%	29.7%	35.0%